AD A107863

AFWAL-TR-81-2045

DAMAGE TOLERANT DESIGN FOR COLD-SECTION TURBINE ENGINE DISKS

United Technologies
Pratt & Whitney Aircraft
Government Products Division
P.O. Box 2691
West Palm Beach, Florida 33402

June 1981

Final Report for Period August 1977 to February 1981

Approved for Public Release; Distribution Unlimited

Prepared for
Air Force Aero Propulsion Laboratory
Air Force Wright Aeronautical Laboratories
Air Force Systems Command
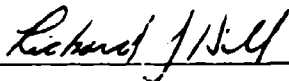Wright-Patterson Air Force Base, Ohio 45433
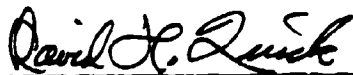
81 11 24 024

Richard J. Hill
Project Engineer

JAMES M. SHIPMAN, Major, USAF
Chief, Components Branch

FOR THE COMMANDER

DAVID H. QUICK, Lt Col, USAF
Acting Director
Turbine Engine Division

AIR FORCE/56780/29 October 1981 — 130

REPORT DOCUMENTATION PAGE		READ INSTRUCTIONS BEFORE COMPLETING FORM
1. Report Number AFWAL-TR-81-2045	2. Govt Accession No. AD-A107 863	3. Recipient's Catalog Number
4. Title *(and Subtitle)* DAMAGE TOLERANT DESIGN FOR COLD-SECTION TURBINE ENGINE DISKS PWH-FR-14442		5. Type of Report & Period Covered FINAL August 1977 to February 1981
		6. Performing Org. Report Number -FR-14442
7. Author(s) Cook, C. H., Johnson, H. E., and Spaeth, C. E.		8. Contract or Grant Number(s) F33615-77-C-2064
9. Performing Organization Name and Address United Technologies Corporation Pratt & Whitney Aircraft Group Government Products Division P.O. Box 2691, West Palm Beach, FL 33402		10. Program Element, Project, Task Area & Work Unit Numbers P.E. 62203F, 3066, 12, 44
11. Controlling Office Name and Address Aero Propulsion Laboratory (AFWAL/POTC) Air Force Wright Aeronautical Laboratories Wright-Patterson AFB, Ohio 45420		12. Report Date June 1981
		13. Number of Pages 241
14. Monitoring Agency Name & Address *(if different from Controlling Office)*		15. Security Class. *(of this report)* UNCLASSIFIED
		15a. Declassification/Downgrading Schedule

16. Distribution Statement *(of this Report)*

    Approved for public release; distribution unlimited

17. Distribution Statement *(of the abstract entered in Block 20, if different from Report)*

18. Supplementary Notes

19. Key Words *(Continue on reverse side if necessary and identify by block number)*

    Damage Tolerant Design
    Fracture Control
    Slow Crack Growth
    Disk Life
    Low Cycle Fatigue

20. Abstract *(Continue on reverse side if necessary and identify by block number)*

This report describes the development, test evaluation, and refinement of a Damage Tolerant Design System for cold-section turbine engine disks. To substantiate the Design System the 42-month effort included the design and test of a functional replacement 2nd-stage fan disk for the F100 engine. This disk would be able to support a 0.030-inch crack for three maintenance intervals without a rapid fracture failure.

    The program was totally successful and resulted in a disk design that was three pounds heavier than the Bill of Material (B/M) disk but had over ten times the B/M life even with a 0.030-inch crack in the bolthole and a 0.020 inch elox crack starter in the rim slot. (Continued)

DD FORM 1473   EDITION OF 1 NOV 65 IS OBSOLETE

20. Abstract *(Continued)*

-- Included in this report are the design criteria and rationale used in creation of the damage tolerant configuration, the testing and analysis methodology, and results as well as recommendations for application and improvements.

DD FORM 1 JAN 73 1473 EDITION OF 1 NOV 65 IS OBSOLETE

CONTENTS

CONTENTS (Continued)

ILLUSTRATIONS

ILLUSTRATIONS (Continued)

ILLUSTRATIONS (Continued)

ILLUSTRATIONS (Continued)

TABLES

GLOSSARY

English Symbols

2a	Crack surface length
A	Area
da/dN	Crack growth rate
f	Frequency, hz
K_{IC}	Value of stress intensity factor at onset of rapid fracture
K_t	Stress concentration factor
N	Engine speed in revolutions per minute
R	Ratio of min. stress to max stress
RT	Room temperature
S	Von Mises equivalent stress
T	Temperature in degrees Fahrenheit

Greek Symbols

δradius	A small change in radial position
Δa	Small crack extension
ΔK_{TH}	Level of stress intensity change marking the onset of crack growth by high frequency fatigue action
2σ	Two standard deviations
σ	Stress in general
σm	Mean stress of a range of stress
$\Delta\sigma$R	A small schange in stress range
σTavg	Average tangential stress
σvib	Peak to peak vibratory stress

Acronyms and Abbreviations:

A/B   Afterburner

A/P   Actual divided by predicted

AMT   Accelerated mission test

Aug   Augmentor

BHOD   Bolthole outside diameter

B/M   Bill of material

conc   Concentrated

cpm   Cycles per minute

3D   Modeled for finite element analysis using all three
            dimensions rather than representation by a plane section

DSINH   Upper and lower hyperbolic sine curve halves joined at a
            common inflection point

EHR   Events history recorder

F/M   Fracture mechanics

°F   Degrees Fahrenheit

HZ   Cyclic rate in cycles per second

LCC   Life cycle cost

Mil   Military

Mils   Measurement in thousandths of an inch

MTBF   Mean time between failures

MUF   Materials utilization factor

NDE   Non-destructive evaluation

N_{prop} Remaining life in cycles of crack propagation

OP Range   Operating range

PWA 99-1   Defined on page 77

SECTION I
SUMMARY

Milestones for the two-phase, 42-month program to Develop, Refine, a; i Evaluate a Damage Tolerant Design System for Turbine Engine Cold Section Disks were successfully met. The program overview is shown in figure 1. Major milestones included:

o   Provision of a preliminary military specification for engine damage tolerance requirements

o   Development of a damage tolerant design system

o   Selection of a current engine disk to demonstrate application and provide a study for design system refinement

o   Selection of a simplified mission to be used to test the damage-tolerant redesign and simulate effects of aircraft missions on cold section disks

o   Procurement of six disk forgings and manufacture of three damage-tolerant disks

o   Characterization of test-hardware material including development of a negative R-ratio material crack growth model

o   Design and approval of a functional-replacement damage-tolerant disk with acceptable Life Cycle Cost payoff

o   Bolthole specimen component life demonstration

o   Disk spin treatment and subsequent ferris wheel life demonstration

o   Evaluation of application results and refinement of the damage tolerant design system

o   Preparation of reports and presentationr.

Task I - Design System Development

- Develop Damage Tolerant Design System For Cold Section (Fan or Compressor) Disks

Phase I

Task II - Engine Disk Selection and Design

- F100 2nd Stage
- Select Damage Tolerant Design For Fabrication Based On Design Matrix

Task III - Disk Fabrication

- Fabricate 3 Disks For Testing

Task IV - Disk Test and Design System Refinement

- Test 3 Disks In Ferris Wheel
- Refine Design System Based on Test Data

Phase II

Task V - Test Hardware Material Characterization and Selection

- Flaw Growth Model Data For Task II

Task VII - Supplementary Material Characterization and Subcomponent Tests

- Negative R-Ratio Flaw Growth Specimens
- Bolthole Verification Specimens

FD 117771A

Figure 1. Program Overview

2

Development of the design system included writing a preliminary Military Specification for Engine Damage Tolerance Requirements (see Appendix A), devising a logical approach to implementing those requirements, assembling a set of computer programs capable of performing the analyses, and constructing a mathematical model of Ti-6Al-4V crack propagation behavior. Refinements to the system were made as required during component demonstration testing to improve predicted vs observed test results.

Engine disk selection involved identifying an engine whose duty cycle is complex, diverse, and well-known, selecting from this engine a cold section disk whose operating environment is well-known, and analyzing the missions in sufficient detail to identify an engine duty cycle and equivalent damage cycles to be employed for test evaluation of a damage-tolerant redesigned disk. The F100 2nd-stage fan disk, used in both the F-15 and F-16 fighters, was selected for this program. The F100 duty cycle is known, as well as its operating environment. In addition, a baseline for this disk had been previously established in Air Force Contract F33615-75-C-2063.

Titanium (Ti-6Al-4V) was selected as the material for this program because of its desirable fracture toughness properties, and the fact that its crack propagation characteristics were well defined, thus requiring only minimal specimen tests to quantify the particular disk heat code within the material's defined scatter band. Using an existing data base for Ti-6Al-4V, an interpolative da/dN vs ΔK model was developed based on the hyperbolic sine and modeling procedures developed during a previous Air Force contract AFML F33615-75-C-5097.

Material was procured from one heat of Ti-6Al-4V in the form of disk forgings sufficient to provide for specimen testing and fabrication of three damage-tolerant design disks as provided in Contract Modification P00003.

Test hardware material characterization involved testing crack propagation specimens taken from one of the purchased disk forgings. Some crack propagation testing was performed to duplicate information

3

in the existing Ti-6Al-4V data base, and some additional testing was performed supplementing the data base. The new data, which duplicated existing data, confirmed that the material purchased for the program is typical Ti-6Al-4V, and that the behavior model constructed using the data base is applicable to the program with minor refinements. The new data that supplemented the data base was used to refine the model in the low stress intensity range where the existing data base was inadequate.

Engine disk design evaluations of four candidate configurations involved completing the matrix shown in figure 2. This matrix evaluation included Life-Cycle-Cost studies and the program goal of providing candidate disks with the capability to live for a minimum of three overhaul periods after initiating a 0.030" surface length crack. Two categories of disk designs comprised the Design Candidate Matrix: designs involving Ti-6Al-4V, which were candidates for fabrication and test, and designs involving materials rejected in the preliminary process of material selection. Inclusion of the latter material comparisons provided additional data substantiating the prior selection of Ti-6Al-4V as a prime damage-tolerant material.

The disk damage tolerant design (DTD) configuration was selected and approved by the Air Force project engineer, Mr. Richard J. Hill (AFAPL, Wright-Patterson Air Force Base), and three DTD disks were fabricated for testing. An additional specimen testing phase (Task VII), prior to disk testing, was added to the program to verify analytically predicted crack propagation life improvements resulting from the planned $500^{\circ}F$ prespin disk treatment. This was successfully accomplished using laboratory-controlled bolthole specimens. From these tests, the need for a modification to the disk prespin treatment became evident and was incorporated in the prespin procedure. Mission cyclic testing of the fully treated DTD disk configuration successfully demonstrated improved crack propagation life to the extent that with 0.030-in. surface length cracks, 140 percent of the 4000 operating hours program life goal was achieved at the boltholes. In addition, active cracks could not be initiated in
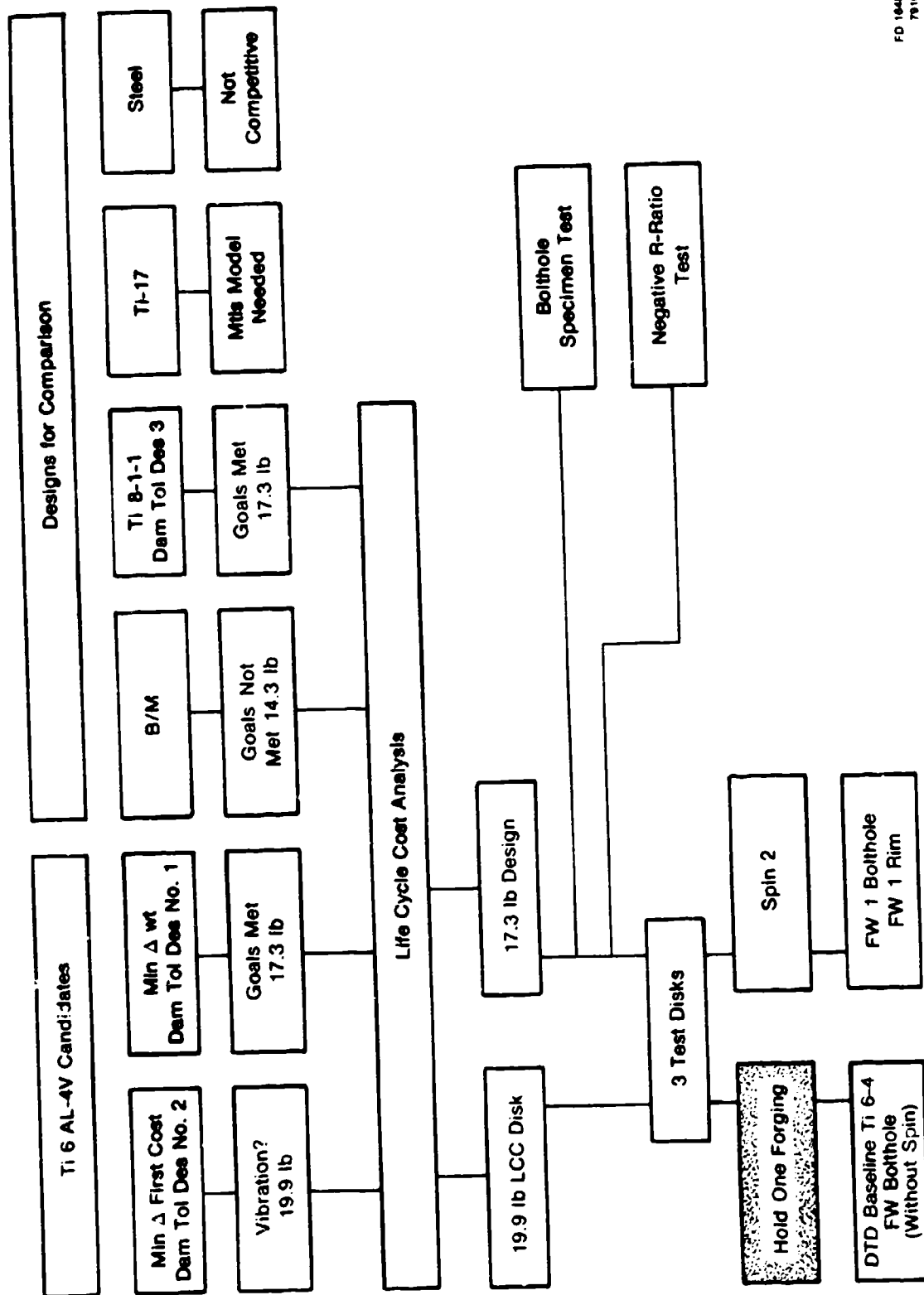
Figure 2. Design Candidate Matrix

rim slots from severe 0.020-in. surface length by 0.010-in. depth ELOX slots during 3500 sawtooth overload cycles, thus demonstrating substantial damage-tolerance capability in the rim.

During the course of applying the damage-tolerant design system and evaluating results, several refinements and an improved understanding of key issues were achieved. A brief summary is contained in Section IX, Conclusions and Recommendations, which follows the detailed discussion sections.

SECTION II

INTRODUCTION

A. BACKGROUND AND OBJECTIVES

Contract F33615-77-C-2064 was a two-phase, 42-month program, culminating with this final report. The overall objective of this program was to develop, refine, and evaluate a damage-tolerant design system for cold-section turbine engine disks. A damage-tolerant design system was successfully established and employed in the design of a functional replacement disk, and was then verified and refined by testing the disk with an induced flaw under accelerated mission cycles. The program goal was to demonstrate damage-tolerant disk design with the capability of operating with 0.030-in. surface length cracks for three overhaul periods.

Fundamental and basic to the damage-tolerant design system was the development of a quantitative design specification similar to MIL-A-8344 for allowable flaw size, shape, orientation, and location applicable to cold-section engine disk materials and design.

The contract was sponsored by the Air Force Aero Propulsion Laboratory, Air Force Systems Command, Wright-Patterson Air Force Base, Ohio, with Mr. Richard J. Hill as Project Engineer. The Pratt & Whitney Aircraft Group Government Products Division Program Manager was Mr. Charles E. Spaeth.

Brief descriptions of all the tasks accomplished under this contract follow.

B. PHASE I - DESIGN SYSTEM DEVELOPMENT (TASK I)

A design system approach was developed utilizing available advanced heat transfer methods, advanced finite element stress analysis techniques, and improved fracture mechanics life prediction techniques to produce damage-tolerant disk designs.

A preliminary military specification, "Damage Tolerance Requirements For Cold Section Turbine Engine Disks", has been written in a manner that closely parallels MIL-A-8344, "Military Specification - Airplane Damage Tolerance Requirements. Embodied in this document are both design criteria and design goals. The design criteria consider flaws in both smooth and notched portions of the disk. In smooth portions the flaws are assumed to be naturally occurring intrinsic defects whose size and orientation have been characterized by the contractor. In notched regions the defects are assumed to have a surface length of 0.030 in. and to be located and oriented as experience with propagating low cycle fatigue cracks would suggest. The design goal was to provide disk designs in which cracks of this nature will not propagate to failure in three overhaul periods, as defined by current usage.

A methodology was developed which is capable of implementing these design criteria and goals by means of a damage integration package. The damage integration package provides a step-by-step design procedure which, when followed to completion, evaluates a disk design relative to its meeting the design goal of tolerating 0.030-in. surface length cracks for three overhaul periods. This is accomplished by collecting all itemized inputs and processing them in proper order through appropriate computer programs.

The integration package interrelates the following:

a. Criteria

b. Initial flaw characteristics

c. Engine duty cycle

d. Material crack growth model

e. Stress intensity factor prediction and crack growth algorithm methods

f. Cumulative damage prediction model

g. Cracked disk residual strength requirements.

8

C.   PHASE II - DESIGN SYSTEM VERIFICATION (TASK II THROUGH VII)

In Phase II the design system was evaluated experimentally. Three functional replacement damage-tolerant design cold section fan disks for the F100 engine were subjected to ferris wheel accelerated mission cycles equivalent to those encountered in the F-15 application.

Phase II consists of five major tasks:

1.   Task II   -   Engine disk selection and design

2.   Task III   -   Disk fabrication

3.   Task IV   -   Disk test and design system refinement

4.   Task V   -   Test-hardware materials characterization and selection

5.   Task VII   -   Supplementary material characterization and subcomponent tests.

1.   Task II - Engine Disk Selection and Design

The disk selected for damage-tolerant design was the F100 engine 2nd-stage fan. The F100 engine is used in the F-15 and F-16 aircraft, and has a well-defined duty cycle. Furthermore, its environment is well-known, and a baseline for this disk had been established in research work under Air Force Contract F33615-75-C-2063, "Structural Life Prediction and Analysis Technology".

Utilizing the design system created in Phase I, analytical disk designs were developed which investigated the individual and synergistic effects of flaw size, shape, orientation, location and material data scatter on the disk life within the design constraints. For the purpose of design comparison, a design matrix was developed. The matrix included life (all failure modes applicable), material type, component cost (recurring and nonrecurring),ease of assembly, stress level, inspectability, weight (component and mating hardware), and engine compatibility. Additionally, the matrix elements were

9

weighted to indicate impact on the total engine according to P&WA's experience with production hardware. A recommendation to the Air Force was made concerning the design to be carried forward through actual testing. The Air Force project engineer reviewed the designs developed by the contractor and approved the recommended design. The criteria for design choice was an interpretation of the created matrix in terms of program goals and cost.

2. Task III - Disk Fabrication

Three damage-tolerant disks were manufactured using Ti-6Al-4V alloy and are functional replacements for the F100 2nd-stage fan disk. Detailed tracking of weight and cost was maintained during the manufacturing process.

3. Task IV - Disk Test and Design system Refinement

After fabrication was completed, two of the three Ti-6Al-4V damage-tolerant design disks underwent a one-cycle overload pre-spin to introduce residual stresses. The disks were accelerated to overspeed at $500^{\circ}F$ and held at this condition until sufficient local inelastic deformation occurred at the notches. The amount of inelastic deformation required to develop the proper residual stresses was determined in Task II. Local beneficial residual stresses occurred at the notches when the disks were unloaded (the large volume of elastic material surrounding the notch draws the inelastic-behaving local material into compression).

Following the overload prespin treatment, one disk was preflawed in 10 boltholes and one in 10 dovetail slots. Disk #1 was subsequently cycled in the ferris wheel under simple sawtooth loading to initiate cracking at the 10 elox preflaws, and to grow the cracks to a 0.030-in. surface length. When the nominal bolthole crack reached ≈ 0.030-in surface length, the disk was then cyclically tested to destruction using 574 simulated engine mission cycles at accelerated loading conditions.

10

Disk #2 which had been preflawed in 10 rim slots was sawtooth cycled to initiate and grow the elox damage to a 0.030-in. surface length crack. After 3500 load cycles there were no detectable initiated cracks from the elox starter slots. It was concluded that the disk had demonstrated substantial damage tolerance capability, and since the last 2000 load cycles were at the limit of the pull bars (significantly higher than engine loading), the test was discontinued to insure sufficient funds and pull bar life to complete the #3 disk test.

Disk #3 although of the same damage tolerant design configuration (ie, weight = 17.3 lb, Ti6-4) was not prespun to introduce the deep compressive residual stresses. Instead, this test provided a baseline disk which utilized a damage tolerant material, and a reduced nominal stress disk profile compared to the Bill of Material (B/M) F100 2nd fan disk manufactured from PWA 1216 (Ti 6-2-4-6). The disk was preflawed in 10 boltholes and sawtooth cycled to initiate and grow the cracks to the required 0.030-in. starting surface length. The disk was then mission cycled using the same accelerated test conditions as disk test #1, and the crack propagated to a near-critical final size of 0.20 in. (surface length) in 275 missions. The test was discontinued in order to save the disk for potential follow-on work to study crack growth behavior in the rim slots (along with disk #2).

A complete strain gage survey of each disk was performed prior to testing. The disk No. 1 ferris wheel test was monitored using advanced acoustic emission technology to detect crack growth. Acoustic emission monitoring was supplemented with eddy current and replication methods as required to correlate crack length with predicted crack growth. For disk tests No. 2 and 3, only replication methods were used in order to accelerate test time and minimize test costs.

Following the mission tests, representative locations from the disks were broken open and examined to determine final crack lengths and depths and variations in crack aspect ratios ($a/2c$ = crack depth/crack length).

11

Life results indicated that the prespin treatment yielded a 2X life improvement under accelerated life testing (which equates to 5X improvement under normal engine operating loads) and that the combination of prespin, material substitution, and 3 lb (21 percent) weight increase for reduced nominal stress was sufficient to achieve 140 percent of the 4000 engine operating hours life goal.

4. Task V - Test Hardware Material Characterization and Selection

The material P&WA chose to characterize for use in the damage-tolerant design (Task II) is Ti-6Al-4V. Three candidate materials that were considered are: (1) Ti-6Al-2Sn-4Zr-6Mo, (2) Ti-6Al-4V, and (3) IN 100.

Titanium was chosen since the engine disk selection is the 2nd-stage fan. Fan weight studies conducted during the F100 engine programs showed that weight penalities of up to 30 percent would be incurred when nickel- or iron-base alloys were substituted for the titanium disks. Of the candidate titanium alloys, Ti-6al-4V was chosen because of its desirable toughness and the fact that its advantageous fracture characteristics were already well defined and only a minimum number of specimen tests from the test disks heat code would be required.

5. Task VII - Supplementary Material Characterization and Subcomponent Tests

During the design system development (Phase I - Task I), the fact that cracks would be growing through regions where substantial residual compressive stresses exist, was recognized. From previous work with Ti-6-4, compressive stresses are known to contribute to and increase the crack growth rates for a constant level of maximum tensile stress. Therefore, this degree of (-) R-ratio degradation for various minimum compression and maximum tension stress levels had to be quantified. Bolthole specimen tests were used to exercise the crack growth model to demonstrate life prediction calibration.

Additionally, life results from the bolthole tests verified a significant life improvement due to the overload treatment; another test conclusion surfaced the fact that in Task II residuals had been overpredicted due to assuming minimum material properties. With this conclusion, the disk spin treatment was modified to utilize typical material properties and to define a higher spin speed (12,150 rpm). The design system was also modified to recognize needed changes as summarized in Section IX. These changes account for the allowable variation in material strength.

SECTION III
INITIAL ENGINE DISK DAMAGE TOLERANT DESIGN SYSTEM

A.   BACKGROUND

To date, gas turbine engine disks have been designed to a fatigue life limit, and therefore must be discarded when this limit is reached so that they do not jeopardize flight safety. It is generally accepted that any disk which fails by gross fragmentation is a hazard because the kinetic energy level in a disk is so high that means of containing large disk fragments are not available short of increasing engine casing weight beyond practical limits for aircraft use.

The task of identifying the safe service life of any particular disk has been complicated by: (1) scatter in low cycle fatigue life; (2) the difficulty of finding minute cracks nondestructively; and (3) uncertainty concerning the remaining life when a crack of a given size is present. Despite these difficulties, a very high level of flight safety has been achieved in the past by recognizing the scatter, determining the safe-life of the limiting members of the population, and avoiding the risk of rapid crack propagation by not operating populations of disks that might contain cracked individuals. The price paid for achieving flight safety in this way has been the cost of throwing away disks with substantial amounts of remaining life.

The development of fracture mechanics has brought significant progress in defining the useful life remaining in a disk that contains a crack. This development has created interest in a second design approach to achieving flight safety and possibly achieving cost benefits in the process. The approach is known as "retirement for cause" through the application of damage tolerant design. Since damage tolerant design practice has merit whether or not "retirement for cause" is associated with it, there is a need for a specification governing the application of fracture mechanics principles to the damage tolerant design of gas turbine disks.

15

B.   ENGINE DISK DAMAGE TOLERANCE REQUIREMENTS

A Preliminary Military Specification, "Engine Damage Tolerance Requirements", comprises Appendix A of this report. Damage tolerance requirements create the need for a methodology to provide designs that meet the requirements. The assemblage of experimental and analytical tools for accomplishing this comprises a Damage Integration Package.

C.   DISK DAMAGE INTEGRATION PACKAGE

The damage integration package provides a step-by-step design procedure which, when followed to completion, provides hardware capable of meeting the design goal of tolerating 0.030 in. surface length cracks for three overhaul periods. This is accomplished by collecting all itemized inputs and processing them in proper order through appropriate computer programs.

The integration package interrelates the following:

1.   Criteria
2.   Initial flaw characteristics
3.   Engine duty cycle
4.   Material crack growth model
5.   Stress intensity factor prediction methods
6.   Cumulative damage model
7.   Cracked disk residual strength requirements.

This concept is illustrated schematically in figure 3.

Discussion of the components of the package begins logically with criteria and the fact that all features of all disks need not be classified Safety of Flight Items.

D.   DISK DAMAGE TOLERANCE CRITERIA

A basic tenet underlying this specification is the conviction that its purpose is to legislate aircraft flight safety rather than to legislate the selection of design concepts or component replacement schemes.

16
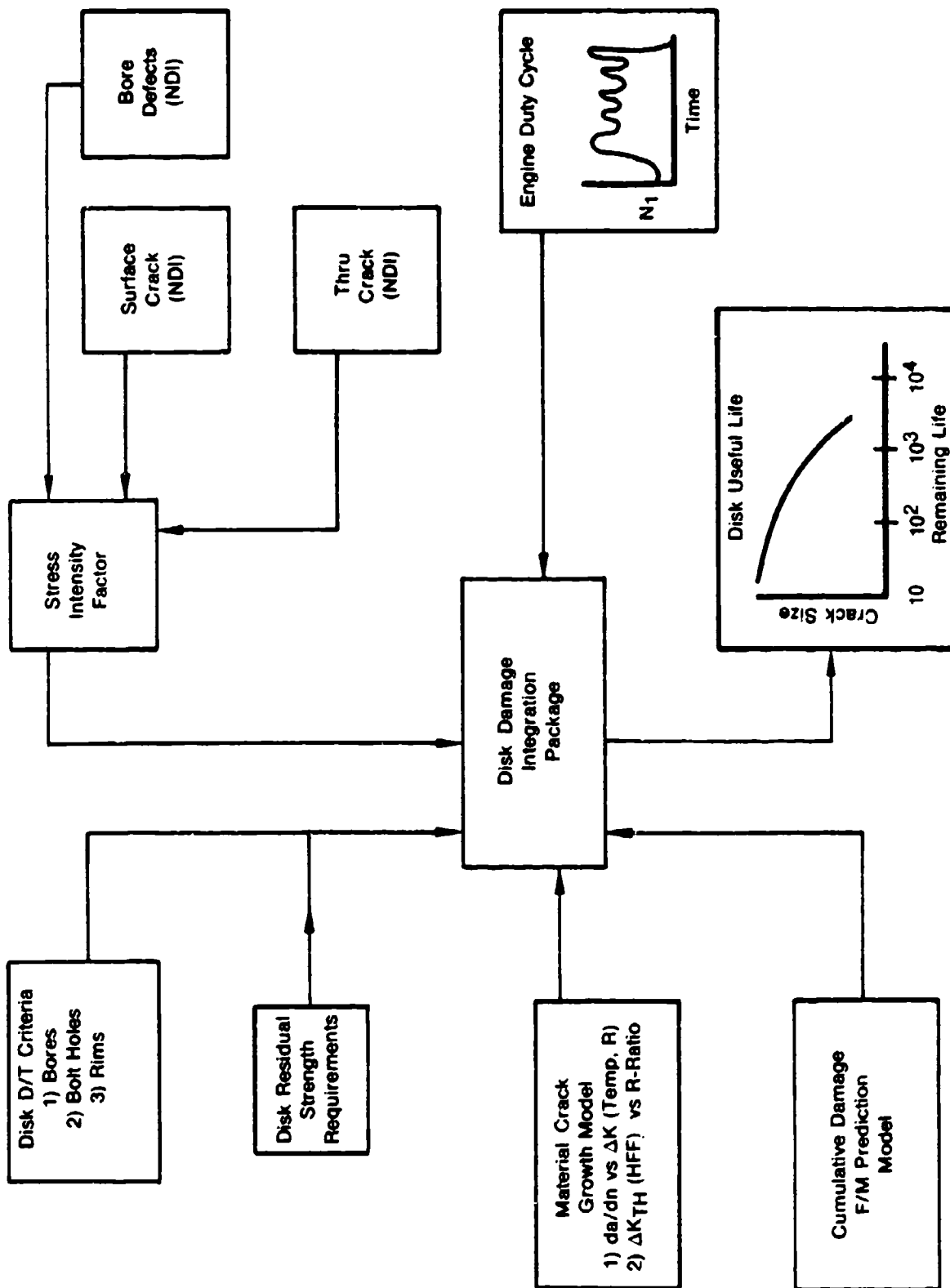
Figure 3. Damage Tolerant Design System.

Aircraft flight safety seems to be a proper subject for legislation while design concepts and component replacement schemes seem to be subjects for design optimization involving Life Cycle Cost analysis, among other criteria.

Of the available options that a designer might elect to investigate, only the damage tolerant option is covered in the specification prepared under this contract. The specification of requirements for aircraft flight safety under a "safe-life" option with statutory retirement should be the subject of another specification. Having specifications for both safe-life and damage tolerant design options would enable the designer to perform a comprehensive design optimization. This, in turn, would provide the design concept and retirement policy most advantageous to the Government.

When aircraft flight safety is recognized as the reason for the existence of damage tolerance requirements, it follows by definition that only safety of flight structures require that the highest levels of confidence be associated with the nondestructive inspection procedure. Under conditions where in-flight shutdown of an engine would not cause direct loss of the aircraft, engine structure would not be classified safety-of-flight structure as defined in the aircraft damage tolerant specification. The significance of classifying engine structures in this way relates to the difference in the non-destructive evaluation (NDE) requirements for the two classes of structure. NDE confidence requirements applicable to safety of flight structure might be beyond the state of the art, and thus might preclude use of "retirement-for-cause" entirely in engines for single engine aircraft, for example. On the other hand, in a multi-engine installation, "retirement-for-cause" might show a cost benefit in spite of occasional release of blades caused by a disk lug failure and the consequent in-flight shutdown. In summary, failure mode and effects analysis must be applied to engine disk components to avoid the safety-of-flight classification where it does not apply and opportunities for the application of "retirement-for-cause" could be created as a result.

18

Where the potential disk fatigue failure is such that safety of flight is involved, the "Preliminary Military Specification, Engine Damage Tolerance Requirements" serves to implement two contract goals; namely, flawed disk residual life and initial flaw size. The residual life goal is that a fatigue crack at a bolthole, rimslot, or other location shall have an expected safe life of three inspection intervals (overhaul periods, if these are defined for the weapons system). Initial flaw size goals are addressed in the section that follows.

E.   INITIAL FLAW CHARACTERISTICS

The design system must treat two categories of initial flaws: (1) surface cracks that occur in strain concentration regions such as boltholes and dovetail slots, and (2) subsurface cracks from inherent material defects that occur in smooth portions of the disk.

For the purpose of this program, the description of initial surface cracks at regions of strain concentration is established by the goals of the program as embodied in the Preliminary Military Specification, Engine Damage Tolerance Requirements. To illustrate, figure 4 has been extracted from the Specification which comprises Appendix A of this report. At location 1, as shown in this illustration a corner fatigue crack would be anticipated and the sum of the crack lengths as measured along the intersecting surfaces that form the corner would initially be 0.030 in. On the other hand, at location 3 a part-through surface crack would be anticipated and its initial surface length, as set by the goals of the program, would be assumed to be 0.030 in. The depth of this crack would be assumed to be 0.015 in. unless experience dictates otherwise.

The growth and instability of subsurface defects, such as voids, porosity, and inclusions can result in failures of disks. Improved processing and stricter quality controls must be enforced to reduce the probability of such failures. The majority of these defects occur in smooth disk sections sufficiently removed from free surfaces and stress gradient effects. The lives of these defects have been

19
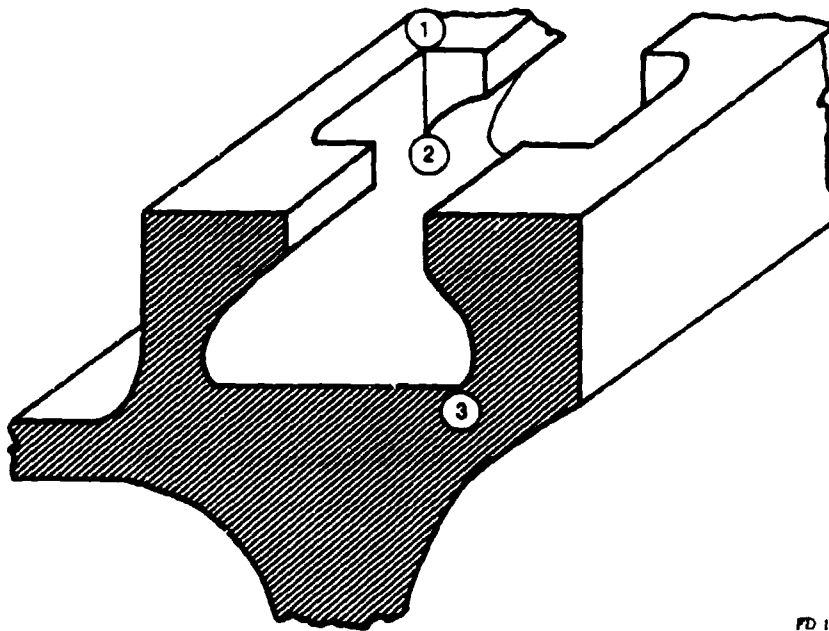
FD 124699

Figure 4. Illustrative Fatigue Crack Locations.

correlated to an equivalent area perpendicular to the disk tangential stress. Therefore, a buried flaw, circular in shape and oriented transverse to the maximum tangential stress, is to be assumed for the bulk of the disk.

Two approaches are recommended for defining initial buried flaw size requirements: (a) probabilistic methods for bore defect allowables (when data are available for material of concern), and (b) deterministic methods when only the NDE limits are known. The "probabilistic" approach recognizes that input data such as initial flaw size, defect orientation, and material da/dN are statistical in nature. This method defines the residual life for the population of disks in service through Monte Carlo techniques where sufficient passes through the simulator are made to insure that the predicted stress versus cycle curves can be plotted with respective mean and lower (2 or 3) bounds determined statistically. The "deterministic" approach assumes an initial flaw size at the inspection limit exists in each component and bases inspection intervals or other actions on

20

properties of the worst member of the population. The initial flaw
size and geometry requirements with their respective disk locations
are further defined in Appendix A, "Preliminary Military Specification
Engine Damage Tolerance Requirements."

The inherent defects and flaws common to the material and its
inspectability must be determined. Cleanliness of materials is
assessed by: (1) reviewing the ultrasonic inspection records to
determine the number of parts that fail to satisfy the acceptance
standard and the size and location of each of the unacceptable
defects; (2) sectioning of reviewed parts to establish the shape,
orientation, and composition of the defects; and (3) cycling of
fatigue specimens removed from disk bores and post-failure
fractographic evaluation to determine the characteristics of flaws
smaller than the acceptance standard. These studies result in a flaw
distribution curve similar to that shown in figure 5, which relates
the fracture plane area of the flaw to the probability of occurrence
in a disk bore of a given volume.

FD 146403
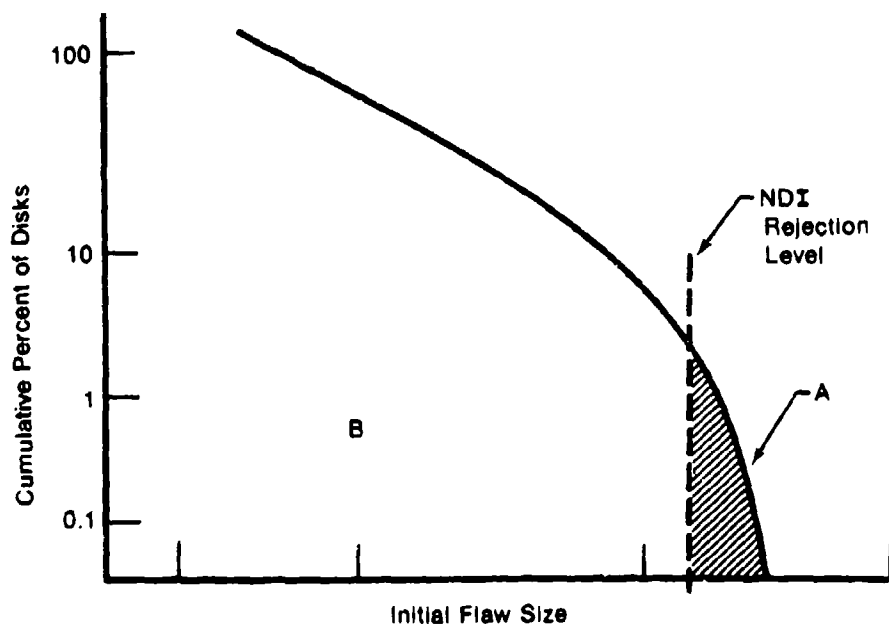
Figure 5. Flaw Distribution Curve for Disks.

21

The fracture plane areas greater than the rejection level, region A, are obtained from review of ultrasonic inspection records. Information for the probabilistic approach, fracture plane areas less than the rejection level, region B, requires extensive material evaluation and specimen testing.

Once the initial flaw description has been established, consideration must be given to the cyclic loading which will propagate the crack.

F.   ENGINE DUTY CYCLE

Duty cycles (figures 6 and 7) have been developed which define equivalent damage simulation based on extensive surveys of F100 operations in the F-15 aircraft and of the TF30 operations in several operational aircraft. The damage simulation profiles, as a function of percent of maximum N_1 rpm versus time, are available and presented in figure 8. A breakdown of the individual subcycles within the missions, as well as a comparison of the test cycle with the actual flight cycles, has been determined and compared with current F100 usage to evaluate the relative number of subcycle events occurring in field service to the subcycles defined for a representative laboratory test. This work has been completed under Air Force Contract F33615-75-C-2063 and has been authorized for use in this contract. F100 duty cycle definition background will be found in Appendix B.

G.   MATERIAL CRACK GROWTH MODEL

A preliminary interpolative model for design configuration purposes was developed for analysis of fatigue crack propagation in Ti 6-4 (AMS 4928). These models provided added modeling flexibility relative to models developed in the following references:

1.   Annis, C.G., R.M. Wallace, and D.L. Sims, "An interpolative Model for Elevated Temperature Fatigue Crack Propagation," AFML-TR-76-176, Part 1 ,November 1976.

22
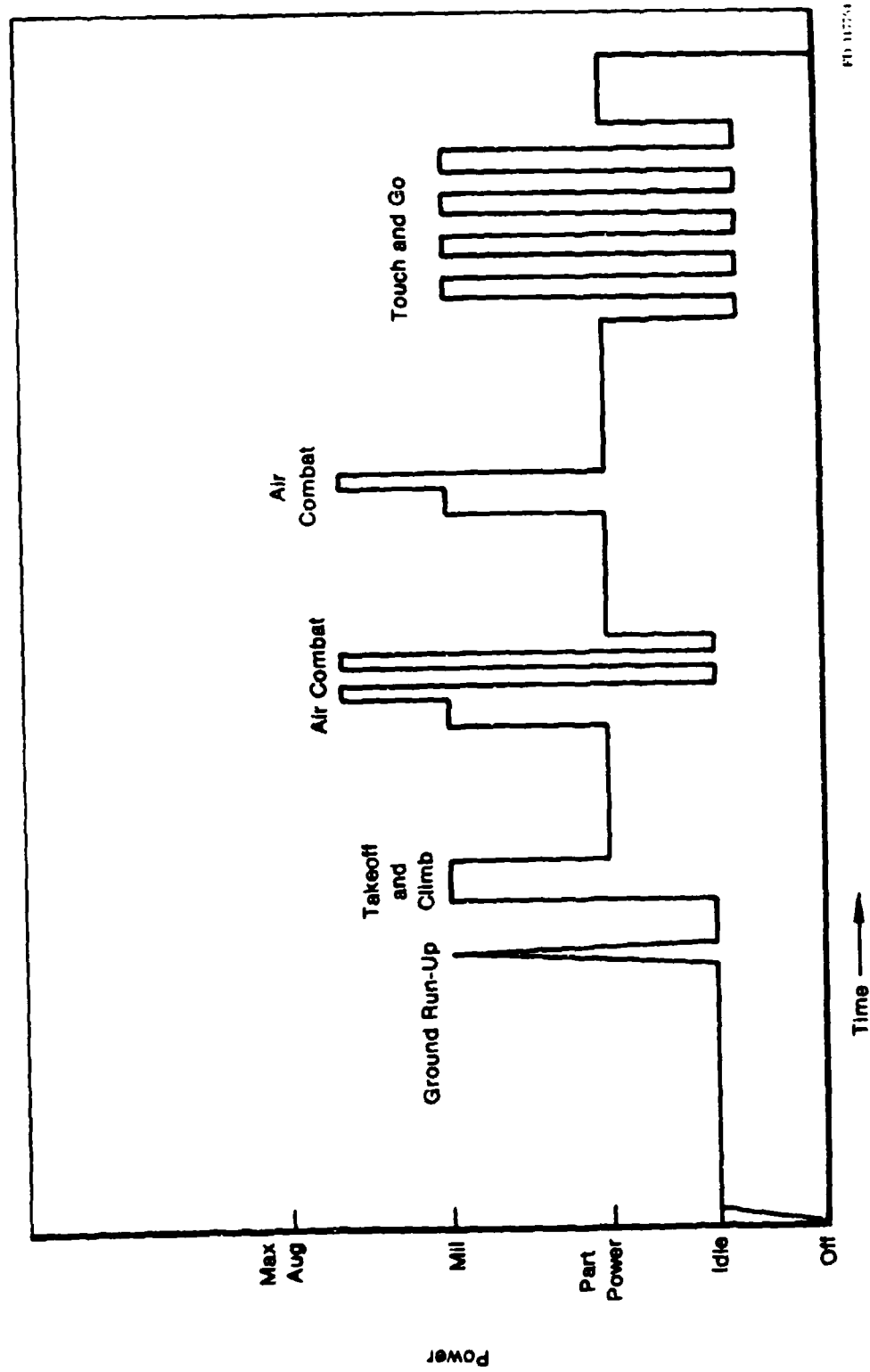
Figure 6. F100 Composite Duty Cycle.
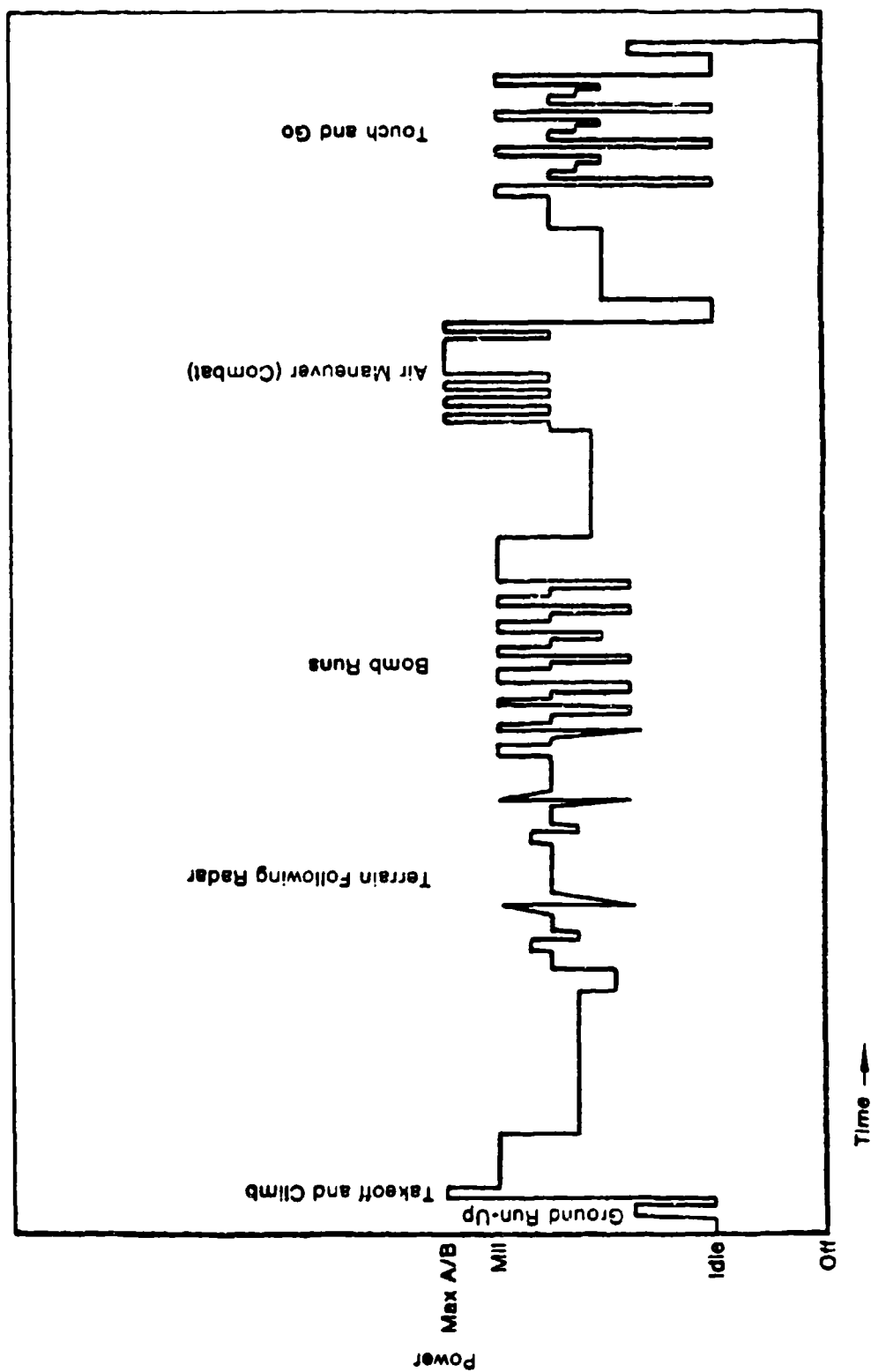
Figure 7. TF30 Composite Duty Cycle.

FD 212317

24
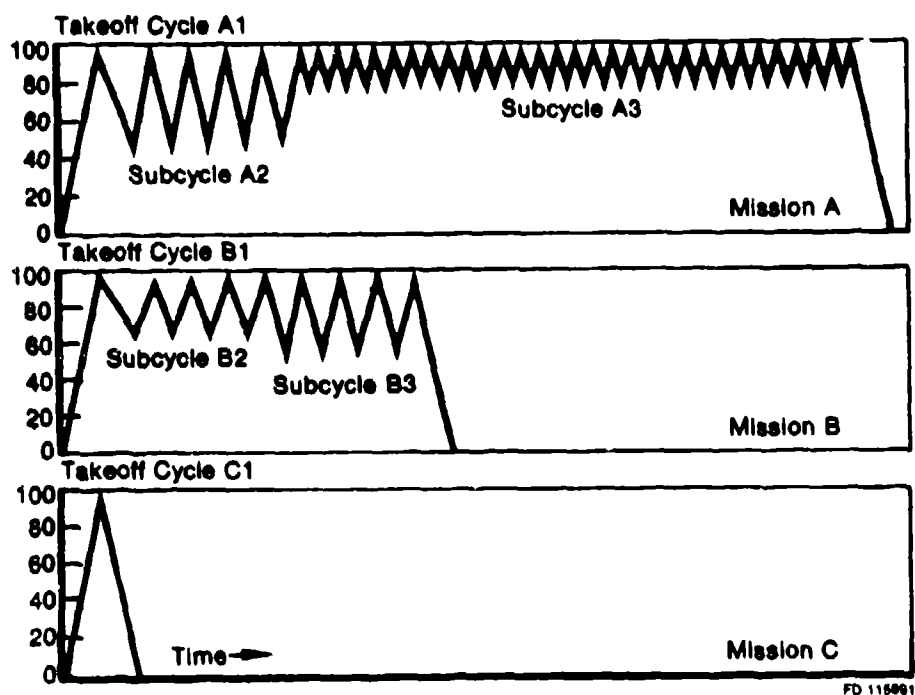
Figure 8. Equivalent Damage Cycle.

2. Wallace, R.M., C.G. Annis, and D.L. Sims, "Application of
   Fracture Mechanics at elevated Temperature," AFML-TR-76-176,
   Part II, April 1977

Two DSINH (Double Hyperbolic Sine) models describe room temperature
crack propagation rates, da/dN, as functions of the applied stress
intensity, K, and positive stress ratios for high (1-30 Hz) and low (10
cpm) frequencies (see figures 9, 10, and 11). A "DSINH" designation
specifies that the coefficients C_1 and C_2 above and below the
inflection points are different as will be discussed in Section VII-C
(Interpolative crack growth model development).

1. $da/dn = C_{1L} \sinh(C_{2L}(\log \Delta K' + C_3)) + C_4$ $\qquad$ ($\log \Delta K \leqslant 10|C_3|$)

2. $da/dn = C_{1U} \sinh(C_{2U}(\log \Delta K'' + C_3)) + C_4$ $\qquad$ ($|C_3| \leqslant \log \Delta K'' \leqslant$ toughness)
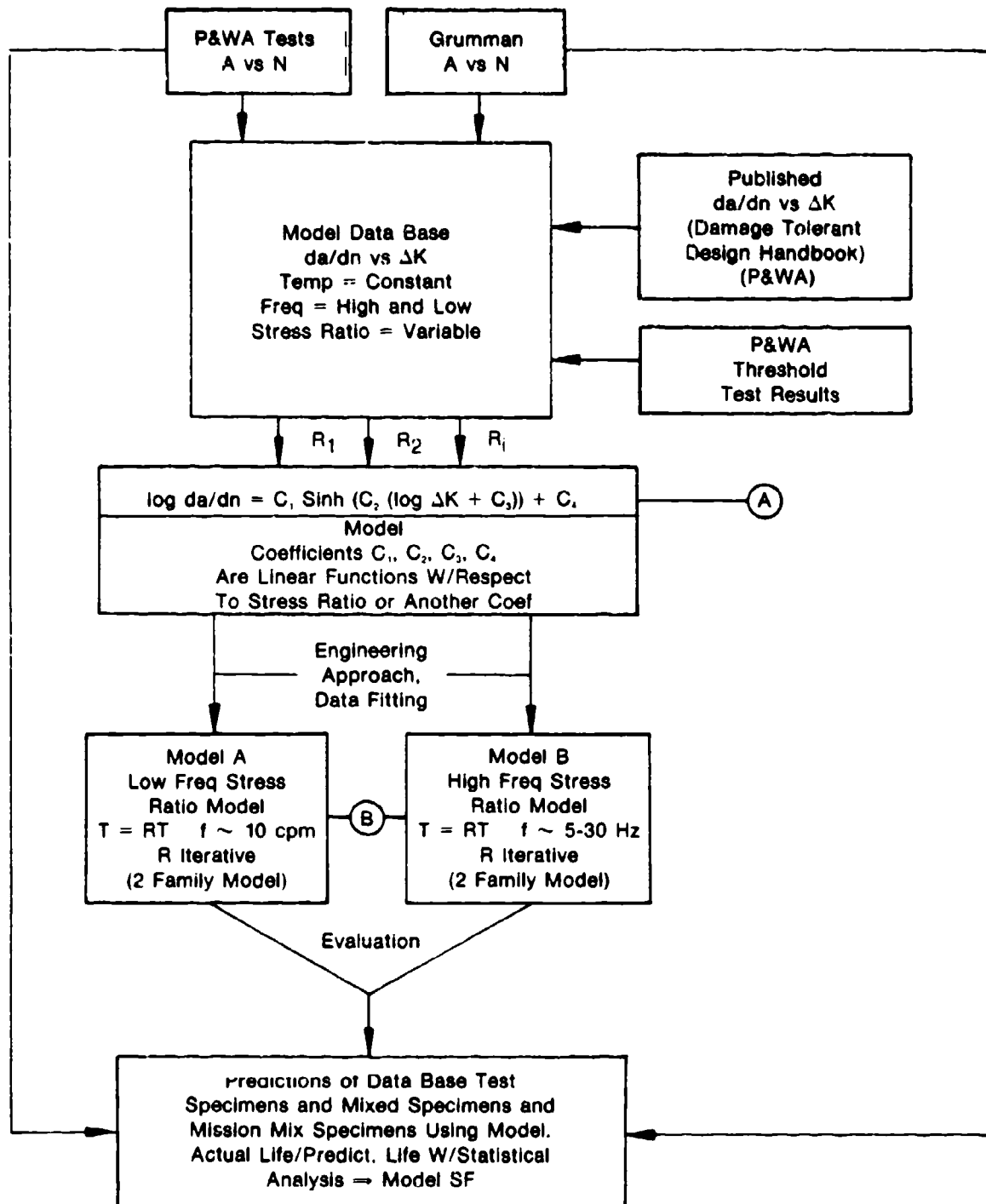
25

Figure 9.   Model Development Flow Chart.

FD 143525

ΔK, MN/m³ᐟ²

TI 6-4
Room Temp
High Frequency
Stress Ratio (R) Model

R = 0.1
R = 0.3
R = 0.5
R = 0.7
R = 0.9

da/dn, in/CYCLE

da/dn, mm/CYCLE

ΔK, KSI√in
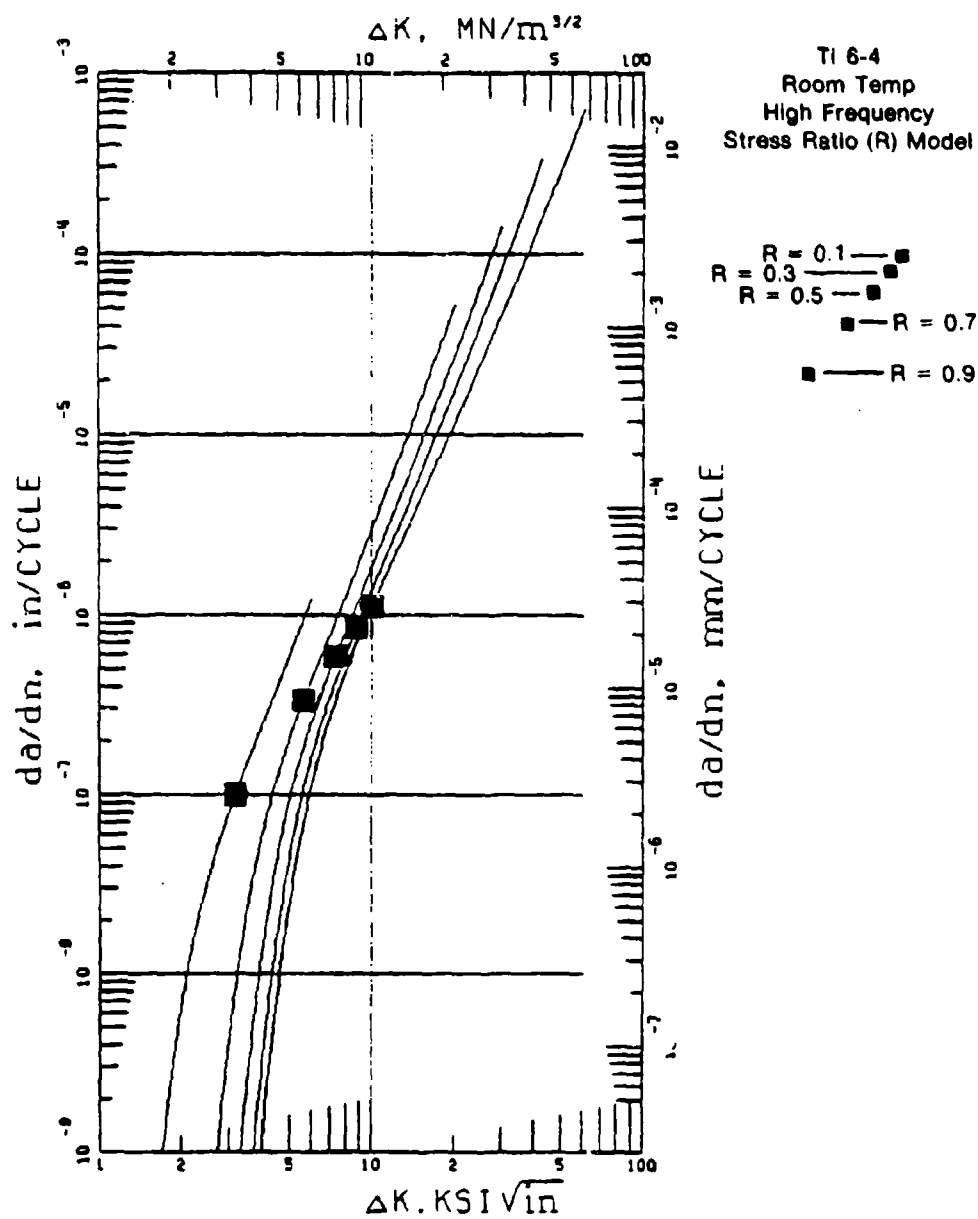
FD 141456

Figure 10.   High-Frequency Stress Ratio Model.
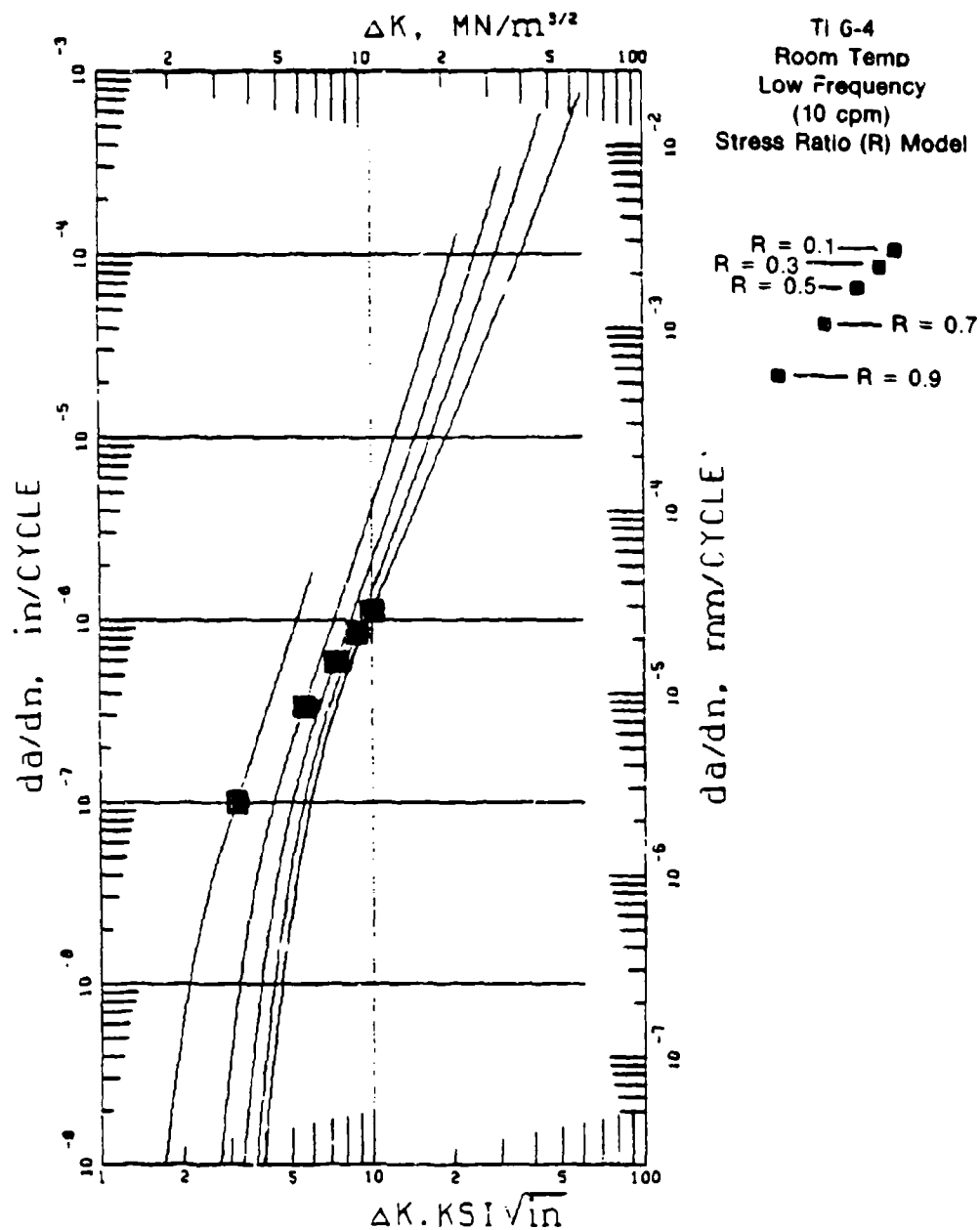
Figure 11. Low-Frequency (10 cpm) Stress Ratio Model.

28

The coefficients are linear functions of stress ratio or the other coefficients. The low- and high-frequency models share common inflection points (for a given R ratio) and share a common lower family. The models were developed from an existing data base to be applicable throughout the crack growth regime from threshold values of ΔK to values of K associated with rapid fracture. The existing data base with its respective modeled curves is shown in Appendix C. To evaluate the accuracy of the model, life predictions were performed for the test specimens used in the data base. The hypothetical crack growth "a" and corresponding cycle count "N" from the evaluations were compared to the actual specimen crack growth to ensure correlative growth shapes. Slight modifications were made to these models as a result of test-hardware material specimen testing.

H. STRESS INTENSITY FACTOR ANALYSIS

To successfully predict crack growth behavior in complicated disk geometries under cyclic stress, sophisticated crack tip stress intensity factor (K) prediction methods are required. K is the parameter which embodies the effect of the stress field, the crack size and shape, and the local structural geometry. P&WA recommends use of the influence function theory derived by J.R. Rice and H. F. Bueckner in life prediction algorithms for complex stress geometry combinations. Details of the theory and procedures for developing the appropriate influence functions are available in the literature and can be obtained in the following references:

1. Rice, J. R., "Some Remarks on Elastic Crack-Tip Stress Fields," Int. Journal of Solids Structures, 1972, Vol. 8, pp 751-758, Pergamon Press.

2. Bueckner, H. F., "A Novel Principle for the Computation of Stress Intensity Factors," Z. Agnew Math Mech 50, pp 526-546, (1970).

3. Bueckner, H. F., "Weight Functions for the Notched Bar," G. E. Report. No. 69-LS-45, pp 3-4, (1969).

4. Cruse, T. A., "Numerical Evaluation of Elastic Stress Intensity Factors by the Boundary-Integral Equation Method," The Surface Crack: Physical Problems and Computational Solutions, ed. J. L. Swedlow, ASME 1972.

5. Besuner, P. M., "Residual Life Estimates for Structures With Partial Thickness Cracks," Mechanics of Crack Growth, ASTM STP 590, ASTM, 1976, pp. 403-419.

6. Hayes, D. J., "A Practical Application of Bueckner's Formulation for Determining Stress Intensity Factors for Cracked Bodies," Int. Journal of Frac. Mechs. 8, No. 2, pp. 157-165, (June 1972).

Influence functions have been developed for the main problem types required for fracture mechanics analyses of engine components. For example, three-dimensional (3-D) part-through surface cracks have varying stress intensity levels along the crack front, and by use of the life prediction algorithm incorporating influence functions developed for 3-D surface or corner cracks in infinite thickness plates, the crack front can be allowed to grow and assume a new shape while reflecting local stress gradient influences on life. Life prediction algorithms for part-through crack geometries such as full or half-elliptical surface and corner cracks should be developed by contractors engaging in damage tolerant design of disks.

Through-crack geometries under symmetrical crack face (shear free) loading can be described with algorithms utilizing two-dimensional (2-D) influence functions. The algorithm in use at P&WA has the capability of addressing six variables in addition to initial crack size for life prediction calculations, see figure 12. Life prediction algorithms based on influence function theory have also been developed to analyze unequal length, through-thickness cracks emanating from opposite sides of the same hole.

P&WA recommends the use of life prediction algorithms using influence function theory for damage tolerant design. This method has the further advantage of reducing the calculation of K to three simple steps:

Parameters

a = Crack Length
x = Location Along Crack

Additional Variables

θ = Notch Angle
R = Notch Radius
L = Notch Length
q = Notch Height
H = Panel Height
W = Panel Width
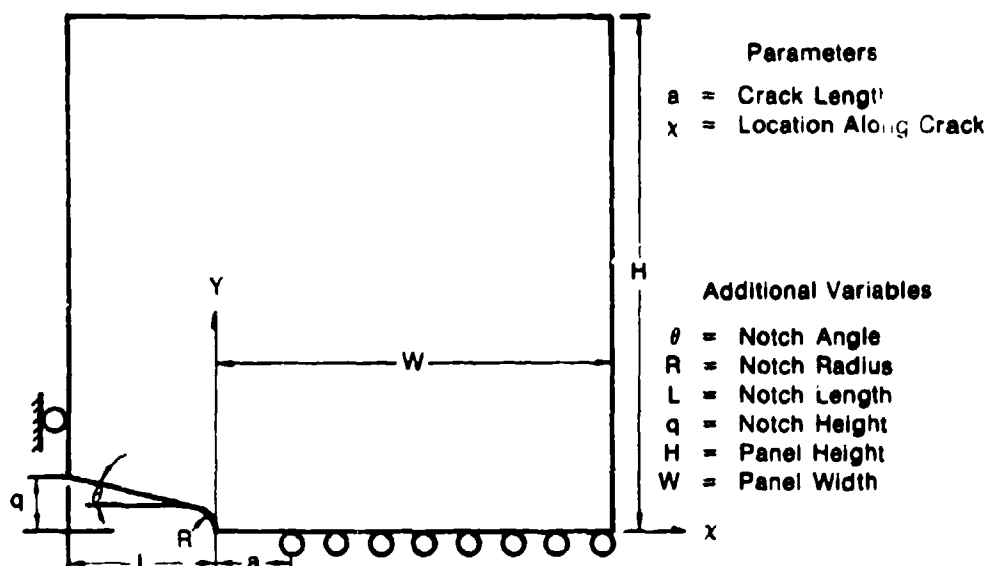
Figure 12. Through-Crack Surface Notch Model (Upper Half Only).

1. Model selection and specification of the problem geometry

2. Calculation of the "uncracked" stress field, defined as that stress in the uncracked solid area to be occupied by the crack

3. Numerical integration to determine K.

An accurate analysis and description of the component's "uncracked" state of stress, at applicable engine conditions, are required. The methods of the stress analyses may range from the stacking of simple 2-D elastic analyses to 3-D MARC plastic analyses in order to model the first order effects of the elasto-plastic material behavior. Although 3-D elasto-plastic analyses are within the current state of the art, due to their complexity and expense such analyses are presently not standard practice for disk stress analysis. However, the state of stress/strain at local concentration regions may be adequately determined using 2-D or 3-D elastic finite-element analyses. To account for local surface plasticity located at concentrated regions, a modified Neuber approach should be used to determine the controlling local surface inelastic stress and strain

31

values from the 2-D or 3-D elastic analyses. The following reference
is available: Neuber, H., "Theory of Stress Concentration for
Shear-Strained Prismatical Bodies with Arbitrary Nonlinear
Stress-Strain Law", Journal of Applied Mechanics, Transactions of The
ASME, December 1961, pp. 544 - 550. Extension of the Neuber method
should be applied to the distribution away from the surface until
calculated elastic stress levels converge to elastic values (i.e.,
below the proportional limit) while maintaining stress equilibrium.
This method of approximating plasticity effects has been substantiated
by evaluating specimen and component fatigue tests. These tests
reflect representative stress/strain concentration regions, i.e.,
boltholes, notches, etc.

The above crack growth life prediction tools and the initial flaw
size criteria must be employed in combination with appropriate damage
accumulation models.

I.   CUMULATIVE DAMAGE MODEL

The empirically derived elastic fracture mechanics correlation of
crack growth (da/dN) rate and crack tip stress intensity factor (K)
is numerically integrated to determine crack size as a function of
cyclic life. In basic form, the relation is:

$$N_{prop} = \int_{a_{initial}}^{a_{final}} \frac{da}{f(\ K,\ R,\ temp,\ freq)}$$

where the numerical integration of this expression will be performed
on a cycle by cycle basis to the defined engine duty cycle simulation.

The integration can be performed in a variety of ways provided
due regard is given to the particular load spectrum and its potential
for producting nonlinear crack growth response. An example of this
effect is the retardation of crack growth during cycles subsequent to
a cycle containing a significant overload. In this connection it is
said that the structure has a memory, since its response to cycle "n"

32

is influenced by the nature of previous cycles (n-1), (n-2), etc. The integration of spectra having this complication must be handled by cumulative damage models which incorporate retardation effects.

Models for crack growth retardation due to overloads are available in the literature for use where significant overloads do occur during operation. Some of the available models that are contained in the P&WA Fracture Mechanics life analysis decks as options are listed below:

1. Willenborg, R., R. M. Engle, and W. A. Wood, "A Crack Growth Retardation Model Using an Effective Stress Concept," AFFDL Tech. Memo 71-1-FBR, 1971.

2. Wheeler, O. E., "Spectrum Loading and Crack Growth," Journal of Basic Engineering, March 1972.

3. Lukas, P. and M. Klesnil, "Transient Effects in Fatigue Crack Propagation," Engineering Fracture Mechanics, Vol.8, No.4, 1976.

4. Gemma, A. E., and D. W. Snow, "Prediction of Fatigue Crack Growth Under Spectrum Loads," presented at the 11th National Symposium on Fracture Mechanics, June 12-14, 1978.

Many problems of practical interest are free of the memory complication and in these cases damage accumulation is said to take place linearly. A general description of Milton A. Minor's rule for linear cumulative damage fatigue is "that the fatigue damage incurred at a given stress level is proportional to the number of cycles at that stress level divided by the total number of cycles required to cause failure at the same level. This damage is usually referred to as the cumulative damage ratio. If the repeated loads are continued at the same level until failure occurs, the cumulative damage ratio should be equal to 1. When fatigue loading involves many levels of stress amplitude, the total damage is a sum of the different cumulative damage ratios and failure should still occur when the cumulative damage ratio sum equals one".

This damage-accumulation rule, where applicable, need not account for stress history (load interaction or load sequence) effects such as severe single overloads that are encountered in airframe structures. Cold secton engine disks have a relatively constant peak amplitude stress profile; therefore, P&WA utilizes this concept as the cumulative damage model for the Fracture Mechanics life prediction techniques. A fan disk load spectrum is shown in figure 8, Section III.F.

Disk residual lives can be predicted when crack growth rates have been determined and residual strength requirements have been established.

J.   RESIDUAL STRENGTH REQUIREMENTS (BURST MARGIN)

Crack propagation effects on residual strength capability must be considered. For disk design, residual strength requirements consist of having adequate burst margin against overspeeds.

A disk is initially designed to exhibit adequate burst margin in the flaw-free state. The relationship between crack size and overspeed capability must remain above safety margins for the entire disk service life. The residual strength (σ_{res}) requirements for disk safety are based on the more limiting of either a 5 percent margin at maximum overspeed rpm, or a 15 percent margin at maximum normal rpm.

The value of (σ_{res}) can be shown to monotonically decrease with increasing crack length by the following expression:

$$\sigma_{res} = \frac{K_{IC}}{f(a)}$$

where:

   K_{IC} = material fracture toughness
   a = instantaneous crack size

Therefore, referring to figure 13 to ensure adequate burst margin in a disk designed to damage tolerance, the design system must include residual strength effects, which will be done as a part of the design effort.

34
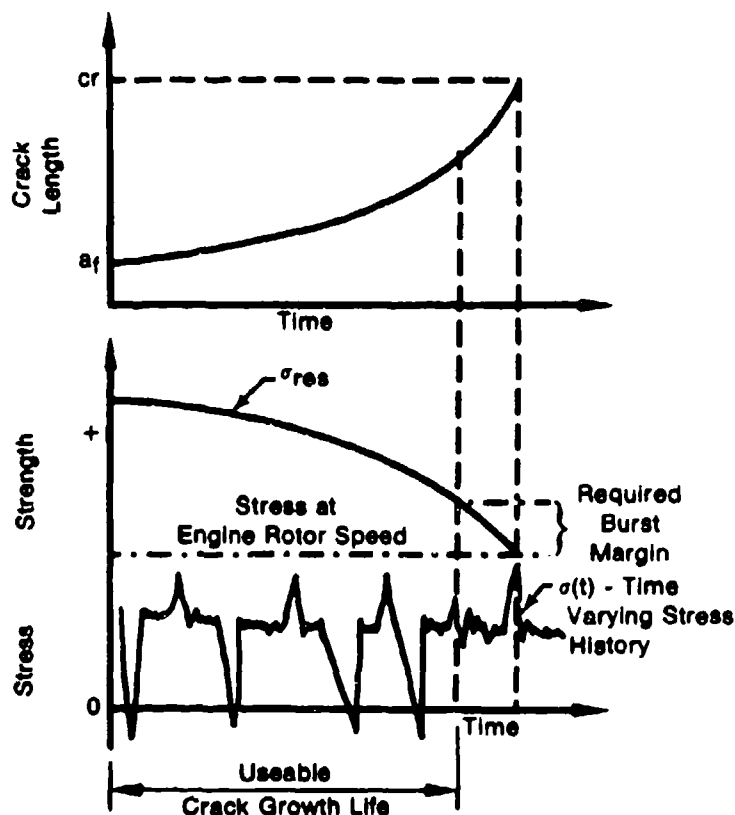
Figure 13. Effect of Crack Damage on Structural Integrity.

K.   RESIDUAL STRENGTH REQUIREMENTS (HIGH-FREQUENCY FATIGUE)

Vibratory-imposed loading from blades must be considered to prevent LCF-HFF interaction and accelerated crack growth rates. Pratt & Whitney Aircraft, in the normal material characterization process, develops high-frequency fatigue threshold ΔK_{TH} (HFF) versus R-ratio crack growth curves of the form shown in figure 14.

The normal progression relative to LCF-HFF interaction behavior is as follows: (1) LCF initiation occurs first followed by (2) low cycle fatigue crack propagation to the $K_{max\ allowable}$ (LCF) corresponding to the high-frequency fatigue threshold ΔK_{TH} (HFF) where, (3) accelerated crack growth rates begin, leading rapidly to critical conditions.

35

From ΔK_{TH} (HFF) vs R-ratio threshold curves and relations of the form,

$$\Delta K_{TH} \text{ (HFF)} = (1 - R) \text{ } K_{max \text{ allowable}}$$

$$R = \frac{\sigma_{steady} - \sigma_{vib}}{\sigma_{steady} + \sigma_{vib}} = \frac{\sigma_{min}}{\sigma_{max}} \text{ at blade-disk coupled frequencies,}$$

the low cycle fatigue maximum allowable stress intensity ($K_{max \text{ allow}}$) will be calculated. The calculated allowable K values are much smaller than those determined from the LCF-related fracture toughness (K_{IC}), and optimistic residual life predictions would result if LCF-HFF interaction is not considered.

36
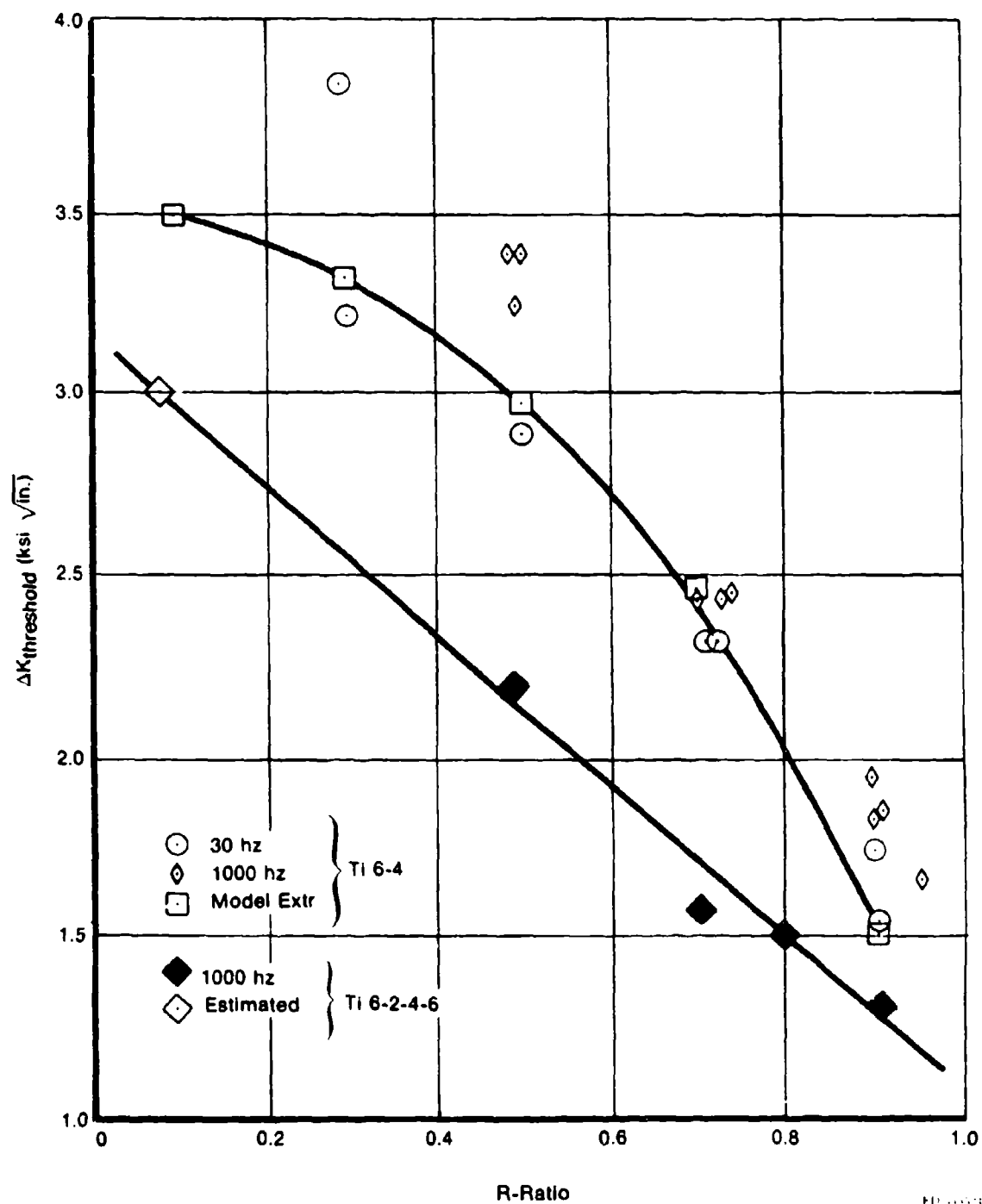
Figure 14. Crack Propagation Threshold Comparison,
Ti 6-4 and Ti-6-2-4-6 (B/M).

SECTION IV

TASK II - ENGINE DISK SELECTION AND DESIGN

A. ENGINE DISK SELECTION

The disk selected for damage tolerant design is the F100 engine 2nd-stage fan. The F100 engine is used in the F-15 and F-16 aircraft, and has a well-defined duty cycle. Further, its environment is well known and a baseline for this disk has been established in research work under Air Force Contract F33615-75-C-2063 "Structural Life Prediction and Analysis Technology".

B. MAJOR DISK DESIGN CONSIDERATONS

Shown in table 1 are the major considerations in the design of a fan or compressor rotor stage. The noteworthy difference in approach between the original F100 fan stage design and the redesign completed under this contract relates to the formation and propagation of cracks resulting from cyclic operation. Crack growth behavior was profoundly affected by the redesign process and will be discussed in depth. Other disk design attributes changed little or not at all and they will receive only passing mention.

Table 1. Major Disk Design Considerations

Original	Current
Yield	Yield
Burst	Burst
Creep	Creep
High Frequency Fatigue	High Frequency Fatigue
o Resonance	o Resonance
o Flutter	o Flutter
o Buffeting	o Buffeting
Low cycle Fatigue	Damage Tolerance

PRECEDING PAGE BLANK-NOT FILMED

C. DAMAGE TOLERANCE GOALS

The damage tolerant design effort had two paramount goals which were: (1) safe operation and (2) economical operation. Conceptually, safe operation of slow crack growth structure results when it is shown that the largest undetected crack-like defect remains subcritical in length throughout the operational interval between inspections. Schematically, this is shown in figure 15 which incorporates specific contractual goals in a graph of crack depth vs mission cycles and time.

The line segments represent the growth behavior of typically propagating cracks at critical locations in a disk bolthole or dovetail slots. The time required for this crack to attain critical length is known as the safety limit. Critical crack length in turbojet engine design practice is influenced not only by a transition from slow to rapid crack growth under normal mission cycle conditions, but also under two other conditions as spelled out in the "Preliminary Military Specification, Engine Damage Tolerance Requirements".
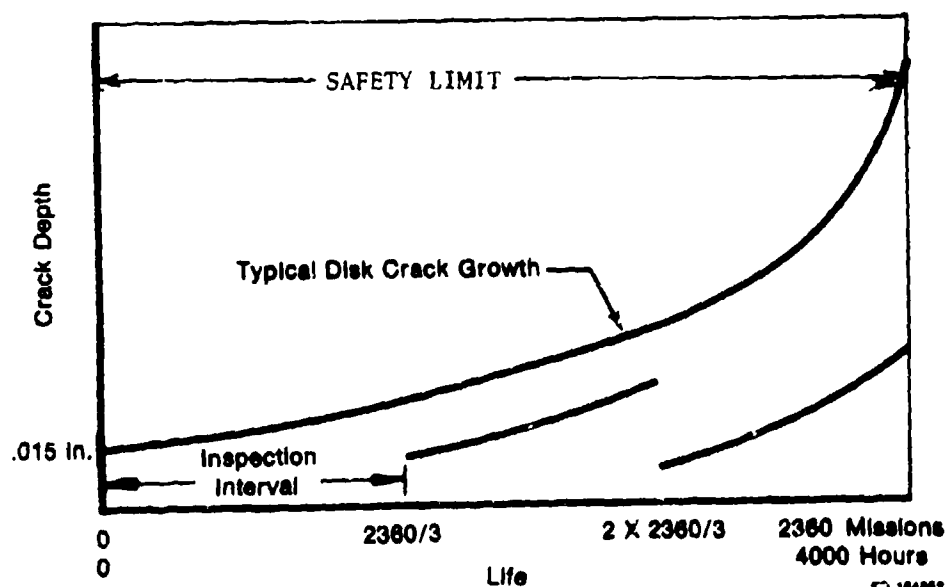
Figure 15. Damage Tolerant Design Inspection Interval Goal.

These other conditions involve momentary overspeeds, which occur infrequently, and high-frequency vibration at levels of vibratory stress in excess of the threshold level for cyclic crack growth. Both of these tend to shorten the safety limit to a degree that will be evaluated quantitatively in a later section.

A critical factor of the residual life analysis is the length assigned to the undetected flaw or crack. The contractually specified value of 0.030 in. surface length was used and the crack was assumed to be semicircular in shape, as specified in the contract. Since the line segments represent typical growth rates, rapidly growing cracks within the crack growth rate scatter band would reach critical length in a time shorter than the safety limit. Airframe damage tolerance practice allows a factor of two in crack growth time to assure safety with faster cyclic crack growth rates. A provision of the Engine Disk Damage Tolerant Design Contract requires use of a factor of three as an initial goal. Thus, figure 15 shows the safety limit partitioned into three inspection intervals.

Slow crack growth structure designed in accordance with this concept will prove reliable provided the means employed to determine the maximum defect size are sufficiently reliable. The rationale employed by the Air Force in selecting a flaw size of 0.030 in. surface length was without doubt to make detection exceedingly probable.

Economics is the principal driver of the inspection interval for obvious reasons. In this regard, the contractual requirement was to employ normal engine maintenance schedules as a guide in selecting the disk inspection interval. F100 fan section components do not have regularly scheduled overhauls as such. On the basis that TF30 engines are overhauled at intervals of 800 to 1200 hours, depending on the model, 1333 hours was selected as the inspection interval goal. Coincidentally, the safety limit under these ground rules becomes equal to the design life specified in the MIL Spec. E5007; namely, 4000 hours.

D. CRACK PROPAGATION DRIVERS

Equivalent damage cycles A, B, and C have been defined as described in Section III-F and as shown in figure 16. A mix consisting of prescribed percentages of these cycles will simulate all of the events, including their frequency of occurrence, that characterize the much more complex mix of actual missions. The subcycle ratios contained in the equivalent damage cycles are shown in figure 17 along with the subcycle ratio which characterizes F100 engine usage in the F-15 aircraft. From the graph it is apparent that a mix of cycles A, B, and C could be devised to have the same ratio of subcycles to major cycles as service and that mission B alone is very close to the desired result. For the purpose of comparative design studies it was deemed acceptable and cost effective to employ mission B alone rather than the mix.

The other potential cyclic crack driver is high-frequency vibration (Section III-K) which will be discussed in relation to figure 18, a Campbell Diagram. The results of dynamic strain measurements in an engine are plotted on this graph of vibration frequency vs fan rotor speed. The slightly curved line, which is nearly horizontal and passes through two data points labeled with dynamic stress levels, is characteristic of fan rotor vibration. At each of the crossings between the curved line and a member of the set of sloped straight lines, a condition of frequency coincidence occurs and results in resonant amplification of shaking forces. A feature worthy of note is that the resonant conditions recorded occurred below the normal operating range of the engine and this contributed to the success of the damage tolerant redesign effort. The indicated dynamic stress levels were measured at a point where gages could reasonably and conveniently be placed as opposed to the inaccessable locations where the potentially affected fatigue cracks are located. This difficulty was overcome by performing a dynamic stress analysis of the rotor assembly using a three-dimensional model of the bladed disk assembly complete with holes and slots. Stress ratios could then be

42
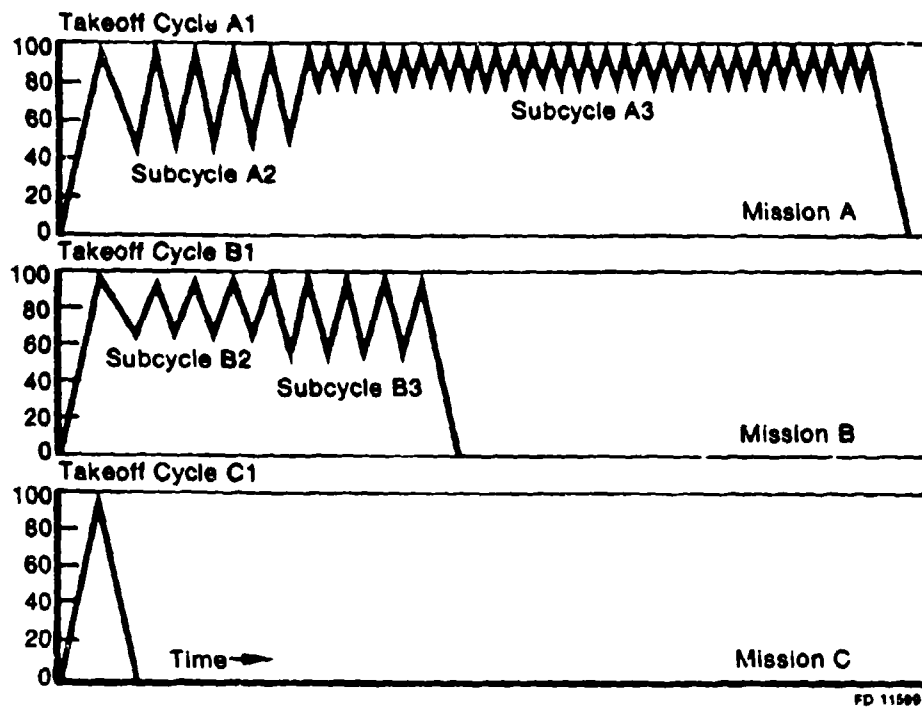
Figure 16. Equivalent Damage Cycles.
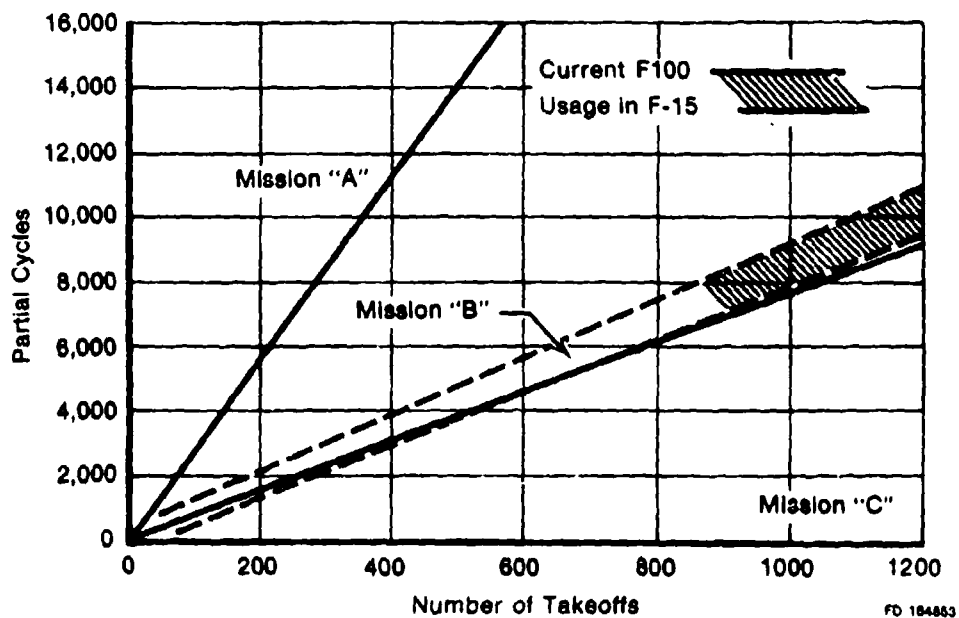
Figure 17. Mission Subcycles.

43
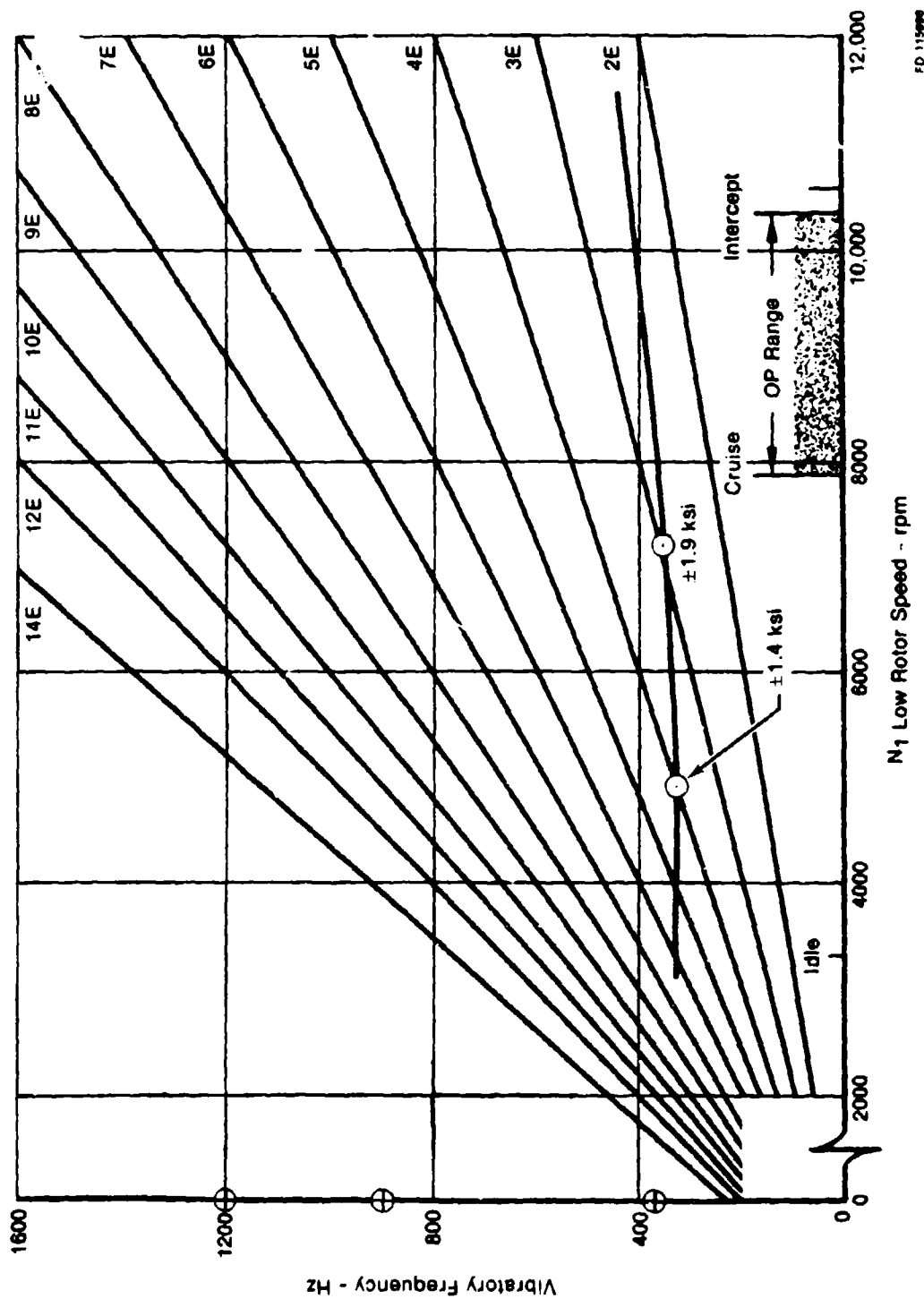
Figure 18. Fan Rotor 2 Campbell Diagram.

44

obtained to relate the vibratory stress at points of concern to the vibratory stress at the strain gage location. With this backgound on goals and drivers, the discussion can move on to the actual design approach.

E.   COMMENTS ON THE DESIGN APPROACH

The notion that a disk may contain a flaw large enough to be detected usin/ /equipment and techniques appropriate for maintenance activity and . (.emain noncritical for an amount of time equal to the original design lifetime inevitably raises the question of weight additions. The reader will note as he continues that material substitution, stress gradient management, or their combination were all insufficient to provide the level of tolerance established as a program goal. A disk designed on the principle that a crack must initiate and grow to reach detectable size is such an efficient structure that weight addition for damage tolerance became inevitable as a supplement to the other techniques that were employed. It is essential, therefore, that the reader understand the major implication of weight addition as a means of providing damage tolerance in engine disks as an across-the-board philosopy.

High thrust-to-weight ratio in the engine is an essential feature of the modern weapons system; hence, additions of weight that do not also provide additional thrust reduce the ability of the system to perform its mission. The investigation to be reported did not concern itself with deterioration in performance of an existing weapons system. Rather, the mission was considered to remain essentially unchanged and the entire weapons system was redesigned to assess the life cycle cost impact of applying a damage tolerant philosophy of engine disk design.

F.   MATERIAL SELECTION

The baseline disk, i.e., the F100 2nd Stage Fan, is Ti-6Al-2Sn-4Zr-6Mo, which was selected for its high strength and ability to resist crack initiation. Low-cycle fatigue, thrust-to-weight ratio, and the requirements of MIL Spec. 5007C were

selected as the primary drivers of the design. However, associated with this high strength capability are low fracture toughness property values in a temperature range from 80 to $200^{\circ}F$. The net result is a disk with minimal tolerance for crack-like defects at the 2nd-stage fan disk normal operating temperatures.

damage tolerant design process began, therefore, with a search for a substitute material which met two primary requirements. The material must be characterized by slow crack growth and high fracture toughness. Additionally, material was required which was adequately characterized with respect to a variety of fatigue and fracture properties. Slow crack growth behavior data were required covering a range of da/dN from 10^{-8} to 10^{-3} for a range of R ratios, temperatures and frequencies.

The tools required to quantify the residual life benefits attributable to substituting Ti6A14V for Ti6A12Sn4Zr6Mo are relative crack growth rates and values of K threshold. Figures 19 and 20 show two values of R ratio where cracks propagate much more slowly in Ti-6-4 than they do in Ti-6-2-4-6. Figure 21 reveals that the difference in stress intensity threshold between Ti6A14V and Ti6246 is least where one would like to see it greatest; namely, at high R ratio values (high steady stress, low vibratory stress). However, any amount of advantage in this factor taken in combination with slower crack growth and greater critical stress intensity makes Ti6A14 very attractive.

Total characterization and excellence in fracture properties dictated the selection of Ti-6A1-4V for use in the program.

Additionally, full characterization of yield, creep and rupture behavior was required for design purposes. Yield and creep data are required because of stringent limits on permanent growth which interferes with interchangeability. The rupture referred to in this design context is more than simply the ordinary ultimate strength. The characteristic referred to relates to disk burst margins and is a measure of the ability of the material to flow and redistribute localized stresses harmlessly in the event of a momentary engine

46
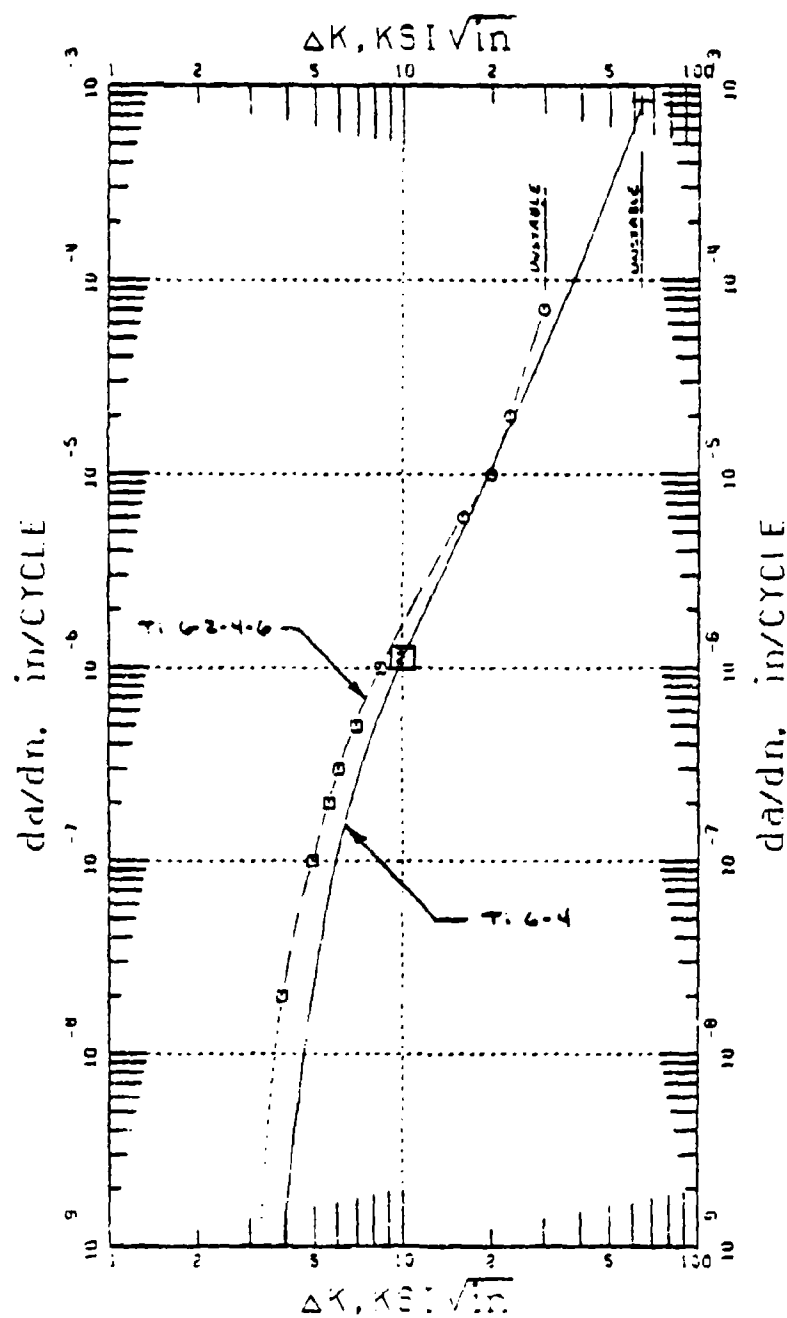
Figure 19. Crack Propagation Comparison of Ti 6-4
With Ti 6-2-4-6, R=0.1, Temp=RT.

47
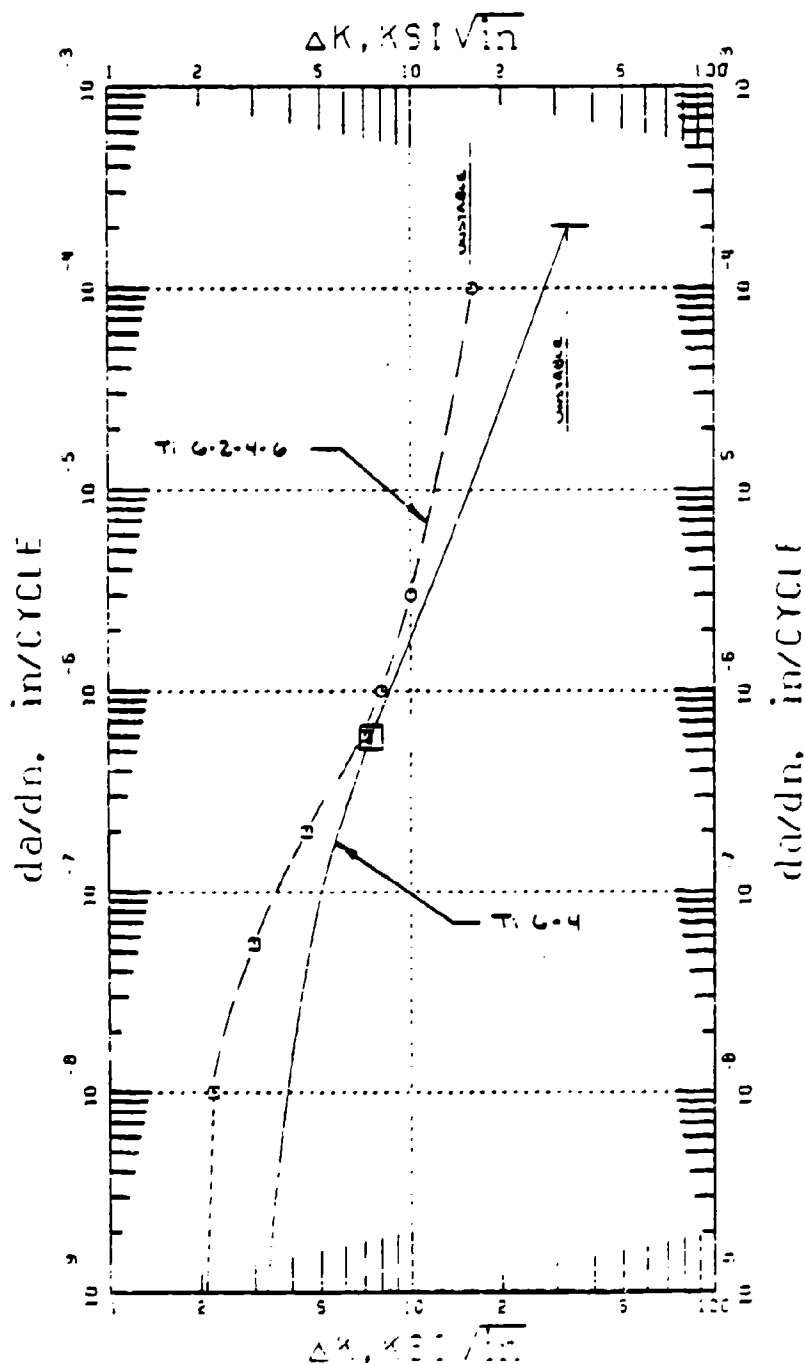
Figure 20. Crack Propagation Comparison of Ti 6-4 With Ti 6-2-4-6, R=0.5, Temp=RT.
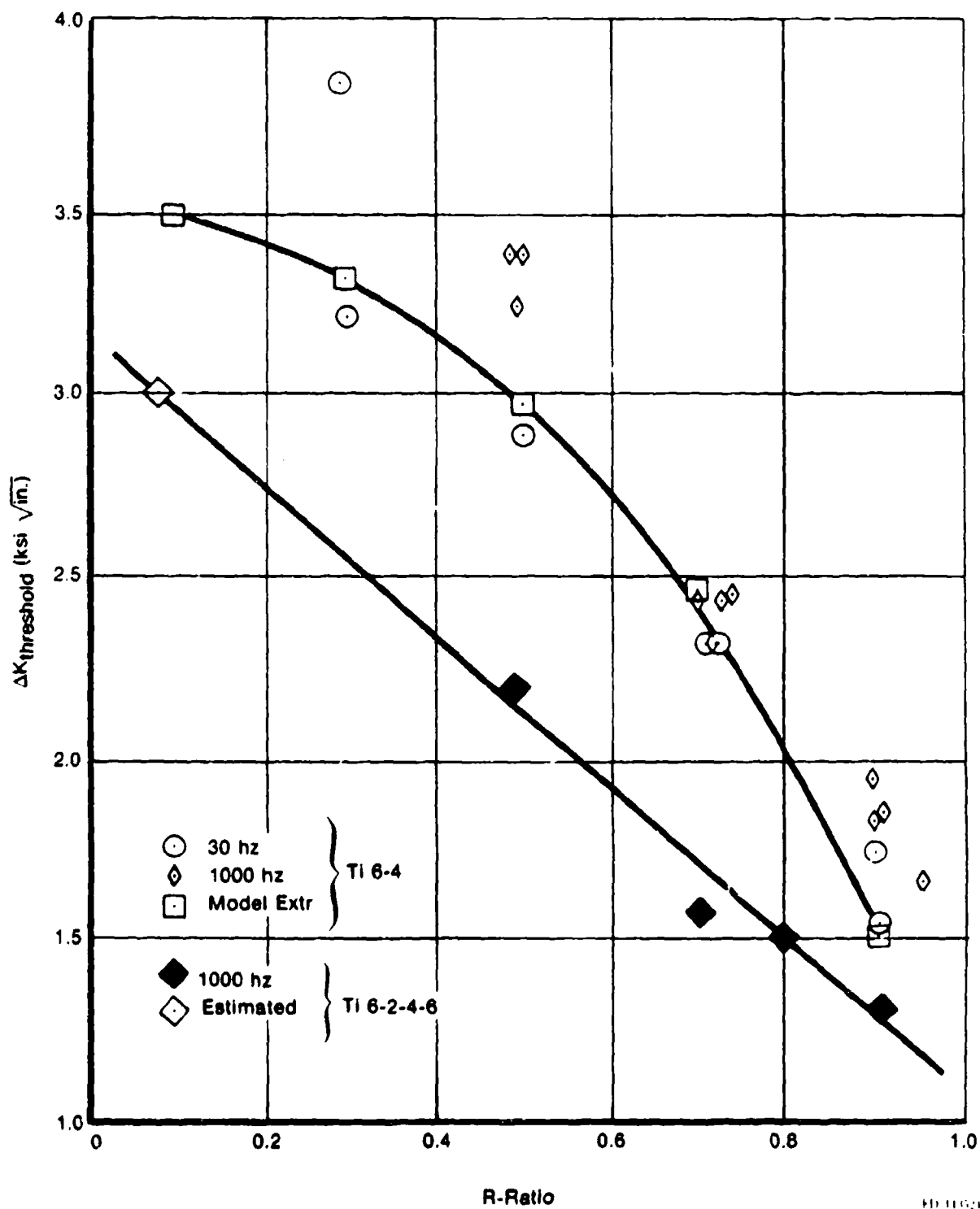
Figure 21. Crack Propagation Threshold Comparison, Ti 6-4
and Ti-6-2-4-6 (B/M).

overspeed condition. In the jet engine community, this property is evaluated by actually bursting several disks, determining for each disk the ultimate material strength and the average tangential stress at burst, and forming for each disk the ratio of the average tangential stress at burst to the ultimate strength of the particular piece of material that went into the disk. The several ratios are evaluated statistically and a material utilization factor (MUF) is determined. A high MUF is obviously an indication of excellence in freedom from initial flaws and high resistance to crack growth under monotonic loading conditions. Ti-6Al-4V exhibits the highest capability of any disk material evaluated by P&WA for this property.

G. STRESS GRADIENT MANAGEMENT

In terms of the goals of the Damage Tolerant Design contract, the greatest challenge is the management of crack growth within a few hundredths of an inch beneath the surface at a strain concentration feature such as the bolthole or the blade attachment features shown in figure 22. A flaw will propagate most rapidly if located at one of these features which magnifies load changes due to throttle movements and produces a large fluctuation in strain.
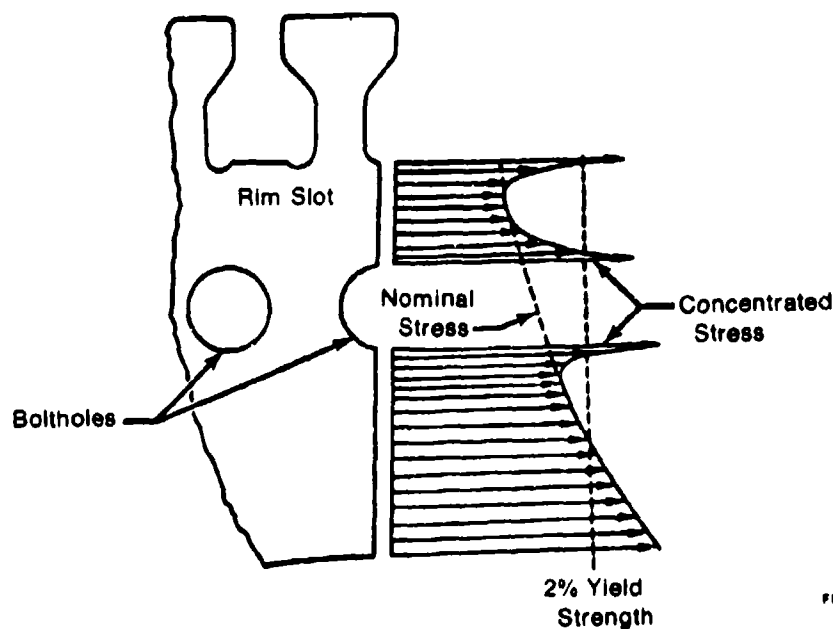
Figure 22. Stress Concentrations.

50

When the disk was designed originally, every effort was made to decrease the strain range because this is the essence of design for long life in low-cycle-fatigue. Consequently, when starting with a disk designed optimally for low-cycle fatigue, there is little the designer can do to further limit strain range short of lowering the nominal stress in the region where the notch feature is located. Since this can only be accomplished by the addition of weight, the designer has the obligation to exhaust other possibilities first. The localized stress at a notch is characterized not only by the stress range, but also by mean stress. In fracture mechanics terminology, ΔK and mean stress effects are reflected in R-ratio shifts to the crack growth (da/dN vs ΔK) curves. The ratio of minimum to maximum stress is referred to as R ratio. At stress concentrations, mean stress, and thus the R ratio, can be manipulated without adding weight whereas the local stress range reflects applied mechanical and thermal stress and cannot be changed apart from additional weight or geometry modifications.

The objective of mean stress relaxation and lowering the local R ratio without adding weight can be accomplished by creating controlled initial loading conditions wherein the material in the immediate vicinity of the notch will plastically deform in tension. Subsequently, when the applied loads are removed, a pattern of residual compressive stress remains. This is analogous to peening but more effective in combating crack growth. While peening is effective in retarding crack initiation, it is ineffective in retarding crack growth in many materials because of its shallow depth.

In order to study the effects of lowering surface stress levels on life, a simple computer simulation was made and a parametric life curve constructed. This curve reflected a 10 percent, 30 percent, and 50 percent decrease in surface stress and the benefit on life.

Growth of a part-through surface crack was simulated in a stress field characterized by a steep linear stress gradient. The effect of near-surface stress redistribution on residual life was approximated by a systematic stepwise reduction of this near-surface stress without

51

significantly changing nominal stress. Figure 23 schematically shows the procedure and the resulting crack depth vs cyclic life for a typical case. The observed effect on residual life has several implications.

1. Since one approach to damage tolerant design involves the introduction of surface compressive residual stress, these sensitivity study results (in conjunction with a MARC non-linear finite element analysis discussed in the following paragraphs) provided guidance in the effort to achieve the desired residual life enhancement.

2. These results provide insight to residual life enhancements that may be expected in other local inelastic stress regions where only elastic analyses are available due to cost and other factors. The approach in these areas will be to utilize the elastic analysis in conjunction with the Neuber analysis method. This more cost-effective technique has been shown to produce residual stress predictions with adequately good correlation to life results. Discussion follows.

Under normal engine operation, occasional overspeeds occur which result in local beneficial stress patterns being introduced at stress concentration features. However, since the material yield properties vary and one cannot depend upon a maximum overspeed to occur in every engine early in its lifetime prior to crack initiation, it is best to introduce the beneficial stress patterns consciously under controlled conditions rather than leaving the process to chance occurrence in the engine. This also provides the opportunity for assuring that adequate levels of beneficial residual stress are introduced.

For the purpose of the Damage Tolerant Design Program, the selected method for obtaining the beneficial residual stress and shift of R ratio at notch features is to place the disk in an evacuated spin pit and expose it to temperature and load conditions that will produce plastic flow and stress redistribution, while providing documentary

52
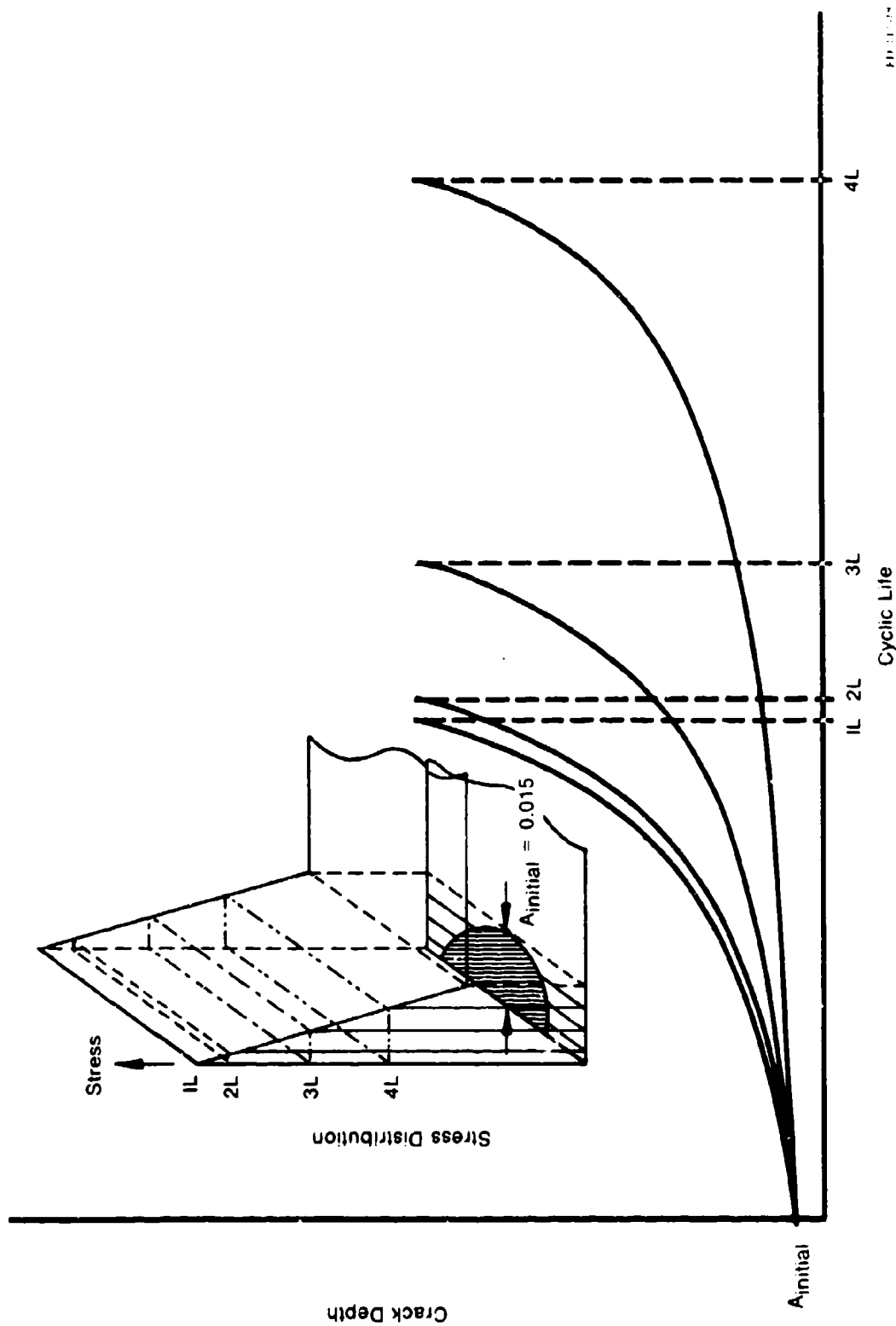
Figure 23. Effect of Near-Surface Stress Redistribution on Cyclic Life of a Part-Through Surface Crack.

evidence that it has occurred. If a carefully measured reference diameter undergoes a small permanent change, then assurance is provided that the desired amount of plastic deformation has occurred at each strain concentrating feature.

To bolster previous studies which support the adequacy of a simple elastic stress analysis with Neuber "correction" for inelastic deformation, a finite element plastic analysis was performed using the MARC computer code to quantify the stress distribution changes. Figure 24 provides the MARC results which illustrate the advantage to be gained by carrying out the spin pit operation at a speed greater than the maximum normal operating speed of service. If spin pit speed of 11,000 rpm was maximum normal operating , the relaxed stress levels (elastic stresses superimposed on residual stresses) would be approximately those labeled MARC plastic at 11,000 rpm. However, if the relaxation has been carried out at 11,000 rpm (overload) and the operating speed is then 10,143, a further reduction in operating stress level results. Both experimental evidence and analytical studies indicate that very significant crack growth rate reduction is accomplished by this technique. A factor of greater than two on residual life was computed and improvements approaching a factor of 5 are supported by experimental data in the discussions that follow.
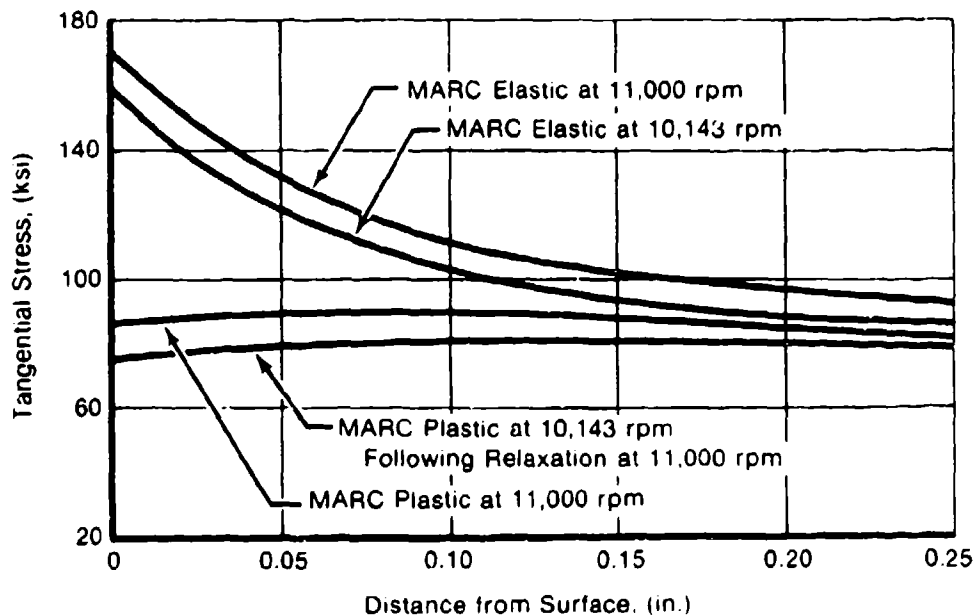
Figure 24. Fan Disk Bolthole MARC Creep Analysis, 500°F.

54

Damage tolerant redesign efforts involved programming the MARC computer code to consider both plasticity and creep relaxation in the vicinity of a disk bolthole. This capability was desired in the design sytem because the introduction of beneficia: residual stress fields around strain concentrating features comprised an important aspect of the intended approach to damage tolerant redesign.

The creep law used for relaxation studies was formulated by bivariate linear interpolation of tabulated TiS-4 creep data contained in the P&WA dwell Low Cycle Fatigue program.

The derived law is:

$$\log_e \epsilon_c = \frac{\log_e S + 0.02147P - 12.2567}{0.004368P + 0.01433}$$

where:

ϵ_c = equivalent creep strain, in./in.

S = Von Mises equivalent stress, psi

P = Larson-Miller parameter = $\frac{T + 460}{1000} (20 + \log_{10} t)$

T = temperature, $^\circ$F
t = time, hr.

This relation was programmed into MARC, and test cases on 1-in. by 1-in. plates under a uniform axial load yielded an excellent play-back of the creep strain-time curve at a constant stress. This law is admissible for creep strains $0.0001 \leqslant \epsilon_c \leqslant 0.01$ and Larson-Miller parameters, $7 \leqslant P \leqslant 21$.

For relaxation analysis, the behavior of the material was assumed to follow the strain hardening rule by which the stress is reduced from one level S_1 to another level S_2 at a constant strain ϵ_1 during a fictitious time shift, $t_2 - t_1$. Using the creep law (1), this time shift is:

$$t_s - t_1 = 10^{20(R-1)} \times t_1^R - t_1$$

where:

$$R = \frac{\log_e S_2 - 12.2567 - 0.01433 \log_e \epsilon_1}{\log_e S_1 - 12.2567 - 0.01433 \log_e \epsilon_1}$$

This strain hardening relation was also programmed into MARC and has been combined with the creep law (1) to generate a creep relaxation program. Figure 25 shows the stress relaxation and creep strain of a 1-in. by 1-in. axially constrained heated plate as predicted by this program.

Conclusions from the rigorous MARC analysis were that assuming MINIMUM material properties, plastic flow and creep deformation would induce the desired residual stresses without inducing unacceptable disk growth; and that 11,000 rpm is the appropriate pre-spin speed for a 500° treatment. This rigorous analysis substantiated the subsequent use of a simpler "disk deck" (a P&WA finite difference tool for analyzing a disk represented by a series of concentric rings) to predict inelastic disk growth and nominal residual stress. Analysis subsequent to the bolthole specimen testing (section VIII-C) revealed that 11,000 rpm is an inadequate treatment process for TYPICAL material properties and that a 12,150 rpm, 500°F prespin is required and will produce plastic flow but not creep. Further comments on design system refinements to account for varying material properties are provided in section IX.

A final topic relating to predicting stress is that accurate prediction of stress concentration is essential. This is straightforward for simple geometry such as boltholes but is difficult for locations with significant 3-dimensional effects such as in the rimslot. P&WA typically uses a superposition of 2D analyses to predict rim stress concentration. For purposes of this contract the rimslot was also analyzed by NASTRAN using the three-dimensional breakup shown in figure 26. Details regarding the three-dimensional analysis will be found in Appendix D. For assessing residuals due to plasticity but no creep, the finer two-dimensional models were used to

56
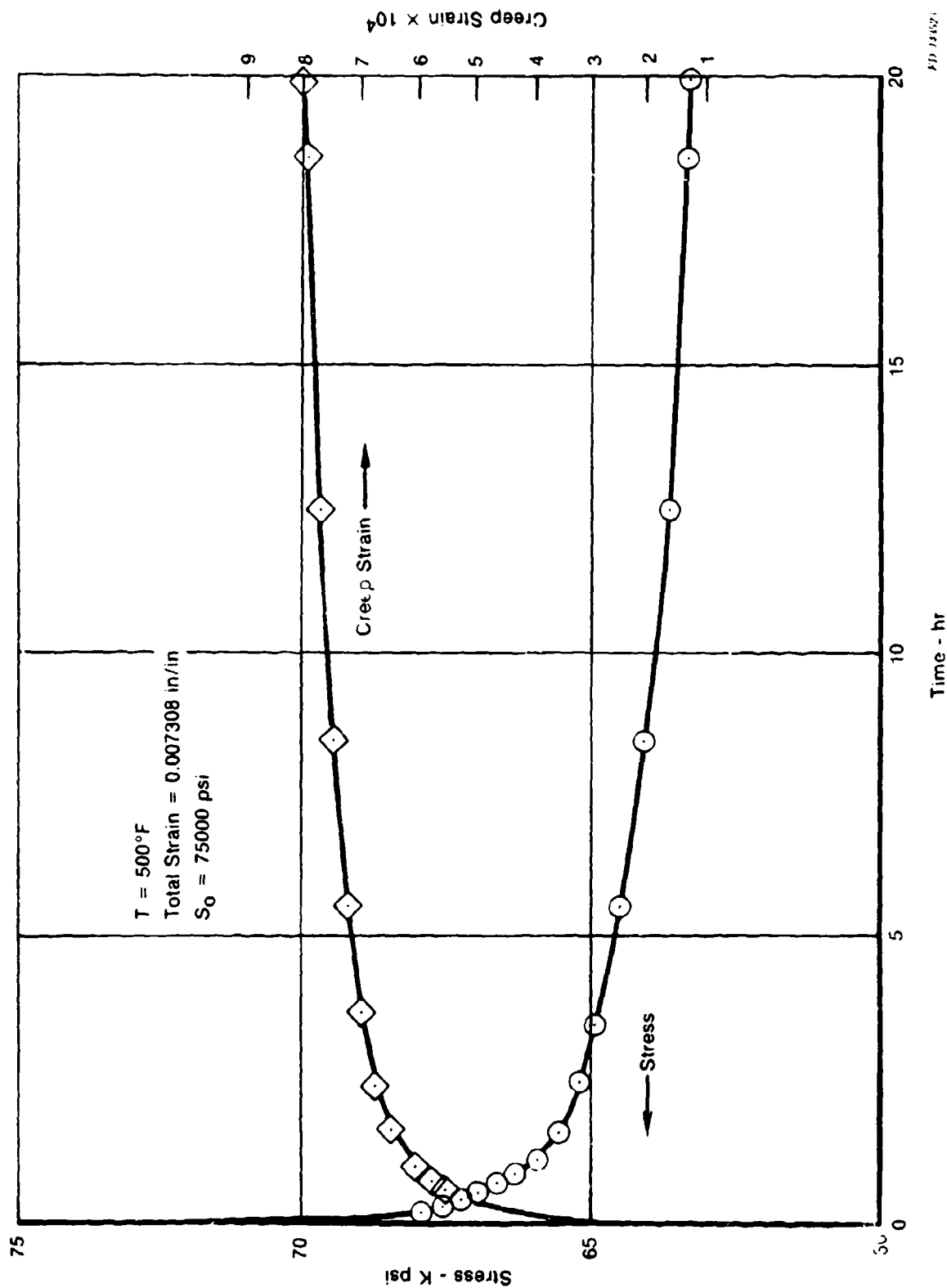
Figure 25. Stress Relaxation of AMS 4 928
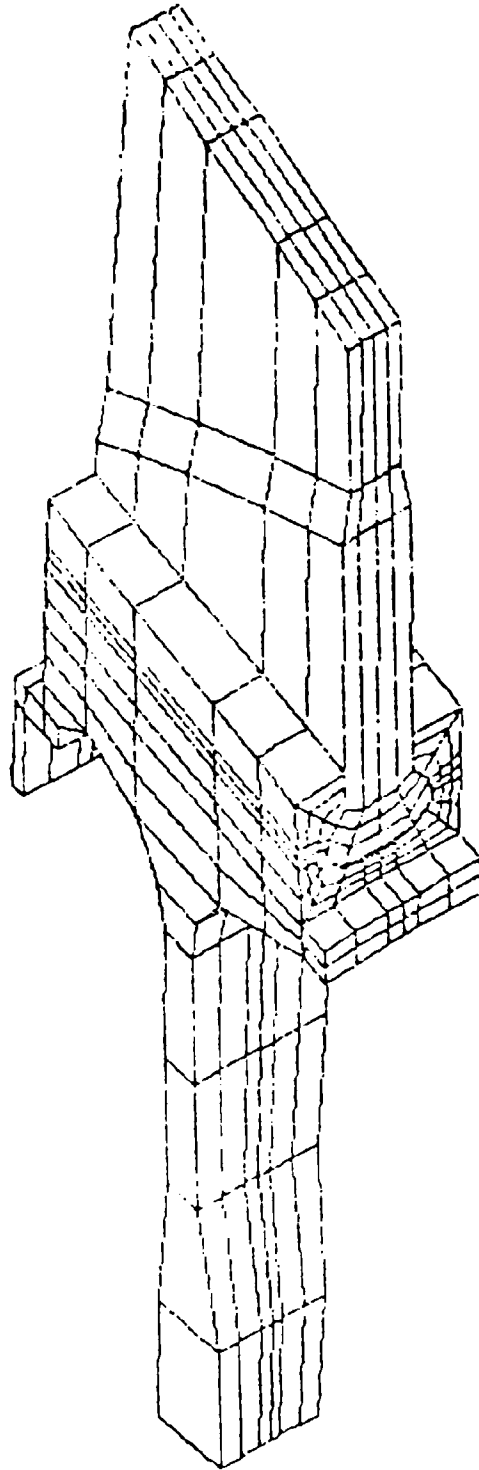
Figure 25. Three-Dimensional Model of Fan Stage Prior to
Addition of Outer Blade Portion.

obtain elastic analyses of the strain concentration regions and Neuber
approximations were applied to the rim region in preference to a MARC
analysis.

A subsequent discussion in Appendix D and summarized in section
IX will assess the accuracy of this rim stress prediction approach.

A final topic relating to stress gradient management is a
frequently expressed concern that beneficial stress patterns may relax
out in service, resulting in less actual life improvement than
anticipated. Reassurance can be taken from the fact that disks which
had experienced 7,000 hr of service exhibited this residual stress
pattern, and life benefits were identified as shown in figure 27.
These disks had received no preservice treatment but had developed the
residual stress patterns during service as time at stress and
temperature accum 'ated. The benefit of having these patterns prior
to any cyclinr ·· ·r than developing them concurrently with cycling
is obvious.
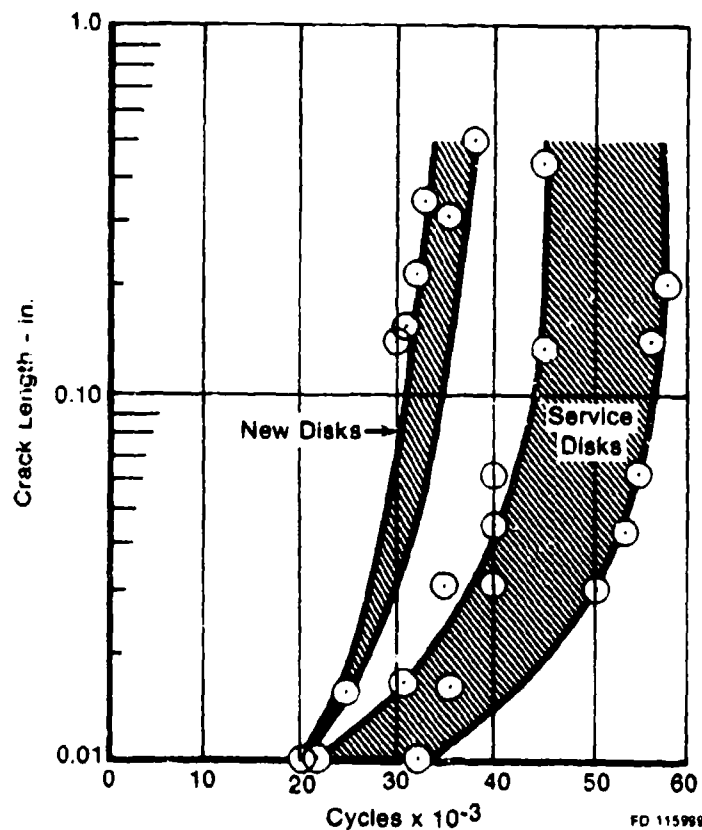
Figure 27. 1963 Residual Life Test Results, Ti-6Al-4V Disks.

59

H.   GENERAL STRESS REDUCTION

In spite of all that the designer can do by material selection and manipulation of localized stress patterns, the goals of 0.030-in. surface length initial cracks and three overhauls for safe, slow crack growth do not appear attainable without weight addition.

It also appears that for components that rotate at high speeds, single load path, slow crack growth structures enjoy an inherent advantage over multiple load path structures. Namely, the design of high-speed machinery is subject to the insidious physical principle that every ounce of weight that is added to the structure adds to the load to be supported, as well as adding load-carrying capability. Thus, the mechanical joints required in a multiple load path structure to replace the conventional disk add weight inordinately. For this reason, the conventional disk configuration was retained and the weight was increased from 14.3 to 17.3 lb of material in the "live" disk. The "live" disk is that portion of the disk consisting of unbroken concentric rings in contrast with the "dead" rim consisting of chunks of material with no tangential load-carrying capability.

I.   DISK CONFIGURATIONS

Figure 28 shows the 17.3 lb damage tolerant disk profile compared to the 14.3-lb original disk profile. The added material modified the stress distribution in the disk as shown in figure 29. Without any special treatment, this disk with 3 lb added weight meets all functional replacement and damage tolerant goals except for slow crack growth from cracks at the bolthole and rim slot regions as shown in figure 30. The "residual stress" treatment increased the safety limit and the inspection interval by a factor greater than two for these critical locations.

In the process of determining that bolthole radial cracking and rimslot bottom radial cracking were the critical fracture modes, many more locations were checked as shown in figure 31. Buried flaws in the bore or web and a surface crack in the upper lug all exhibited safety limits greater than 15,000 missions. The safety limit for a crack propagating circumferentially from bolthole to bolthole was slightly greater than for the features identified as life-limiting locations.

60

Bill of Material Design
14.3 lb

Damage Tolerant Design No. 1
17.3 lb

FD 184866
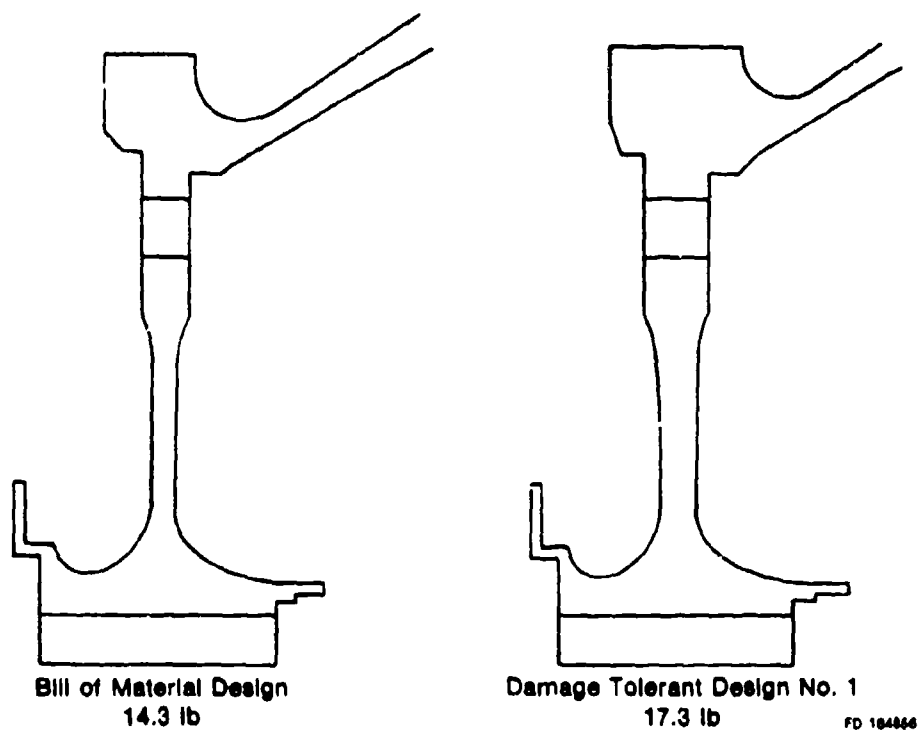
Figure 28.   F100 2nd-Stage Fan Disk Designs.

FD 115994A
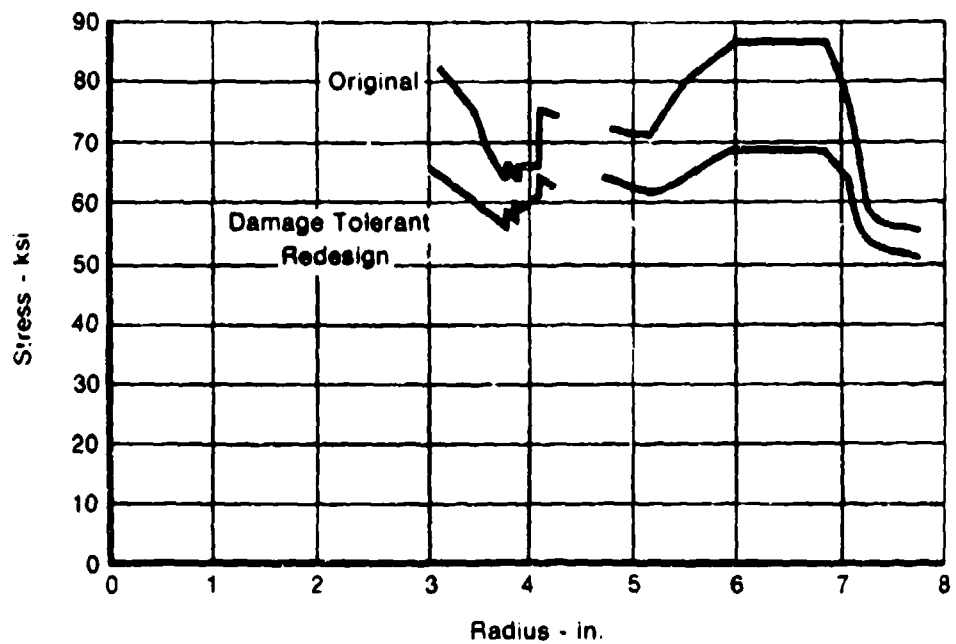
Figure 29.   Fan Disk Tangential Stress Profile.
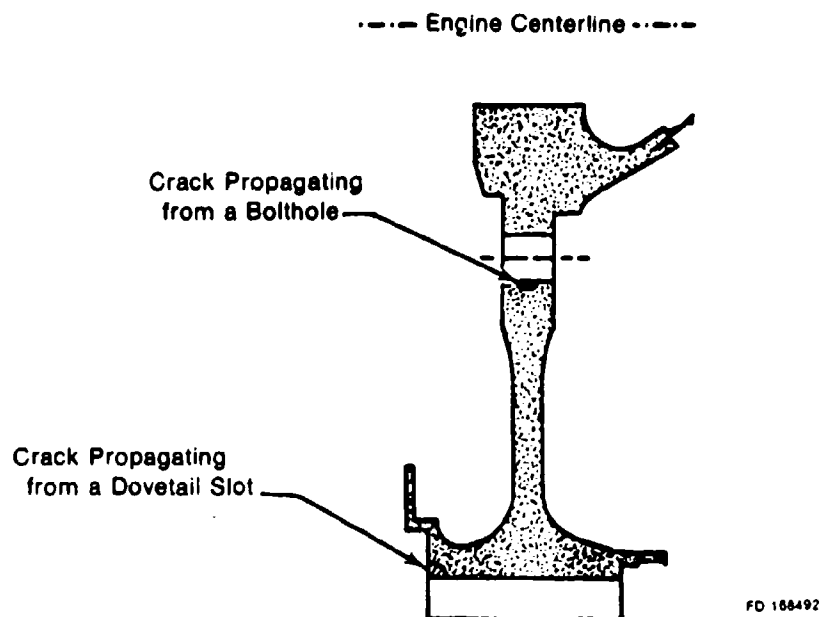
Figure 30. Life-Limiting Features of Damage-Tolerant Disk.
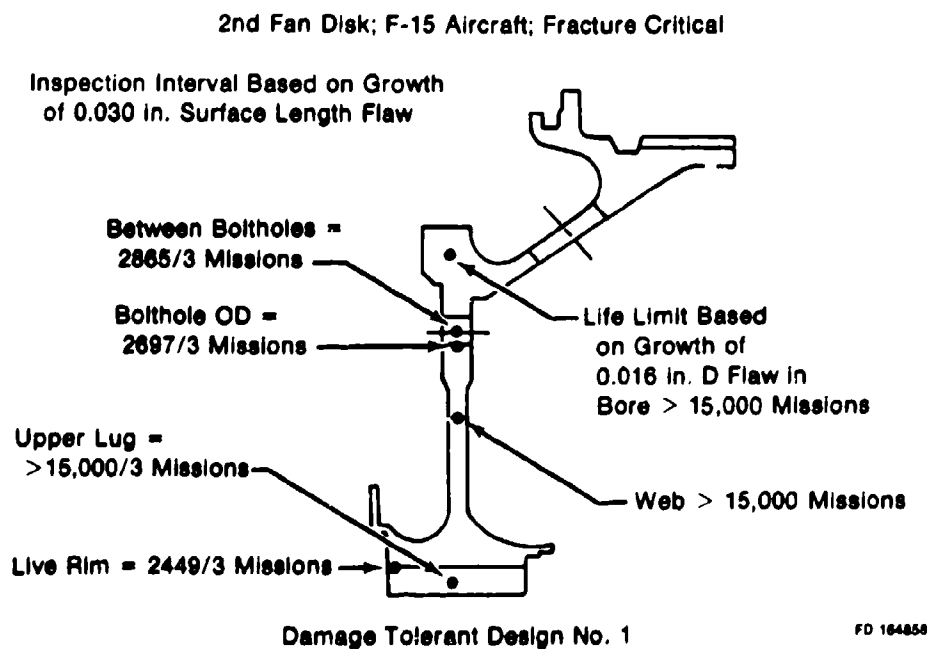
Figure 31. Disk Life Limits.

Thus, the results of fracture mechanics analysis indicate that the desired degree of damage tolerance is achieved by the combination of Ti-6Al-4V, crack growth retardation resulting from the spin treatment, and 3 lb of additional material. Included in the damage tolerance assessment are the following: slow crack growth, the possibility of an overspeed occurring at the end of an inspection interval, and repeated exposure to a vibratory stress peak which occurs during low-speed operation. On a typical basis, the slow crack growth life computed with due consideration of overspeed and high-frequency fatigue exceeded 2300 missions at all bolthole and dovetail slot locations. These reinspectable areas determine the inspection interval. Buried flaws, on the other hand, are not reinspectable using current technology. For this reason, the calculated residual crack growth life of bore and web regions has no bearing on the inspection interval, but instead determines the total useful life of the disk.

As indicated in figure 31, the configuration referred to was given the designation, damage tolerant design No. 1. A second damage tolerant design that could be fabricated from the same Ti-6Al-4V forging was desired to provide an option for the program. An alternative means of enhancing the bolthole life has been investigated in Contract F33615-77-C-5023 "Fan Disk Life Extension." Bolthole cold work has been shown to provide the degree of enhancement needed for this region of the disk; however, no comparable scheme presently exists which will enhance the rim slot to the necessary degree. Consequently, a determination was made of the additional nominal stress reduction required to bring the dovetail slot life up to the desired level. A 19.9-lb disk with cold-worked boltholes meets all damage tolerant design criterial in terms of slow crack growth resulting from mission cycles.

Additionally, the bolthole region meets the established goals of damage tolerance when overspeed and vibration are also considered. Concerning the dovetail region, the damage tolerance and vibration are

63

also considered. The debate centers around the degree of conversatism inherent in the assumptions used to determine vibratory stress levels in the fracture critical areas.

Damage tolerant design No. 1 met all criteria despite the conservatism inherent in the vibratory stress levels. Because of the potential that the 19.9-lb coldwork bolthole disk has, it was designated damage tolerant design No. 2 pending resolution of the vibratory stress doubt. The safety limits of damage tolerant configurations 1 and 2 are compared in table 2. Therein is shown the magnitude of the reduction in safety limit attributable to adding the burst criterion. Also shown is the fact that in locations where a high level of compressive residual stress has been achieved, either by stress relaxation or by bolthole cold work, the addition of vibratory stress to the F100 2nd-stage damage tolerant configurations produced no reduction in life beyond that which was produced by addition of the burst criterion. Where deep compressive residual stress does not exist, sensitivity to high-cycle fatigue crack propagation exists and vibratory stress levels must be accurately known.

Table 2. Safety Limits of Damage Tolerant Disks

Location On Disk	Damage Tolerant Design No. 1			Damage Tolerant Design No. 2		
	Basic F/M (Missions)	Overspeed Burst (Missions)	High Freq. Vibration (Missions)	Basic F/M (Missions)	Overspeed Burst (Missions)	High Freq. Vibration (Missions)
Upper Lug	15,000	15,000	15,000	15,000	15,000	15,000
Web	15,000	15,000	9,500	15,000	15,000	9,600
Live Rim	2,449	2,343	Burst Limited	2,260	2,240	Possible Problem
Bolthole OD	2,697	2,479	Burst Limited	4,054	3,547	Burst Limited
Between Boltholes	2,865	2,840	Burst Limited	2,865	2,840	Burst Limited

J.   LIFE CYCLE COST ANALYSIS

Life Cycle Cost (LCC) was a dominant factor in the selection of
the configuration to be fabricated and tested. Table 3 represents the
results   of   LCC   analysis   of   several   damage   tolerant   candidate
configurations   and   the   baseline   configuration   looked   at   from   a
conventional LCF approach to disk life management and also from a
damage tolerant approach to disk life management.   In column 2, the
materials considered in the study are identified.   In addition to the
Ti6-2-4-6, which is used in the Bill of Material, and Ti6-4, which was
used in the program, Ti8-1-1 was included since it is an extensively
characterized   material   with   an   excellent   military   service   record.
Entries in column 3 identify three disk geometries by weight and the
corresponding   condition   of   the   boltholes.   These   have   been   previously
identifed as: (1) 14.3 lb, B/M,   (2) 17.3 lb damage tolerant design
No. 1, and   (3) 19.9 lb damage tolerant design No. 2.   For the B/M
disk, PWA 99-1 defines a proprietary sequence of manufacturing steps
aimed at enhancing life in terms of cycles to crack initiation.   For
the damage tolerant design No. 1 disks, spin denotes the treatment
employed to enhance the crack propagation life through stress gradient
management, while for damage tolerant design No. 2, cold work denotes
the treatment employed to enhance crack propagation life.   As noted in
column 4, two levels of initial inspection capability to be applied
only   to   new   disks   using   the   manufacturer's   facilities   were
investigated. Use of 0.005-in. depth of initial defect assumes that
the goals of a P&WA/AFML joint program to characterize inspection
capability are met and that this standard can be applied at least to
the initial inspection.   Use of 0.015-in. depth reflects the more
conservative goal established for the damage tolerant contract.   For
the   damage   tolerant   redesigns,   the   level   of   field   inspection
capability was assumed to be 0.015-in. depth with a surface length of
0.030 in. according to damage tolerant design goals.   The several
results of LCC analyses can be selectively paired to isolate and
evaluate the cost impact of the different variables in the study.

Table 3. Life Cycle Cost Study Results.

(1)	(2)		(3)	(4) Inspection Depth (in.)	(5) Acquisition Cost, $ (Millions)	(6) Shipping, Disassembly and Inspection Cost, $ (Millions)	(7) Weight Penalty Cost, $ (Millions)	(8) Total Cost, $ (Less Base) (Millions)
		Weight (lb)	Treatment					
Low-Cycle Fatigue	Ti-6Al-2Sn-4Zr-6Mo	14.3	PWA 99-1*	N/A	20.9	2.5	Base	23.4
Damage Tolerant Design	Ti-5Al-2Sn-4Zr-6Mo	14.3	PWA 99-1	0.005	9.2	17.3	Base	26.5
Damage Tolerant Design (3)	Ti-8Al-1V-1Mo	17.3	Spin	0.015	9.3	11.5	2.5	23.3
Damage Tolerant Design	Ti-6Al-4V	17.3	Spin	0.005	8.3	5.8	2.5	16.6
Damage Tolerant Design (1)	Ti-6Al-4V	17.3	Spin	0.015	8.3	11.5	2.5	22.3
Damage Tolerant Design	Ti-6Al-4V	19.9	Cold Work	0.005	8.3	5.8	4.6	18.7
Damage Tolerant Design (2)	Ti-6Al-4V	19.9	Cold Work	0.015	8.3	11.5	4.6	24.4

Preliminary estimates of Life Cycle Cost (LCC) indicate that the achieved inspection interval is sufficiently long to result in a 40% saving for the damage tolerant design disk relative to its baseline. The flaw detection capability assumed in this particular comparison was the P&WA/AFML objective, i.e., 0.005-in. depth. A groundrule of the LCC analysis was that the engine and airframe could be redesigned as required to allow the basic mission to be accomplished in spite of a modest reduction in thrust-to-weight ratio of the engine. Erosion of weapons sytem capability as a result of applying this damage tolerant philosophy and approach to an existing weapons system would require evaluation using an approach different from the LCC approach employed here.

*Defined on page 65.

Ground Rules for the LCC Analysis follow.

It is assumed that capital equipment requirements are the same among the various designs and will not affect relative assessments. Furthermore, the cost of initial surface defect inspection is assumed the same for all disks.

The life cycle considered in this study is for a fleet of 540 aircraft (1080 engines/disks) operating an average of 25 hours per month for twenty years under existing maintenance and support concepts. Under consideration for comparative acquisition purposes are 1703 (including spares) second stage disks.

A field inspection schedule involving eddy current inspection of all discs in service is imposed on the various disk alternatives according to design assessments relating to disk material, weight, and initial stress gradient associated with strain concentration features.

All costs are in 1979 dollars and the discount rate used was ten percent.

Columns 5, 6, and 7 of table 3 contain the major elements of LCC associated with fan disks. Disk acquisition costs, column 5, reflect both the differing raw material costs of the several alloys and the fact that replacement B/M disks are needed under the traditional LCF approach to disk life management. Costs in column 6 reflect the fact that fan modules for an F100 engine would remain intact at the squadron maintenance facility, so that disassembly of the modules and inspection of the disks would necessitate transportation to a depot. The significantly higher cost for Ti6-2-4-6 reflects the short inspection interval it would have if managed on a slow crack growth basis rather than a crack initiation (LCF) basis. Use of the same cost for Ti6-4 and Ti8-1-1 reflects the fact that the same inspection interval was used for disks of both alloys. Fracture properties of the two alloys are so similar that any real difference between them is obscured at present by insufficient crack growth data relative to the negative R ratio regime associated with stress gradient management.

67

The figures in column 7 reflect the increase in LCC corresponding to a particular weight increase. The following concepts were employed in arriving at the weight/cost relation:

1. There would be no appreciable reduction in mission capability.

2. Damage tolerant design philosophy was assumed to be applied at the inception of a new weapons system so that the only given was the mission to be accomplished. These groundrules allowed the design of an optimum airframe/damage tolerant engine combination to accomplish the given mission.

    Putting into an existing weapons system an engine which had been redesigned to provide damage tolerance was an unacceptable approach for the damage tolerant design contract. The reason for this is that modest compromises in mission capability would be unavoidable. However modest a compromise might be, it is controversial and is something not reduceable to an LCC increment.

3. All costs for a fleet of 540 aircraft employed in F-15 type operation would be included.

4. The useful life of the weapons system would be 20 years, during which time the engine would experience 9,600 hr comprising 5664 missions; a mix of 79 percent Air Combat, 9 percent Ground Trim, 8 percent Low Level Combat, and 4 percent Functional Check Flight.

Costs in column 8 must be used in a comparative way only because the unspecified base cost is omitted from the totals. The difference between any two figures in column 8 does represent a cost saving or a cost increase, since the base cost then falls out. Damage tolerant design No. 1 is lower in cost than either No. 2 or 3 since material cost for No. 3 is more than for No. 1 and the weight penalty cost increase for 2.6 additional pounds significantly affects No. 2. It is clear from the chart that the cost of all three drops as the inspection capability improves, thereby providing strong incentive for NDE progress.

68

The life cycle cost advantage (which the damage tolerant design disk developed under this contract enjoys relative to an F100 Bill of Material (B/M) 2nd stage fan disk) is very sensitive to assumed initial flaw size; i.e., NDE inspection capability. The contractual goal of 0.030 in. surface length (0.015 in. depth) was appropriate at the outset of this contract. On this basis, the damage tolerance of the design developed under this contract is essentially beyond comparison with the F100 B/M disk which it functionally replaces.

The safety limits were calculated based on the time required for the maximum probable initial flaw or defect to grow to critical condition and cause component failure. With a 0.030 in. surface length crack in a bolthole, the B/M disk safety limit is less than 800 hours, whereas the safety limit of damage tolerant redesign disk #1 exceeds 4000 hours. In keeping with the contract groundrule requiring three inspection intervals within the safety limit life, the limit of 800 hours for the B/M disk would be logistically and economically impractical.

In contrast, requiring three inspection intervals within the safety limit life of the damage tolerant design disk would mean that disk inspections would coincide with scheduled shop visits thereby greatly reducing the cost of employing the damage tolerant approach to disk management philosophy. Recent B/M work is exploring a cryogenic spin pit treatment to improve damage tolerance and screen for small flaws. This work appears promising to extend B/M life toward (but not meeting) this contract's damage tolerance objectives. See Section III C.

Three and one half years of rapid advancement have brought NDE technology to the point where it is realistic to make life cycle cost comparisons on the basis of an assumed initial flaw size of 0.005 in. depth rather than 0.015 in. depth. Reference to Table 3 shows that, on this basis, the damage tolerant disk design reduces by 40 percent the cost of supplying the fleet with 2nd stage fan disks throughout the twenty-year life of the weapons system.

K. DESIGN SUMMARY

LCC results from table 3 have been entered into table 4 (the Design Summary Matrix) for the baseline and for the three configurations which have potential for meeting all damage tolerant design program goals. The baseline fails to meet these goals because the more ambitious inspection capability must be achieved to make this disk viable on a slow crack growth management scheme. However, it is anticipated that the B/M disk will be safe when managed on a crack-initiation basis, i.e., run to the life predicted for crack initiation in one per thousand and retire all disks. Damage tolerant design No. 1 meets all program goals despite the conservative approach taken in projecting high-frequency stress levels into the strain concentration regions of the disk rim dovetail slots. Damage tolerant design No. 2 meets all program goals except for a gray area involving high-frequency fatigue propagation of a crack originating in a dovetail slot. The uncertainty is caused by the uncalibrated degree of conservatism in projecting high-frequency stress levels from the point of measurement to the strain concentration regions. Damage tolerant design No. 3, as previously discussed, differs from No. 1 only in material, and at most would require fine tuning to meet all program goals.

Entries in table 4 which have not previously been discussed will now be addressed.

Functionality: Each damage tolerant redesign disk is the functional equivalent of the Bill-of-Material disk, and changes to adjacent hardware were kept to an absolute minimum. Since thickening of the disk at the bolt circle radius was unavoidable, modification of mating part axial lengths will be required.

Life (Luke Hours): This represents the calculated minimum operational time required to initiate a crack in the limiting notched feature of the disk or to propagate a preexisting internal flaw to failure. Minimum is defined as the shortest time for any member of a population of 1000 disks in the case of crack initation and of a

70

Table 4. Design Summary Matrix

Configuration Factor	Baseline	Damage Tolerant Design No. 1	Damage Tolerant Design No. 2	Damage Tolerant Design No. 3
Material	Ti-6Al-2Sn-4Zr-6Mo [1]	Ti-6Al-4V	Ti-6Al-4V	Ti-8Al-1V-1Mo
Bolthole Treatment Stress (Critical)	PWA 99-1 ($\sigma\, t_{avg}$)	PWA 99-1, Hot Spin $\sigma\, t_{avg}$	Cold Work Vibration	PWA 99-1, Hot Spin $\sigma\, t_{avg}$
Functionality	Base	Spacer Change	Spacer Change	Spacer Change
Life (Luke Hours)	3,160	10,000	10,000	10,000
Burst Margin	1.275	1.275	1.275+	1.275+
Weight, lb	14.3	17.3	19.9	17.3
Resonance (Speed and Stress)	Base	Improved	Improved	Improved
Life Cycle Cost ($ Millions)	(2)	22.3	24.4	23.3
Inspectability	Base	Improved	Improved	Improved
Maintainability	Base	Improved	Improved	Improved
Manufacturability	Base	Special Spin	Cold Work	Special Spin

(1) Defined on page 65.
(2) Cost basis compatible with contract goals not available.

71

population of 10,000 disks (each one assumed to contain a flaw) in the case of crack propagation. All three damage tolerant designs have the capability of safely withstanding a maximum overspeed condition on the last flight occurring in the inspection interval.

Resonance (Speed and Stress): Vibratory qualities of the redesigns remain the same as the Bill-of-Material stage. Changes inside the bolt circle of a disk such as this have a negligible effect upon the resonant characteristics. Likewise, modest changes to the web thickness produce negligible effects. Since the disk rim and blades were unchanged and the material stiffness-to-density ratio remained essentially constant, the redesign process caused no significant change in vibratory characteristics.

Reliability: Even though the reliability of the B/M disk operated under traditional LCF ground rules is expected to be very high, it must be said that the damage tolerant redesigns are even higher. Lower stresses and defect tolerant materials provide additional margin of safety. The usage for this additional margin must be established by investigations which are to follow.

Life Cycle Cost: The LCC differences between damage tolerant candidate configurations is small. The B/M configuration is eliminated from the damage tolerant category by the selection of 0.015-in. initial flaw depth as the goal for the damage tolerant design contract.

Inspectability: The three candidates have essentially the same inspectability advantage relative to the B/M, i.e., NDE capability consistent with damage tolerant program goals is adequate for all three candidates, whereas the B/M cannot pass this requirement.

Maintainability: The candidate disks have been given an improved maintainability rating because they are believed to have a greater tolerance for handling damage. While careful handling is a requirement for all disks, handling requirements for the B/M disk

would have to be more strict than for the damage tolerant redesigns because the B/M disks have higher stress levels, more rapid crack propagation, and smaller critical crack lengths.

Manufacturability: Each of the designs requires a manufacturing step that the B/M does not. The special spin has a historical precedent in the thousands of proof spins that were routinely conducted by P&WA over the years. Consequently, this is not viewed as a deviation from accepted manufacturing processing. The development work on bolthole cold work will be completed in a timely manner under Air Force Contract F33615-77-C-5023. "Fan Disk Life Extension" so this is viewed as an acceptable manufacturing technique though it is innovative in terms of jet engine disk manufacture.

L. DESIGN SELECTION

Recommendation: When all factors were taken into consideration and weighed according to P&WA experience, damage tolerant design No. 1 emerged as the recommended candidate. It required the least added weight, it had the lowest LCC, and convervatism in projecting vibratory stress levels from strain gage locations to incipient crack locations caused no problem with meeting the vibratory threshold criterion for damage tolerance.

Approval for the selection of damage tolerant design No. 1 was received from the Air Force project engineer. Accordingly, the program proceeded as shown in figure 2, with the fabrication of two disks to the approved configuration. One to evaluate damage tolerance in the boltholes and the second to evaluate rimslot damage tolerance. The configuration of the third test disk was held open pending outcome of first two disks. After successfully completing the first two tests, the third forging was used to manufacture a ferris wheel test version of damage tolerant design No. 1 which was tested without the prespin residuals in order to establish a baseline.

SECTION V

TASK III - DISK FABRICATION

Material was procured from one heat of Ti-6Al-4V in the form of six disk forgings sufficient to provide for specimen testing and the fabrication of three damage tolerant design disks as provided in Contract Modification P00003. The material analysis is presented in table 5.

Table 5. Material Analysis Report.

Specification: AMS4928H SUPP PWA S-4928G
Conditions of Forgings: Forgings in shipment were solution treated at 1745°F ± 15°F for 1 hr, water-quenched, annealed at 1300°F ± 15°F, for 2 hr, then aircooled.

Mechanical property acceptance of listed forgings based on results from integral test ring per forging which conforms to material specifications listed above are:

Serial	Test Identity	Yield ksi 0.2% Offset	Ultimate Strength ksi	Elongation in./in. Percent	Reduction Of Area, (Percent)
2022	112	141.1	152.8	11	32
2023	112	141.9	153.4	14	40
2024	112	141.5	152.3	13	41
Spec Min.		120	130	10	20
Design Typ.		140	150	15.0	42

Two test disks were machined suitable for prespinning and provided at no cost to the contract. Total GPD expenditure for these disks was $24,031 which included $16,220 to outside vendors. A cost breakdown is provided in table 6.

A manufacturing savings of $1,030 was realized by elimination of machining operations for splines and airflow holes in the hub. These flight requirement features are not required for the test disks.

To put these test disk costs in perspective with a routine production cost for the damage tolerant design:

Cost of B/M F100 2nd Disk (Ti6-2-4-6)	$4,070
Cost Change to Substitute Ti6-4 Design	-550
Cost Change to Provide Spin Treatment	+200
Total Cost per Disk	$3,720

75

Table 6. Cost of Two Test Disks
(No Cost to Contract)

Item	Cost, ($)	
Forgings (2)	7,559	(1978 Expenditure)
Machine Forgings to Disk Profile	9,770	
Broach Blade Slots in Disks	1,987	
Inspection	1,066	(1979 Expenditure)
Material Control (Handling)	2,714	
Misc Manufacturing	935	
Total	24,031	

A third disk specimen, configured for ferris wheel testing only, was fabricated. This disk was fabricated without the hub since no prespin treatment would be given.

SECTION VI

TASK VI - DISK TEST AND DESIGN SYSTEM REFINEMENT

A. BACKGROUND AND OBJECTIVES

Having developed and applied a Damage Tolerant Design System to redesign an F100 fan disk, life assessment tests were required in order to evaluate the design system predictions and to identify needed refinement. Two critical locations identified in figure 32 were selected for life testing. Test disk No. 1 received the spin treatment and was tested to determine bolthole outer diameter (BHOD) life. Test disk No. 3 provided BHOD life without benefit of the spin treatment. Test disk No. 2 which was also prespun, evaluated the rim slot bottom location. The following general discussion of test results is supplemented by a detailed test laboratory report provided as Appendix E.

B. SPIN TREATMENT

Two fully-bladed disks were hot-spun (figure 33) to induce beneficial residual stress (figure 34) at the stress concentration features.

The first disk scheduled for prespinning was instrumented with thermocouples and eight high temperature strain gages (See Appendix E). The instrumentation was concentrated at the peak stress locations at bolthole O.D. and rimslot bottom which were to be preflawed prior to mission testing.

The two disks were then prespun at 500°F to the analytically predicted speed required to achieve the optimum bolthole residual stresses while remaining within allowable growth tolerances. The 500° insured that spin induced residuals severe enough to provide local reverse yielding during unloading will not relax at hot shut-down engine operating temperatures (200°-300°).

Results are summarized in Table 7. Bolt circle radius growth received special inspection before and after spin. The spin speed had been selected by declaring 0.002 in.-0.004 in. to be the acceptable

77
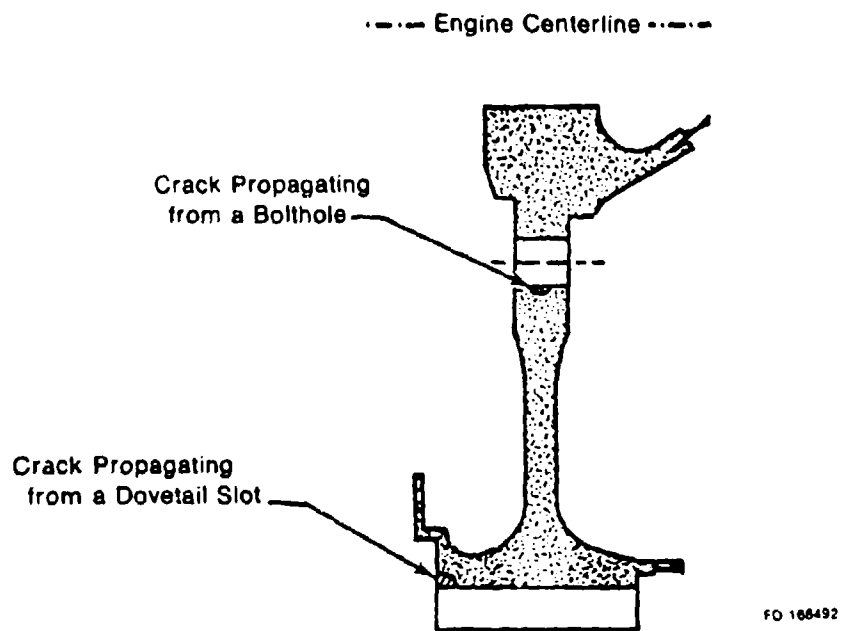
Figure 32.   Life Test Locations on Damage Tolerant Disk.

Figure 33.   Spin Pit Residual Treatment Assembly.
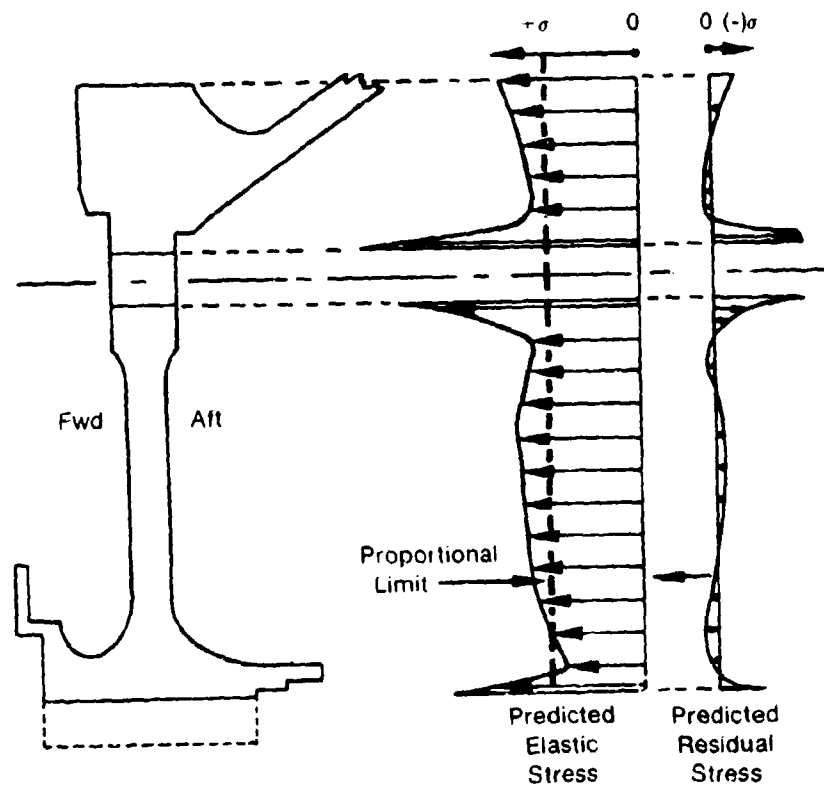
Figure 34. Predicted Spin Pit Stress.

Table 7. Spin Pit Measurements

Location	Parameter	Measured	Predicted	Actual / Predicted
Bolt Circle	δ_{radius}	0.0038 in.	0.002 in. to 0.004in.	Good
BHOD	σmax	–	186 ksi	–
	$\sigma residual$	–	-70 ksi	–
Rim FWD	σmax	82 ksi	149 ksi	0.55
	$\sigma residual$	+12 ksi	-46 ksi	–
Rim AFT	σmax	78 ksi	103 ksi	0.76
	$\sigma residual$	+13 ksi	-8 ksi	–

range of growth and by selecting the initial spin speed with elastic-plastic analysis. This analysis predicted that 12,150 rpm would yield the minimum acceptable growth (0.002 in.) although this elastic-plastic prediction was recognized as having a significant error band due to hub geometry. Post-spin growth results indicated 0.0038 in. change in bolt circle radius and substantiated the adequacy of the spin. Due to the large plastic deformation in the boltholes, the strain gages failed during load. Because analytical prediction (Neuber upload and kinematic ha .: ng with perfect plasticity unload) indicated that significant reverse yielding would accompany 0.002 in. growth, it was concluded that a near-optimum beneficial residual had been successfully induced in the boltholes.

The rim slot bottom strain gage results indicated that the stress prediction system was very conservative. Measured stress (Table 7) indicated that no plasticity or beneficial residual stress was produced in this location; in fact, only the residual tensile stress due to bore plasticity was measured.

These rim results are both good and bad. The bad part is that no significant residual stress was induced in the rim slot but the good part is that due to reduced stress levels, residual stress may not be required to meet program life goals. A discussion with AFAPL Program Manager R. J. Hill resulted in agreement to continue the rin. test program to define the life benefit due to lower design stress, material substitution, and tensile residual stress due to bore plasticity. Redefinition of the rim slot ferris wheel loading requirements and life prediction was required. A review of the rim stress prediction system was conducted. If it is required to reduce the conservative 2-D stress prediction, a 3-D finite element analysis may be utilized. See Appendix D.

C. FERRIS WHEEL BOLTHOLE LIFE TEST

Elox damage (0.020in. long X 0.005in. wide X 0.010in. deep) in 10 of the 30 boltholes was provided to hasten initiation to a 0.030-in. surface length precrack. The disks were then cycled for 2000 cycles

with simple sawtooth loading to initiate and grow the elox starter cracks to the required 0.030 in. surface length, before mission testing began.

An accelerated life test (stress higher than normal engine operating stresses) was used to minimize ferris wheel test time for the bolthole location (figure 35). Initial predictions of bolthole stress and life were based on the simplifying assumptions that:

1) Ferris wheel $K_T \approx$ Spin pit K_T

2) Stress distribution due to hub removal is negligible

Subsequent to the life test, these assumptions were found to yield an unacceptable error in life prediction. Disk stress reanalysis and NASTRAN verification were used to refine these predictions.

Table 8 indicates in the stress summary box that the ferris wheel measured stress vs. predicted stress (using normal engine K_t) differ by 11 percent (155 ksi and 140 ksi, respectively). The use of normal engine K_t to predict ferris wheel bolthole stress caused the inaccuracy. The nature of the difference is that in the ferris wheel, blade centrifugal load is simulated using hydraulic jacks but disk centrifugal load is absent. This difference between ferris wheel loading and normal engine loading modifies the ratio of radial stress to tangential stress which in turn modifies the K_t. In addition, some of the beneficial spin-induced residual stress at the bolt hole location was sacrificed when the bore was removed to make ferris wheel testing possible. The initial life prediction of 1600 cycles (figure 36) incorrectly assumed these stress variations were insignificant in terms of life, and required revision.

The previously mentioned assumptions are generally valid for current conventional designs but proved invalid for the life-enhanced damage tolerant design (a simple illustration to explain this stress sensitivity is given in figure 37). Using a K_t corrected for ferris wheel loading, the current life prediction correlation (667 missions
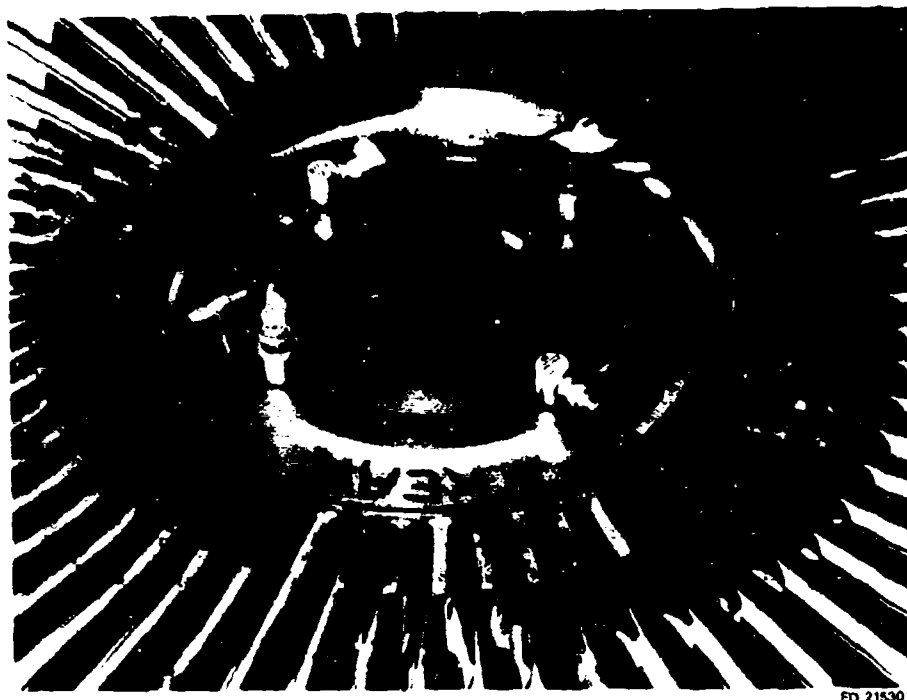
FD 215301

Figure 35. Ferris Wheel Testing.

Table 8. Ferris Wheel Stress Measurements

		Disk Deck			Disk Deck		NASTRAN	
Location	Para-Meter	Measured (ksi)	Pre-Pred. (ksi)	Actual Pred. (ksi)	Post-Pred. (ksi)	Actual Pred. (ksi)	Post-Pred. (ksi)	Actual Pred. (ksi)
BHOD	σ_{conc}	155	140	1.11	160	0.97	161	0.96
Bore	σ_{hoop}	92	100	0.92	–	–	96	0.96
Web	σ_{hoop}	69	70.5	0.98	–	–	68	1.01
Web	σ_{radial}	58	55	1.05	–	–	57	1.02
Rim_{fwd}	σ_{conc}	81	105	0.77	–	–	–	–
Rim_{aft}	σ_{conc}	73	96	0.76	–	–	–	–

82
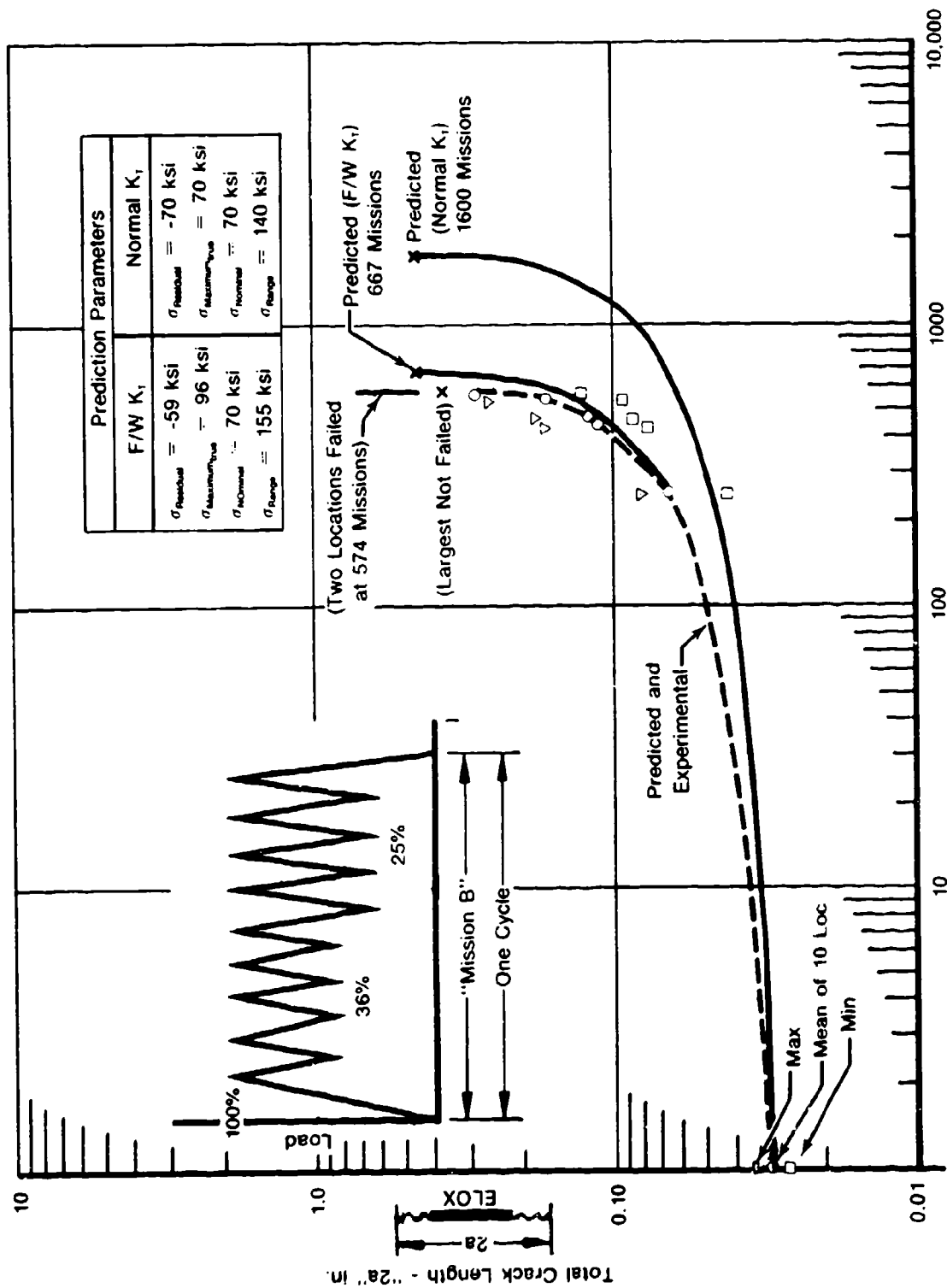
Figure 36. E.T. Bolt Hole Disk F/W Tests.

FD 202316

83

Damage Tolerant Treatment Involves

- Material Substitution
- Overload Induced Residuals
- Reduced Stress Range

Damage Tolerant Treatment Improves Life and Increases Sensitivity of Life to Stress Error Because:

Reduced Stress

Schematic Only

Small ΔN (Current Designs)

Large ΔN (Dam Tol Design)

σ or S

$\Delta\sigma$

N (Life)

Summary:
Reduced Stress Moves the Design to Flatter Portion of S-N Curve with Resultant Accentuated Sensitivity in Life Results

Normal vs Overload Residuals

$\{$ Normal Residual $\}$

Assume $\Delta\sigma_{Range} = 0.2\ \sigma_{Range}$ due to K, change

if $\sigma_R + \Delta\sigma_R = 1.20\ \sigma_R$,
$\sigma_w + \Delta\sigma_w = 1.25\ \sigma_w$
(Amplified 1.25:1.2 Due to R = -0.2)

Time

σ_{Range}

$\{$ Overload Residual $\}$

if $\sigma_R + \Delta\sigma_R = 1.20\ \Delta\sigma$,
$\sigma_w + \Delta\sigma_w = 2.0\ \sigma_w$
(Amplified 2:1.2 Due to R = -4.0)

Time

σ_{max}

Summary: Large -R Causes Very Amplified % Variation in σ_{max} with Resultant Accentuated Sensitivity in Life Results

Figure 37. Illustration of Stress-Range Sensitivity.

FD 207151

84

predicted versus 574 missions actual, see figure 36) indicates the
fastest of the 10 bolthole cracks failed at 86 percent of the predicted
typical crack growth behavior. This is within a reasonable scatter
band. Furthermore, by using these substantiated prediction
techniques, the accelerated (high stress) ferris wheel results can be
stated in terms of equivalent engine hours of life under normal
operating stress levels (figure 38). When interpreted in this manner,
the demonstrated bolthole life is 140 percent of our ambitious goal of
4000 hours after 0.030 in. surface length crack.

The subsequent baseline bolthole (test No. 3) verification test
was to demonstrate life for the damage tolerant design configuration
without the benefit of the 500°F overload prespin treatment which
introduces deep local compressive residual stresses. Some local
inelastic notch behavior was expected on the first ferris wheel load
cycle, and considerable additional crack growth capability over the
Bill of Material Ti 6-2-4-6 disk was predicted.

This disk was also preflawed in 10 boltholes and cycled for 500
sawtooth cycles to grow the starter cracks to 0.030 in. surface length.
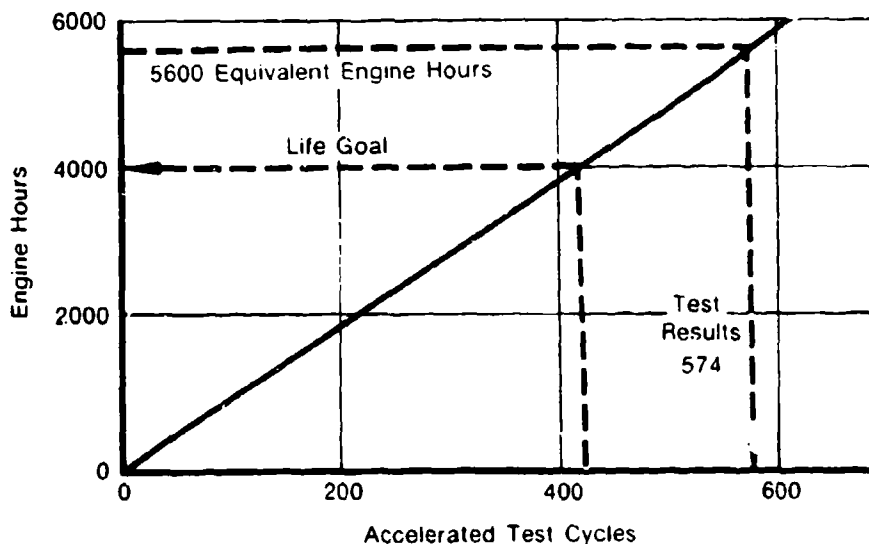
FD 203326

Figure 38. Testing Results Exceeded Life Goals, Disk No. 1.

The disk was then mission cycled using the same stress levels as disk No. 1 with the intent of stopping the test when the largest crack reached approximately 0.20 in. surface length. The objective was to preserve the disk for additional rim crack propagation testing (possible follow-on contract) at a later date.

The life prediction correlation (figure 39) shows the largest crack to have reached 0.189 in. in 275 mission cycles, which translates to approximatly a factor of 2 decrease in life compared to disk test No. 1 (figure 36) which received the prespin treatment.

A close examination of figures 39 and 40 indicates that:

o   a 2:1 life improvement is attributed to the pre-spin residuals alone (even though the accelerated life test reduces the benefit), i.e., on basis of equivalent engine hours at engine operating stress (figure 40) an actual 5:1 benefit has been predicted/demonstrated.

o   Crack growth prediction for deep compressive (prespin) residuals ($R < -1.0$) was very accurate

o   Crack growth prediction for normal-loading induced residuals ($R > -0.13$) was conservative and consistent with prior bolthole specimen testing at similar R-ratios and loading (Section VIII-C).

o   The crack growth design goal of 4000 hours (or 2360 missions, figure 15) was surpassed by 40 percent and the very early "conservative" design system predictions (2697 mission or 4570 hrs) was exceeded by 22 percent. This indicates acceptable margins on other previously discussed design requirements such as overload residual.

Photographs of typical bolthole cracks trepanned from disks No. 1 and No. 3 are provided in figures 41 through 44. Note that the half-penny aspect-ratio assumption is justified and that the barely

86
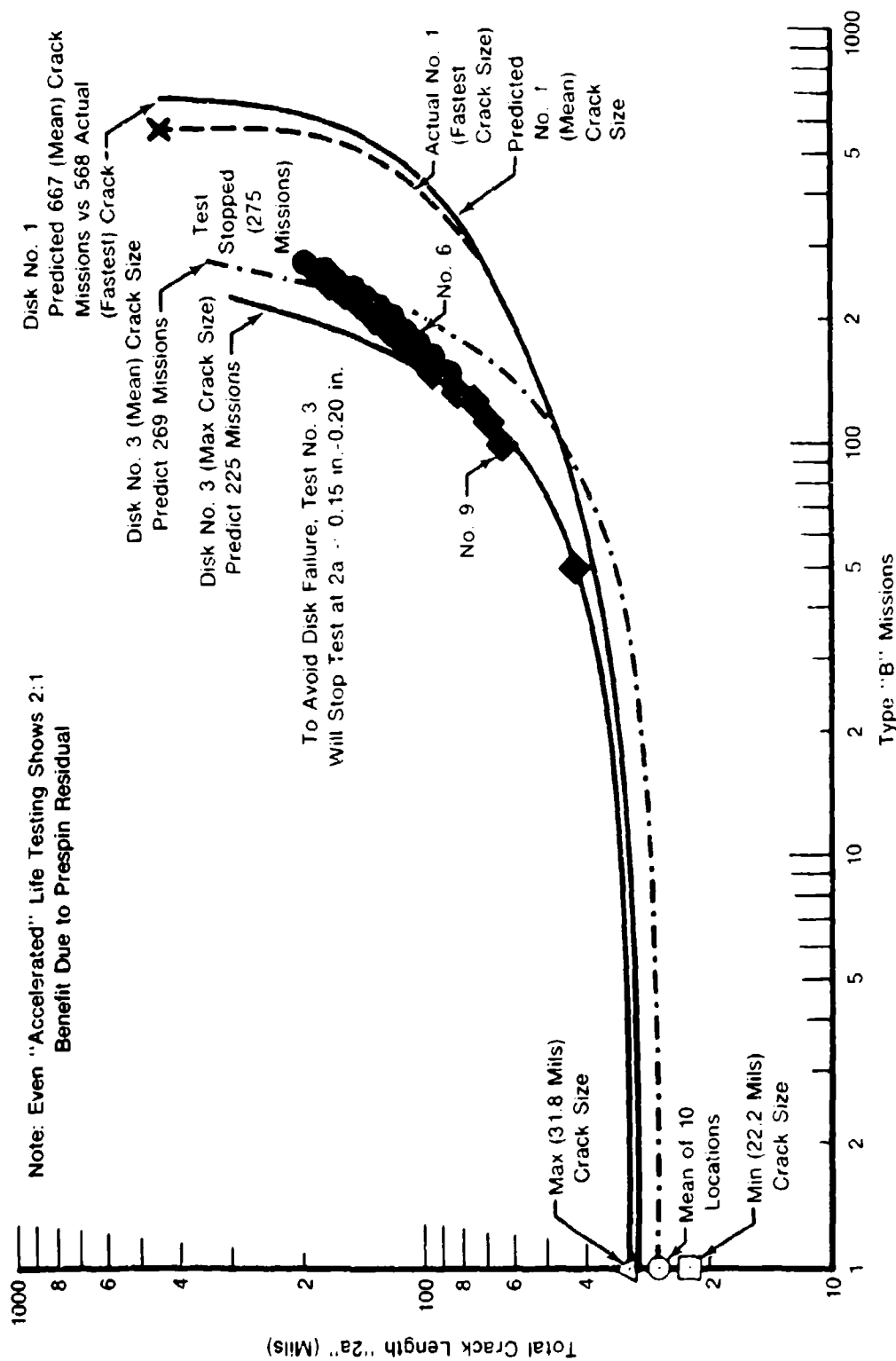
Figure 39. DTD Bolthole F/W Test, Disk No. 3 Prediction vs (Actual and Predicted) Disk No. 1.
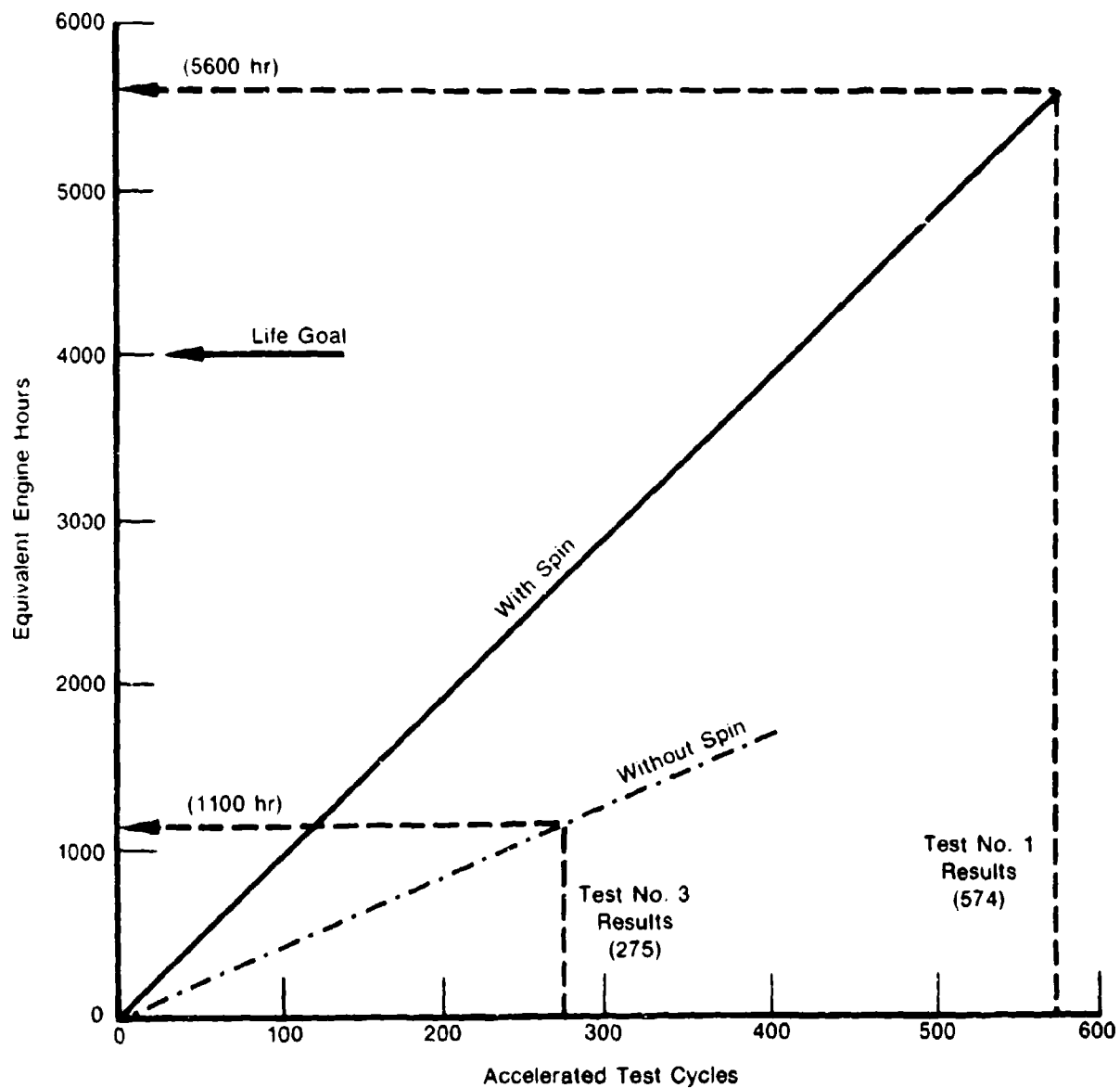
Figure 40. Damage tolerant Disk Bolthole vs No-spin Baseline
(Corrected for A/P Calibration).

88

Figure 31. Typical brittle fracture. Test No. A-35-35.
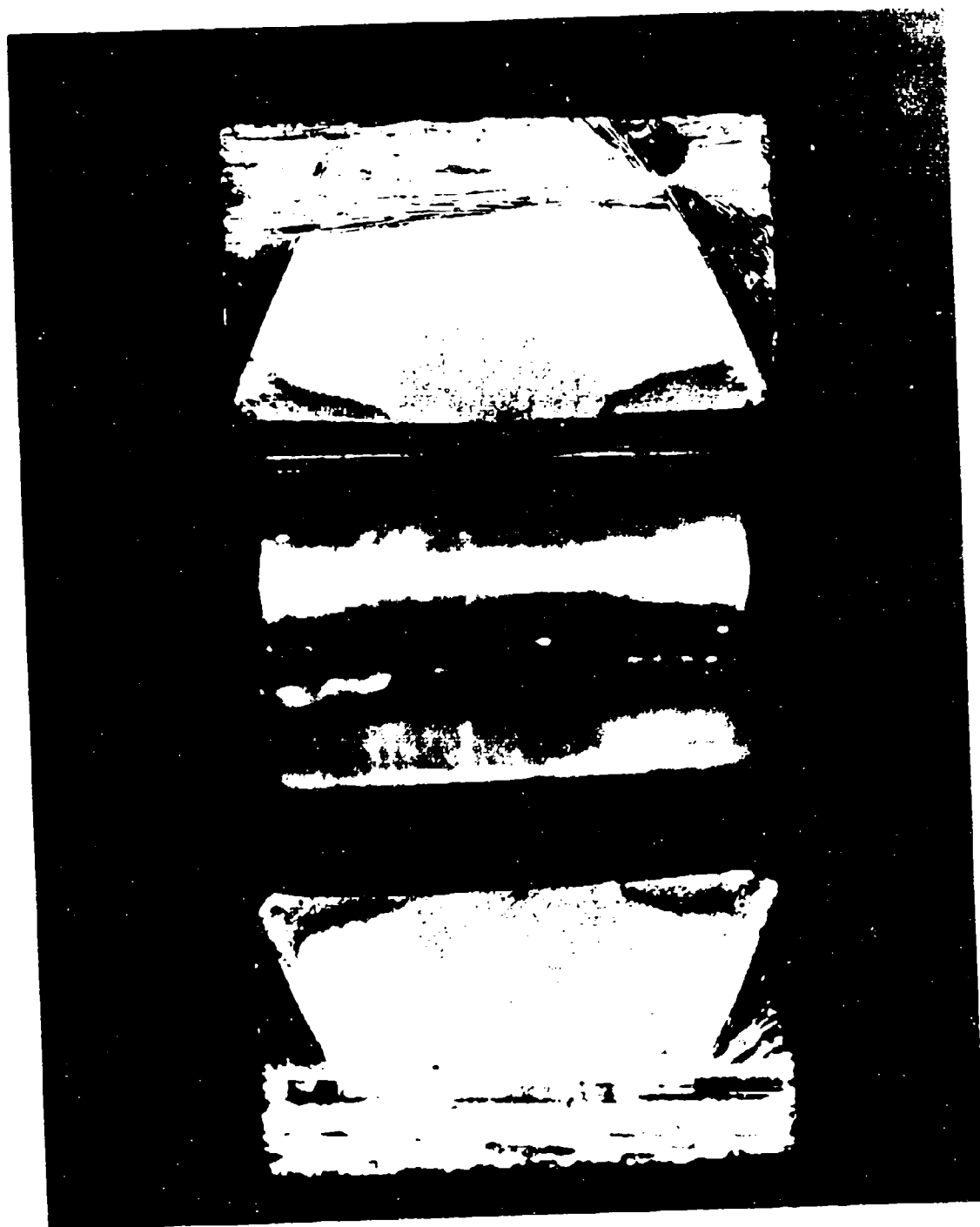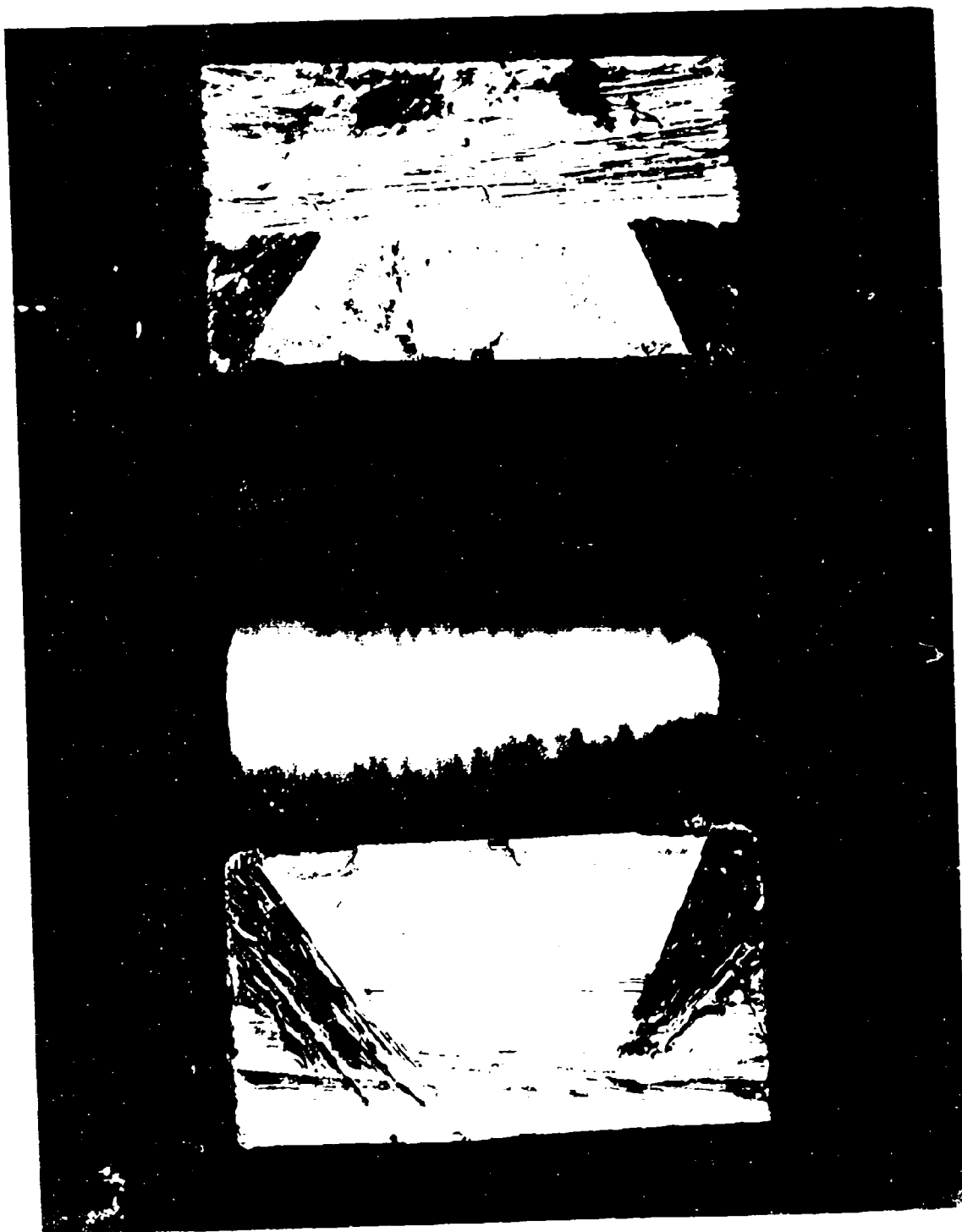
Figure 41. Largest Unruptured Bolthole Crack, Disk No. 1, BH #16.
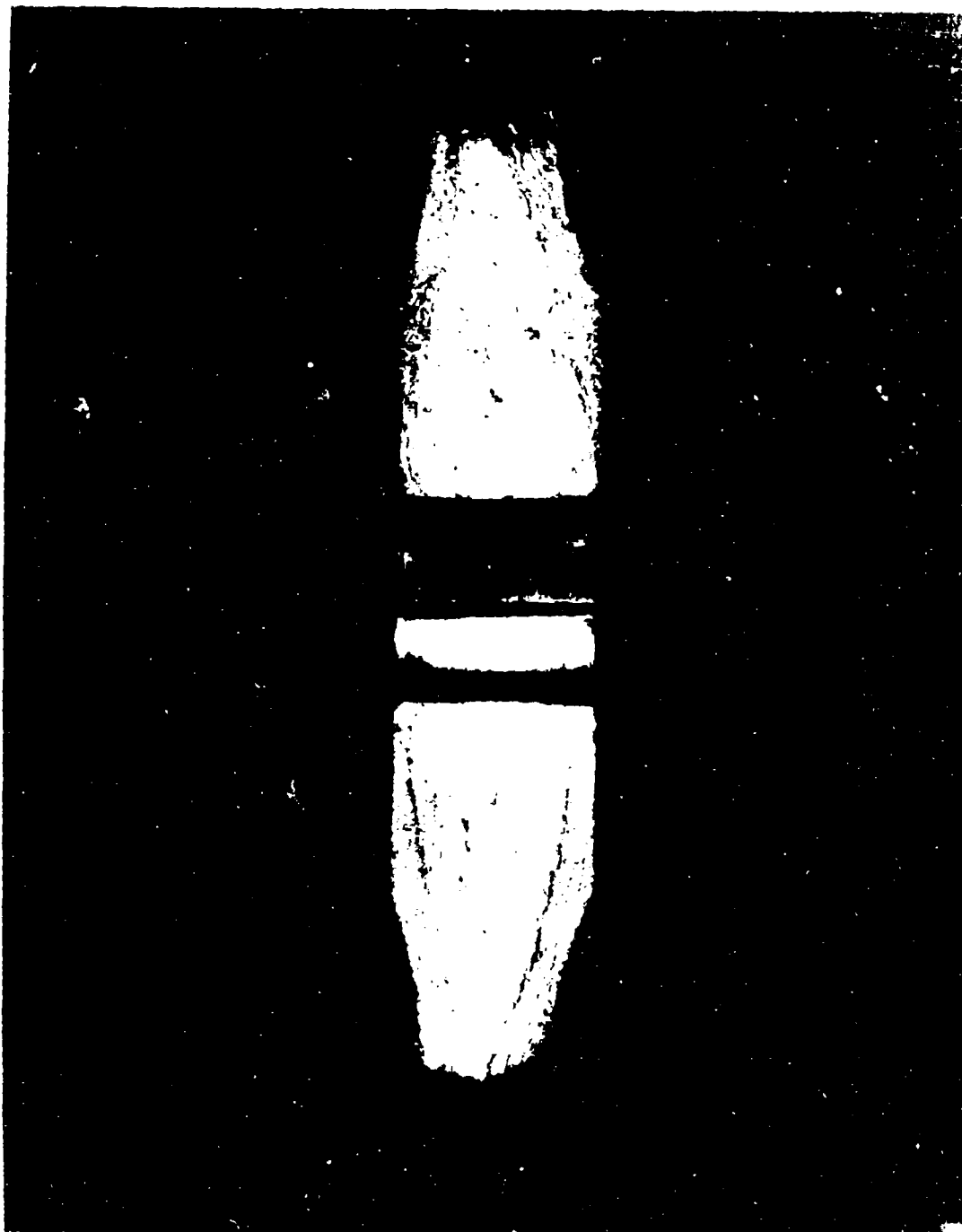
Figure 43. Secondary Rupture Surfaces, Test No. 1, Weld (180° around from primary fracture).

91
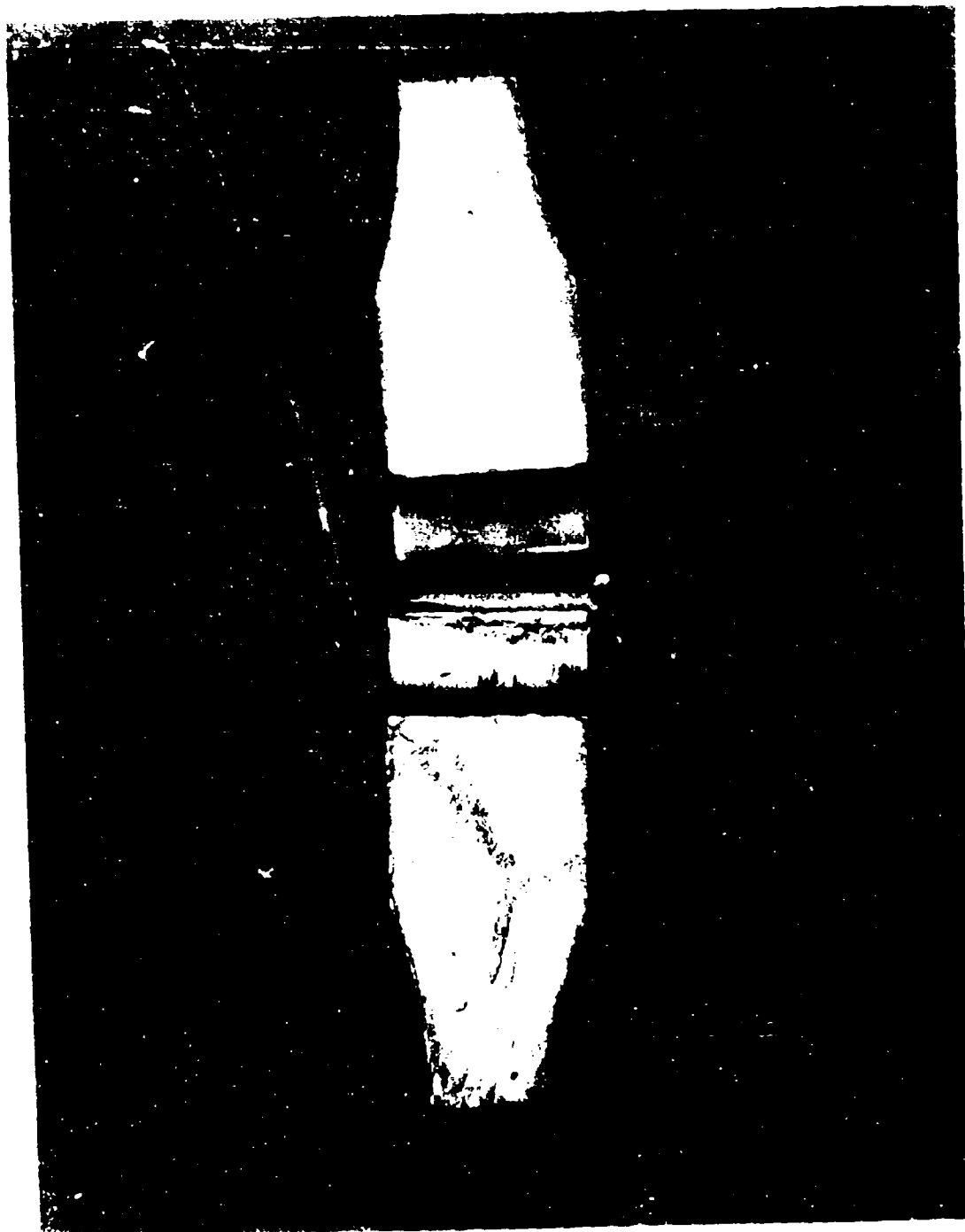
Figure 12. Primary Rupture Surface, Disk No. 1, 6h x20.

visible "final" crack size in figure 44 indicates that failure occurs as a thru crack becomes imminent (consistent with figure 36 prediction of final crack size).

D.   FERRIS WHEEL RIM LIFE TEST

The rim was tested using Test Disk No. 2 and consideration was given to the very conservative stress predictions illustrated in table 8 and discussed previously. The predicted live rim max stress location was eloxed as illustrated in figure 45. A crack growth (elox-to-0.030-in precrack) prediction was made by assuming that the severe elox damage would immediately initiate an active crack. After 1500 cycles and no crack growth the test loading was increased to the hydraulic system limit (producing stresses in Table 8) and 2000 additional cycles were applied without achieving an active crack. Testing was terminated to conserve program funds and allow evaluation of the test results illustrated in figure 46. This evaluation led to the conclusion that, due to the very low rim stress levels disclosed by the ferris wheel strain gages (Table 8) and unanticipated by the conservative 2-D rim stress system, testing the rim to failure without rework to amplify rim stress would not be cost effective. Program schedule and funds precluded this rework, so test No. 2 was concluded on the positive note that even at rim stresses significantly above engine operating stress a severe 0.020-in. long and 0.010-in. deep elox slot remained dormant. A close examination of the higher-stressed (Table 8) bolthole precracking revealed that the growth rate (slope of curve in figure 47) was valid only after a significant delay in initiation to an active crack. This clearly illustrates the intrinsic damage tolerance due to Ti 6-4 material behavior.

Front Face

Rear Face

(20) Elox Slots

0.010
0.006

0.022
0.018

0.100 ± 0.005

Section B-B

Bore

B

On Both Front and Rear Face
Elox 10 Slots Evenly
Spaced Around Rim

No. 60   No. 1   No. 2   No. 3   No.4   No.5   No. 6   No. 7

B

20°

Elox Slots
in Acute
Corners

View A

Front Face

Rear Face

0.120
± 0.005

0.010
0.008   Deep

0.004
0.006

View A. Expanded

FD 212913
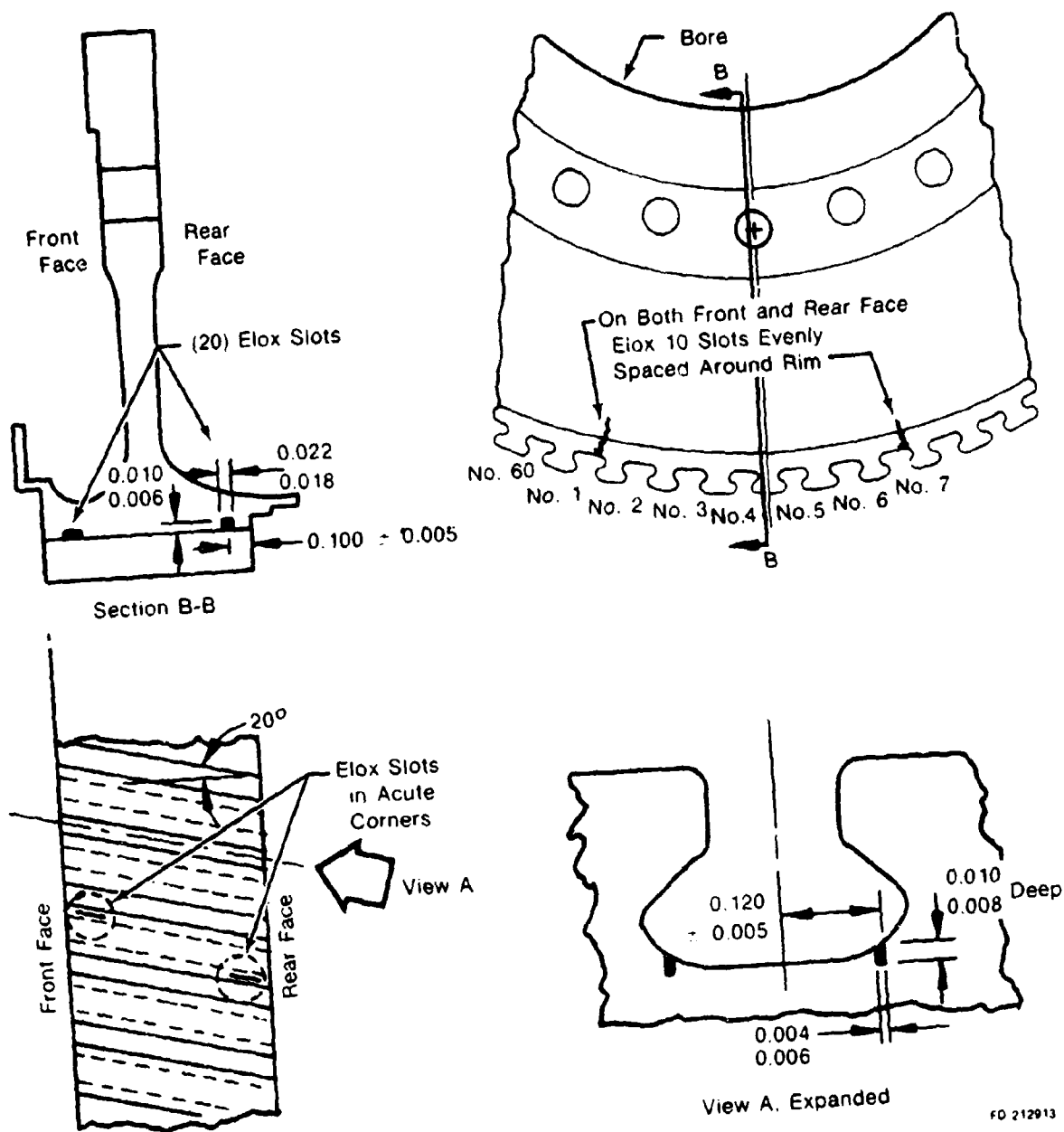
Figure 45.   Rim Elox Damage.
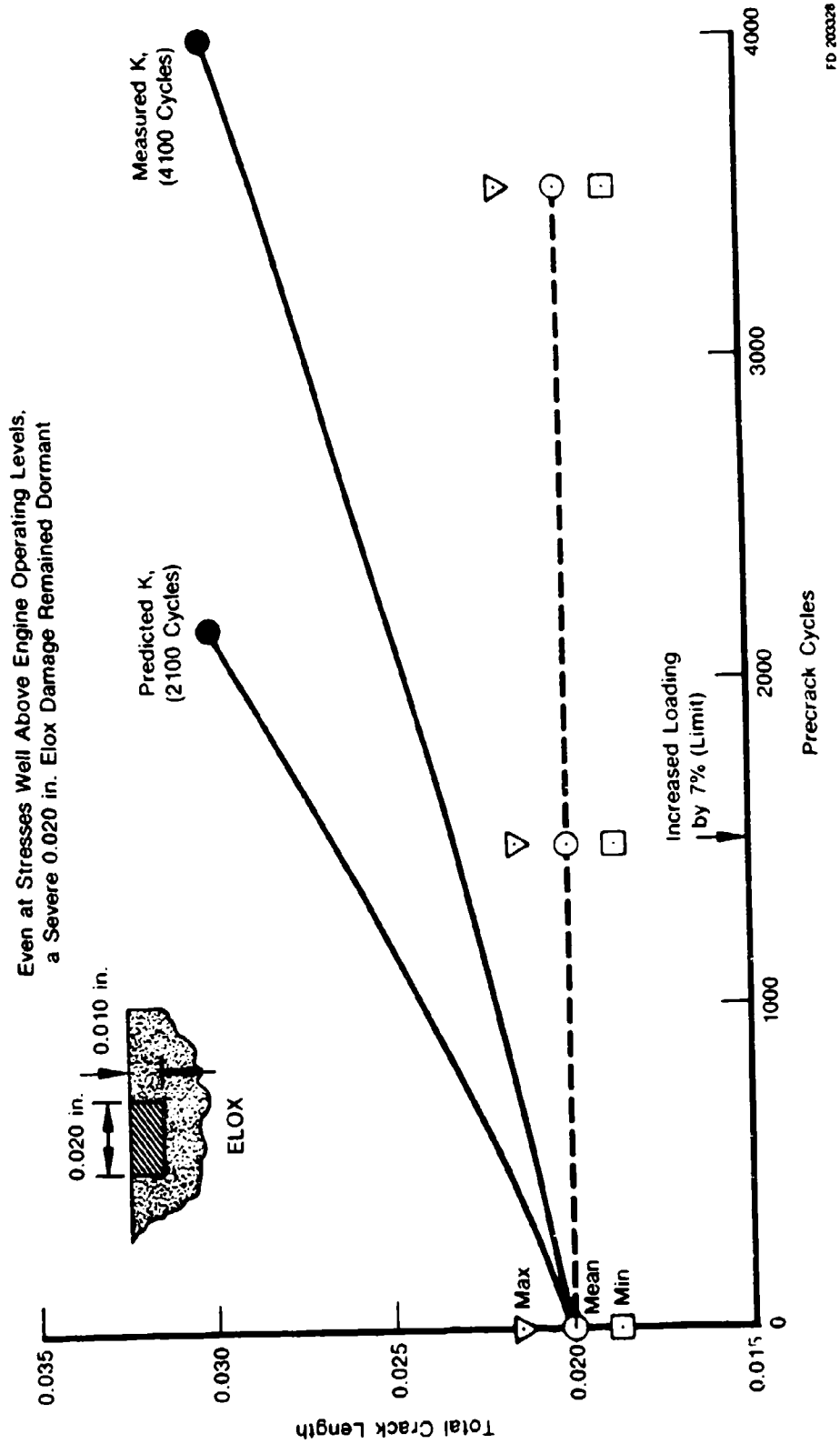
Figure 46. Ferris Wheel Rim Test.

FD 203328
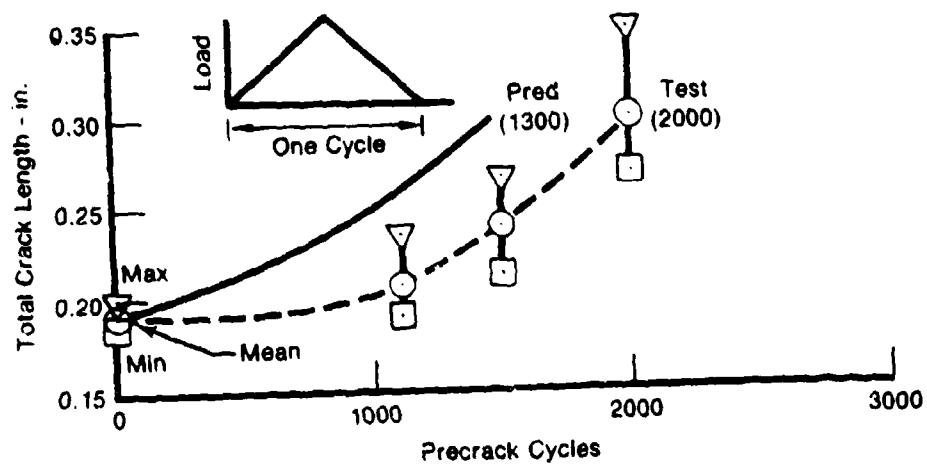
Figure 47.   Ferris Wheel Disk Test No. 1 Bolthole Precrack.

SECTION VII
TASK V - TEST-HARDWARE MATERIAL CHARACTERIZATION

A. BACKGROUND AND OBJECTIVES

The material P&WA chose to characterize for evaluating damage tolerant disk designs was Ti-6Al-4V.

Basic impetus in choosing Ti6Al-4V was to utilize a damage tolerant material in the contract which had a well characterized data base and would therefore require minimal additional testing. From this data base an interpolative crack growth model (da/dN vs K could be developed.

Titanium was chosen since the engine disk selection is the 2nd-stage fan. Fan weight studies conducted during the F100 engine programs showed weight penalties of up to 30 percent by substituting steel or iron-base alloys for the titanium disks. Of the candidate titanium alloys, Ti 6-4 was chosen because of its fracture toughness properties and large fracture mechanics data base thus requiring only a minimum number of specimen tests from the test disks heat code. The following is a description of the type tests run with Ti 6-4 specimens in the program, and the procedure utilized to develop the required da/dN vs K crack growth model for residual life analysis.

B. MATERIAL TESTS

Two types of testing were accomplished during the contract. One series of tests was used to demonstrate that the material purchased for this contract was typical of the material in the Ti6Al-4V data base, the other to supplement the fracture mechanics data base.

Forgings purchased for the contract were solution treated at 1745°F ±15°F for 1 hour, water quenched, annealed at 1300°F ±15°F for 2 hours and air cooled.

Specimens fabricated from the integrally forged test rings were used to qualify and accept the material. These test results are shown

97

in Table 5 compared to design typical and minimum specified values. All tests were run in accordance with ASTM E8-69 "Tension Testing of Metallic Materials."

In addition to conventional properties (tensile, yield, reduction in area, elongation, etc.) to qualify the material as typical Ti6Al-4V, a minimal number of fracture mechanics tests were run. These were intended both to verify the interpolative da/dN model developed from previously existing data, and to extend the data base at some conditions where insufficient data existed during the interpolative model development.

First, in July of 1978, the limited initial fracture mechanics testing covering four R-ratios confirmed that the Ti6Al-4V heat code "CDCH" used in this contract had comparable crack growth rate properties to the interpolative models Ti6-4 (AMS 4928) data base.

The data showed that a conservative representation of the material behavior was made by the crack growth model (section III-G) for regions where minimal data existed or where extrapolations were required during the model development. A comparison of the preliminary model predicted behavior and resultant data is shown in figures 48 through 54.

Comparisons of predicted da/dN vs ΔK (per the interpolative model) and observed da/dN vs ΔK from the specimens are shown first, followed by comparisons of predicted and observed crack size "a" versus cycles "N" for the same specimens.

C. INTERPOLATIVE CRACK GROWTH MODEL DEVELOPMENT

Early in the program effort, Section III-G, development of the interpolative da/dN vs ΔK material crack growth model for Ti6Al-4V was initiated. The interpolative model was required in order to perform residual life analysis at various mission conditions and had to include variable R-ratio ($R = \sigma_{min}/\sigma_{max}$), temperature, and frequency effects as provided by the data base.
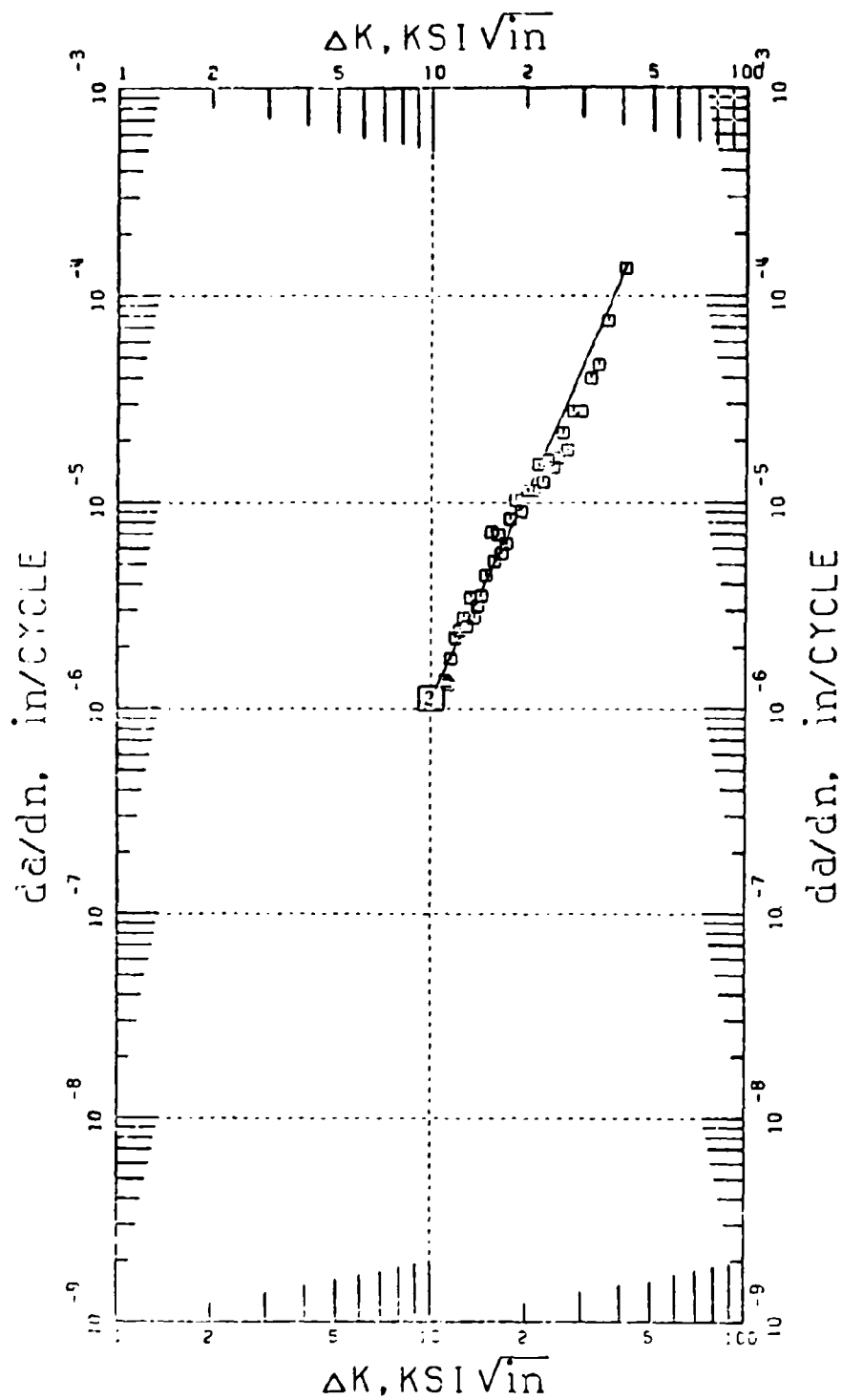
Figure 48. Ti6-4 Model Substantiation.
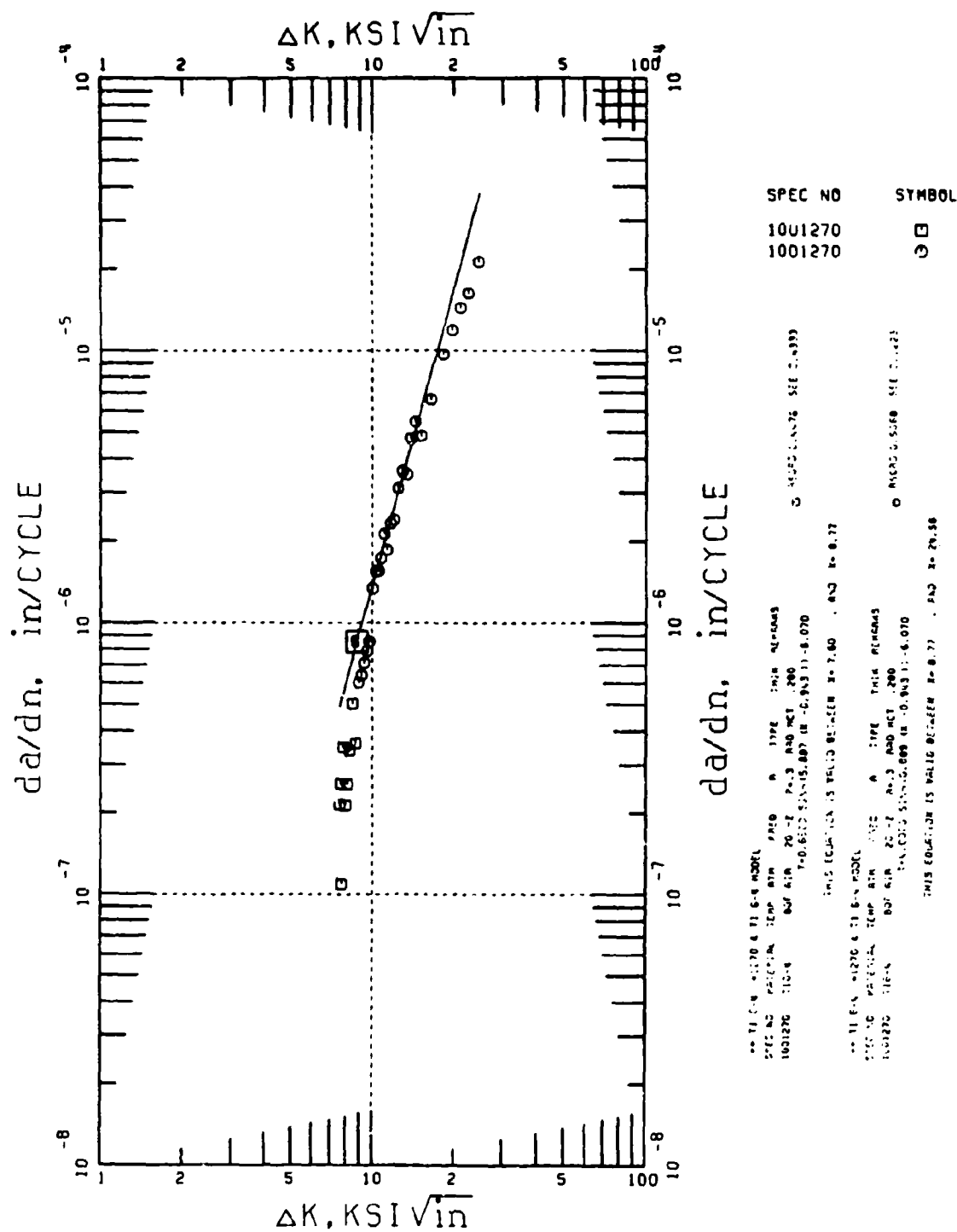
Figure 49. Ti6-4 Model Substantiation.
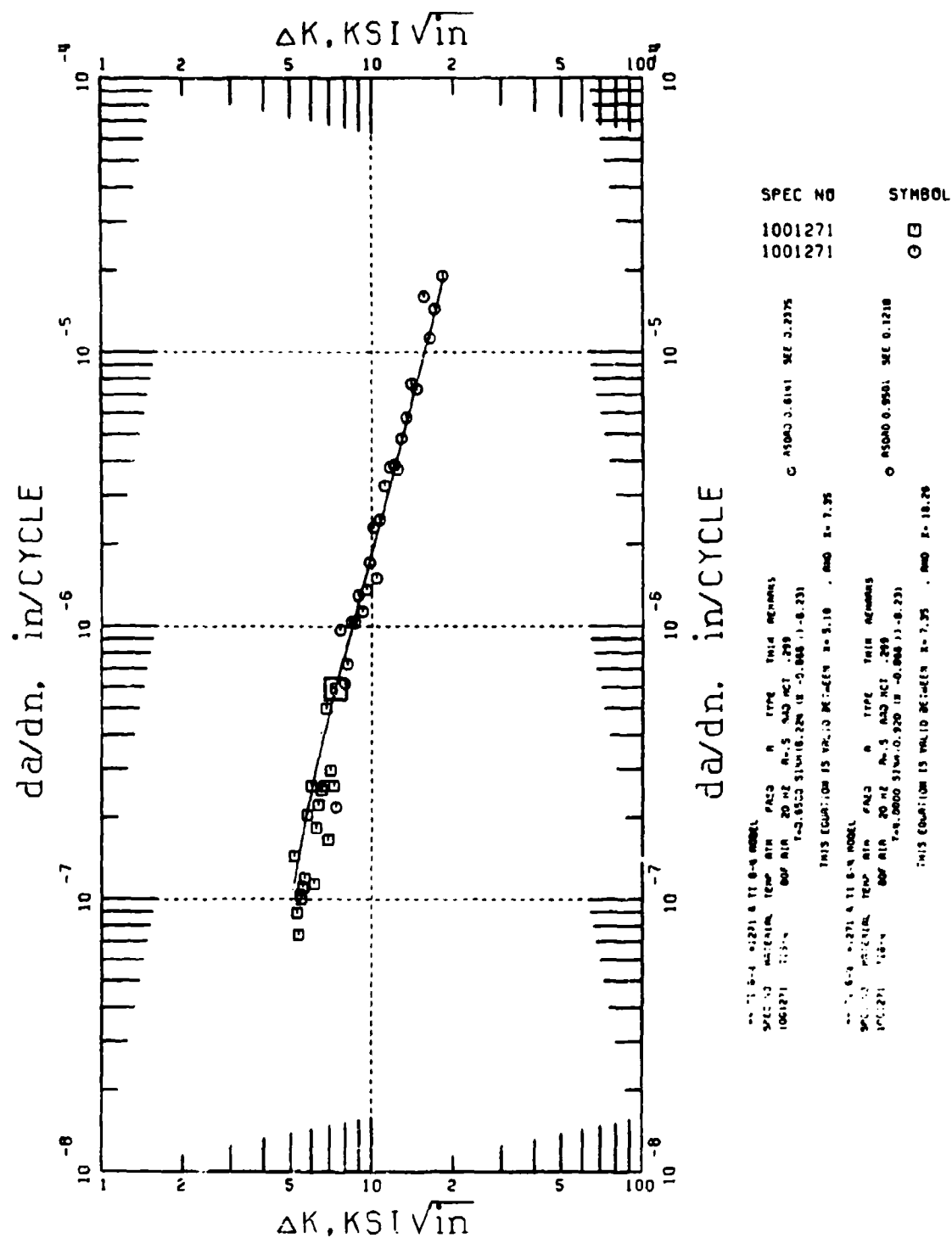
Figure 50. Ti6-4 Model Substantiation.
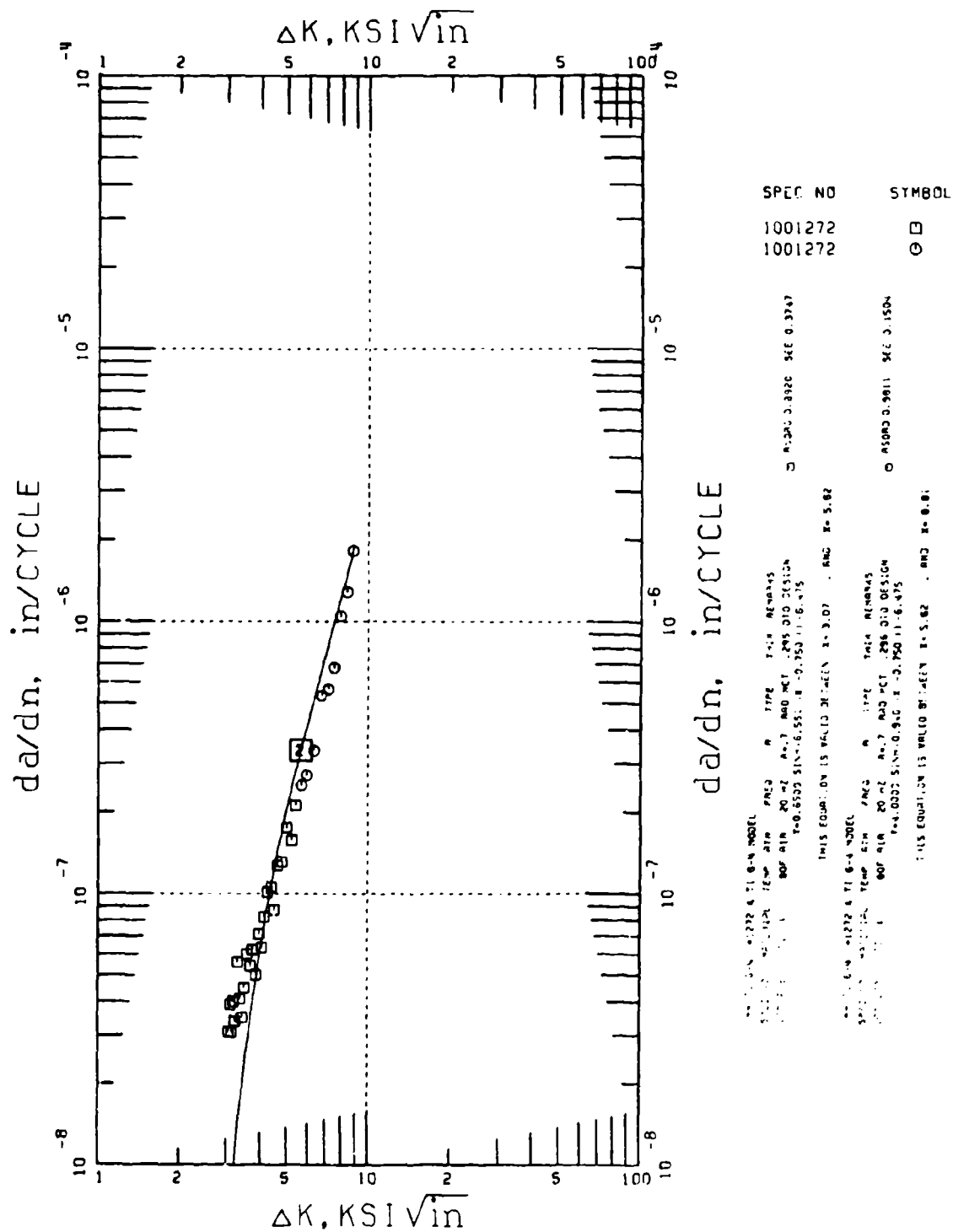
Figure 51.   Ti6-4 Model Substantiation.
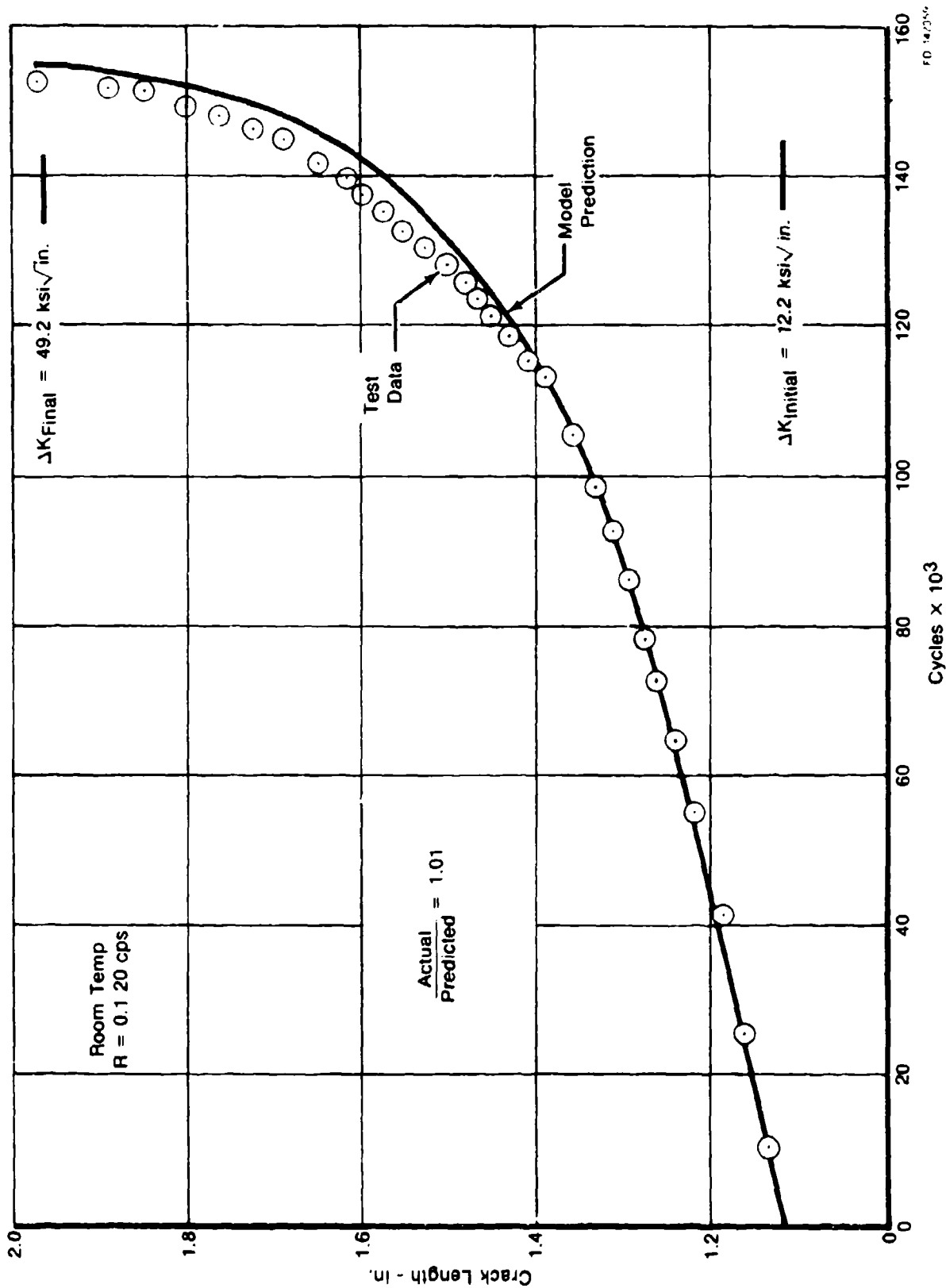
Figure 52. Ti6-4 Model Prediction of Specimen Number 1001269 (3) With Test Results.

103
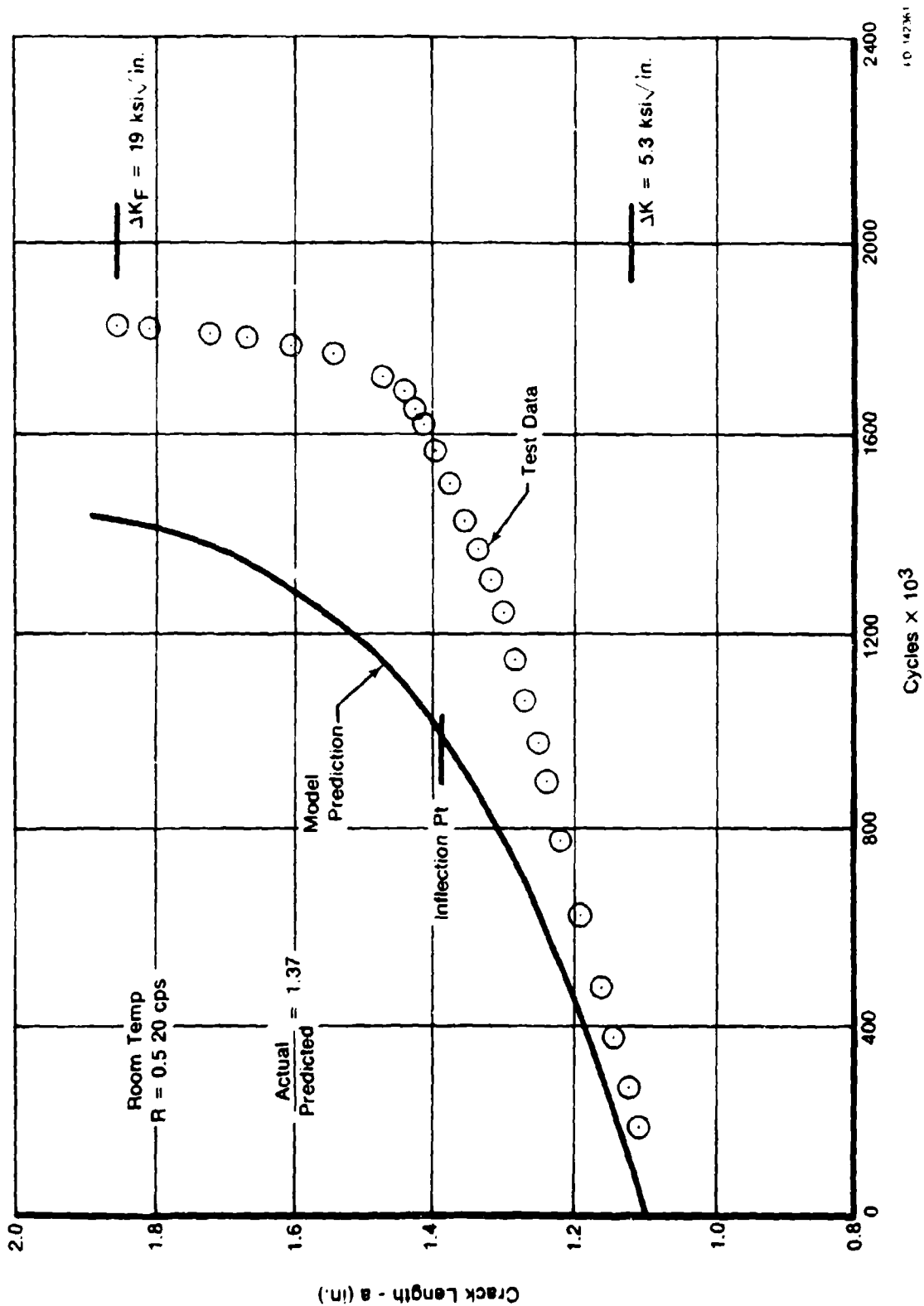
Figure 53. Ti6-4 Model Prediction of Specimen Number 1001271 (S) With Test Results.

104
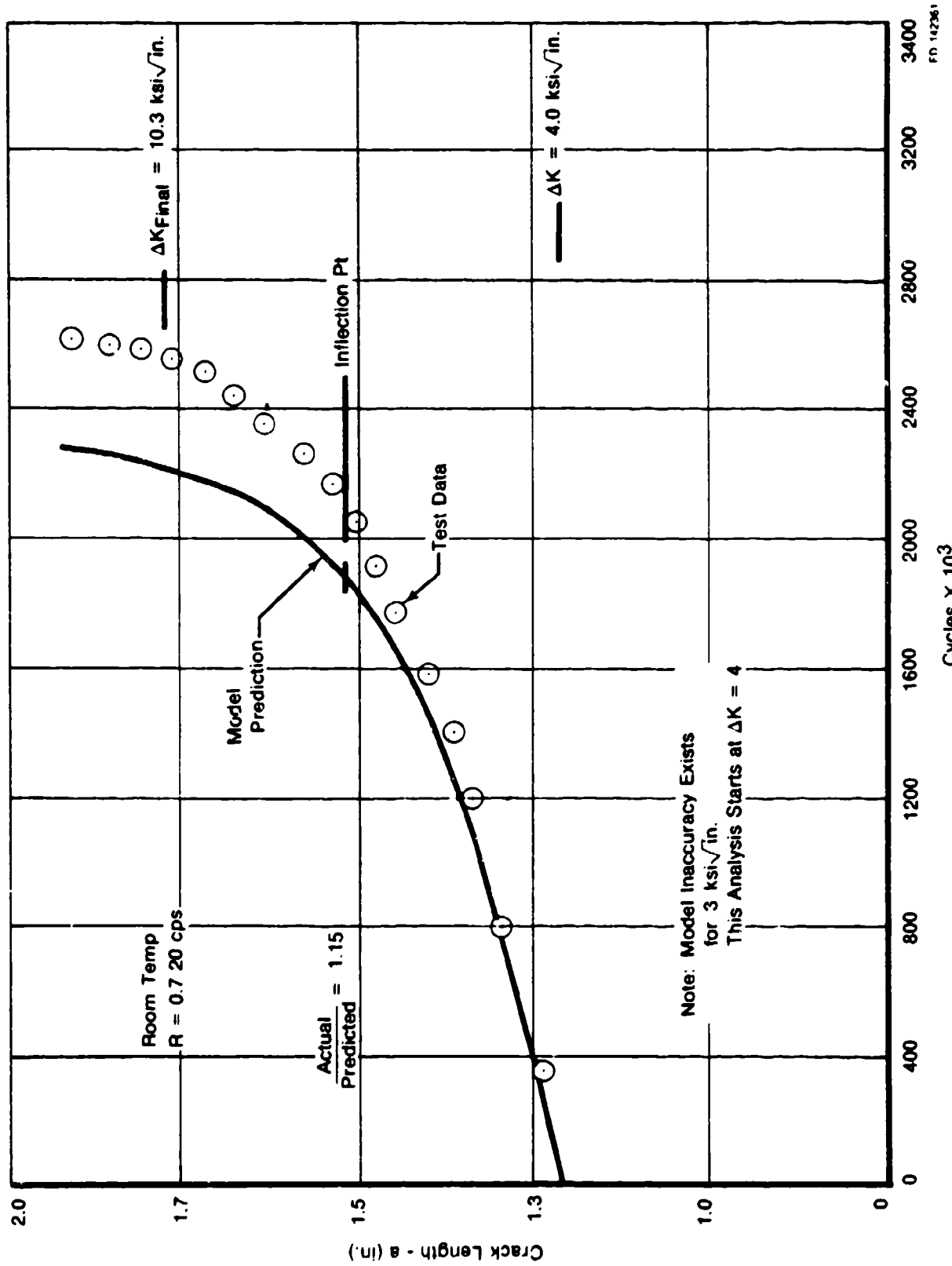
Figure 54. Ti6-4 Model Prediction of Specimen Number 1001271 (4) With Test Results.

A flow chart describing the model development procedure is shown in figure 55, and was planned as a logical extension of the modeling procedures developed and refined during AFML contract F33615-75-C-5097 "Application of Fracture Mechanics at Elevated Temperature".

The fracture mechanics data base was compiled from existing East Hartford Pratt Whitney Commercial Products Division testing, Grumman testing, and published damage tolerant design handbook curves.

From this data, a preliminary constant temperature, variable R-ratio model, for two frequency conditions, low and high frequency, was constructed. The low frequency model includes data run at $\leq$ 10cpm, whereas a very slight improvement in growth rates (slower) was noted in data available for frequencies $10 \longrightarrow 20$Hz. This was modeled as a separate high frequency model. The models were developed using the hyperbolic sine relationships developed in the AFML contract previously mentioned, and utilized four controlling parameters.

The defining equation for instantaneous growth rate is as follows:

$$da/dn = C_1 \sinh C_2 (\log \Delta K + C_3) + C_4$$

where: C_1, C_2, C_3, and C_4 affect the da/dn curve
as shown in figure 56.

Modeling guidelines at P&WA, when this modeling effort began, included the requirement that the mathematical relationship of C3 and C4 to the variables R-ratio, temperature, and frequency be described by straight lines.

To improve data fit, adhere to the linear modeling constraints, and not allow curves to unrealistically cross within R-ratios at a given temperature or frequency, a slight modification to the basic hyperbolic equation was implemented during development of the preliminary interpolative model. This simple innovation allowed different C_1 and C_2 coefficients to be used above and below the inflection point of any particular curve. The other modeling procedures remained consistent with then current procedures. This is shown schematically in figure 57.

106
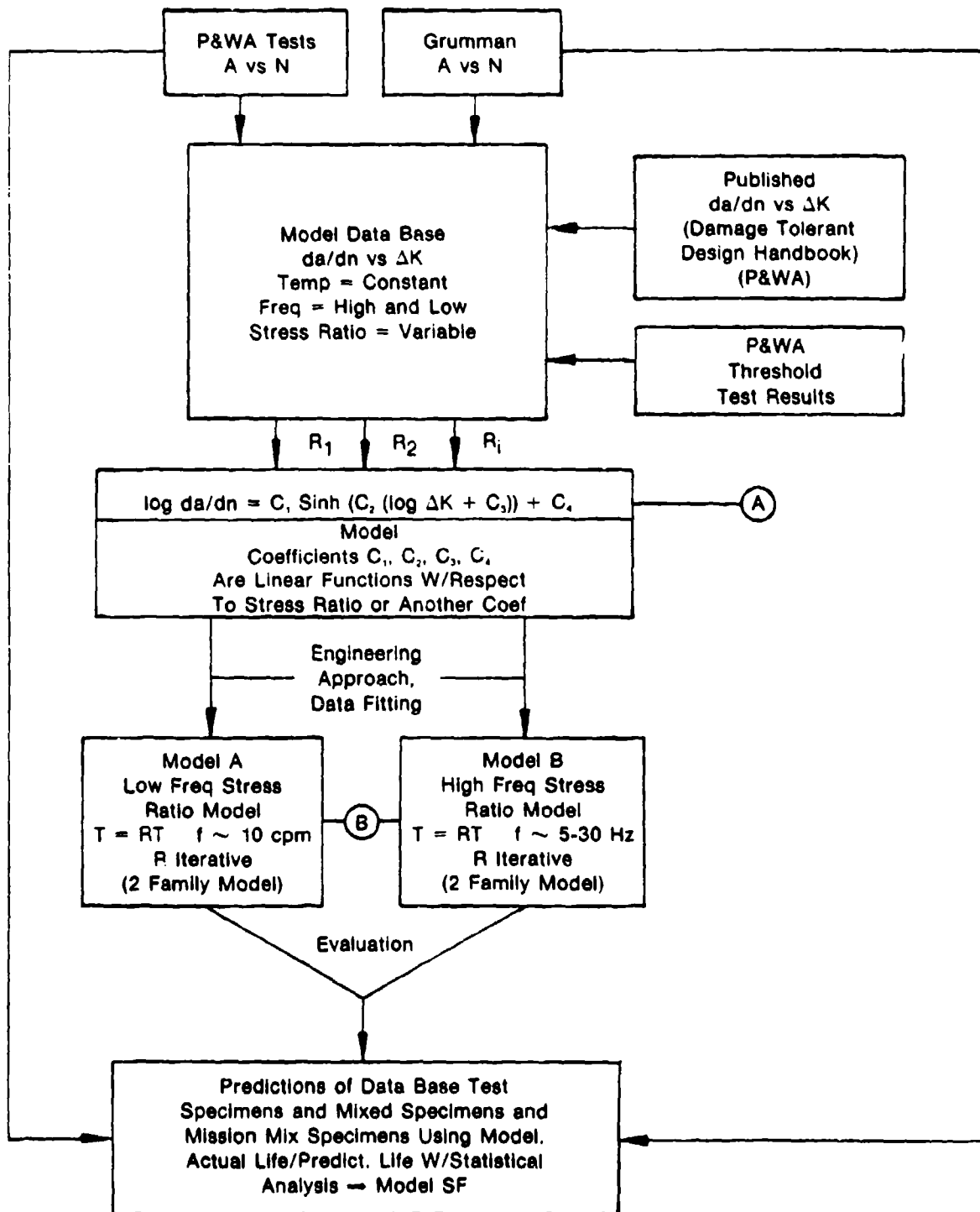
Figure 55. Model Development Flow Chart.
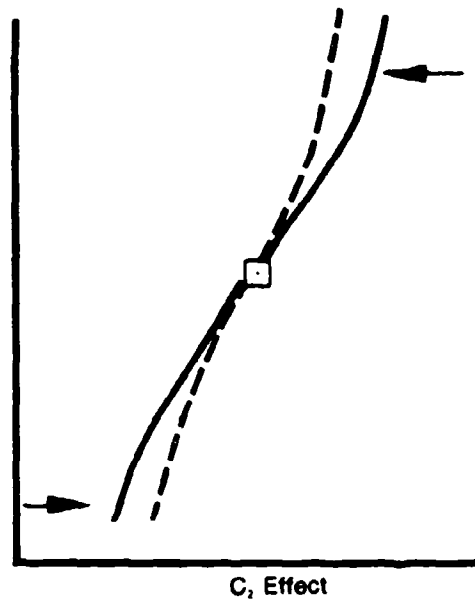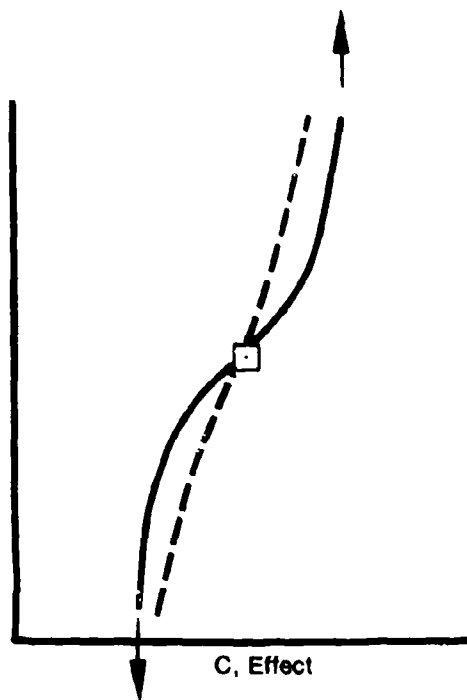
C₁ and C₂ - Shaping Coefficients
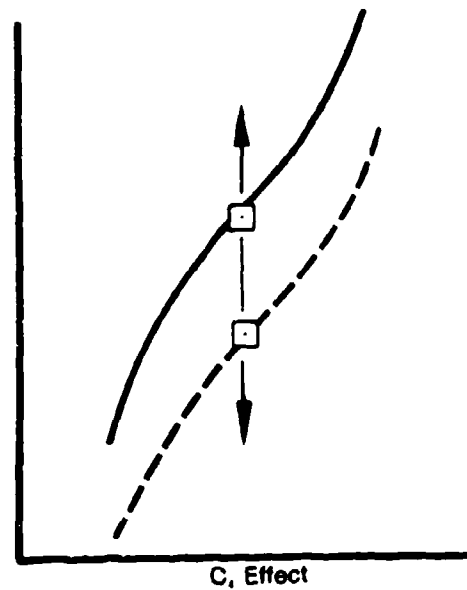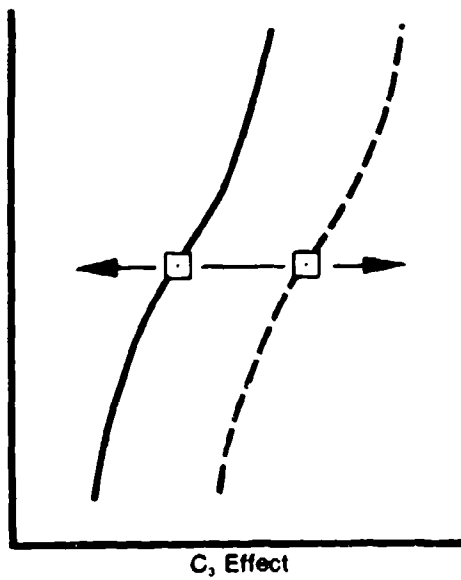
C₃ and C₄ - Inflection Point Locating Coefficients

FD 207099

Figure 56.   Coefficient Effects on Sinh Shapes.

108
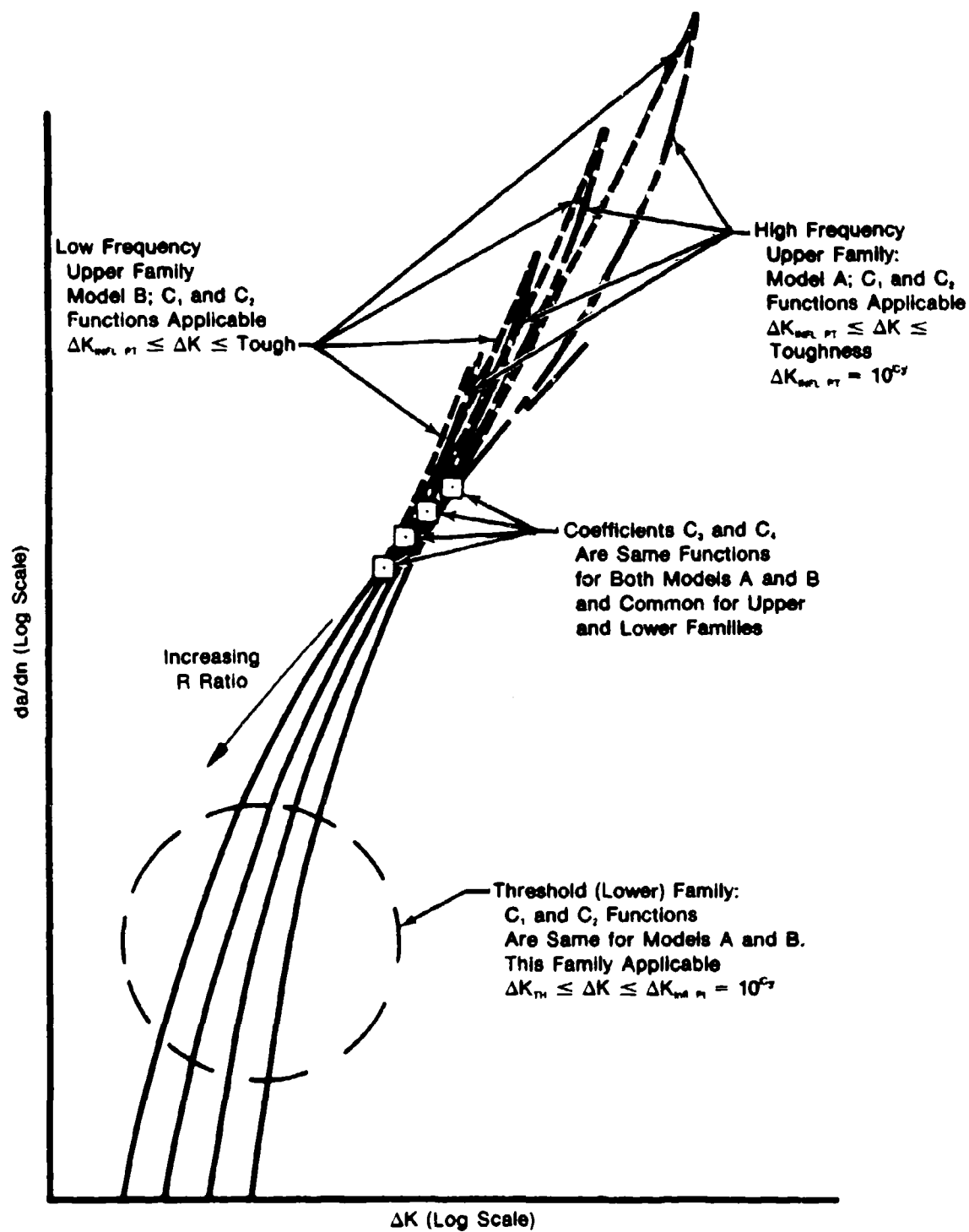
Figure 57. General Form For Preliminary Ti6-4 Model.

Elevated temperature da/dN data up to 650°F have been compared with the resultant iso-temperature model, and yielded acceptable results. For the preliminary model (see figure 58) the resultant analytical curves of da/dN vs K for various R-ratios are shown in figs 59 and 60 for the high and low frequencies. Analytical curves with data are included in Appendix C, along with model coefficients and statistical actual/predicted specimen life correlation plots.

Subsequent to this effort, the modeling procedures were refined by relaxing the requirement that related crack growth curves have inflection points that plot on a straight line. Relaxing this requirement was of some help in fitting the data with a single sinh curve rather than one above and another below the inflection point.

A replacement model was begun which incorporated the same data base, and is intended to provide equivalent accuracy in the (+) R-ratio regime. The replacement model was to have been refined to include (-) R-ratio capability using the additional data from task VII (supplementary material characterization and subcomponent tests, see section VIII following).
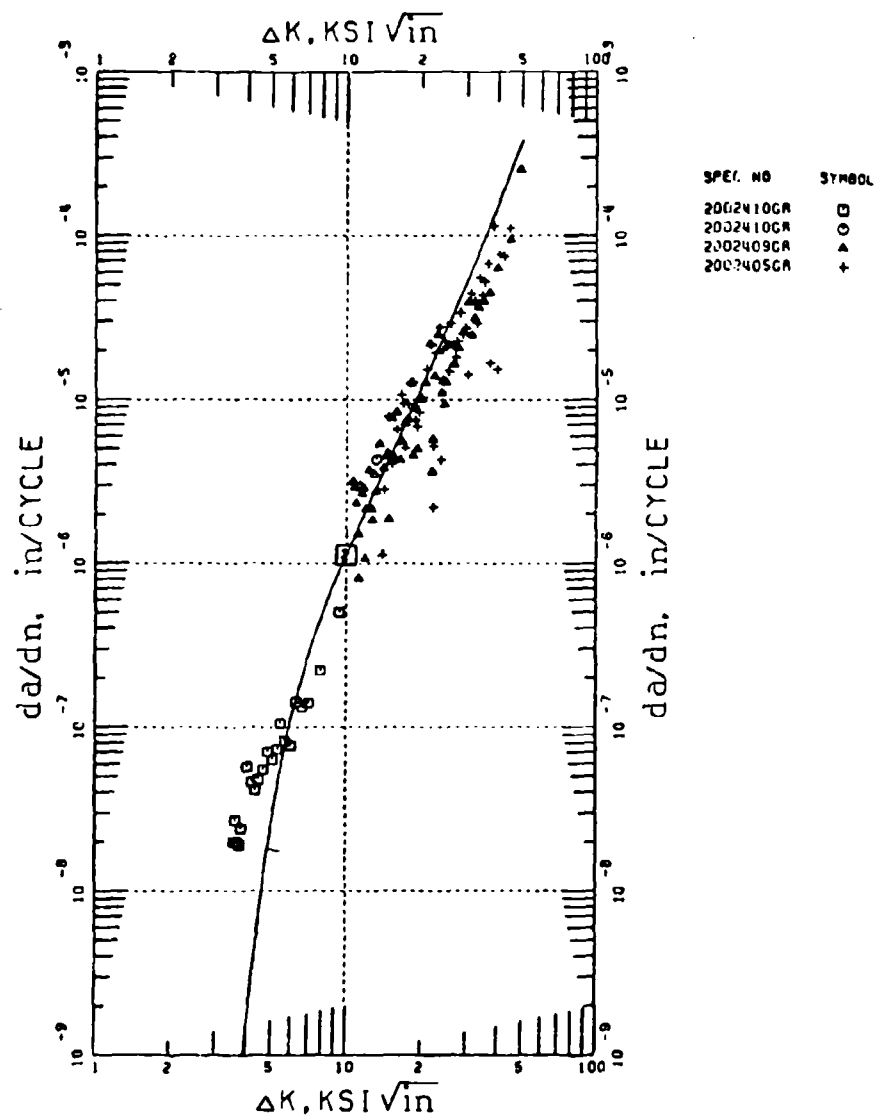
Figure 58.   Room Temperature Model Compared at 300°F.

111
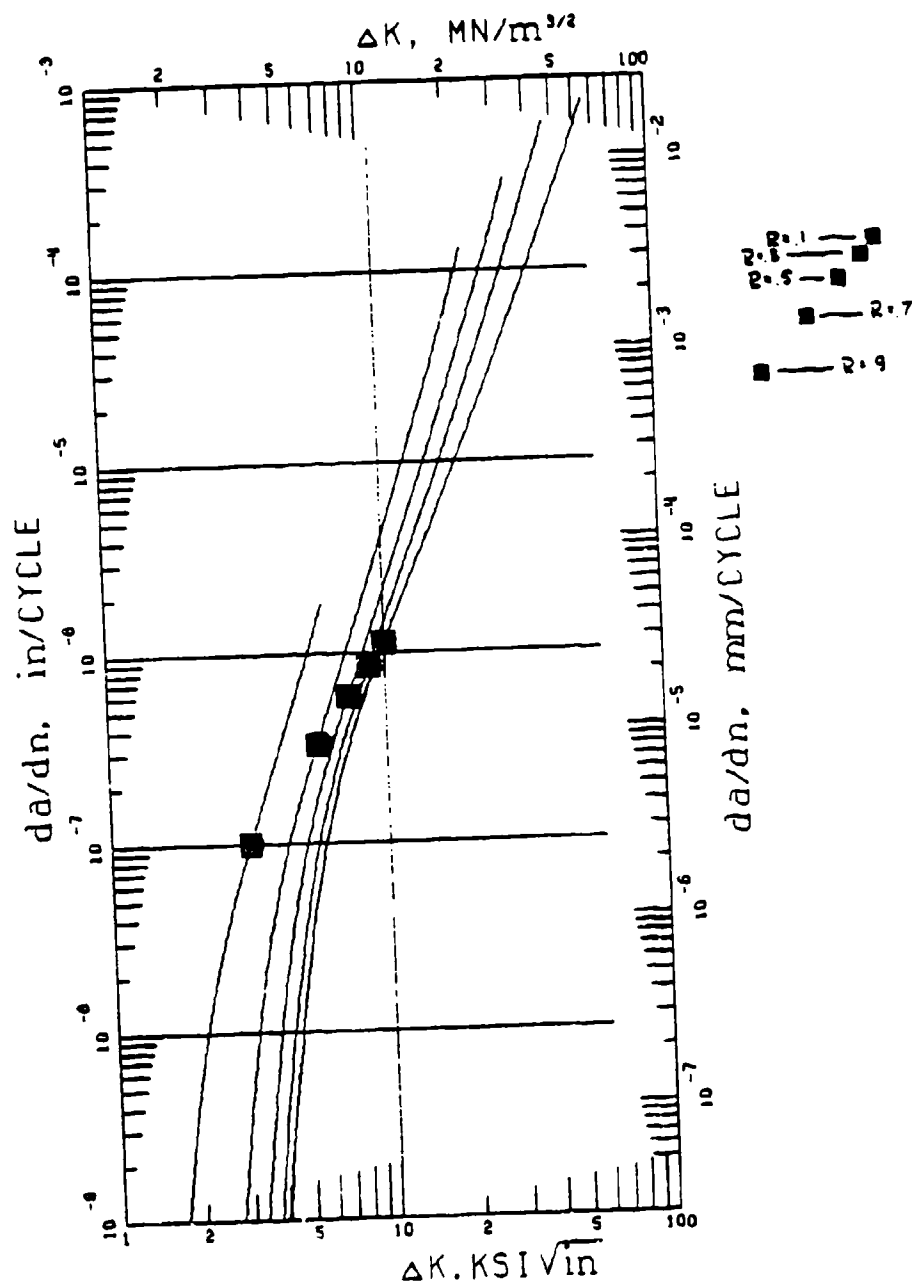
Figure 59. Ti 6-4 RT Low Frequency (10 cpm) Stress Ratio Model.

112
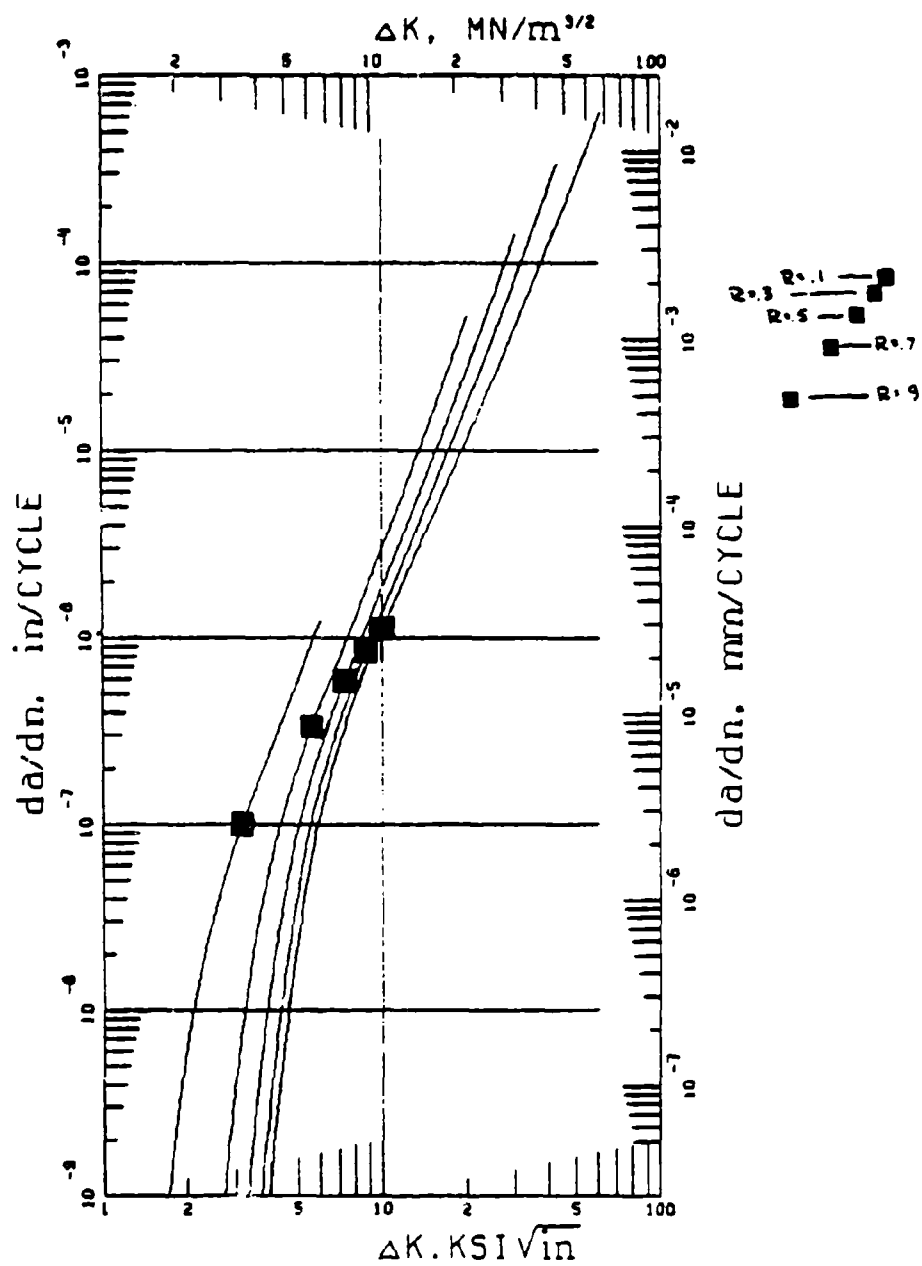
Figure 60.   Ti 6-4 RT High Frequency Stress Ratio Model.

SECTION VIII
TASK VII - SUPPLEMENTARY MATERIAL CHARACTERIZATION
AND SUBCOMPONENT TESTS

A.   BACKGROUND AND OBJECTIVES

During Task V (Material Characterization) limited test data indicated that Ti 6-4 exhibited a faster crack growth rate for the same maximum stress if compressive stresses were added to the applied stress range (i.e., (-) R-ratio degraded). It became necessary therefore to quantify these effects in order for the damage tolerant design system to correctly predict crack growth life at notch regions where deep compressive residual stresses are to be induced. To accomplish this, a supplementary data acquisition task was added to the program with the following twofold requirement:

o   provide crack growth data to extend the da/dN model to values of negative R-ratio consistent with the deep beneficial compressive residuals induced as part of the damage tolerant treatment.

o   provide life prediction calibration data for notched subcomponent (bolthole) specimens (satisfy last step in Fig 55).

Ti-6Al-4V material from the six disk forgings described in Section V was used to machine eight fracture mechanics compression specimens (figure 61) and ten bolthole specimens (figure 62).

The fracture specimens were specified for negative R-ratio testing to refine the interpolative material model of da/dN vs ΔK in the range of $-3.0 < R < -0.5$. The need for this data was to refine the replacement sinh material model used for crack growth prediction. The improved material model was to have been calibrated to the bolthole test specimens and used to predict ferris wheel test life.

The bolthole specimens were delivered to GPD's test lab and divided into groups of three to evaluate crack growth rate for:
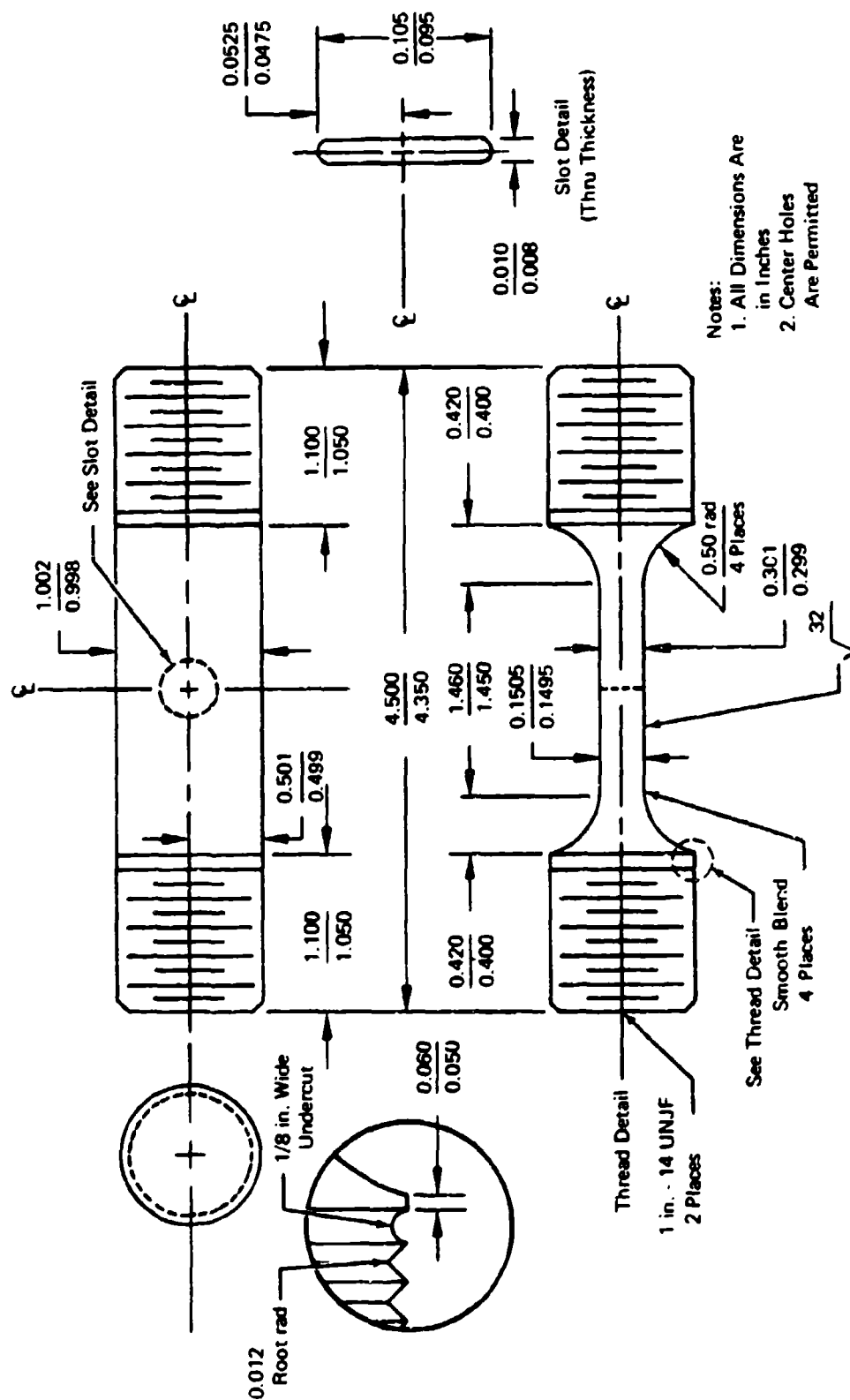
Figure 61. Thick-Section Center-Notched Specimen.

FO 184166

116

NOTES:

1 Holes Ⓐ Must Be Loc on Centerplane Ⓐ Within 0.001 Fir and Perpendicular With Surfaces Ⓐ, Ⓑ, Ⓒ, and Ⓓ Within 0.001 Fir Break Edges of Holes Ⓐ 0.010-0.020 rad both sides

2 Surf Ⓐ Must Be on Common Plane With Surf Ⓑ, and Surf Ⓒ on Common Plane With Surf Ⓓ, With 0.0005 Fir

3 Machine Centerhole Ⓑ to Fin Dim per MMT Engineering Instructions. Appropriate Instructions to Accompany this Drawing

See Figure 63

4 This Drawing Replaces Drawing No. FML 96327A

Ⓐ 0.6255 / 0.6250 dia
Ream or Bore Smooth
2 Holes Thru
Per Note 1

1.446 ref

$\frac{0.725}{0.721}$ Ⓐ 3 Ⓐ $\frac{0.725}{0.721}$

Ⓑ One Hole Thru, Machine Per Note ③

Ⓑ

$\frac{0.960}{0.940}$ 1.805 / 1.795 | 1.805 / 1.795 | $\frac{0.960}{0.940}$

5.500 ref

Attachment Sect. | Gage Sect. | Attachment Sect.

Surf Ⓐ

Surf Ⓑ

Surf Ⓒ

Surf Ⓓ

$\frac{0.750}{0.740}$ $\frac{0.750}{0.74C}$

32GAA

$\frac{0.750}{0.740}$ R

4 Places.
Blend Smoothly.
No Undercuts or
Ridges Permitted

0.500 Ref

$\frac{0.251}{0.249}$

$\frac{0.251}{0.249}$

$\frac{0.073}{0.072}$

$\frac{0.146}{0.144}$

Ⓐ

Sect. A-A

FD 184165

Figure 62. Bolthole Specimen.

117

1. No beneficial residual stress treatment

2. Precrack prior to "residual" treatment

3. Precrack after "residual" treatment.

The third group of three specimens was subjected to fifty cycles of load/unload to stabilize the work-hardening characteristics of the σ-ϵ hysteresis. Then all specimens were submitted for eloxing of a 0.005 in. (thick) by 0.010 in. (deep) by 0.020 in. (long) slot in the bolthole (figure 63). The eloxed slots were then cyclically loaded to a precrack size (0.030 in. surface length) and subsequent growth rates monitored during cyclic testing.

B. SPECIMEN CONFIGURATIONS

To acquire crack growth rate data (da/dN) for negative R-ratio, the thick section compression specimen was used (figure 61) in-lieu of the standard compact tension specimen. This provided compression-tension-compression loading capability.

To verify the material crack growth rate model, to verify the 500°F prespin treatment, and to calibrate the life prediction system; GPD's standard bolthole specimens (figure 62) were used. These subcomponent specimens are a required step in GPD's development of a calibrated damage integration package. For the purposes of this study, elox damage was used to initiate cracks in the desired location (figure 63) and a simple sawtooth cycle was used to precrack the specimens and to induce crack growth to failure.

C. BOLTHOLE SPECIMEN TESTS

Ten bolthole specimens were subjected to variations of damage tolerant treatment and tested as described in Table 9. Although the sample size is small, the observable trends in life results (figure 64) indicate that:

1) relative to Ti 6-2-4-6, slow crack growth rate in Ti 6-4 substantiates significant intrinsic damage tolerant capability

118

2) a significant further life improvement is caused by the overload treatment process.

3) treatment can be enhanced by controlling the sequence of thermo-mechanical loading (although residuals induced at ambient will not be entirely retained at engine operating temperatures).

4) life improvement (due to inducement of residual stress) increases significantly as test stress is decreased to engine operating levels.

5) Ti 6-2-4-6 with overload treatment (cryo spin) may also be a viable damage tolerant option ---discussion follows

0.145

Chamfer

0.297

0.020

0.030

ELOX Slot

View A-A
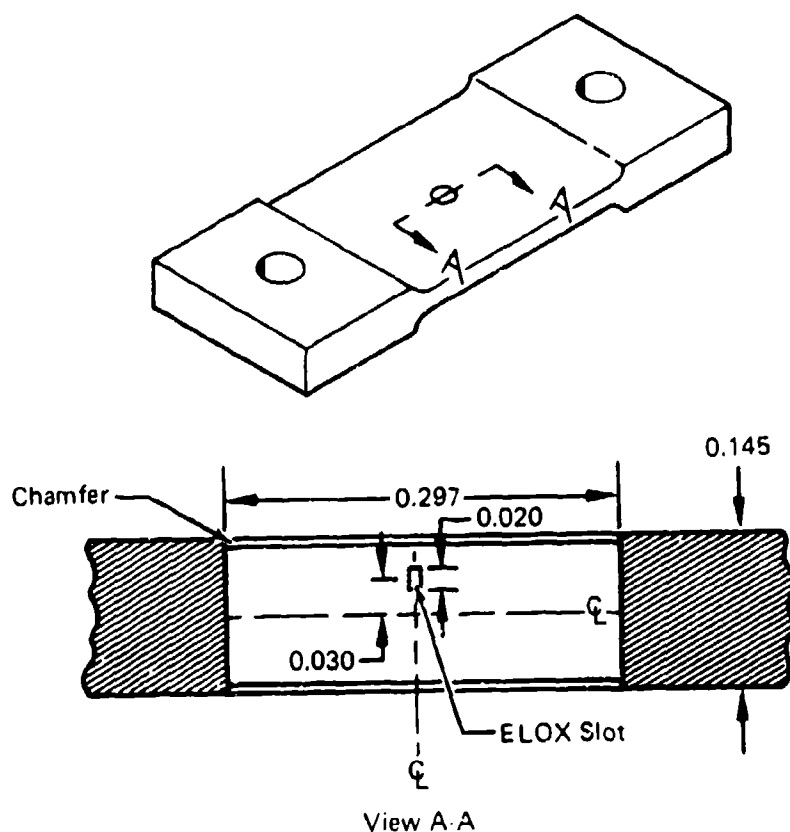
ELOX Slot Dimensions: 0.020-in. Length x 0.010-in. Depth x 0.005-in. Width

FD 184167

Figure 63. Flawed Bolthole Specimen.

119

TABLE 9. BOLTHOLE SPECIMEN TESTS

Sequence of Precrack vs Overload Treatment	Specimen No.	Elox Size (in.)	Cycles To 0.030 in. Crack	2a[1] at 2250 Cycles (in.)	Cycles From 0.030 in. To Failure	
A. BaseLine (No Overload)						
1) Elox	(1)	0.020	1500	0.050	2698	
	(2)	0.020	1500	0.040	2522	2650
	(3)	0.020	1500	0.048	2718	
B. Crack → Treat[2]						
1) Elox	(4)	0.020	1250	0.048	3500	
2) Precrack	(5)	0.020	1500	0.046	3221	
3) Treat	(6)	0.020	1500	0.047	3446	
C. Treat[2] → Crack						3300
1) 50 Cycles	(7)	0.019	1643	0.036	3600	
2) Treat	(8)	0.020	1600	0.039	2724	
3) Elox						
4) Precrack						
D. Crack → Treat[3]	(9)	0.019	1110	0.050	3700	
						3700
E. Treat[3] → Crack → Treat (2nd)	(10)	0.028	243	0.055	3700	

NOTES:
1) 2a = Crack surface length.
2) Test at Ambient, 70 Ksi, R = 0.05, 10 cpm following treatment, i.e., 500° Unload after "500°F, 70 Ksi (Nominal) K_t = 2.55" Overload
3) Same test except ambient unload after the 500°F overload.

Test life results (3300 cycles) indicate that the optimum beneficial residual (to yield 4100 cycles) had not been achieved. After study, it was recognized that the Task II prediction of creep-stress relaxation effects, which was based on assuming min-property creep behavior, was inconsistent with the typical property material being tested. Reanalysis indicated that for typical strength material the optimum disk residuals can be achieved by increasing the spin treatment speed to the point where reverse-yield residuals are achieved at the bolthole during subsequent unload (i.e., no creep deformation occurs in typical material).

A design system refinement resulted from this investigative effort. It was recognized that in a production-line treatment process, a means of varying treatment spin speed to account for

ACCELERATED LIFE TEST

Baseline, Ti 6-2-4-6
(Analytical Prediction)

Ti 6-2-4-6 with "Cryo" Treatment
(Related Test Data)

Baseline, Ti 6-4
(3 Specimens)

Ti 6-4 with Overload Residuals
(5 Specimens)

Ti 6-4 with Overload Residuals
Including Ambient Unload
(2 Specimens)

Ti 6-4 with Maximum
Overload Residuals
(Analytical Prediction)

ENGINE LOADING LEVEL

Baseline, Ti 6-4
(Analytical Prediction)

Ti 6-4 with Maximum Overload Residuals
(Analytical Prediction)

Ti 6-2-4-6, σ_{Range} = 178 ksi

Ti 6-4, σ_{Range} = 178 ksi

Ti 6-4, σ_{Range} = 120 ksi

5000+

2650

3300

3700

4100

3200

Life, Sawtooth Cycles
(0.030 in. — Failure)

0   1000   2000   3000   4000   5000   6000   7000   8000   9000   10,000+

FD 212914

Figure 64. Bolthole Specimen Testing.

121

variation in material strength would be required. In general this would be accomplished using semi-empirical speed selection curves correlated to forging specimen strength. Verification that the desired residual stresses were in fact induced would be achieved by post-spin measurement of disk growth.

Another significant result of the bolthole specimen testing was to compare data trends from this program against the cryogenic T16-2-4-6 bolthole testing results, and to recognize the cyro-spin process as a potential damage tolerant treatment not previously evaluated. Subsequent to the selection process in this program, a related GPD effort to evaluate spin treatment of T16-2-4-6 disks at cyrogenic temperature produced impressive results. By capitalizing on T16-2-4-6's lack of negative R-ratio degradation (compressive portion of applied stress cycle is not damaging), a significant life improvement (figure 64) can be achieved by inducing beneficial residuals. Note that the primary intent of the cyro-spin treatment is to reliably inspect for damage by screening for flaws significantly smaller that the A_i = 0.015-in. assumed by this program. In summary, the tools and techniques developed or refined in this program are applicable to a cryogenic-spin damage tolerant treatment process which when applied to T16-2-4-6 may offer damage tolerant design potential.

D. CRACK GROWTH SPECIMEN TEST AND LIFE PREDICTION CALIBRATION

The need for this testing was to extend the replacement-sinh material model (section VII-C) into the negative R-ratio range. Prior to this testing an existing preliminary model had been extrapolated into the negative R-ratio based on limited data at R = -1.0 (section VII--C). This existing model was found to correlate with excellent agreement with the bolthole specimen data (see figures 65, 66, 67, 68).

The initial effort to extend the replacement-sinh model using the seven new datapoints in the range $(-0.5) > R > (-1.0)$ produced a model which yielded unrealistic trends. During attempts to correlate with bolthole crack growth data the replacement-sinh model erroneously

• 25% Life Conservatism for Existing Extrapolated Model
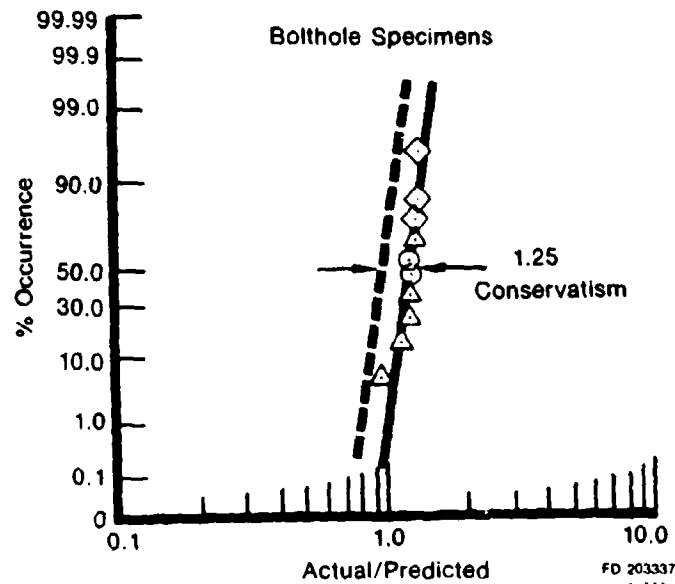
Figure 65.   Bolthole Specimen Life Correlation.
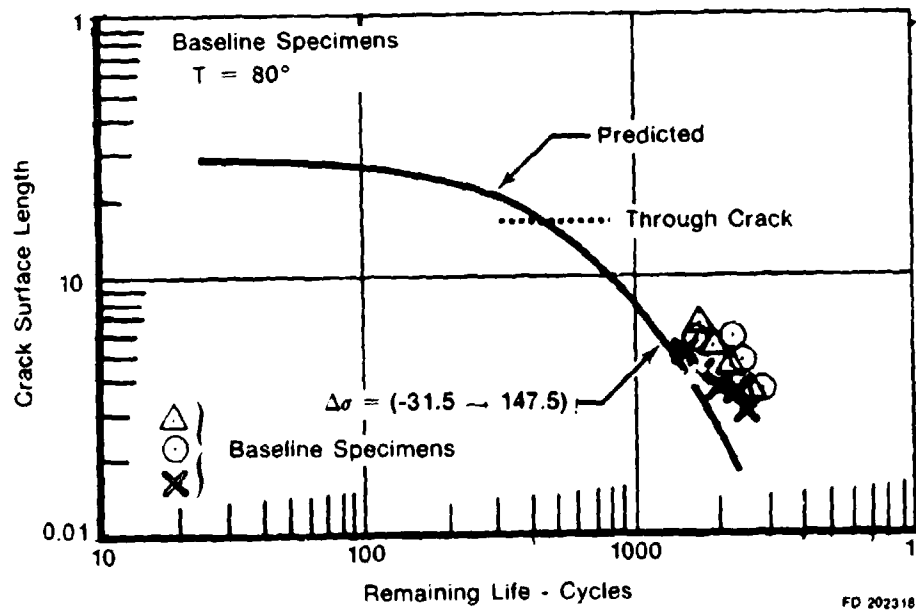
Figure 66.   AMS 4928 (Ti 6-4) D.T. Bolthole Correlation.
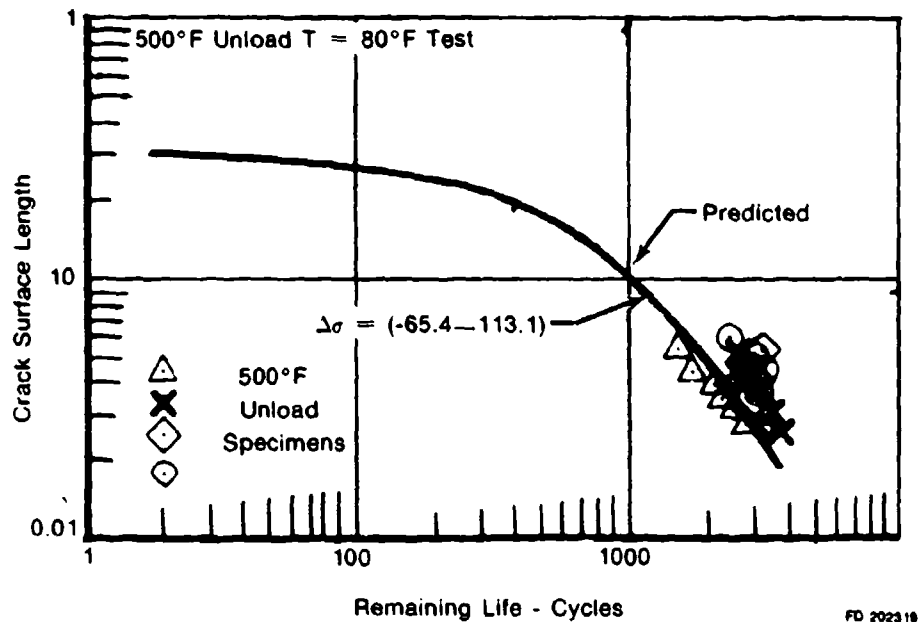
Figure 67.   AMS 4928 (Ti 6-4) D.T. Bolthole Correlation.
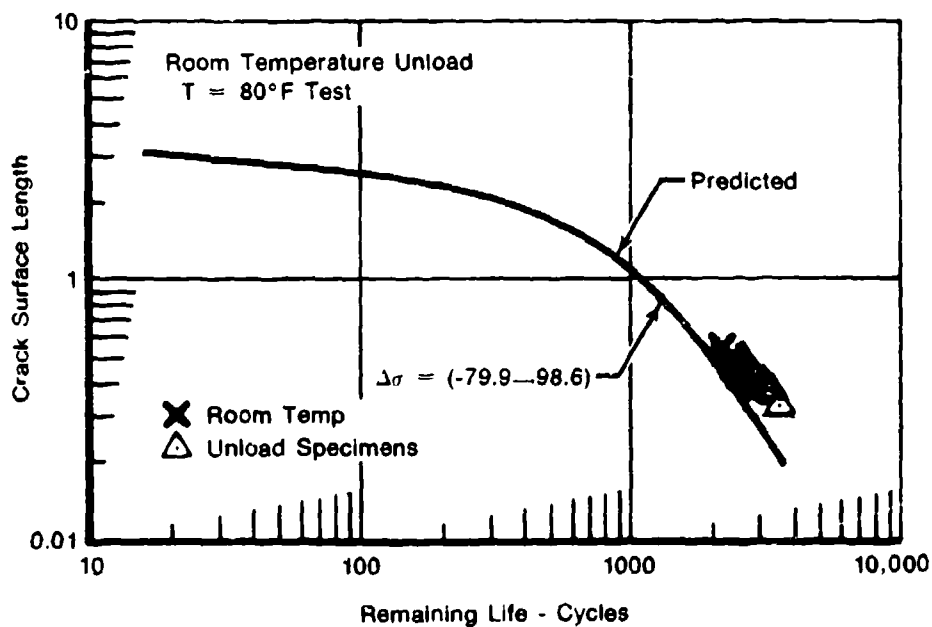
Figure 68.   AMS 4928 (Ti 6-4) D.T. Bolthole Correlation.

124

predicted that beneficial residual treatement decreased life. This indicated that the model was predicting too much negative ratio degradation within certain (-) R-ratio regions. This was largely due to the unequal crack lengths, both front to back and both sides, on the through-thickness specimens. We suspected an unplanned bending moment to be the cause. However, we could find no correlation between crack length differential and deviation from expected da/dN behavior, as would have resulted had the specimens experienced bending in addition to the tension-compression loading. Thus we were unable to incorporate these test results in our Ti6-4 da/dN model. Since currently, the Ti6-4 replacement-sinh model has been determined to be valid only for $R \geqslant 0$, the preliminary-sinh model which correlated well with test data was then used to predict disk life.

SECTION IX
SUMMARY, CONCLUSIONS, AND RECOMMENDATIONS

A.   INTRODUCTION

The preliminary design specification produced in this contract is modeled after the aircraft damage tolerant design specification and provides a nucleus which can be expanded through subsequent contracts (e.g., Hot Section Turbine Engine Disks and Retirement for Cause) to arrive at a comprehensive and mature document. The design system successfully demonstrated in this contract using a cold section disk is adaptable to hot section disks, other rotating components, and nonrotating structures. As a tool to assess existing designs it has been successfully applied in a variety of Air Force programs, including F100 Structural Assessment, TF30 Life Verification, and F100 Cryogenic Spin.

Selection of the F100 2nd-stage fan disk as the test hardware to be used in this contract was approved by the Air Force. It was shown that turbine engine cold section disks can be made damage tolerant by materials selection, modest weight addition, and residual stress treatments that do not constitute a radical departure from industry state of the art. The cost to manufacture damage tolerant disks was tracked and it was concluded that initial disk cost differences do not figure prominently in the determination of engine Life Cycle Cost.

In the case of the F100 2nd-stage fan disk the contract-stipulated assumption of 0.030 in. surface length flaw eliminated the Ti 6-2-4-6 B/M disk as a viable candidate. This led to a damage tolerant design in Ti 6-4 which satisfies the contract requirement to safely operate with 0.030 in. initial flaws. This design, when operated to its prescribed inspection interval, has approximately the same Life Cycle Cost as the B/M operated on a safe-life basis. Improving the NDE capability to reliably detect a 0.010 in. surface length flaw would make both disks viable on a common basis; i.e., with inspection intervals equal to one-third of their

127

respective safety limits. On this basis, the damage tolerant redesign achieves a 40 percent Life Cycle Cost saving relative to the B/M. Improved NDE capability, with residual stress achieved by cryogenic spin treatment would also allow consideration of Ti 6-2-4-6 damage tolerant designs which may meet the contract intent and be lighter than Ti 6-4 designs. Recent work, outside this contract, with cryogenic treatment of Ti 6-2-4-6 appears promising in this respect.

Ferris wheel testing to an accelerated mission test cycle established that the target life of 4000 engine operating hours was surpassed by the damage tolerant design disk. Application experience, strain gage data, and crack growth data were translated into refinements of the design system and are described in this report. A summary of activities, conclusions, and recommendations associated with each Phase and Task of this contractual effort is provided as follows.

B.   PHASE I, TASK I - DESIGN SYSTEM DEVELOPMENT

1.   A Preliminary Military Specification of Engine Damage Tolerance Requirements was provided.

The preliminary design specification produced in this contract is modeled after the aircraft damage tolerant design specification and provides a nucleus which can be expanded through subsequent contracts (e.g., Hot Section Turbine Engine Disks and Retirement for Cause) to arrive at a comprehensive and mature document.

2.   An initial design system was defined, developed and documented.

The design system successfully demonstrated in this contract using a cold section disk is adaptable to hot section disks, other rotating components, and non-rotating structures. As a tool to assess existing designs it has been successfully applied in a variety of Air Force programs, including F100 Structural Assessment, TF30 Life Verification and F100 Cyrogenic Spin

128

C.   PHASE II, Task II - ENGINE DISK SELECTION AND DESIGN

1. Selection of the F100 2nd-stage fan disk as the test-hardware
    to be used in this contract was approved.

2. Formal Air Force approval of the F100 composite duty cycle
    and of the equivalent damage cycle was received.

3. Damage tolerant redesign features were defined and   consisted
    of Ti 6-Al-4V in place of Ti 6-2-4-6, hot spin residual stress
    patterns   in   stress   concentration   regions,   and   geometry
    modifications as required to meet program objectives.

4. Design and selection, with Air Force approval, of damage
    tolerant concept No. 1 was completed. It required the least
    added weight, had the lowest Life-Cycle-Cost and was found to
    meet all program goals.

    Discussion: Turbine engine cold section disks can be made
    damage   tolerant   by   materials   selection,   modest   weight
    addition and spin treatments that do not constitute a radical
    departure from industry state of the art. The life cycle
    cost savings that result are very sensitive to the level of
    NDE technology available. In the case of the F100 2nd stage
    fan disk the contract-stipulated assumption of 0.030 in.
    surface length flaw eliminated the Ti 6-2-4-6 B/M disk as a
    viable candidate. This led to a damage tolerant design in
    Ti 6-4 which, at approximately the same acquisition cost and
    LCC as the B/M, satisfies the contract requirement for safely
    operating with 0.030 in flaws. An additional conclusion is
    that improving NDE capability to the level of 0.010 in.
    surface length flaws would allow a 40 percent savings in LCC
    for   the   Ti6-4   damage   tolerant   design.   Improved   NDE
    capability also allows consideration of Ti-6-2-4-6 damage
    tolerant designs which may meet this contract intent and be
    lighter than Ti 6-4 designs. Recent work, outside this
    contract, with cryogenic treatment of Ti 6-2-4-6 appears
    promising in this respect.

129

D. PHASE II, Task III - DISK FABRICATION AND HARDWARE STATUS

1. Fabrication of three test disks was completed at no cost to the contract.

   Other manufacturing requirements included provision of spin arbors, ferris wheel pull-bars, etc. The cost to manufacture damage tolerant disks was tracked and the conclusion reached is that initial disk cost differences do not figure prominently in the determination of engine Life Cycle Cost.

2. Disk number 1 was fabricated and tested to destruction in the bolthole.

3. Disk number 2 was fabricated and tested in the rim region, demonstrating much damage tolerance, and was not destroyed. It can be reoperated and retested to provide additional useful information concerning rim safety limit.

4. Disk number three was tested in the bolt holes and not destroyed. It can also be reoperated to provide additional rim safety limit information.

E. PHASE II, Task IV - DISK TEST AND DESIGN SYSTEM REFINEMENT

1. The target life of 4000 engine operating hours was surpassed.

2. Spin pit treatment effects were quantified by measuring crack growth behavior during ferris wheel testing.

   Test disks No. 1 and No. 2 received spin pit treatment and ferris wheel life testing to assess damage tolerance at bolthole and rimslot locations. Test disk #3 was ferris wheel tested without the spin pit treatment to provide a bolthole baseline.

130

3. Significant design system refinements were identified and are discussed in section IX-H.

F. PHASE II, Task V - TEST-HARDWARE MATERIAL CHARACTERIZATION

1. Test-hardware material characterization accomplished the goals for which it was prescribed, ie., the portion of the new data that duplicated the prior-existing data base confirmed that the material purchased to make damage tolerant disks in this program was typical and that the crack propagation behavior model constructed from the data base was applicable.

G. PHASE II, Task VII - SUPPLEMENTARY MATERIAL CHARACTERIZATION AND SELECTION

1. Seven fracture specimens were tested to acquire additional da/dN data for the range of $(-0.5) \geqslant R \geqslant (-1)$.

2. Ten bolthole specimens were tested to quantify the significant life improvement of the damage tolerant treatment and to verify calibration of the life prediction system.

Discussion: The difficulty of extending material crack growth models to large negative R-ratios was demonstrated by the inability to utilize the negative R-ratio data to generate an acceptable replacement material crack growth model. Fortunately the preliminary extrapolated crack growth model previously described was found to correlate conservatively with bolthole specimen data and provided accurate disk life predictions.

The bolthole specimens, although a supplementary task, proved to be indispensable. They focused attention to the need to account for acceptable variation in material strength, guided our evaluation of adequacy of the crack growth model, provided a low-cost preview to disk results, and allowed revision to the pre-spin plan.

131

H. DESIGN SYSTEM RECOMMENDATIONS

1. Normal variations in material properties necessitate several specific considerations for damage tolerant design of disks. These are:

a) Manufacturing production post-spin is to be selected based on forging strength qualification testing for each heat of disk material.

b) Disk growth should be "designed" using both minimum and typical material properties. Post-spin growth measurement is to be used to substantiate having achieved the proper treatment

c) Local inelastic behavior at stress-concentration features should consider use of maximum (upperbound) stress-strain and/or creep behavior to avoid optimistic prediction of beneficial residual stress.

2. Stress prediction procedures may require revision to accommodate "damage tolerant" and/or "retirement for cause" design philosophy. Specifically:

a) Damage tolerant structures, by nature of their using large beneficial residual stresses and achieving long life (figure 37), are very life sensitive to even small variations in stress

b) Significant stress predictior conservatism such as may be the case in the broach slot bottom of 3-dimensionally complex rims, is acceptable for "safe life" design philosophy but causes unacceptable overdesign (weight, costly material, etc.) in application of "damage tolerant" philosophy. A more rigorous 3D stress analysis may be required. Subsequent programs should provide further investigation of the following three-dimensional aspects of rim stress:

132

o   effect of blade untwist

o   effect of rim flexibility

o   effect of broach slot angle

o   effect of shroud fixity

o   effect of thermal gradients (hot section disks)

o   effect of complex geometry such as intersecting
        cooling holes, curved broach, slots for
        coverplate retention, etc.

Disks number two and three from this contract were
tested so as to facilitate their usage for a
follow-on rim analysis investigation.

c)   Costly, inelastic stress-concentration analysis is
        seldom required. The state of elastic stress/strain
        at local concentration regions can be adequately
        determined using 2-D or 3-D elastic finite-element
        analyses. To account for local surface plasticity
        located at strain concentration regions, a modified
        Neuber approach should be used to determine the
        controlling local surface inelastic (residual) stress
        values based on the 2-D or 3-D elastic analyses. The
        reference to the Neuber formulation is found in
        section III-H of this report. The term "modified"
        Neuber approach implies the use of a kinematic-
        hardening perfect-plasticity assumption for modeling
        the reverse yield situation. The Neuber method
        should be applied to the distribution away from the
        surface until calculated elastic stress levels
        converge to elastic values (i.e., below the
        proportional limit) while maintaining stress
        equilibrium. This method of approximating plasticity
        effects has been substantiated by correlation with
        specimen and component fatigue tests. Note that this
        does not preclude

133

requirements for inelastic (plasticity/creep) analysis for overall disk residual growth and corresponding "global" residual stress distribution.

3. A sophisticated analytical system of crack growth prediction is required. Specific recommendations relating to this contract include:

a) the "damage integration package" must recogn'ze the influence of R-ratio variation (vs. crack depth) due both to local and "global" residual stresses

b) a material crack-growth model with extension to large values of negative R-ratio is required. This model must be calibrated to component specimen testing to insure proper "blending" of (+) R-ratio and (−) R-ratio models.

c) to successfully predict crack growth behavior in complicated disk geometries under cyclic stress, sophisticated crack tip stress intensity factor (ΔK) prediction methods are required. ΔK is the parameter which embodies the effect of the stress field, the crack size and shape, and the local structural geometry. P&WA recommends use of the influence function theory derived, by J.R. Rice and H.F. Bueckner in life prediction algorithms for complex stress/geometry combinations. Details of the theory and procedures for developing the appropriate influence functions are available in the literature and can be obtained in the references found in section III-H of this report. Life prediction algorithms for part-through crack geometries such as full- or half-elliptical surface and corner cracks should be developed by contractors engaging in damage tolerant design of disks.

134

d) The empirically derived elastic fracture mechanics
    correlation of crack growth rate (da/dN) and crack
    tip stress intensity factor (ΔK) is numerically
    integrated to determine crack size as a function of
    cycle life. In basic form, the relation is:

$$N_{propagation} = \int_{a_{initial}}^{a_{final}} \frac{da}{f(\Delta K, \ R, \ temp, \ freq)}$$

where the numerical integration of this expression
will be performed on a cycle by cycle basis to the
defined engine duty cycle simulation.

The integration can be performed in a variety of ways
provided due regard is given to the particular load
spectrum and its potential for producing non-linear
crack growth response. An example of this effect is
the retardation of crack growth during cycles
subsequent to a cycle containing a significant
overload. In this connection it is said that the
structure has a memory, since its response to cycle
"n" is influenced by the nature of previous cycles
(n-1), (n-2), etc. The integration of spectra having
this complication must be handled by cumulative
damage models which incorporate retardation effects.

e) Models for crack growth retardation due to overloads
    are available in the literature for use where
    significant overloads do occur during operation.
    Some of the available models that are contained in
    the P&WA Fracture Mechanics life analysis decks as
    options are listed in Section III of this report.

135

Recognize that the damage tolerant design approach
employed in this contract was to apply that one
overpowering overload under controlled conditions so
that crack growth under all subsequent cycles would
be retarded. It must also be recognized that the
mission cycling of many turbine engine disks is like
that of the F100 2nd stage fan in that the mission
events produce differing minimum stress values but a
common maximum stress value. Under these conditions,
simple linear crack growth response is to be
expected. On the other hand, turbine disk stresses
are driven by thermal gradients in addition to
centrifugally induced stress. Consequently, the
opportunities for crack tip "blunting" by
mission-related overloads increase and the likelihood
of having to employ non-linear F/M increases
correspondingly.

APPENDIX A
MILITARY SPECIFICATION
ENGINE DAMAGE TOLERANCE REQUIREMENTS

1. SCOPE

1.1 This specification contains the damage tolerance requirements for aircraft flight safety when the design option of "retirement for cause" is applied to aircraft gas turbine engine cold section disks classified as safety of flight structure. Also specified herein are the conditions which determine when gas turbine engine disks must be classified as safety of flight structure. Acceptable levels of mean time between failure (MTBF) and confidence are specified for safety of flight structure. For structure not so classified, levels of MTBF and confidence are left to be determined by design optimization. The objective is to protect safety of flight structure from potentially deleterious effects of concentrated cyclic strains and of material, manufacturing and processing defects through control of stress levels, use of fracture mechanics design concepts, proper material selection and control, manufacturing and process controls and the use of careful inspection procedures. Requirements for aircraft flight safety when the "safe-life" design option is selected are outside the scope of this specification.

2. APPLICABLE DOCUMENTS

2.1 The following documents, of the issue in effect on date of invitation for bids or request for proposal, form a part of this specification to the extent specified herein:

SPECIFICATIONS

   Military

   MIL-E-5007   Engines,   Aircraft,   Turbojet,   and
                   Turbofan, General Specification for

STANDARDS

Military

MIL-STD-1534   Engines, Aircraft, Gas Turbine, Technical
Design Requirements

(Copies of documents required by suppliers in connection with specific
procurement functions should be obtained from the procuring activity
or as directed by the contracting officer.)

3.0 REQUIREMENTS

3.1 General requirements. Detailed damage tolerance requirements are
specified in various categories as a function of design concept and
degrees of inspectability which are defined in 6.2. The Contractor
shall demonstrate that all damage tolerant safety of flight structures
comply with the detailed requirements in a minimum of one of these
categories (one design concept and one inspectability level). Design
concepts utilizing multiple load paths and crack arrest features may
be qualified under the appropriate inspectability level(s) as either
slow crack growth or fail-safe structure. Single load-path structure
without crack arrest features must be qualified at the appropriate
inspectability levels as slow crack growth structure. The Contractor
shall perform all of the analytical and experimental work necessary to
demonstrate compliance with the damage tolerance analyses and tests as
specified herein and in MIL-E-5007, MIL-STD-1534 and the procurement
contract. This effort involves residual strength and crack growth
analyses and tests. The analyses shall assume the presence of low
cycle fatigue cracks placed in the most unfavorable location and
orientation with respect to the applied stress and material properties
and of subsurface defects that have been characterized in size,
location and orientation in bores and webs. The crack growth analyses
shall predict the growth behavior of these flaws in representative
chemical, thermal, and sustained and cyclic stress environments to
which that portion of the component shall be subjected in service.
The design flight-by-flight ∩ ·ess spectra and chemical and thermal

138

environment shall be developed by the Contractor and approved by the procuring activity. Interaction effects, such as variable loading and representative environment, shall be accounted for.

3.1.1 Initial flaw (crack) assumptions. Disk low cycle fatigue cracking shall be assumed to derive from two basic sources: (1) manufacturing or material process related defects. These occur predominately in large volume disk regions such as bores and webs where less material working is observed. These defects manifest themselves as either subsurface microstructural voids, metallic or nonmetallic inclusions, or heat treatment quench cracks; and (2) cracking occurring from local material with even smaller initial flaws (e.g. surface distress during machining) being cyclically deformed. These cracks are predominately observed in local stress concentration regions, and are due to either mechanical, thermal, or combined thermal-mechanical fatigue loading.

3.1.1.1 Initial crack size assumptions. Lacking documentary guidance of superior nondestructive inspection (NDE) capability, disk damage tolerant evaluations shall assume a 2 x 0.0XX in. (surface length) part through surface crack at each disk stress concentration feature. If special improved nondestructive inspection (NDE) techniques are developed and incorporated at the production and overhaul facilities, smaller initial cracks may be assumed. This shall require demonstration that the assumed crack size can be repeatedly detected with adequate (See footnote) probability and confidence levels. If proof spin techniques are employed by the Contractor initially and by the Government in the course of inspection, it is possible that smaller initial crack sizes based on analytically determined critical crack size at proof stress levels may be assumed.

3.1.1.1.1 Hole initial crack assumption. Disk bolthole failure data and bolthole specimen experience indicate that material, surface finish and bolthole length directly impact the crack initiation location (i.e., corner crack or bolthole surface crack). Therefore, initial crack assumptions for holes shall be categorized as to

finished and unfinished holes in thin and thick material. A finished surface shall imply application of polishing techniques and chamfering, whereas an unfinished hole implies an as-machined condition with no chamfering.

a. Hole (finished)

    (1) Thickness > 0.10 in. -   assume a single surface crack (length = 2.0 x 0.0XX in.; depth = 0.0XX in.)

    (2) Thickness ≤ 0.10 in. -   assume a single corner crack (0.0XX in. x 0.0XX in.)

b. Hole (unfinished - no chamfer)

    (1) Thickness ≥ 0.10 in. -   assume a single corner crack (0.0XX in. x 0.0XX in.)

    (2) Thickness < 0.10 in. -   assume a single through crack 0.0XX in. deep

3.1.1.1.2 Rim slot initial crack assumptions. Initial crack assumptions for disk rim slots shall be categorized by either axial or circumferential rim slot design. The assumed initial crack type (i.e., corner crack or surface crack) shall depend on the interactions between local stress concentrations, broach angle effects, and axial through thickness stress intensification effects. The Contractor must demonstrate suitable techniques for defining where low cycle fatigue (LCF) cracks will initiate.

---

*Definition of adequate inspection capability can be more realistically addressed in a program with broader scope. To be meaningful the investigation must include hot section as well as cold section disks. Avoidance of unwarranted conservatism requires that the investigation employ probabilistic methods rather than deterministic methods. A program that fulfills these requirements is the Retirement for Cause program, so the definition of adequate probability and confidence should come therefrom.

3.1.1.1.2.1 Axial rim slots. At the disk rim region assume the
following initial crack sizes following evaluation of candidate
designs to establish anticipated corner or center slot surface crack
locations. Lower rim regions and upper lug regions shall both be
considered.

*a. For indicated corner crack initiations assume a part
through corner crack of 0.0XX in. x 0.0XX in.

*b. For indicated center slot crack initiations assume a
2 x 0.0XX-in. surface length crack with depth of 0.0XX in.

3.1.1.1.2.2 Circumferential rim slots. The design of damage tolerant
circumferential rim attachments must consider two regions as shown in
figure A-1.

*a. Blade entry slot. For hoop loading the more limiting of
two locations and the associated initial crack size
assumptions for a blade entry slot shall determine its
residual life capability. Assume a 0.0XX-in. x 0.0XX-in.
corner crack at location (1) of figure A-1 and a
2 x 0.0XX-in. length surface crack with 0.0XX-in. depth at
location (2) of figure A-1.

*b. Dovetail slot bottoms (circumferential cracks). For tooth
bending loads at the dovetail slot limiting local stress
concentration at location (3) in figure A.1 assume a
2 x 0.0XX-in. length surface crack with 0.0XX-in. depth.

3.1.1.1.3 Bore and web initial defect assumptions. The probability
of manufacturing or material processing defects occurring in large
mass volume regions of disks shall be considered in damage tolerant
design evalutions. There are two possible approaches which can be
utilized depending on the extent of available data.

141
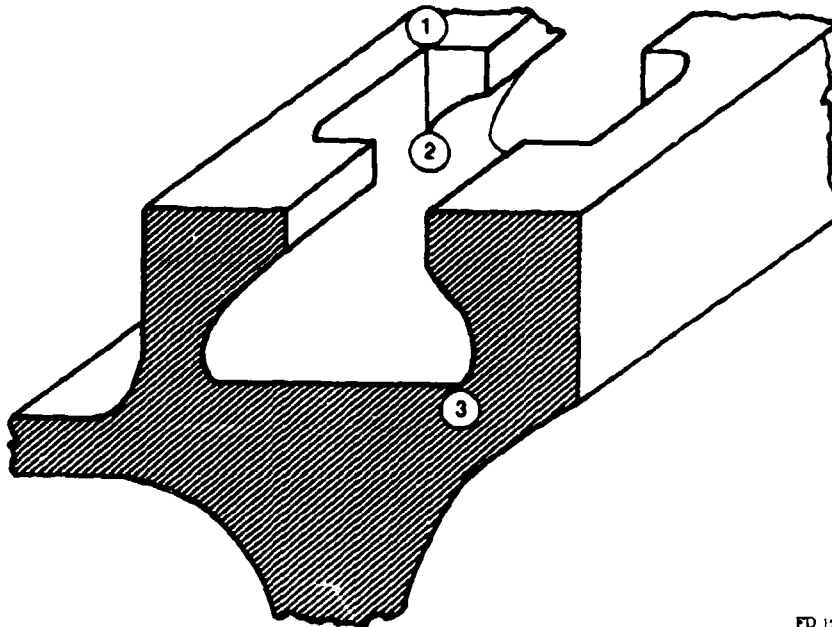
FD 124899

Figure A-1. Cicumferential Dovetail Configuration.

a. Probabilistic approach. This residual life approach is
    based on a Monte Carlo Variable Flaw Distribution method,
    and provides the most realistic answers for a given disk
    population. This method may be used provided sufficient
    vendor defect information exists to establish both the
    material flaw distribution curves and flaw preferential
    orientation trends. Figure A-2 provides a schematic of
    this method. The flaw distribution curves shall be
    truncated at the upper end based on NDE limits.

b. Deterministic approach. This residual life approach is
    based on a unique initial defect size assumption and should
    be used when insufficient data is available to define the
    Monte Carlo Model distribution curves. Bore and web
    initial defect sizes shall be set at the NDE acceptance
    limits, and assumed to exist in every disk of the
    population.

142
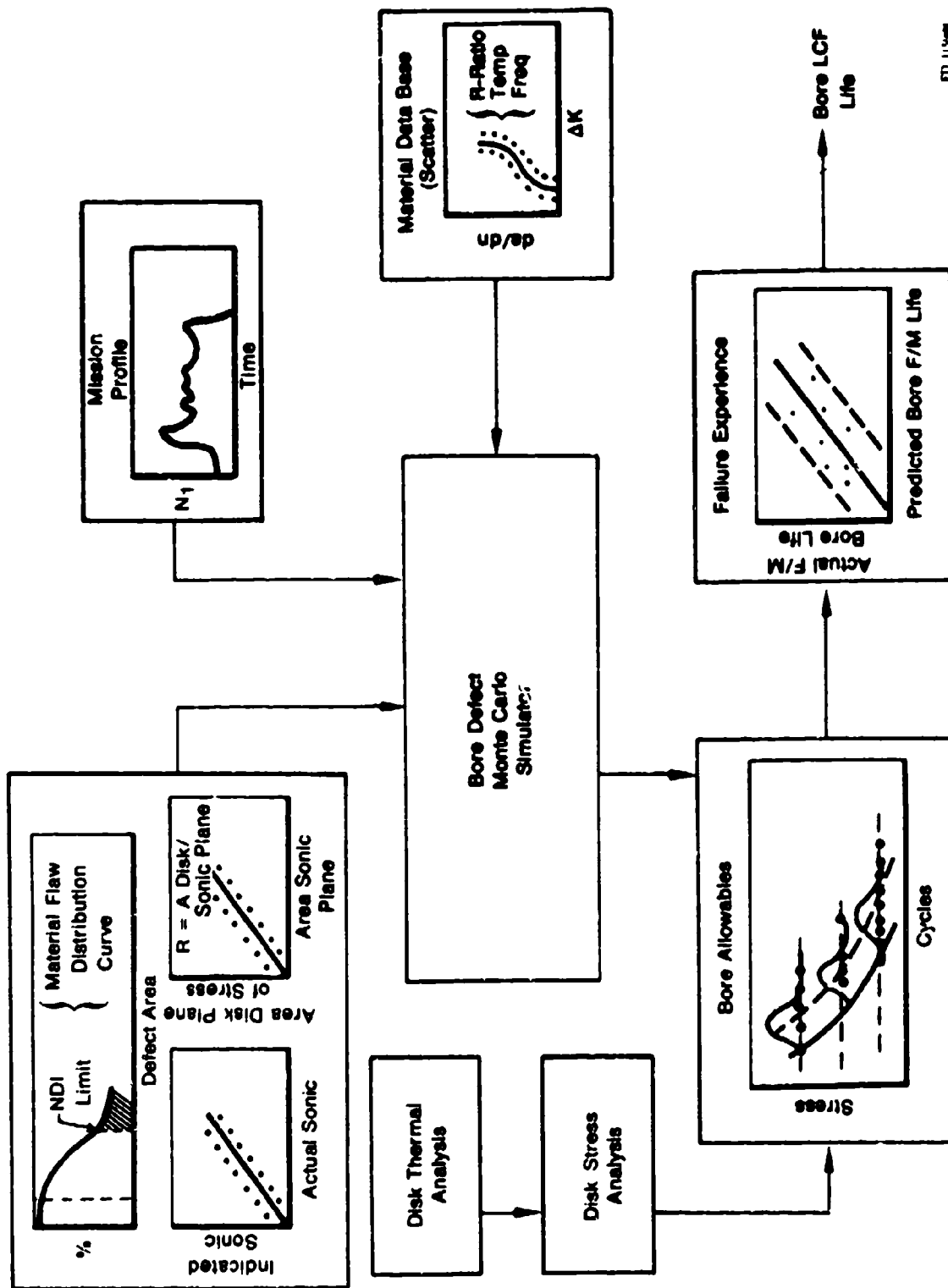
Figure A-2. Bore Defect Fracture Mechanics (F/M) System.

143

3.1.1.2 Continuing damage. Cyclic crack growth behavior of some stress concentration regions is discontinuous as a result of specific geometry conditions (finite width, thickness, etc.). Slow crack growth is observed to terminate at one free edge before reinitiation and continued crack growth from another location occurs. An example of this is disk balance weight flange holes with small edge distances at which initiation and growth to the free edge occurs. Subsequent to this, reinitiation and growth to failure occurs from the diametrically opposite face of the hole.

a. When ... growth from an assumed initial crack is terminated due to local geometry effects and reinitiation occurs from a secondary location, the stress field assumed for continuing crack growth analysis shall include the influence of the prior crack's inability to transmit load.

b. The initial assumed crack size for a continuing crack growth analysis (i.e., secondary crack location) shall be determined by analysis considering geometry and loading).

3.1.1.3 Remaining structure damage.

3.1.1.3.1 Fail-safe multiple load path. The damage assumed to exist in the alternate load path at the location of primary failure in fail-safe multiple load path structure at the time of and subsequent to the failure of a primary load path shall be as follows:

a. Multiple load path dependent structure. It shall be assumed that the original defects in the dependent paths grew and attained 2 x 0.0XX surface length simultaneously. A crack growth analysis shall be performed to determine the crack growth in the alternate path corresponding to propagation from 2 x 0.0XX in., (surface length) to failure in

---

*If special NDE techniques are used small intial crack sizes may be assumed in rim locations. This special NDE capability must be demontrated and incorporated at the overhaul facilities to utilize these benefits at the initial disk design phase.

the primary path. Load increases which result from fracture in the primary path and affect the secondary path must be included in the analysis.

b.   Multiple load path independent structure. The same as 3.1.1.1 plus the amount of crack growth which occurs prior to load path failure.

3.1.1.3.2 Fail-safe crack arrest structure. For structure classified as fail-safe crack arrest, the primary damage assumed to exist in the structure following crest of a rapidly propagating crack shall depend upon the particular geometry and environment.*

3.1.2 In-Service Inspectable.

3.1.2.1 In-service inspection flaw assumption: The smallest damage which can be presumed to exist in the structure after completion of a depot or base level inspection shall be as specified in 3.1.1.1.

3.1.2.2 Galling limits. Galling limits (i.e., permissible depth of surface damage) for upper lug disk blade contact surfaces shall be defined based on a maximum pseudo-stress intensity allowable, $K_{max\ allowable}$ (LCF), predicted from appropriate material high-frequency fatigue vibratory threshold (K_{th} HFF) properties at steady-state operating conditions. This relationship follows:

$$\text{Assume } K_{max\ allowable}(LCF) = \frac{K_{th}\ (HFF)}{(1 - R)}$$

$$\text{where } R = \frac{\sigma_{steady} - \sigma_{vib/2}}{\sigma_{steady} + \sigma_{vib/2}},$$

σ_{steady} = Maximum operating stress neglecting vibratory stress

σ_{vib} = Peak-to-peak vibratory stress

$K_{th}\ (HFF) = f(R,\ Temp)$

---

*Failsafe crack arrest behavior is extremely uncommon in turbine engine cold section disks, but occurs with significant frequency in hot section disks. Rim slots in hot section disks crack when hot rims occur in combination with cool bores. Cracks sometimes arrest and sometimes continue to rupture. Requirements should be developed in the follow-on contract concerned with hot section disks.

K_{th} (HFF) vs R-ratio material property curves utilized in this evaluation at various temperatures shall be developed during basic material characterization.

3.1.3 Residual strength requirements. The minimum residual strength requirements for cold section disks shall be determined on the basis of burst margin capability and the ability to resist rapid crack propagation resulting from dynamic stressing. To meet damage tolerant design requirements the relationship between crack size and overspeed capability shall remain above safety margins for a slow crack growth or fail-safe interval corresponding to (XX) times the inspection intervals (contract goal). This requires the design to exhibit adequate burst margin after the last cycle of the most limiting interval predicted for all disk geometries. Definition of dynamic disk activity must be documented experimentally and it must be shown that the growing crack does not attain the length corresponding to threshold stress intensity. Residual strength requirements in terms of burst margins shall be as specified in MIL-E-5007. The residual life analysis shall utilize simulated missions to be defined by the Contractor, subject to Government approval, and must include equivalent engine duty cycle damage.

3.2 Specific requirements. Specific damage tolerance requirements for "slow crack-growth" structure, "fail-safe multiple load path" structure, and "fail-safe crack arrest" structure are specified in 3.2.1, 3.2.2 and 3.2.3, respectively.

3.2.1 Slow crack growth structure. Of the degrees of inspectability in accordance with 6.2.6, only depot or base level inspectable and in-service noninspectable are applicable to slow crack growth structures. The frequency of inspection for both shall be as stated below unless otherwise specified in the appropriate contractual documents.

Depot or base level inspectable - Once in the interval determined
as specified in 3.2.3.1

146

In-service noninspectable -   Once at the end of one design
lifetime.

3.2.1.1 Depot or base level inspectable. The damage which can be
presumed to exist in the structure after completion of a depot or base
level inspection shall be that specified for slow crack growth
structure in 3.1.2. These damage sizes shall not grow to critical
size and cause failure of the structure due to the application of the
requirements of MIL-E-5007 after (XX) times the inspection interval.

3.2.1.2 In-service noninspectable. The initial damage size as
specified in 3.1.1.1 shall not grow to critical size and cause failure
of the structure due to the application of the requirements of
MIL-E-5007 at the end of one design lifetime.

3.2.2 Fail-safe multiple load path structure. The degress of
inspectability as specified in 6.2.6, which can be applicable to
fail-safe multiple load path structure, are in-flight evident
inspectable, depot or base level inspectable and in-service
noninspectable. Disk constructions in this classification will
include but not be limited to those design configurations where
multiple load paths are employed to support a single blade row. To be
included along with multiple load path structures is redundancy of
engines; i.e., two or more identical blade rows performing identical
functions and supported by their respective disks in their respective
locations in or on the airframe. Several conditions must be met
before these disks can be considered fail-safe as well as multiple
load path. The conditions are as follows:

a.   The weapon system must have one-engine-out capability.

b.   The disk must release blades rather than large disk
      fragments.

c.   The construction of the engine cases must provide
      protection to the airframe, control equipment and other
      engine or engines.

147

3.2.2.1 Inspection intervals. The frequency of inspection for each of the inspectability levels shall be as stated below unless otherwise specified in the appropriate contractual documents.

In-flight evident inspectable - Once per flight.

Depot or base level inspectable - Once in the interval determined as specified in 3.2.3.1.

In-service noninspectable - Once at the end of one design lifetime.

3.2.2.2 Residual strength requirements and damage growth limits. There are two sets of residual strength requirements and damage growth limits for fail-safe multiple load path structure. The first set applies to the required residual strength and damage growth limits for intact structure, (i.e., the structure prior to a load path failure), and the second set applies to the remaining structure subsequent to a load path failure. These are described in 3.2.2.2.1 and 3.2.2.2.2, respectively.

3.2.2.2.1 Intact structure. The requirements for the intact structure are a function of the depot or base level inspectability of the intact structure for damage sizes which are less than a load path failure, (i.e., subcritical cracks and small element failures). If the structure is depot or base level inspectable the smallest damage sizes which can be presumed to exist in the structure after completion of a depot or base level inspection shall be those as specified in 3.1.2. These damage sizes shall not grow to a size such as to cause load path failure due to the application of the requirements of MIL-E-5007 after (XX) times the inspection interval. If the structure is not depot or base level inspectable for subcritical flaws or small element failures which are less than a load path failure, either by virtue of small critical flaw sizes or inspection problems, the initial material and manufacturing damage as specified in 3.1.1 shall be assumed and it shall not grow to the size required to cause load path failure due to the application of the requirements of MIL-E-5007 at the end of one design lifetime.

148

3.2.2.2.2 Remaining structure subsequent to a load path failure. Subsequent to load path failure, the minimum assumed damage in the remaining alternate structure as specified in 3.1.1.3.1 shall not grow to a size such as to cause loss of the disk due to the application of the requirements of MIL-E-5007 after (XX) times the inspection interval minus the time prior to load path failure.

3.2.3 Fail-safe crack arrest structure. The degree of inspectability as specified in 6.2.6 which can be applicable to fail-safe crack arrest structure is depot or base level inspectable.

3.2.3.1 Inspection intervals. The frequency of inspection shall be once in the shortest of the intervals determined by taking the residual life of each disk in an assembly and dividing by (XX), the number of required inspections.

3.2.3.2 Residual strength requirements and damage growth limits. There are two sets of residual strength requirements and damage tolerance limits for fail-safe crack arrest structure. The first set applies to the intact structure prior to unstable crack growth and arrest. The second set applies to the remaining structure subsequent to encountering unstable crack growth and arrest. These are described in 3.2.3.2.1 and 3.2.3.2.2, respectively.

3.2.3.2.1 Intact structure. The requirements for the intact structure are a function of the depot or base level inspectability for damage caused by unstable crack growth and arrest. If the structure is depot or base level inspectable, the smallest damage sizes which can be presumed to exist in the structure after completion of a depot or base level inspection shall be those as specified in 3.1.2. These shall not grow to a size to cause unstable crack growth in (XX) inspection intervals. If the structure is not depot or base level inspectable for subcritical flaws, the initial material and manufacturing damage as specified in 3.1.1.1 shall be assumed and it shall not grow to critical size by the requirements of MIL-E-5007 in one design lifetime.

149

3.2.3.2.2 Remaining structure subsequent to crack arrest. The remaining structure at the time of the unstable crack growth shall be able to sustain the load as specified in MIL-E-5007. In addition, subsequent to the unstable growth and arrest, damage as specified in 3.1.1.3.2 shall not grow to a size such as to cause catastrophic loss of the engine due to the application of the load in the specified minimum periods of unrepaired usage. The loads and minimum period of unrepaired service usage for depot or base level inspectability shall be the same as those specified for fail-safe multiple load path structure.

4. QUALITY ASSURANCE PROVISIONS

4.1 Design Data. Design data shall be generated as required to support the analysis effort.

4.2 NDT demonstration program. Where designs are based on initial flaw size assumptions less than those as specified in 3.1.1.1a, a non-destructive testing demonstration program shall be performed by the contractor and approved by the procuring activity to verify that all flaws equal to or greater than the design flaw size will be detected to the specified reliability and confidence levels. The demonstration shall be conducted on each selected inspection procedure using production conditions, equipment and personnel. The defective hardware used in the demonstration shall contain cracks which simulate the case of tight fabrication flaws. Subsequent to successful completion of the demonstration program, specifications on these inspection techniques shall become the manufacturing inspection requirements and may not be changed without a requalifying program subject to procuring activity approval.

5. PREPARATION FOR DELIVERY

   NOT APPLICABLE

6. NOTES

6.1 Intended use. This specification is intended for use in the design for all new military aircraft turbine engine cold section disks

for the procuring activity. Mandatory selection of the damage tolerant design option is not intended.

6.2 Definitions

6.2.1 Design option. A design option is one of two or more approaches to the task of making the likelihood of aircraft loss extremely low. For example, design for damage tolerance with a policy of retirement for cause or design for safe-life with a policy of mandatory retirement at a prescribed limit.

6.2.2 Retirement for cause. Retirement for cause is the practice of retiring a part from service only after a crack has been detected by nondestructive inspection.

6.2.3 Safe-life. Safe-life is the service time required for the most fatigue prone member of a population of parts to grow a crack of a prescribed size that is safe whether or not it is detectable.

6.2.4 Safety of flight structure. That structure whose failure could cause direct loss of the aircraft, or whose failure if it remained undetected could result in loss of the aircraft. Engine cold section disks will not be considered safety of flight structures when two or more engines power the weapons system and the following conditions are met:

a. The weapons system design provides one-engine-out safe-flight capability.

b. The design of the disks is such that blade release occurs rather than disk fragmentation.

c. The construction of the engine provides for the containment of released blades and disk lug portions.

6.2.5 Design concepts. The design concepts to be used in conforming to engine damage tolerance requirements shall be in accordance with the following definitions.

6.2.5.1 Slow crack growth structure. Slow crack growth structure consists of those design concepts where flaws or defects are not allowed to attain the critical size required for unstable rapid propagation. Safety is assured through slow crack growth for

151

specified periods of usage depending upon the degree of inspectability. The strength of slow crack growth structure with subcritical damage present shall not be degraded below a specified limit for the period of unrepaired service usage.

6.2.5.2 Crack arrest fail-safe structure. Crack arrest fail-safe structure is structure designed and fabricated such that unstable rapid propagation will be stopped within a continuous area of the structure prior to complete failure. Safety is assured through slow crack growth of the remaining structure and detection of the damage at subsequent inspections. Strength of the remaining undamaged structure will not be degraded below a specified level for the specified period of unrepaired service usage.

6.2.5.3 Multiple load path fail-safe structure. Multiple load path fail-safe structure is designed and fabricated in segments (with each segment consisting of one or more individual elements) whose function it is to limit or contain localized damage and thus prevent complete loss of the structure. Safety is assured through slow crack growth in the remaining structure to the subsequent inspection. The strength and safety will not degrade below a specified level for a specified period of unrepaired service usage.

6.2.5.3.1 Multiple load path-dependent structure. Multiple load path structure is classified as dependent if, by design, a common source of cracking exists in adjacent load paths at one location due to the nature of the assembly or manufacturing procedures. An example of multiple load path-dependent structure is individual members joined by common fasteners with common drilling and assembly operations.

6.2.5.3.2 Multiple load path-independent structure. Multiple load path structure is classified as independent if by design, it is unlikely that a common source of cracking exists in more than a single load path at one location due to the nature of assembly of manufacturing procedures.

152

6.2.6 Degree of inspectability. The degree of inspectability of safety of flight structures shall be established in accordance with the following definitions.

6.2.6.1 In-flight evident inspectable. Structure is in-flight evident inspectable if the nature and extent of damage occurring in flight will result directly in characteristics which make the flight crew immediately and unmistakably aware that significant damage has occurred and that the mission should not be continued.

6.2.6.2 Depot or base level inspectable. Structure is depot or base level inspectable if the nature and extent of damage will be detected utilizing one or more selected nondestructive evaluation (NDE) procedures. The inspection procedures may include NDE techniques such as penetrant, X-ray, ultrasonic, etc. Accessibility considerations may include removal of those components designed for removal.

6.2.6.3 In-service noninspectable structure. Structure is in-service noninspectable if either damage size or accessibility preclude detection during one or more of the above inspections.

6.2.7 Residual life. Residual life is the interval of service time required for a crack that narrowly escaped detection by NDE to grow to such a length that rapid fracture is imminent.

6.2.8 Minimum assumed initial damage size. The minimum assumed initial damage size is the smallest crack-like defect which shall be used as a starting point for analyzing residual strength and crack growth characteristics of the structure.

6.2.9 Minimum assumed in-service damage size. The minimum assumed in-service damage size is the smallest damage which shall be assumed to exist in the structure after completion of an in-service inspection.

6.2.10 Frequency of inspection. Frequency of inspection is the number of times that a particular type of inspection is to be conducted during the service life of the aircraft turbine engine.

153

6.2.11 Minimum period of unrepaired service usage. Minimum period of unrepaired service usage is that period of time during which the appropriate level of damage (assumed initial or inservice) is presumed to remain unrepaired and allowed to grow within the structure.

6.2.12 Threshold stress intensity change. Threshold stress intensity change is the level of stress intensity change below which a crack is nonpropagating and above which a crack is propagating.

6.3 Ordering data. MIL-E-5007 and MIL-STD-1534 or later issues will be used in conjunction with this specification.

APPENDIX B
F100 DUTY CYCLE DEFINITION BACKGROUND

The first operational F-15 was delivered to the Tactical Air Command in November 1974. Shortly after the F-15 became operational, a team of Air Force and Pratt & Whitney Aircraft engineers began a series of interviews with TAC pilots from the F-15 Training Squadron and the Operational Test and Evaluation Squadron in an attempt to identify the flight envelope, throttle movements, and time at various power conditions for the wide variety of missions conducted by the two squadrons. The pilots readily admitted it was difficult to accurately recount the actions taken during the very active air combat missions. The F100 engine, however, has an electromechanical device, called an Events History Recorder (EHR) mounted on the engine. This device receives a variety of engine parameters that permit the clocking of total engine operating time, time at high temperature and the number of throttle excursions. The information recorded by the EHR was then compared to the pilot interview information. Follow-up discussions were held with the pilots to verify that the engineering data reasonably portrayed the mission being flown.

The F100 EHR data (time, cycles, time at temperature) from thousands of flights has been obtained. From this statistical base the expected number of throttle excursions (cycle) and time at rated temperature has been determined and extrapolated for the life of the engine for Luke AFB training squadron, and Langley AFB operational squadron. Accelerated Mission Testing (AMT) has been constructed consistent with this projected usage and at the same usage intervals, the AMT engines and the high-time field engines have been disassembled and compared with excellent correlation, confirming the test and usage predictions. Figure B-1 graphically shows how the usage is established. Periodic interviews are conducted to keep the engineering mission profile current with operational usage. For example, a change in mission mix ratio between air combat mission and ground support can significantly change the throttle excursion rates.

155
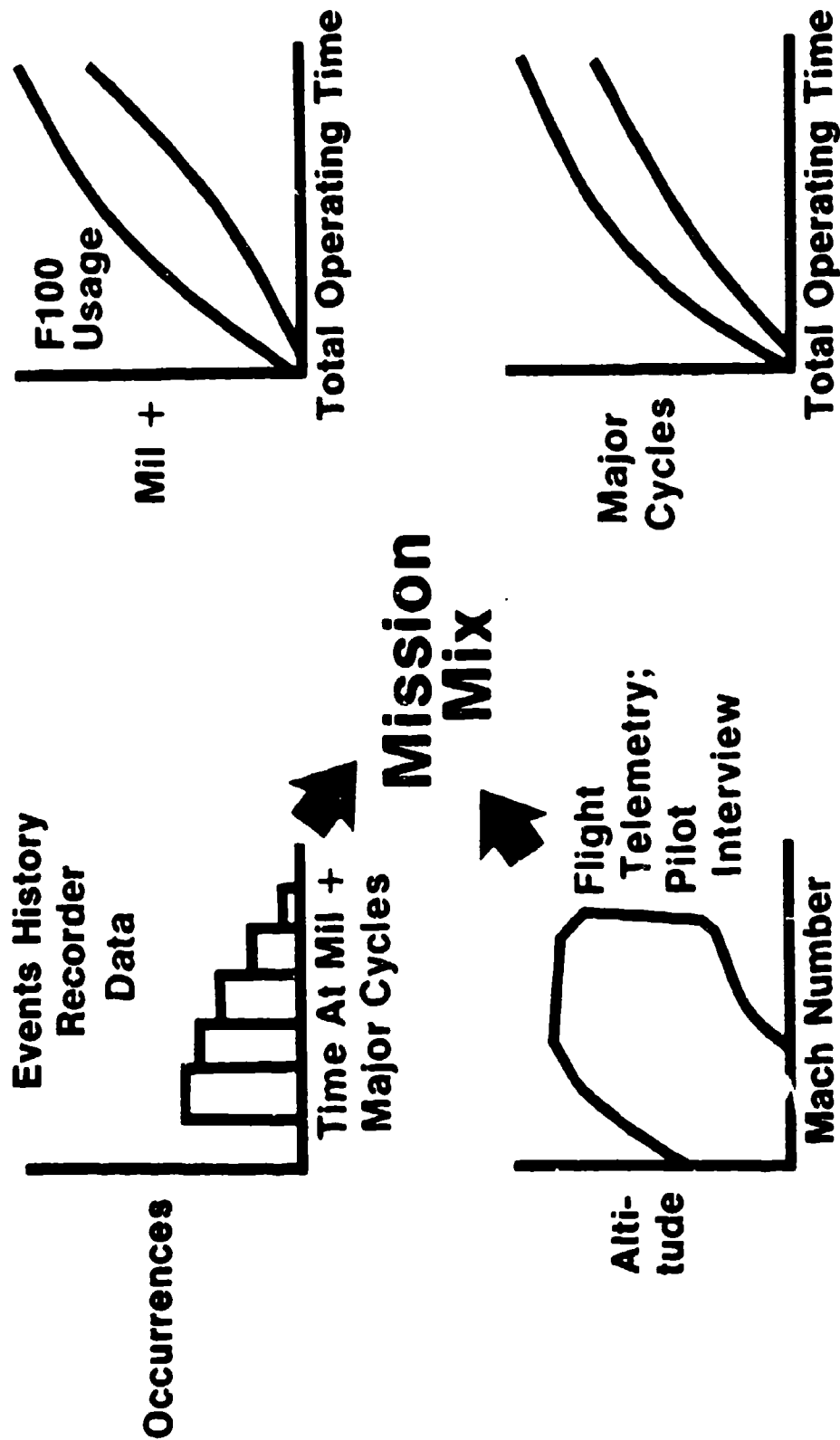
Figure B-1 Actual Field Use

156

APPENDIX C
CRACK GROWTH MODEL DATA BASE

On the following pages, the individual da/dN vs K curves from the crack growth models of Section III.G are shown with the pre-contract data base information superimposed.
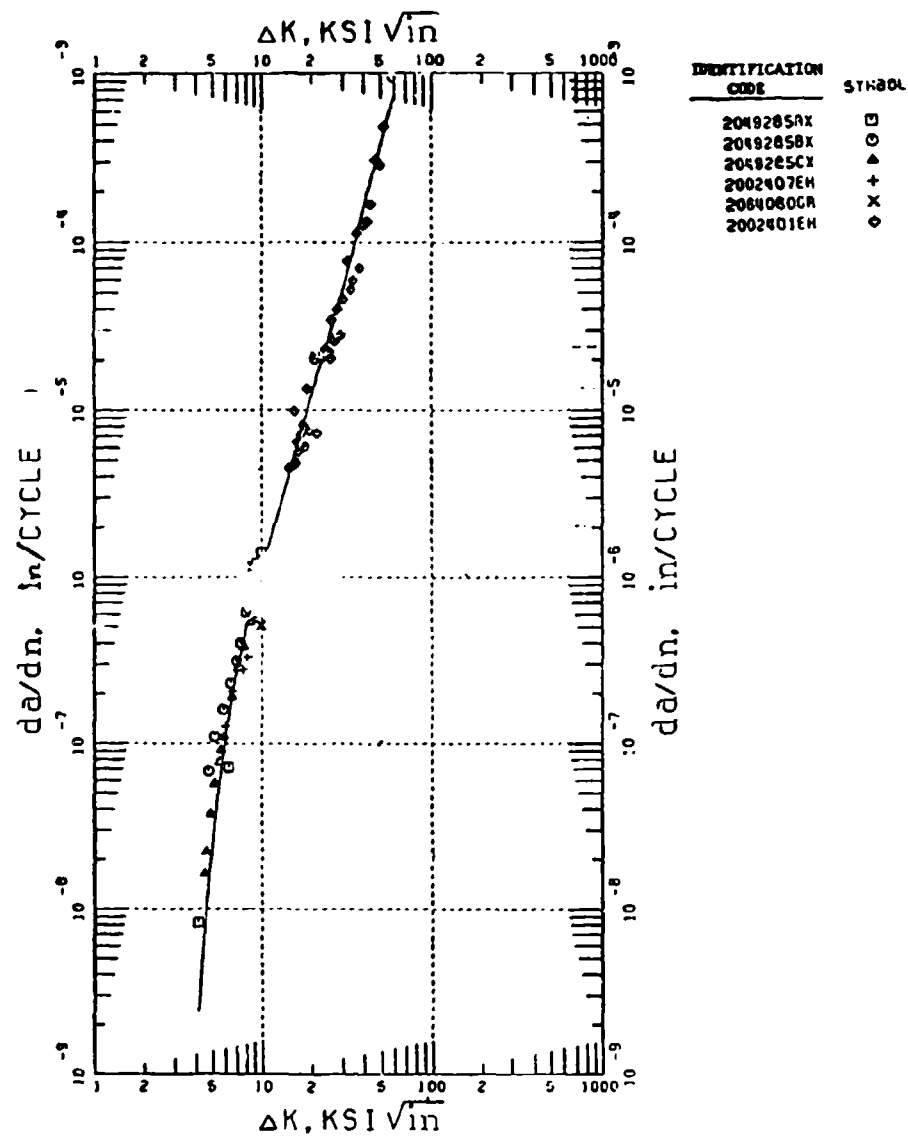
Figure C-1.   Crack Propagation, Ti 6-4; RT, R=0.1, 10 cpm.
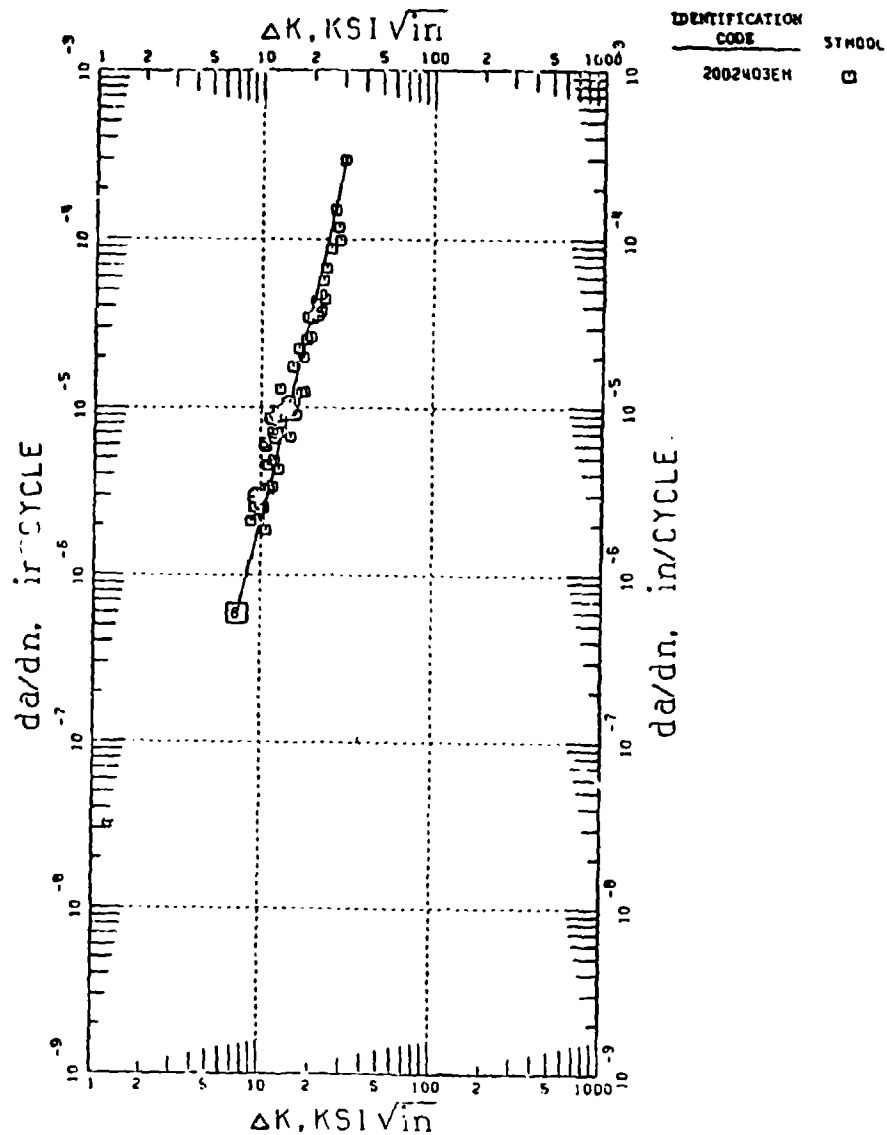
Figure C-2. Crack Propagation, Ti 6-4; RT, R=0.5, 10 cpm.

159
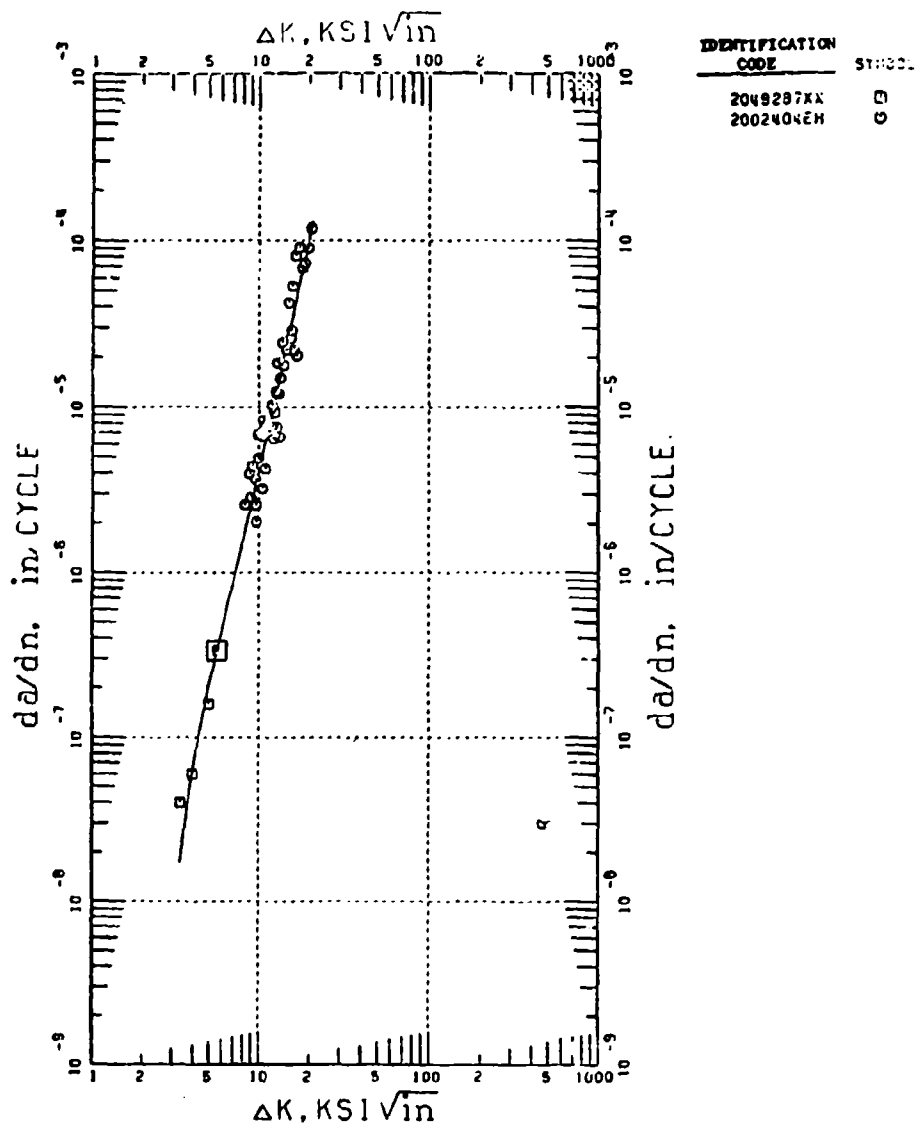
Figure C-3. Crack Propagation, Ti 6-4; RT, R=0.7, 10 cpm.
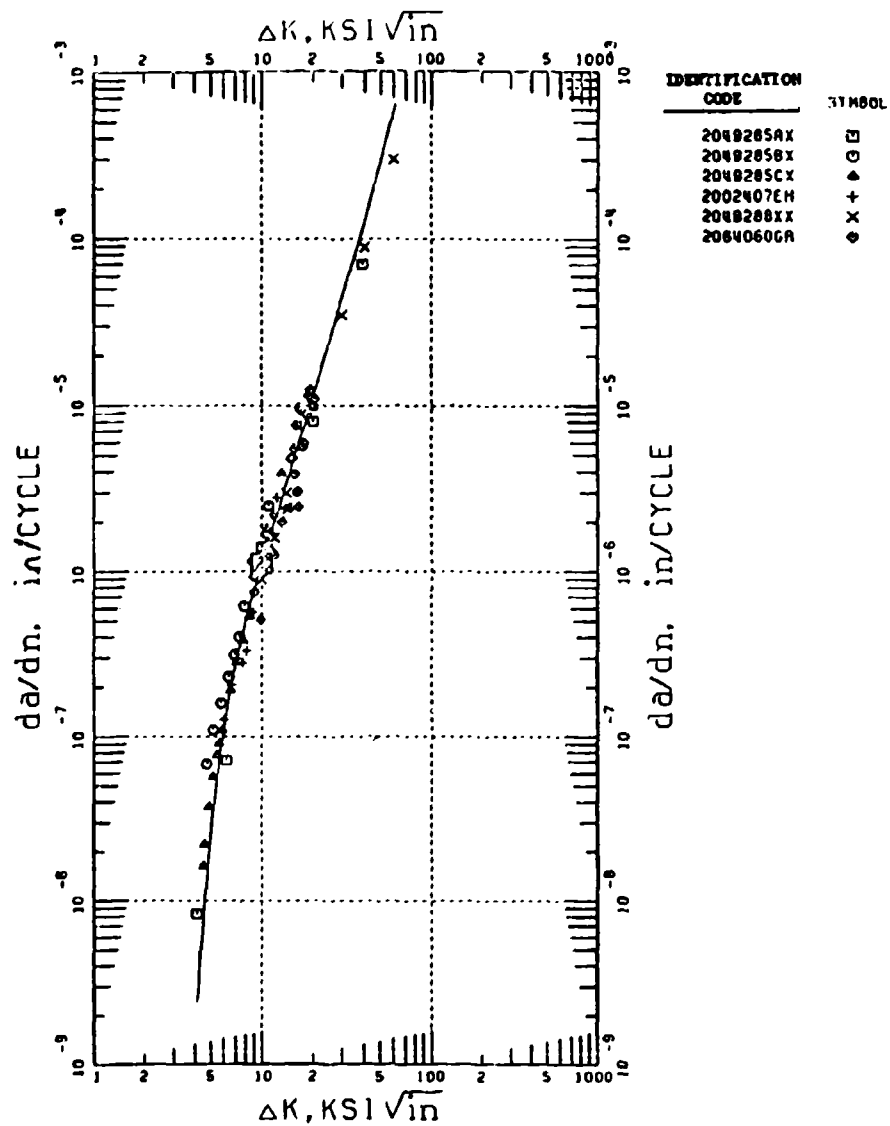
Figure C-4. Crack Propagation, Ti 6-4; RT, R=0.1, 1-30 Hz.
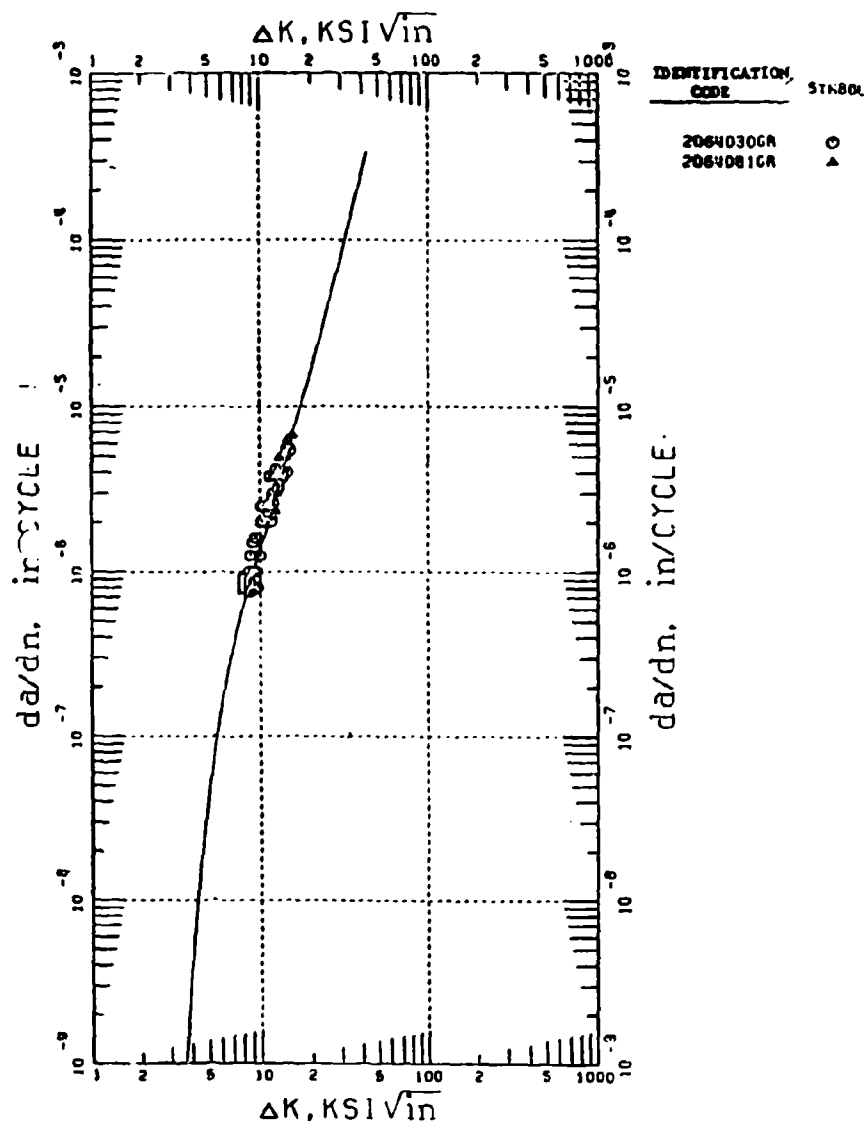
Figure C-5. Crack Propagation, Ti 6-4; RT, R=0.3, 1-30 Hz.
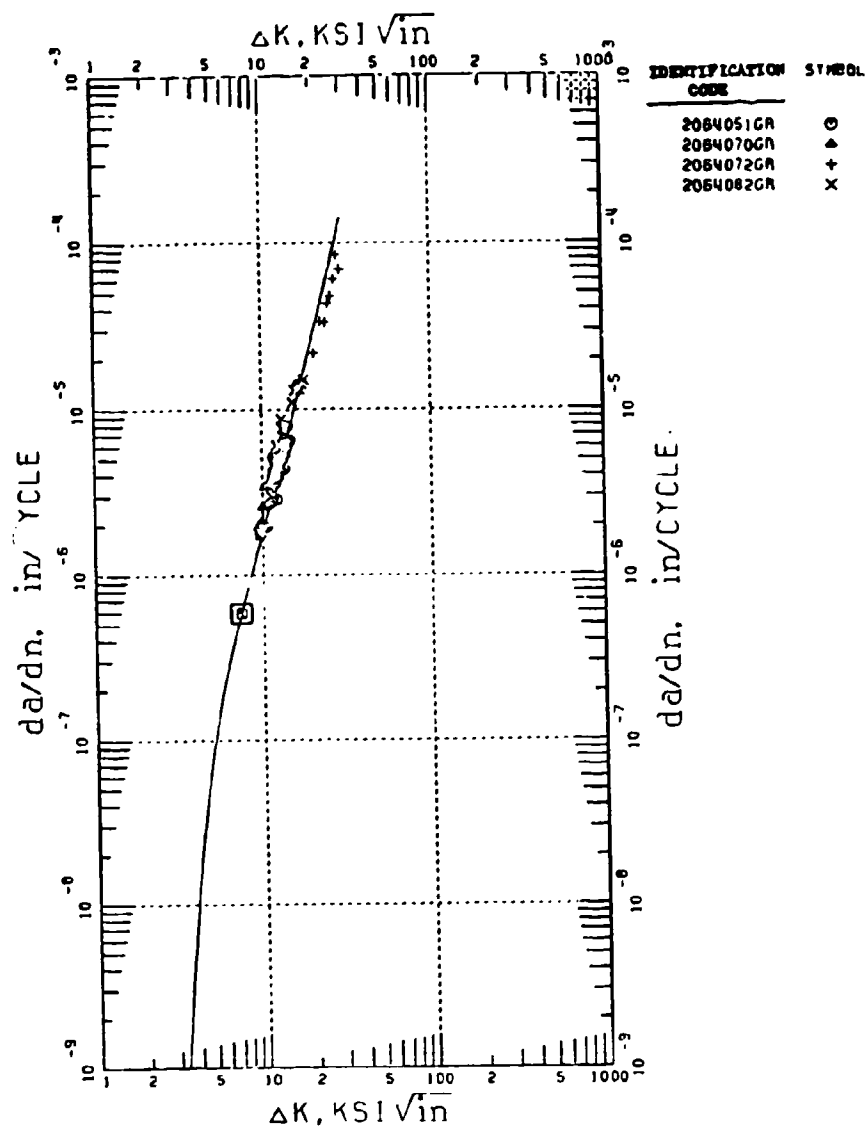
Figure C-6. Crack Propagation, Ti 6-4; RT, R=0.5, 1-30 Hz.

163
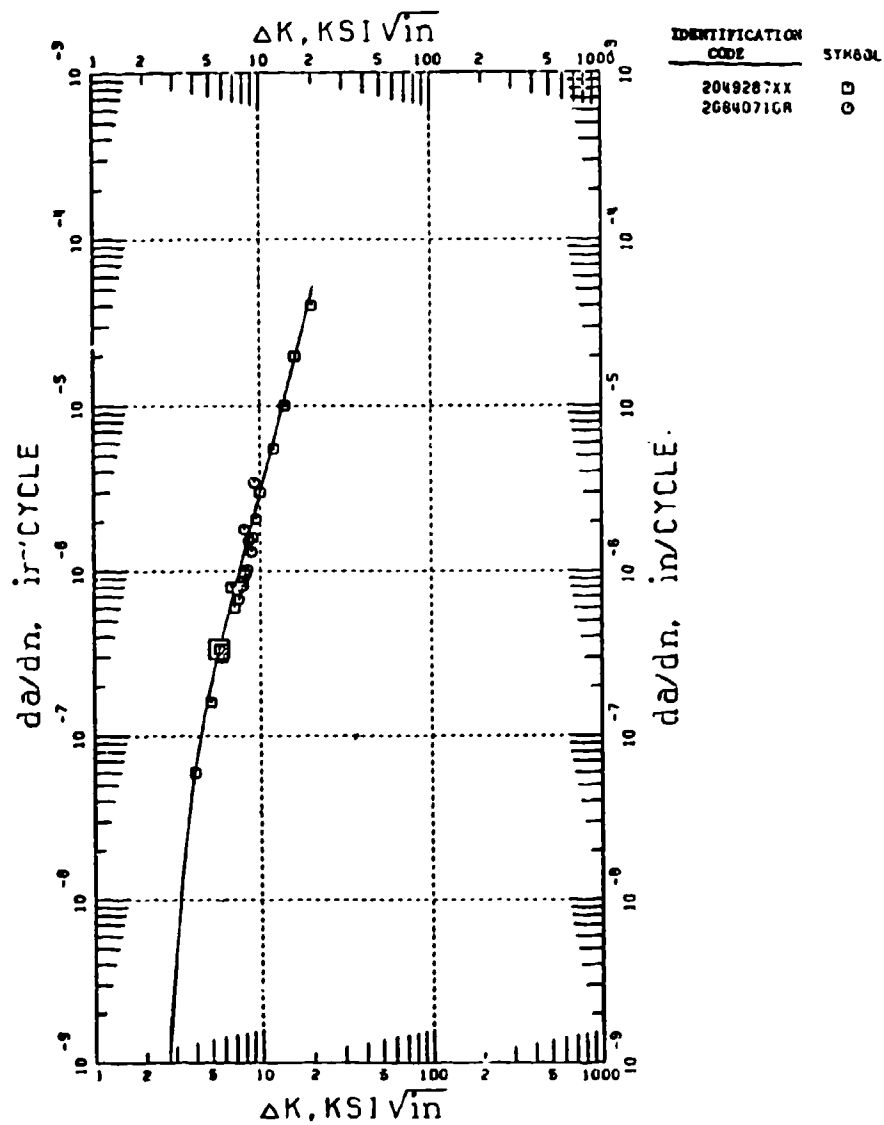
Figure C-7. Crack Propagation, Ti 6-4; RT, R=0.7, 1-30 Hz.

164
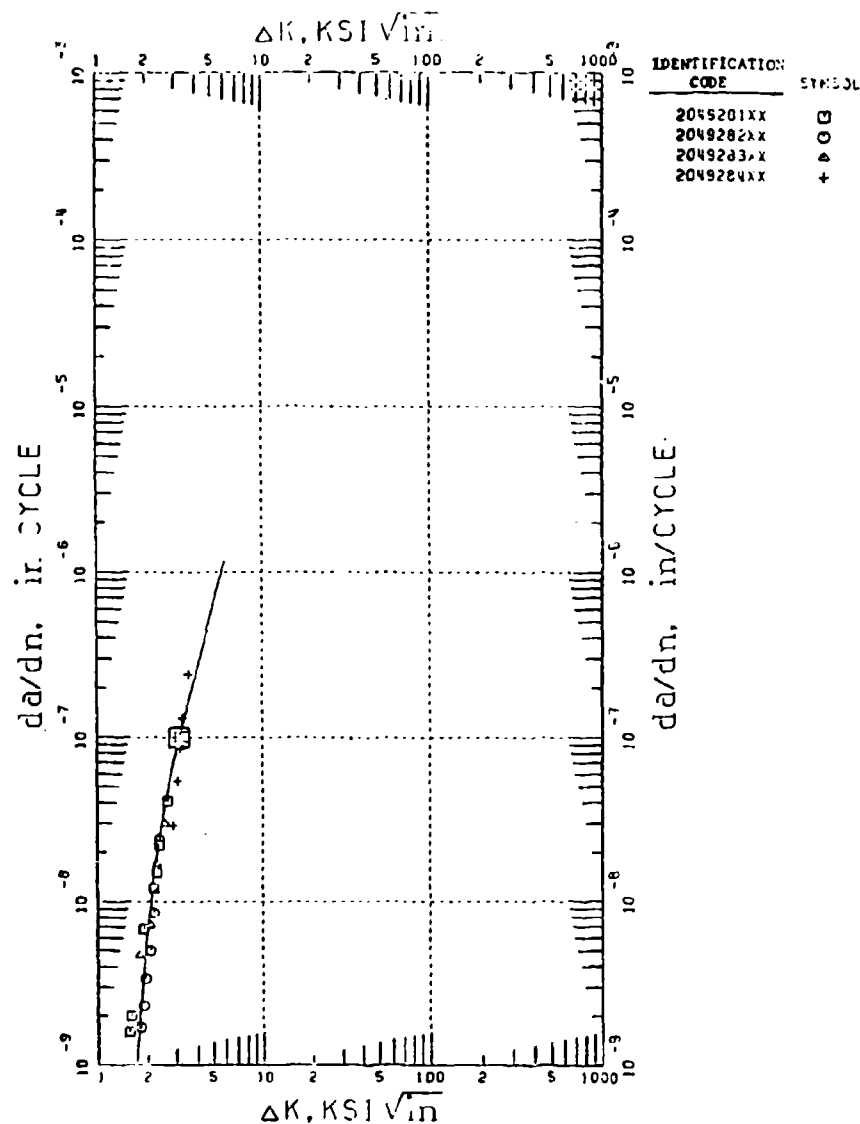
Figure C-8. Crack Propagation, Ti 6-4; RT, R=0.9, 1-30 Hz.

APPENDIX D

RESULTS OF 3-DIMENSIONAL FINITE ELEMENTS ANALYSIS

A three-dimensional model of the entire F100 2nd-Stage Fan Rotor was run on NASTRAN both for centrifugal stress and for three nodal diameter vibratory motion.

The detail of the breakup around the dovetail attachment is shown in figure D-1, whereas the overall modeling technique of the disk, attachment region, blade and shroud is shown in figure D-2. Figure D-3 shows the distribution of centrifugal stress over an imaginary cutting plane through a disk lug between two blade dovetails. The isometric vividly portrays the complexity of the stress distribution.

The stress-producing contributions of centrifugal load, bending moment, and geometry are made clear as a result of the study depicted in figures D-4, D-5 and D-6. These results identify moment and broach angle as strong drivers along with centrifugal load.

This analysis had two intended uses. The first was to correlate with dynamic strain gage data to estimate dynamic stresses in stress-concentration locations which were not instrumented.

The second use was to substantiate the adequacy of superimposing 2D analyses to assess static concentrated stress. This second usage proved misleading. Subsequent strain gage data (Section VI) indicated that the 2D rim analysis system too conservatively predicts rim slot bottom stress. This analysis was probably misleading as it enforced plane-section-remains-plane at a location where stiffness influence of the highly cambered and twisted airfoil violates the assumption. Current 3D analysis, independent of this contract, is assessing influence of rim geometry (rim width): (rim thickness): (web thickness) and airfoil camber, twist, and loading. We believe that our 2D system is accurate for typical compressor stages, is acceptably conservative for "safe-life" design of fan stages, but for

"retirement-for-cause" or damage-tolerant design philosophy it may require replacement with a "calibrated" 3D stress system for fan rims with complex 3D characteristics.

Current studies are using NASTRAN, a system of preprocessors for model construction, a full airfoil model with higher-order plate elements (for economy), 20-node brick elements for attachment and disk rim, and disk interface boundary conditions from routine design tools to model this complex structure.
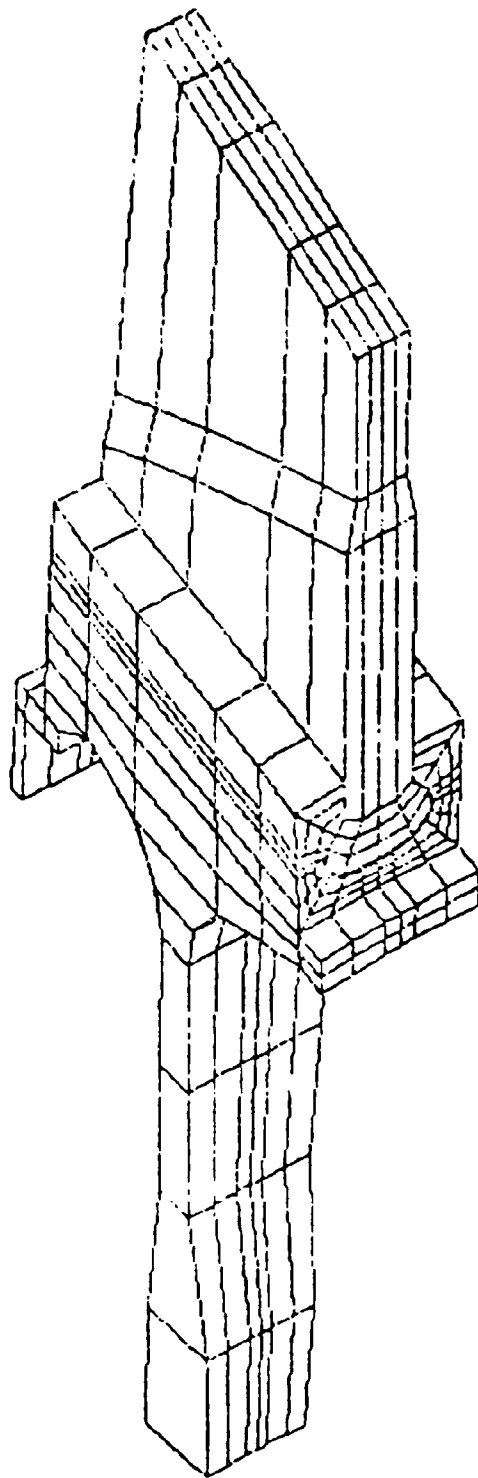
Figure D-1. Disk Segment and Lower Blade Portion.
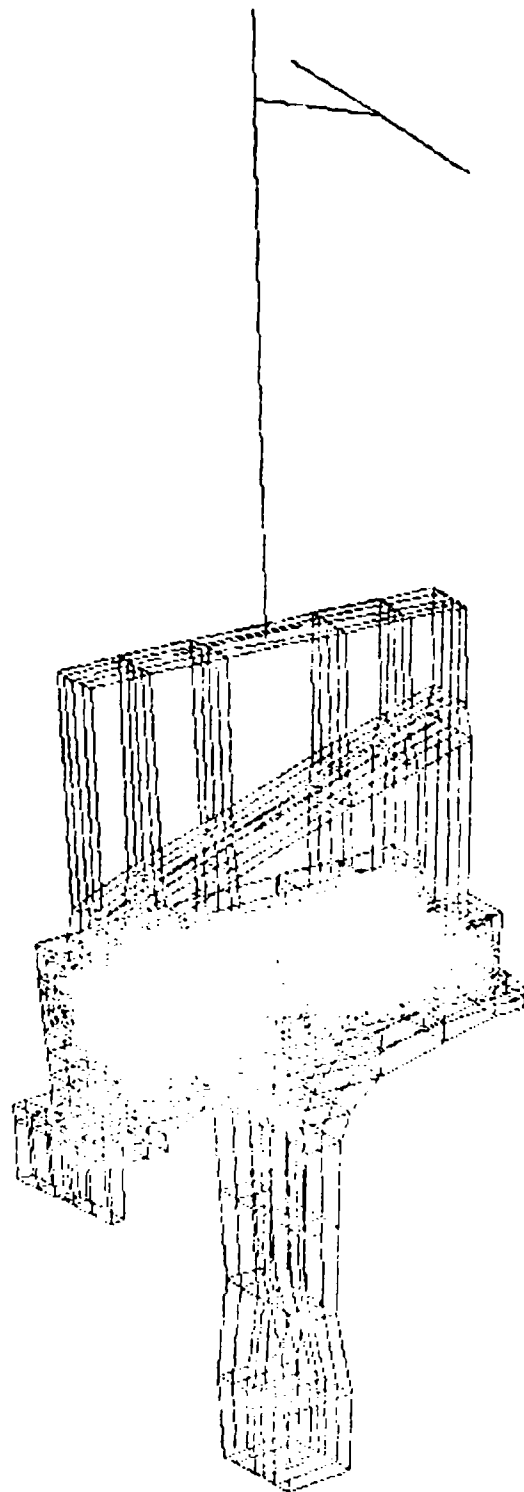
Figure D-2. Disk Segment With Lower Blade Showing Addition of
Upper Blade and Shroud

170
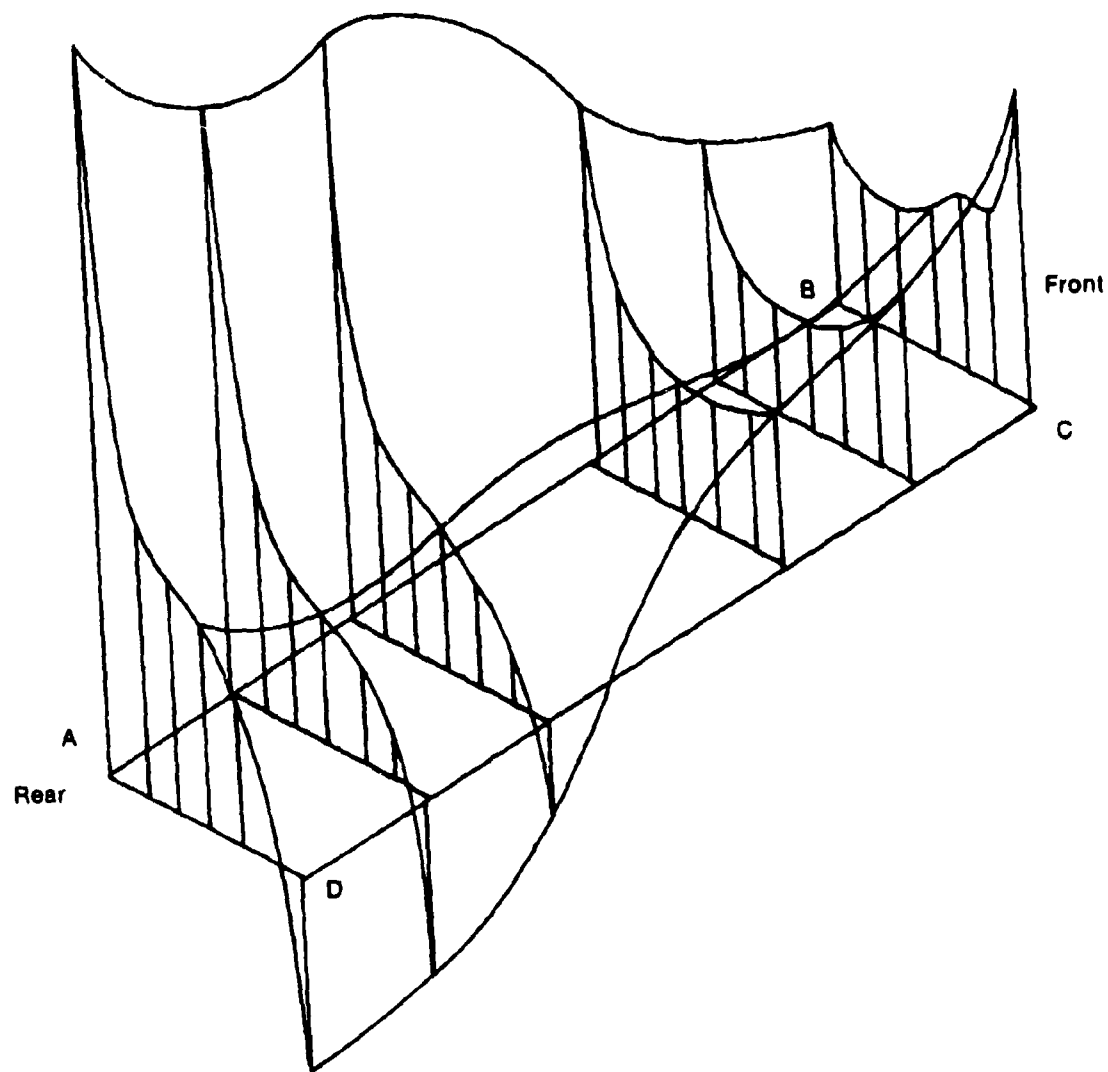
Figure D-3. Stress on Minimum Lug Cross Section.

171
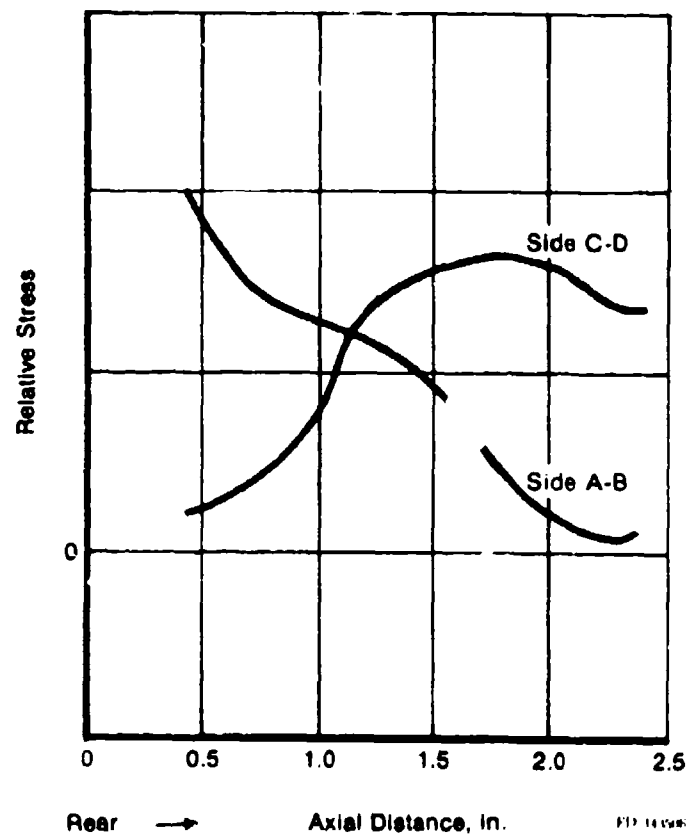
Figure D-4. B/M Disk Centrifugal Load and Tangential Moment.

172
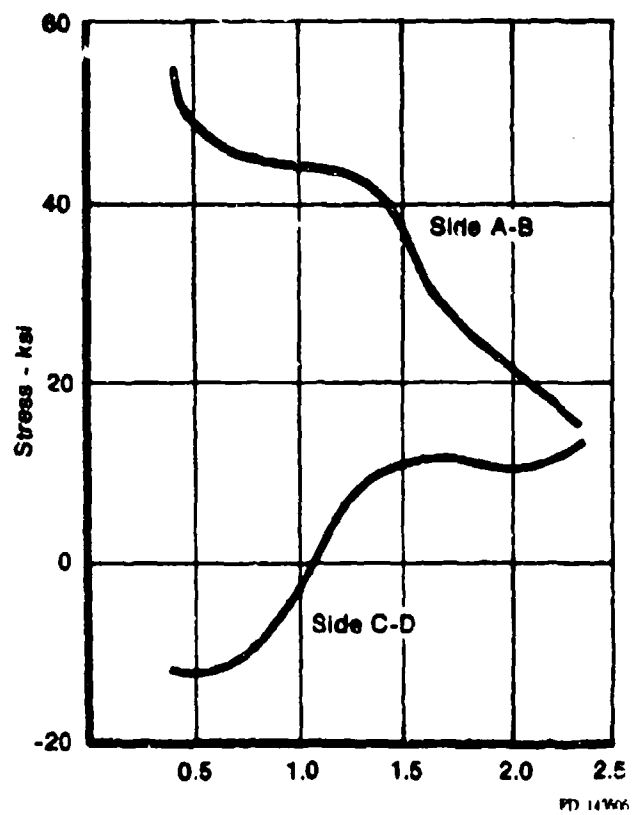
Figure D-5. B/M Disk Centrifugal Load.
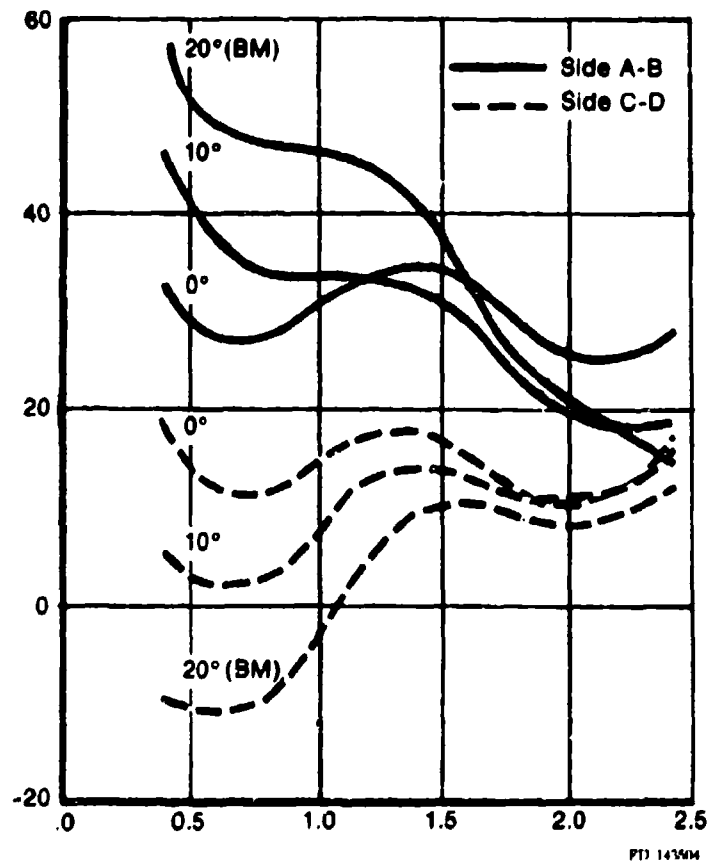
Figure D-6. Effect of Broach Angle on Stress Distribution.

APPENDIX E
TEST LAB REPORTS

Test lab results of the aforementioned spin pit and ferris wheel work were extracted from GPD document FMMT 22361 by M.S. Mills and J.J. Weber.

BACKGROUND

These disk tests were to support an overall design program (Contract F33615-77-C-2064) to develop, refine and evaluate a damage tolerant design (DTD) system for a disk capable of operating with 0.030 inch surface length cracks for three overhaul periods.

The basic DTD disk design is a "beefed up" prespun version of the F100 bill-of-material (B/M) 2nd stage fan disk, P/N 4040002 of different material. In addition to the prespinning procedure, changes include thickening of the bore and web for reduced stress in critical locations, and respecifying the material from PWA 1216 (Ti 6-2-4-6) to AMS 4928 (Ti 6-4) for increased fracture toughness.

Part Name:	Damage Tolerant Design Fan Disk (Hereafter designated DTD)
Part Number:	SKD 5379 MP, GKJ 9396, GKJ 0411 (Residual Spin Flawed Bolthole DTD Disk 1 and Residual Spin Flawed Rim DTD Disk 2)
	SKD 9980 (Flawed Bolthole Baseline DTD Disk 3, not Prespun)
Serial Numbers:	BJE 141 (Hereafter designated Disk 1)
	BJE 142 (Hereafter designated Disk 2)
	BJE 143 (Hereafter designated Disk 3)
Material	AMS 4928, TI-6Al-4V

175

TEST CONFIGURATION, PROCEDURE AND RESULTS

Strain gages and chromel/alumel thermocouples were installed to measure the strain and temperature distribution on disks 1 and 2 at 500°F. A three leadwire system was installed to minimize strain gage drift due to temperature variations. Disk 1 was instrumented more fully than disk 2 to establish the strain and oven calibration (figures E-2 and E-3, respectively). A layout of oven and spin assembly in the spin rig configuration is shown in figure E-1. The first spin acceleration of disk 1 was conducted only to 10,000 rpm to corroborate analytical design predictions prior to the full speed test. The complete strain data and corresponding test temperatures are in tables E-1 and E-2, respectively, for disks 1 and 2. The resultant room temperature residual strain values for disks 1 and 2 are also contained in table E-1. Figures E-6 through E-9 are plots of table E-1 for disk 1.

FERRIS WHEEL TEST PORTION

Prior to the ferris wheel test, the two prespun DTD disks had their bores removed to create proper nominal disk stresses within the limit of drawbar pull load capability. Disk 3 was the "non-treated" baseline disk for disk 1 and therefore not spin tested; it was machined directly into the ferris wheel configuration (thus having a different part number than disks 1 and 2). Prior to ferris wheel testing, disks 1 and 3 were elox preflawed in ten boltholes (figure E-4). Disk 2 was elox preflawed at two locations in each of ten rim slots (figure E-5).

A ferris wheel strain survey was first carried out on disks 1 and 2 instrumented per figures E-4 and E-5, with resultant strains in tables E-3 and E-4, respectively. Figures E-10 and E-11 show the ferris wheel setup for disk 1 including the mounted acoustic emission probes. In figures E-12 and E-13, ferris wheel strain data from table E-3 are plotted. A close-up of disk 2 slot instrumentation is figure E-14 with strain data graphed on figures E-15 through E-18.

176

Inspection techniques applied to the ferris wheel LCF portion of this test included replication, fluorescent penetrant inspection (FPI), eddy current (EC), and acoustic emission (AE). Replication wasused as the primary inspection method. FPI was discontinued after use only on disk 1, as the elox flaws caused excessive bleedout of the penetrant and therefore inaccurate measurements. Results of the EC and AE inspections are contained in FMMT 23292. EC and AE were also discontinued after use only on disk 1 due to inconclusive results caused by signal interference from the elox flaws and malfunctioning equipment, respectively.

Replications (acetyl cellulose plastic film, 0.034 mm thick) were taken for all elox flaws to determine initial baseline preflaw dimensions. Figure E-20 shows a typical elox flaw for each disk. After cycling began, periodic replications were performed under partial load in the ferris wheel to enhance crack detail.

The disks were first sawtooth load cycled to attain about 0.030 inch crack initiation and then mission cycled for crack propagation evaluation (cycles defined in figure E-19). Replication crack propagation data are detailed in tables E-5 and E-6 for disks 1 and 3, respectively. Figures E-22 and E-23 contain crack growth data from tables E-5 and E-6 (no cracks were detected on disk 2 after a total of 3500 sawtooth cycles). Disk 1 was LCF tested to failure, while LCF testing on disks 2 and 3 was discontinued at imminent fracture.

Replication photos in figure E-21 show a typical bolthole crack growth progression.

Five cracked boltholes in disk 1 and three in disk 3 were: (1) sectioned out of the respective disks; (2) heat-tinted for one hour at 600°F; (3) and broken open to expose the fracture faces. This was to determine crack depths at test termination. This data is contained in table E-7. Figures E-24 and E-25 show a representative bolthole fracture face set for each disk. Data from tables E-5 and E-6 were converted to change in crack growth per change in number of cycles

177

(da/dN) tables E-8 and E-9, respectively. The two boltholes on disk 1 which failed through (1C and 2C) were viewed by the scanning electron microscope (SEM). These fractures are shown in figures E-26 through E-28.

DISCUSSION OF RESULTS

Spin Test

At 8,000 rpm, the last speed where all readable gages were operable on disk 1, the maximum strain occurred in the bolthole (gage 5, figure E-2). It reached 4300 microinch/in. However, extrapolating the data for gages 3, 5, 6, 7 to 12,150 rpm (by linear regression, which resulted in a fair amount of conservatism) indicated strains well into yielding for the bolthole gages. At 500°F, minimum strain to cause 0.2 percent yield is about 6440 microinch/in. for AMS 4928. The extrapolated strains for gages 3, 5, 6 and 7 were 5150, 9180, 9500, and 8880 microinch/in., respectively. This yielding resulted in a reported residual growth of about 0.004 inches in the bolt circle diameter for both disks 1 and 2.

Comparing rim slot bottom stresses on disk 1 (strain gages 1, 2, 3 and 4) to those previously measured on the B/M disk at 10,000 rpm (P/N 4040002, PWA 1216 Titanium) showed significant differences. Stresses were lowered about 34 percent on the front side in the slot root bottom (live rim) for disk 1 versus the B/M. They were reduced about 48 percent on the rear side. These lowered stresses, compared to the B/M disk, are due to the thickened bore and web on the DTD disk. This fact should increase life in the rim for the DTD disk. Data were not available in the boltholes on the B/M disk for similar comparison.

The spin strain data, plotted in figures E-6 through E-9, showed yielding occurred somewhere above 11,000 rpm. Note also in figures E-6 through E-9 (rim slot locations) that some residual tension occurred at the end of the deceleration portion of the run. The plastic yielding of the bore to the bolt circle area (about 0.004 inch growth

178

in the bolt circle diameter and the elastic material around it (rim)
should cause the bore to bolthole area to be in compression and the
rim in tension. Rim gages 1,3 and 4 (disk 1) showed this tension in
the rim after the residual spin while bolthole gages 5 and 6 (disk 2)
confirmed compression (table E-1). This will lower the operating
stresses at the boltholes and thereby increase bolthole life. Table
E-2 indicates an approximate 150°F differential between the bore and
hub. However, strain data reported *ᵈ ᵥ spinning indicates only
strain due to speed, and not due to thermᵤᵢ stresses.

FERRIS WHEEL TEST

Strain Survey

Disks 1 and 3 were designated for bolthole testing and disk 2 for
the rim test. Disk 1 was predominently strain gaged in the boltholes
(figure E-11) and disk 2 in the rim (figure E-14). Disk 3 (not strain
gaged) was the baseline disk for disk 1.

The highest strain occurred in the midspan of the bolthole, out-
board side. It peaked at 9770 microinch/in. for 18,890 lbs/slot (gage
11, figures E-4 and E-12). This was well beyond the 0.2 percent yield
point at room temperature (8500 microinch/in.). However, the bolthole
was starting from a compressive residual state. If the residual com-
pressive strain values of gages 5 or 6 of disk 2 in table E-1 are
added, net peak strain would be somewhat reduced resulting in elastic
response. This would provide additional ferris wheel LCF life in the
residual treated DTD disk 1 over the baseline DTD disk 3.

Strains decreased moving <u>outboard of the bolthole edges</u> (shown in
figure E-13). Peak strain occurred on the front side, and reached
6190 microinch/in. at 18,890 lbs/slot (strain gage 5, figure E-4).

Bore (modified for ferris wheel test) <u>midspan</u> strains
(circumferential) were repeatable to within 1 percent between disks 1
and 2 , where maximum strain reached 6050 microinch/in. (strain gage
30, figure E-4).

The web strains were repeatable to about 3 percent between disk 1 and 2. The circumferential web stresses at 18,890 lbs/slot attained 71,500 psi and 71,800 psi (front and rear, respectively, using averages and $E = 16.6 \times 10^6$ psi, $v = 0.35$). The radial web stresses at the same load were measured at 60,150 psi with a small $\pm$ 3450 psi bending stress toward the rear (drawbar load axis positioned to minimize bending).

The disk slot strains had consistently shaped profiles (figures E-15 through E-18), where strains peaked at 7140 microinch/in. near the front edge (acute corner) of the lug bearing radius (Location Q, figures E-5 and E-16). Figures E-16 and E-18 illustrate more variation in strain between lugs than figures E-15 and E-17. This may be due to the variable drawbar-to-disk contact pattern in the highly stressed lug load bearing surfaces.

No strains other than bolthole values approached the minimum required strain to yield AMS 4928 (even disk 2 strains extrapolated to 18,890 lbs/slot). This implied these other measured areas should have sufficiently more ferris wheel life than the boltholes and therefore be of lesser concern.

FERRIS WHEEL TEST

Tables E-5 and E-6 contain the ferris wheel crack history (via replication) for disks 1 and 3 (the residual spun disk and its baseline, respectively). For disk 2, no cracks were detected propagating from the rim elox flaws after a total of 3500 sawtooth cycles (see figure E-19 for duty cycle definition). This indicated the rim area for disk 2 was very "damage tolerant" of elox flaws.

Bolthole cracks propagated noticeably faster during ferris wheel sawtooth cycling in disk 3 than disk 1, even though they started from a shorter mean elox length (0.0141 inches vs. 0.020 inches). Figure E-22 shows this well. Tables E-7 and E-9 also confirmed the crack growth rate for baseline disk 3 was always higher than disk 1 for sawtooth cycling.

The web strains were repeatable to about 3 percent between disk 1 and 2. The circumferential web stresses at 18,890 lbs/slot attained 71,500 psi and 71,800 psi (front and rear, respectively, using averages and $E = 16.6 \times 10^6$ psi, $v = 0.35$). The radial web stresses at the same load were measured at 60,150 psi with a small $\pm$ 3450 psi bending stress toward the rear (drawbar load axis positioned to minimize bending).

The disk slot strains had consistently shaped profiles (figures E-15 through E-18), where strains peaked at 7140 microinch/in. near the front edge (acute corner) of the lug bearing radius (Location Q, figures E-5 and E-16). Figures E-16 and E-18 illustrate more variation in strain between lugs than figures E-15 and E-17. This may be due to the variable drawbar-to-disk contact pattern in the highly stressed lug load bearing surfaces.

No strains other than bolthole values approached the minimum required strain to yield AMS 4928 (even disk 2 strains extrapolated to 18,890 lbs/slot). This implied these other measured areas should have sufficiently more ferris wheel life than the boltholes and therefore be of lesser concern.

FERRIS WHEEL TEST

Tables E-5 and E-6 contain the ferris wheel crack history (via replication) for disks 1 and 3 (the residual spun disk and its baseline, respectively). For disk 2, no cracks were detected propagating from the rim elox flaws after a total of 3500 sawtooth cycles (see figure E-19 for duty cycle definition). This indicated the rim area for disk 2 was very "damage tolerant" of elox flaws.

Bolthole cracks propagated noticeably faster during ferris wheel sawtooth cycling in disk 3 than disk 1, even though they started from a shorter mean elox length (0.0141 inches vs. 0.020 inches). Figure E-22 shows this well. Tables E-7 and E-9 also confirmed the crack growth rate for baseline disk 3 was always higher than disk 1 for sawtooth cycling.

180

Figure E-23 shows the same events occurred in mission cycling.
Up to the point where disk 1 mean crack lengths became much larger and
closer to failure than disk 3 (past 445 mission cycles, table E-5),
disk 3 had higher ferris wheel mission cycle crack growth rate than
disk 1 (comparing tables E-8 and E-9).

Past 445 mission cycles, the crack growth rate for disk 1 took a
quick turn toward failure, which occurred after a total of 2091 saw-
tooth and 568 mission cycles. Primary failure site was bolthole 20.
The failure resulted in the separation of disk 1 into two halves.
Disk 3 approached this comparable point, then further testing on it was
discontinued (after a total of 1200 sawtooth and 275 mission cycles).

The final mean aspect ratio for the residually treated disk 1 was
1.94:1, 10 percent higher than the average for baseline (untreated)
disk 3.

Boltholes 10 and 20 were studied with a SEM (scanning electron
microscope). This was to assure no material anomalies existed.
Figure E-26 shows a clearly defined thumbnail shaped fatigue crack for
bolthole 10 (secondary failure hole), and that the fatigue had prog-
ressed normally for Ti-6Al-4V (AMS 4928). This is clearly shown by
the transgranular fatigue with striations well defined in many areas.
Bolthole 20 (primary failure hole) showed a poorly defined thumbnail
pattern (figure E-27). In region B of bolthole 20 located the same
distance from the elox slot as region A in bolthole 10, similar
transgranular fatigue with well defined striations in many areas was
seen (figure E-27). Figure E-28 views the crack surface progressing
from a transition region C (reference figure E-27) containing few
striated areas with very little integranular or tensile (dimpled)
fatigue to a region D of overstress. This region 'D' of overstress
has within it areas of mixed tensile (dimpled) and intergranular
fatigue. Bolthole 6 on baseline disk 3 was examined by SEM for
comparison and showed the same fatigue pattern as bolthole 10 on
disk 1.

181

As a point of interest, bolthole 12 on disk 1, <u>inboard side</u>, had an elox flaw similar to the others on the disk. After disk failure, replication of this location showed no cracks propagating from this elox flaw.

REFERENCES

1. Monthly R&D Status Report, C.E. Spaeth, Program Manager, "Develop, Refine and Evaluate a Damage Tolerant Design System for Cold Section Turbine Engine Disks", dated 31 March 1980.

2. FMMT 22035, M.S. Mills to S.P. Stone, "Room Temperature Spin Strain Survey of F100 2nd Stage Fan Disk and Blades", dated 13 July 1980.

3. FMMT 23292, P.V. Young to C. Spaeth, "Use Nondestructive Evaluation to Detect Crack Initiation in a Damage Tolerant Designed F100 2nd Fan Disk," dated 3 November 1980.

4. Monthly R&D Status Report, C.E. Spaeth, Program Manager, "Develop, Refine and Evaluate a Damage Tolerant Design System for Cold Section Turbine Engine Disks," dated 24 April 1980.

5. Dimensional Inspection Record Sheet of Pre- and Post-Spin Tested DTD Disk 1, dated 22 February 1980.

6. Internal Correspondence, C. Cook to J. Weber/M. Mills, "Ferris Wheel Test Plan for DTD #1", dated 14 July 1980.

7. MDL Work Request and Report No. 55-148, H.R. Nesor to M.S. Mills, SEM Study of Damage Tolerant Design Disks Bolthole Fracture Faces, dated 17 March 1981.

ME&T STEADY STATE SPIN STRAIN DATA AT 500°F
AMS 4928 TITANIUM DISK DERIVED FROM F100 2ND STAGE FAN DESIGN
DAMAGE TOLERANT DESIGN, DISKS 1 AND 2. (REFERENCE FIGURE E-2 FOR S/G LOCATIONS)

Disk #1

Gage	Run	500°F Strain (micro in/in.) for Speed (rpm) of:																
		0*	2000	4000	6000	8000	10000**	11000	11500	12000	12150	10000	8000	6000	4000	2000	0	Ort***
1	1	0	-	720	1430	2390	3660	-	-	-	-	-	-	-	-	-	0	0
1	2	0	110	490	1160	2150	3640	4250	4780	5820	6100	4700	3890	3170	2140	-	1040	1100
2	1	0	-	750	1490	2470	3770	-	-	-	-	-	-	-	-	-	0	0
2	2	0	200	700	1440	2450	3740	4550	5060	5980	6260	4810	3820	2780	1740	-	760	870
3	1	0	-	480	1240	2190	3460	-	-	INOPERATIVE							0	0
3	2	0	-	-	-	-	-	-	-									
4	1	0	-	570	1230	2130	3300	-	-	-	-	-	-	-	-	-	0	0
4	2	0	120	480	1110	2040	3230	4000	4520	5450	5690	4400	3630	2800	1920	-	950	1040
5	1	0	-	1100	2490	4300	6180	-	-	-	-	INOPERATIVE						0	0
5	2	0	230	960	2100	3710	5790	-	-	-	•	•	•	•	•	•	•	
6	1	0	-	1130	2440	4180	-	-	-	-	INOPERATIVE						0	0
6	2	0	-	-	-	-	-	•	•	•	•	•	•	•	•	•	•	
7	1	0	-	960	2160	3850	-	-	-	INOPERATIVE								
7	2	0	-	-	-	-	-	•	•	INOPERATIVE								
8	1	0	-	-	-	-	-	-	-	INOPERATIVE								
8	2	0	-	-	-	•	•	•	•	INOPERATIVE								

Disk #2

Gage	Recorded Residual Strain Only (Maximum rpm was 11,950)
5	-1580
6	-1520

* Recording System set for zero initial output prior to acceleration

** Run #1 to only 10,000 rpm for preliminary design analysis check prior to full speed run #2

*** Residual strain measured after test at room temperature

TABLE E-2

AVERAGE TEST TEMPERATURES DURING SPIN TESTS FOR RESIDUAL STRESS
INDUCEMENT

AMS 4928 TITANIUM DISK DERIVED FROM F100 SECOND STAGE FAN DESIGN
DAMAGE TOLERANT DESIGN DISKS 1 AND 2*

(REFERENCE FIGURE E-3 FOR T/C LOCATIONS)

Thermocouple	Temperature (°F $\pm$ 10°F)
1	501
2	498
3	491
4	495
5	518
6	520
7	518
8	521
9	500
10	501
11	355
12	353

*Oven Calibration Repeatability Tests of Disk
1 Used to Establish Temperature During Test
of Disk 2

TABLE E-3
MMT FERRIS WHEEL STEADY STATE STRAIN DATA AT ROOM TEMPERATURE
AMS 4928 TITANIUM DISK DERIVED FROM F100 2ND STAGE FAN DESIGN
DAMAGE TOLERANT DESIGN, DISK 1   (REFERENCE FIGURE E-4)

Strain (Micro in./in.) for Load (lbs) at Each Blade Slot of:

Gage	Run	8000	12000	16000	17000	18000	18890	18000	17000	16000	12000	8000
1	1	2180	3380	4630	4910	5220	5470	5200	4920	4630	3540	2550
	2	2260	3440	4630	4970	5280	5530	5250	4970	4650	3540	2580
2	1	1990	3020	4080	4310	4570	4650	4530	4210	3900	2900	2000
	2	2020	3020	4070	4320	4580	4770	4510	4170	3870	2850	1960
3	1	1860	3000	4180	4460	4750	4980	4710	4450	4200	3190	2250
	2	1950	3030	4190	4490	4780	5010	4730	4480	4190	3140	2230
4	1	1920	2910	4000	4230	4510	4700	4470	4140	3800	2770	1890
	2	1940	2920	3990	4260	4520	4720	4460	4090	3780	2720	1850
5	1	2510	–	–	–	–	6150	–	–	–	–	2540
	2	2560	–	–	–	–	6190	–	–	–	–	2460
6	1	2190	–	–	–	–	5380	–	–	–		2210
	2	2250	–	–	–	–	5410	–	–	–	–	2140
7	1	2020	–	–	–	–	4890	–	–	–	–	2000
	2	2060	–	–	–	–	4930	–	–	–	–	1950
8	1	2790	–	–	–	–	6920	–	–	–	–	2910
	2	2860	–	–	–	–	6970	–	–	–	–	2790
9	1	2390	–	–	–	–	5880	–	–	–	–	2460
	2	2450	–	–	–	–	5930	–	–	–	–	2380
10	1	2110	–	–	–	–	5130	–	–	–	–	2120
	2	2150	–	–	–	–	5160	–	–	–	–	2050
11	1	3760	5730	7900	8450	9120	9620	9360	8770	8200	6250	4230
	2	3830	5830	8100	8650	9270	9770	9340	8710	8160	6150	4130
12	1	3800	5770	7860	8390	9030	9530	9200	8650	8080	6170	4170
	2	3880	5820	7970	8520	9130	9620	9070	8470	7930	5970	3990
13	1	1040	–	–	–	–	2460	–	–	–	–	980
	2	1040	–	–	–	–	2440	–	–	–	–	930
14	1	1070	–	–	–	–	2520	–	–	–	–	1030
	2	1070	–	–	–	–	2500	–	–	–	–	980
15	1	1040	–	–	–	–	2500	–	–	–	–	1020
	2	1050	–	–	–	–	2490	–	–	–	–	990
16	1	•	•	•	•	INOPERATIVE			•	•	•	•
	2	•	•	•	•	INOPERATIVE			•	•	•	•
17	1	3550	5430	7500	8040	8660	9150	8900	8330	7800	5950	4070
	2	3630	5500	7630	8190	8720	9280	8870	8280	7750	5830	3960
18	1	3700	5620	7650	8130	8720	9160	8820	8250	7690	5820	3910
	2	3780	5660	7710	8220	8720	9230	8720	8130	7600	5680	3790
19	1	3710	5640	7730	8260	8900	9370	9100	8500	7940	6030	4100
	2	3780	5680	7810	8360	8880	9440	9010	8390	7840	5860	3940
20	1	3610	5500	7510	8000	8600	9040	8760	8190	7640	5800	3920
	2	3680	5520	7570	8070	8580	9100	8640	8070	7550	5670	3790

186

FERRIS WHEEL STEADY STATE STRAIN DATA AT ROOM TEMPERATURE
AMS 4928 TITANIUM DISK DERIVED FROM F100 2ND STAGE FAN DESIGN
DAMAGE TOLERANT DESIGN, DISK 1   (REFERENCE FIGURE E-4)

Strain (Micro in./in.) for Load (lbs) at Each Blade Slot of:

Gage	Run	8000	12000	16000	17000	18000	18890	18000	17000	16000	12000	8000
21	1	1340	-	-	-	-	3450	-	-	-		1070
	2	1350	-	-	-	-	3280	-	-	-	-	1290
22	1	1200	-	-	-	-	2900	-	-	-	-	1190
	2	1210	-	-	-	-	2890	-	-	-	-	1160
23	1	790	-	-	-	-	1960	-	-	-	-	820
	2	800	-	-	-	-	1970	-	-	-	-	810
24	1	760	-	-	-	-	1840	-	-	-	-	750
	2	780	-	-	-	-	1830	-	-	-	-	730
25	1	1240	-	-	-	-	2980	-	-	-	-	1180
	2	1250	-	-	-	-	2900	-	-	-	-	1140
26	1	1250	-	-	-	-	3010	-	-	-	-	1240
	2	1250	-	-	-	-	2980	-	-	-	-	1200
27	1	990	-	-	-	-	2340	-	-	-	-	1010
	2	1000	-	-	-	-	2330	-	-	-	-	980
28	1	980	-	-	-	-	2310	-	-	-	-	940
	2	1000	-	-	-	-	2300	-	-	-	-	930
29	1	2230	-	-	-	-	5360	-	-	-	-	2210
	2	2260	-	-	-	-	5370	-	-	-	-	2090
30	1	2490	-	-	-	-	6030	-	-	-	-	2480
	2	2530	-	-	-	-	6050	-	-	-	-	2530

MMT FERRIS WHEEL STATIC STRAIN DATA AT ROOM TEMPERATURE
AMS 4928 TITANIUM DISK DERIVED FROM F100 2ND STAGE FAN DESIGN
DAMAGE TOLERANT DESIGN, DISK 2   (REFERENCE FIGURE E-5)

Strain (Micro in./in.) for Radial Load (lbs) at Each Blade Slot of:

Gage	Run	8000	10000	12000	14000	15000	16000	17000	17700	17000	16000	12000	8000
1	1	1830	2260	2730	3160	3370	3600	3840	4030	–	–	–	–
	2	1800	2250	2580	3220	3410	3630	3860	4060	–	–	–	–
2	1	2130	2630	3180	3700	3950	4200	4490	4680	–	–	–	–
	2	2090	2620	3170	3740	3970	4240	4510	4750	–	–	–	–
3	1	2040	2570	3160	3390	3630	3920	4210	4430	–	–	–	–
	2	1930	2510	3030	3580	3800	4070	4380	–	–	–	–	–
4	1	1830	2250	2680	3140	3330	3550	3790	3950	–	–	–	–
	2	1800	2200	2640	3110	3300	3510	3730	3870	–	–	–	–
5	1	1300	1610	1960	2320	2480	2640	2830	2950	–	–	–	–
	2	1300	1620	1970	2290	2480	2640	2800	2880	–	–	–	–
6	1	1250	1580	1850	2290	2440	2610	2770	2880	–		–	–
	2	1280	1550	1900	2200	2380	2520	2640	2680	–	–	–	–
7	1	780	980	1180	1450	1540	1670	1750	1840	–	–	–	–
	2	790	990	1210	1420	1540	1620	1720	1760	–	–	–	–
8	1	820	1030	1230	1460	1550	1700	1790	1830	–	–	–	–
	2	820	970	1220	1380	1520	1590	1680	1710	–	–	–	–
9	1	1270	1590	1890	2310	2470	2640	2860	2940	–	–	–	–
	2	1300	1590	1930	2270	2430	2580	2770	2810	–	–	–	–
10	1	1500	1870	2230	2620	2780	2890	3030	3110	–	–	–	–
	2	1420	1720	2070	2420	2680	2880	3030	3040	–	–	–	–
11	1	920	1130	1360	1590	1680	1780	1900	1980	1860	1760	1350	890
	2	920	1140	1370	1600	1710	1810	1920	1990	1900	1880	1380	920
12	1	930	1150	1380	1610	1720	1820	1930	2000	1890	1790	1380	900
	2	920	1140	1360	1600	1720	1820	1930	2010	1920	1810	1390	920
13	1	2390	2990	3590	4230	4520	4840	5180	5350	5060	4780	3590	2400
	2	2400	3000	3620	4240	4530	4830	5130	5360	5020	4750	3520	2310
14	1	2350	2930	3530	4150	4420	4720	5030	5220	5020	4720	3500	2330
	2	2340	2930	3550	4160	4450	4730	5020	5240	5000	4720	3460	2280
15	1	2840	3410	3970	4600	4830	5180	5520	5760	5760	5640	5180	–
	2	2810	3400	4000	4680	5000	5280	5590	5820	5710	5610	5040	2800
16	1	2210	2740	3370	4030	4260	4550	4840	4730	4580	4210	3140	2000
	2	2300	2860	3460	4030	4310	4580	4860	5040	4760	4370	3210	2040
17	1	2580	3210	3840	4530	4780	5160	5530	5800	5730	5590	4820	3400
	2	2600	3200	3920	4630	4980	5300	5650	5910	5770	5630	4720	3250
18	1	2320	2890	3540	4240	4460	4770	5080	5290	4760	4360	3170	1910
	2	2380	2970	3620	4210	4470	4740	5010	5210	4660	4240	3000	1850
19	1	1640	1960	2270	2620	2730	2930	3110	3240	3360	3250	2620	1870
	2	1620	1910	2080	2580	2750	2910	3090	3210	3220	3120	2460	1900
20	1	610	690	790	880	910	950	990	1020	850	750	560	430
	2	640	710	780	850	880	930	960	1000	900	800	590	440
21	1	–	–	INOPERATIVE			–	–	–	–	–	–	–
	2	–	–	INOPERATIVE			–	–	–	–	–	–	–
22	1	1770	2110	2510	2890	3010	3160	3350	3480	3220	3000	2290	1560
	2	1710	2040	2390	2740	2900	3060	3240	3380	3270	3050	2290	1550

MMT FERRIS WHEEL STATIC STRAIN DATA AT ROOM TEMPERATURE
AMS 4928 TITANIUM DISK DERIVED FROM F100 2ND STAGE FAN DESIGN
DAMAGE TOLERANT DESIGN, DISK 2   (REFERENCE FIGURE E-5)

Strain (Micro in./in.) for Radial Load (lbs) at Each Blade Slot of:

Gage	Run	8000	10000	12000	14000	15000	16000	17000	17700	17000	16000	12000	8000
23	1	2180	2760	3290	3870	4080	4400	4700	4910	4930	4830	4220	3130
	2	2240	2800	3310	3890	4160	4420	4700	4920	4830	4750	4040	2950
24	1	2910	3580	4320	5070	5310	5660	6000	6250	6260	5960	4600	3140
	2	2840	3510	4220	4920	5240	5560	5910	6160	6020	5700	4320	2840
25	1	2850	3460	4020	4640	4860	5180	5620	5720	5830	5740	5400	4400
	2	2960	3570	4100	4690	4950	5210	5490	5700	5620	5550	5120	4000
26	1	3680	4340	5090	5890	6140	6490	6890	7140	6940	6610	5440	3940
	2	3430	4110	4830	5530	5840	6170	6500	6770	6720	6370	5140	3620
27	1	2030	2530	3040	3580	3790	4040	4340	4520	4400	4250	3580	2570
	2	2000	2500	3010	3560	3830	4070	4330	4520	4380	4240	3540	2480
28	1	2090	2610	3190	3770	4000	4270	4570	4770	4630	4470	3600	2440
	2	2090	2620	3170	3730	4000	4240	4510	4720	4610	4450	3580	2410
29	1	2120	2650	3220	3730	3940	4220	4510	4700	4620	4470	3810	2860
	2	2130	2670	3170	3730	3990	4240	4510	4710	4570	4410	3730	2720
30	1	2150	2650	3210	3770	3980	4230	4490	4670	4450	4270	3320	2190
	2	2120	2630	3170	3700	3920	4170	4410	4590	4350	4170	3220	2100
31	1	2150	2710	3160	3590	3690	3860	4030	4160	-	INOPERATIVE		
	2	1970	2450	2850	3380	3690	4020	4270	4460	3900	3780	3330	2440
32	1	1850	2300	2820	3320	3520	3760	4030	4200	4080	3920	3140	2130
	2	1840	2300	2800	3280	3510	3740	3980	4160	4050	3910	3130	2110
33	1	1520	1900	2290	2670	2830	3030	3250	3380	3240	3120	2600	1940
	2	1490	1870	2230	2650	2840	3030	3230	3380	3260	3120	2600	1900
34	1	-	-	-	INOPERATIVE				-	-	-	-	-
	2	-	-	-	INOPERATIVE				-	-	-	-	-
35	1	1310	1630	1950	2280	2420	2590	2770	2870	2750	2630	2180	1600
	2	1270	1600	1900	2250	2420	2580	2750	2880	2770	2640	2180	1570
36	1	1400	1740	2100	2460	2600	2780	2950	3080	2950	2810	2180	1460
	2	1390	1730	2080	2440	2600	2760	2920	3060	2960	2810	2170	1450
37	1	1180	1460	1650	2120	2540	2760	2950	3070	2990	INOPERATIVE		-
	2	-	-	-	INOPERATIVE				-	-	-	-	-
38	1	1050	1310	1600	1870	1990	2130	2280	2380	2270	1970	1650	1100
	2	1050	1320	1590	1880	2010	2150	2270	2380	2260	2140	1650	1080
39	1	1540	1920	2300	2680	2830	3030	3250	3380	3230	3100	2600	1930
	2	1500	1870	2240	2640	2840	3010	3210	3370	3290	3160	2670	1970
40	1	1690	2100	2540	2980	3160	3380	3600	3770	3630	3480	2780	1880
	2	1670	2090	2500	2950	3140	3350	3560	3720	3610	3470	2760	1850
41	1	2070	2580	3080	3630	3880	4120	4380	4580	4430	4270	3580	2600
	2	2110	2620	3120	3660	3870	4150	4430	-	INOPERATIVE			-
42	1	2100	2620	3160	3720	3940	4210	4470	4650	4530	4330	3390	2280
	2	2080	2590	3110	3640	3900	4120	4360	4540	4350	4170	3220	2120
43	1	1620	2020	2420	2850	3020	3230	3460	3610	3500	3360	2800	2000
	2	1590	1990	2380	2820	3030	3230	3440	3600	3480	3330	2740	1930
44	1	1530	1900	2320	2730	2890	3080	3300	3440	3320	3190	2540	1710
	2	1510	1880	2270	2670	2870	3030	3230	3380	3280	3150	2500	1680

MMT FERRIS WHEEL STATIC STRAIN DATA AT ROOM TEMPERATURE
AMS 4928 TITANIUM DISK DERIVED FROM F100 2ND STAGE FAN DESIGN
DAMAGE TOLERANT DESIGN, DISK 2
(REFERENCE FIGURE E-5)

Disk 2: Ferris Wheel (Micro in./in.) for Radial Load (lbs) at Each Blade Slot

Gage	Run	8000	10000	12000	14000	15000	16000	17000	17700	17000	16000	12000	8000
45	1	1790	2210	2650	3100	3280	3500	3740	3880	3730	3590	3000	2210
	2	1750	2190	2600	3060	3270	3480	3700	3880	3750	3600	2990	2160
46	1	1790	2200	2660	3090	3240	3450	3660	3790	3530	3370	2580	1680
	2	1720	2130	2550	2980	3160	3360	3550	3690	3510	3350	2560	1670
47	1	1230	1520	1830	2140	2260	2420	2590	2690	2530	2420	2020	1480
	2	1200	1490	1780	2110	2270	2410	2570	2690	2600	2490	2090	1530
48	1	1850	1950	2210	2520	2650	2800	2980	3100	3120	2010	2620	2120
	2	1760	2080	2380	2730	2810	2920	3030	3150	3080	3000	2730	2070

TABLE E-5
CRACK LENGTH VS. NUMBER OF FERRIS WHEEL CYCLES
OUTBOARD BOLTHOLE ELOX REPLICATION INSPECTION DATA
AMS 4928 TITANIUM DISK DERIVED FROM F100 2ND STAGE FAN DESIGN
DAMAGE TOLERANT DESIGN DISK 1

(See Figure E-19 for Ferris Wheel Duty Cycle Definition)

Bolthole	Beginning Elox Width	Beginning Elox Length	Sawtooth Cycles			Mission Cycles				
			1177	1500	2000	250	420	445	545	568
2	0.0073	0.0196	0.0212	0.0237	0.0270	0.0413	0.0790	0.0855	0.1220	0.1370
4	0.0075	0.0205	0.0210	0.0222	0.0282	0.0656	0.1355	0.1470	0.2250	0.2670
6	0.0075	0.0205	0.0228	0.0241	0.0298	0.0794	0.1439	0.1630	0.2764	0.3450
8	0.0073	0.0198	0.0223	0.0264	0.0311	0.0647	0.0960	0.1135	0.1610	0.1933
10	0.0073	0.0200	0.0220	0.0260	0.0281	0.0535	0.0769	0.0880	0.1580	0.1866
12	0.0075	0.0195	0.0225	0.0230	0.0288	0.0760	0.1360	0.1525	0.2250	0.3266
14	0.0074	0.0200	0.0220	0.0238	0.0258	0.0604	0.1176	0.1278	0.1810	0.2115
16	0.0070	0.0195	0.0201	0.0242	0.0349	0.0777	0.1386	0.1418	0.2260	0.2610
18	0.0070	0.0200	0.0220	0.0267	0.0312	0.0588	0.1036	0.1278	0.1850	0.2090
20	0.0070	0.0202	0.0225	0.0263	0.0314	0.0794	0.1662	0.1805	0.3000	0.4200*
Minimum Crack Length		0.0195	0.0201	0.0222	0.0258	0.0413	0.0769	0.0855	0.1220	0.1370
B/H		12	16	4	14	2	10	2	2	2
MEAN (Average)		0.02000	0.0218	0.0246	0.0296	0.0657	0.1193	0.1327	0.2059	0.2559
Maximum Crack Length		0.0205	0.0228	0.0267	0.0349	0.0794	0.1662	0.1805	0.3000	0.4200
B/H		6	6	18	16	20	20	20	20	20

*Primary Failure Site

TABLE E-6. CRACK LENGTH VS. NUMBER OF FERRIS WHEEL CYCLES
OUTBOARD BOLTHOLE ELOX REPLICATION INSPECTION DATA. AMS 4928
TITANIUM DISK DERIVED FROM F100 2ND STAGE FAN DESIGN
DAMAGE TOLERANT DESIGN DISK 3

(See Figure E-19 for Ferris Wheel Duty Cycle Definition)

Bolt-Hole	Beginning Elox Width	Beginning Elox Length	Sawtooth Cycles					Mission Cycles		
			300	500	900	1100	1200	50	100	115
2	0.0053	0.0138	0.0148	0.0165	0.0213	0.0232	0.0261	0.0352	0.493	-
4	0.0048	0.0133	0.0153	0.0178	0.0218	0.0242	0.0274	0.0385	0.0545	-
6	0.0060	0.0142	0.0262	0.0192	0.0252	0.0282	0.0310	0.0427	0.0605	0.0642
8	0.0053	0.0142	0.0153	0.0183	0.0230	0.0267	0.0300	0.0430	0.0647	0.0685
10	0.0052	0.0143	0.0152	0.0177	0.0230	0.0258	0.0287	0.0377	0.0530	-
12	0.0055	0.0145	0.0150	0.0152	0.0182	0.0202	0.0222	0.0259	0.0357	-
14	0.0055	0.0142	0.0158	0.0168	0.0207	0.0230	0.0247	0.0293	0.0405	-
16	0.0048	0.0143	0.0154	0.0173	0.0208	0.0225	0.0253	0.0350	0.0594	-
18	0.0050	0.0140	0.0150	0.0167	0.0200	0.0222	0.0243	0.0303	0.0428	-
20	0.0053	0.0141	0.0150	0.0179	0.0215	0.0232	0.0262	0.0324	0.0456	-
Minimum Crack Length		0.0133	0.0148	0.0152	0.0182	0.0202	0.0222	0.0259	0.0357	
B/H		4	2	12	12	12	12	12	12	
MEAN		0.0141	0.0153	0.0173	0.0216	0.0239	0.0266	0.0350	0.0506	
Maximum Crack Length		0.0145	0.0162	0.0192	0.0252	0.0282	0.0310	0.0430	0.0647	
B/H		12	6	6	6	6	6	8	8	

TABLE E-6. CRACK LENGTH VS. NUMBER OF FERRIS WHEEL CYCLES (Cont.).
OUTBOARD BOLTHOLE ELOX REPLICATION INSPECTION DATA. AMS 4928
TITANIUM DISK DERIVED FROM F100 2ND STAGE FAN DESIGN
DAMAGE TOLERANT DESIGN DISK 3

(See Figure E-19 for Ferris Wheel Duty Cycle Definition)

Bolthole	Mission Cycles									
	125	135	150	165	175	190	200	210	220	225
2	-	0.0580	-	-	-	0.0876	-	-	-	-
4	-	0.0704	-	-	-	0.0974	-	-	-	-
6	0.0697	0.0754	0.0850	0.0943	0.1022	0.1086	0.1146	0.1240	0.1316	0.1360
8	0.0743	0.0818	0.0890	0.0992	0.1060	0.1140	0.1224	0.1268	0.1354	0.1416
10	-	0.0685	-	-	-	0.0910	-	-	-	-
12	-	0.0448	-	-	-	0.0631	-	-	-	-
14	-	0.0482	-	-	-	0.0686	-	-	-	-
16	-	0.0613	-	-	-	0.0834	-	-	-	-
18	-	0.0530	-	-	-	0.0762	-	-	-	-
20	-	0.0581	-	-	-	0.0764	-	-	-	-
Minimum Crack Length B/H	-	0.0448	-	-	-	0.0631	-	-	-	-
B/H		12				12				
Mean	-	0.0620	·	-	-	0.0866	-	-	-	-
Maximum Crack Length B/H	-	0.0818	-	-	-	0.1140	-	-	-	-
B/H	-	8	-	-	-	8	-	-	-	-

193

TABLE E-6. CRACK LENGTH VS. NUMBER OF FERRIS WHEEL CYCLES (Cont.).
OUTBOARD BOLTHOLE ELOX REPLICATION INSPECTION DATA. AMS 4928
TITANIUM DISK DERIVED FROM F100 2ND STAGE FAN DESIGN
DAMAGE TOLERANT DESIGN DISK 3

(See Figure E-19 for Ferris Wheel Duty Cycle Definition)

Bolthole	Mission Cycles					
	230	235	245	255	265	275
2	-	0.1126	-	0.1304	-	0.1400
4	-	0.1240	-	0.1360	-	0.1488
6	0.1404	0.1492	0.1568	0.1670	0.1784	0.1892
8	0.1444	0.1520	0.1608	0.1710	0.1820	0.1882
10	-	0.1090	-	0.1174	-	0.1268
12	-	0.0826	-	0.0921	-	0.1012
14	-	0.0936	-	0.0988	-	0.1076
16	-	0.1052	-	0.1162	-	0.1266
18	-	0.0960	-	0.1070	-	0.1176
20	-	0.0950	-	0.1054	-	0.1146
Minimum Crack Length		0.0826		0.0921		0.1012
B/H	-	12	-	12	-	12
MEAN	-	0.1119	-	0.1241	-	0.1361
Maximum Crack Length		0.1520		0.1710		0.1892
B/H	-	8	-	8	-	6

TABLE E-7. OCULAR EXAMINATION DATA. FINAL CRACK LENGTH
VS. DEPTH OF SEVERAL BOLTHOLES FOR FERRIS
WHEEL LCF TEST OF AMS 4928 TITANIUM DISK
DERIVED FROM F100 2ND STAGE FAN DESIGN
DAMAGE TOLERANT DESIGN DISKS 1 AND 3

(See Figure E-19 for Ferris Wheel Duty Cycle Definition)

Disk 1 Bolthole	Final Crack Length[3]	Final Crack Depth[3]	Elox Slot Depth	Final Aspect Ratio
2	0.1480	0.0750	0.0105	1.97:1
6[1]	0.3780	0.2050	0.0098	1:84:1
10	0.1960	0.1010	0.0098	1:94:1
16	0.2720	0.1360	0.0097	2.00:1
20	0.4300	0.2230[2]	0.0100	1:93:1
Mean				1:94:1
Disk 3 Bolthole				
2	0.1480	0.0820	0.0104	1.80:1
6[1]	0.2030	0.1150	0.0106	1.77:1
12	0.1075	0.0630	0.0114	1.71:1
Mean				1.76:1

(1) Figures E-24 and E-25 show heat tinted fracture faces of each, respectively.

(2) Normal crack pattern depth was about 0.2230 inches; however, the last several cycles produced additional striations for a total depth of about 0.38 inches.

(3) Includes elox length and depth.

TABLE E-8. CRACK GROWTH RATE FOR FERRIS WHEEL LCF TEST OF AMS 4928
TITANIUM DISK DERIVED FROM F100 2ND STAGE FAN DESIGN
DAMAGE TOLERANT DESIGN DISK 1
(Reference Table E-5 for Data Used in Table E-8)
da/dN (Mils/Cycle)

Bolthole	Sawtooth Cycles			Mission Cycles				
	0-1177	1177-1500	1500-2000	0-250	250-420	420-445	445-545	545-568
2	0.0014	0.0077	0.0066	0.0572	0.2218	0.2600	0.3650	0.6522
4	0.0004	0.0037	0.0120	0.1496	0.4112	0.4600	0.7800	1.8261
6	0.0020	0.0040	0.0114	0.1984	0.3794	0.7640	1.1340	2.9826
8	0.0021	0.0127	0.0094	0.1344	0.1841	0.7000	0.4750	1.4043
10	0.0017	0.0124	0.0042	0.1016	0.1376	0.4440	0.7000	1.2435
12	0.0025	0.0015	0.0116	0.1888	0.3529	0.6600	0.7250	4.4174
14	0.0017	0.0056	0.0040	0.1384	0.3365	0.4080	0.5320	1.3261
16	0.0005	0.0127	0.0214	0.1712	0.3582	0.1280	0.8420	1.5217
18	0.0017	0.0146	0.0090	0.1104	0.2635	0.9680	0.5720	1.0435
20	0.0020	0.0118	0.0102	0.1920	0.5106	0.5720	1.1950	5.2174
Minimum da/dN	0.0004	0.0015	0.0040	0.0572	0.1376	0.1280	0.3650	0.6522
B/H	-	12	14	2	10	16	2	2
Mean da/dN	0.0016	0.0086	0.0100	0.1442	0.3156	0.5364	0.7320	2.1635
Maximum da/dN	0.0025	0.0146	0.0214	0.1984	0.5106	0.9680	1.1950	5.2174
B/H	12	18	16	6	20	18	20	20

TABLE F-9. CRACK GROWTH RATE FOR FERRIS WHEEL LCF TEST OF AMS 4928 TITANIUM DISK DERIVED FROM F100 2ND STAGE FAN DESIGN DAMAGE TOLERANT DESIGN DISK 3

(Reference Table E-6 for Data Used in Table E-9)

da/dN (Mils/Cycle)

Bolthole	Sawtooth Cycles					Mission Cycles				
	0-300	300-500	500-900	900-1100	1100-1200	0-50	50-100	100-115	115-125	100-135
2	0.0033	0.0085	0.0120	0.0095	0.0290	0.1820	0.2820	-	-	0.2486
4	0.0067	0.0125	0.0100	0.0120	0.0320	0.2220	0.3200	-	-	0.4543
6	0.0067	0.0150	0.0150	0.0150	0.0280	0.2340	0.3560	0.2467	0.5500	0.1629
8	0.0037	0.0150	0.0118	0.0183	0.0330	0.2603	0.4340	0.2533	0.5800	0.2143
10	0.0030	0.0125	0.0133	0.0740	0.0290	0.1800	0.3060	-	-	0.4429
12	0.0017	0.0010	0.0075	0.0100	0.0200	0.0740	0.1960	-	-	0.2600
14	0.0053	0.0050	0.0098	0.0115	0.0170	0.0920	0.2240	-	-	0.2200
16	0.0037	0.0095	0.0088	0.0085	0.0280	0.1940	0.4880	-	-	0.0543
18	0.0033	0.0085	0.0083	0.0110	0.0210	0.1200	0.2500	-	-	0.2914
20	0.0030	0.0145	0.0090	0.0085	0.0300	0.1240	0.2640	-	-	0.3571
Minimum da/dN B/H	0.0017	0.0010	0.0075	0.0100	0.0170	0.0740	0.1960	-	-	0.0543
	12	12	12	12	14	12	12			16
Mean da/dN	0.0040	0.0120	0.0106	0.0119	0.0267	0.1682	0.3120	-	-	0.2706
Minimum da/dN B/P	0.0067	0.015	0.0150	0.0185	0.0330	0.2600	0.4880	-	-	0.4543
	6	6	6	8	8	8	16			4

197

TABLE E-9. CRACK GROWTH RATE FOR FERRIS WHEEL LCF TEST
OF AMS 4028 TITANIUM DISK DERIVED FROM F100 2ND STAGE FAN DESIGN
DAMAGE TOLERANT DESIGN DISK 3
(Reference Table E-6 for Data Used in Table E-9)

da/dN (Mils/Cycle)

Bolthole	Mission Cycles									
	125-135	135-150	150-165	165-175	135-190	175-190	190-200	200-210	210-220	220-225
2	–	–	–	–	0.5382	–	–	–	–	–
4	–	–	–	–	0.4909	–	–	–	–	–
6	0.5700	0.6400	0.6200	0.7900	0.6036	0.4267	0.6000	0.9400	0.7600	0.8800
8	0.7500	0.4800	0.6800	0.6800	0.5855	0.5333	0.8400	0.4400	0.8600	1.2400
10	–	–	–	–	0.4091	–	–	–	–	–
12	–	–	–	–	0.3327	–	–	–	–	–
14	–	–	–	–	0.3709	–	–	–	–	–
16	–	–	–	–	0.4018	–	–	–	–	–
18	–	–	–	–	0.4218	–	–	–	–	–
20	–	–	–	–	0.3327	–	–	–	–	–
Minimum da/dN B/H	–	–	–	–	0.3327 12	–	–	–	–	–
Mean da/dN	–	–	–	–	0.4487	–	–	–	–	–
Maximum da/dN B/H	–	–	–	–	0.6036 6	–	–	–	–	–

TABLE E-9. CRACK GROWTH RATE FOR FERRIS WHEEL LCF TEST
OF AMS 4928 TITANIUM DISK DERIVED FROM F100 2ND STAGE FAN DESIGN
DAMAGE TOLERANT DESIGN DISK 3
(Reference Table 6 for Data Used in Table 9)

da/dN (Mils/Cycle)

Bolthole	Mission Cycles								
	225-230	190-235	230-235	235-245	235-255	245-255	255-265	255-275	265-275
2	-	0.5556	-	-	0.8900	-	-	0.4800	-
4	-	0.5911	-	-	0.6000	-	-	0.6400	-
6	0.9800	0.9022	1.7600	0.7600	0.8900	1.0200	1.1400	1.1100	1.0800
8	0.5600	0.8444	1.5200	0.8800	0.9500	1.0200	1.1000	0.8600	0.6200
10	-	0.4000	-	-	0.4200	-	-	0.4700	-
12	-	0.4333	-	-	0.4750	-	-	0.4550	-
14	-	0.5556	-	-	0.2600	-	-	0.4400	-
16	-	0.4844	-	-	0.5500	-	-	0.5200	-
18	-	0.4400	-	-	0.5500	-	-	0.5300	-
20	-	0.4133	-	-	0.5200	-	-	0.4600	-
Minimum da/dN B/H	-	0.4000 10	-	-	0.2600 14	-	-	0.4400 14	-
Mean da/dN	-	0.5620	-	-	0.6105	-	-	0.5965	-
Maximum da/dN R/P	-	0.9022 6	-	-	0.9500 8	-	-	1.1100 6	-

199
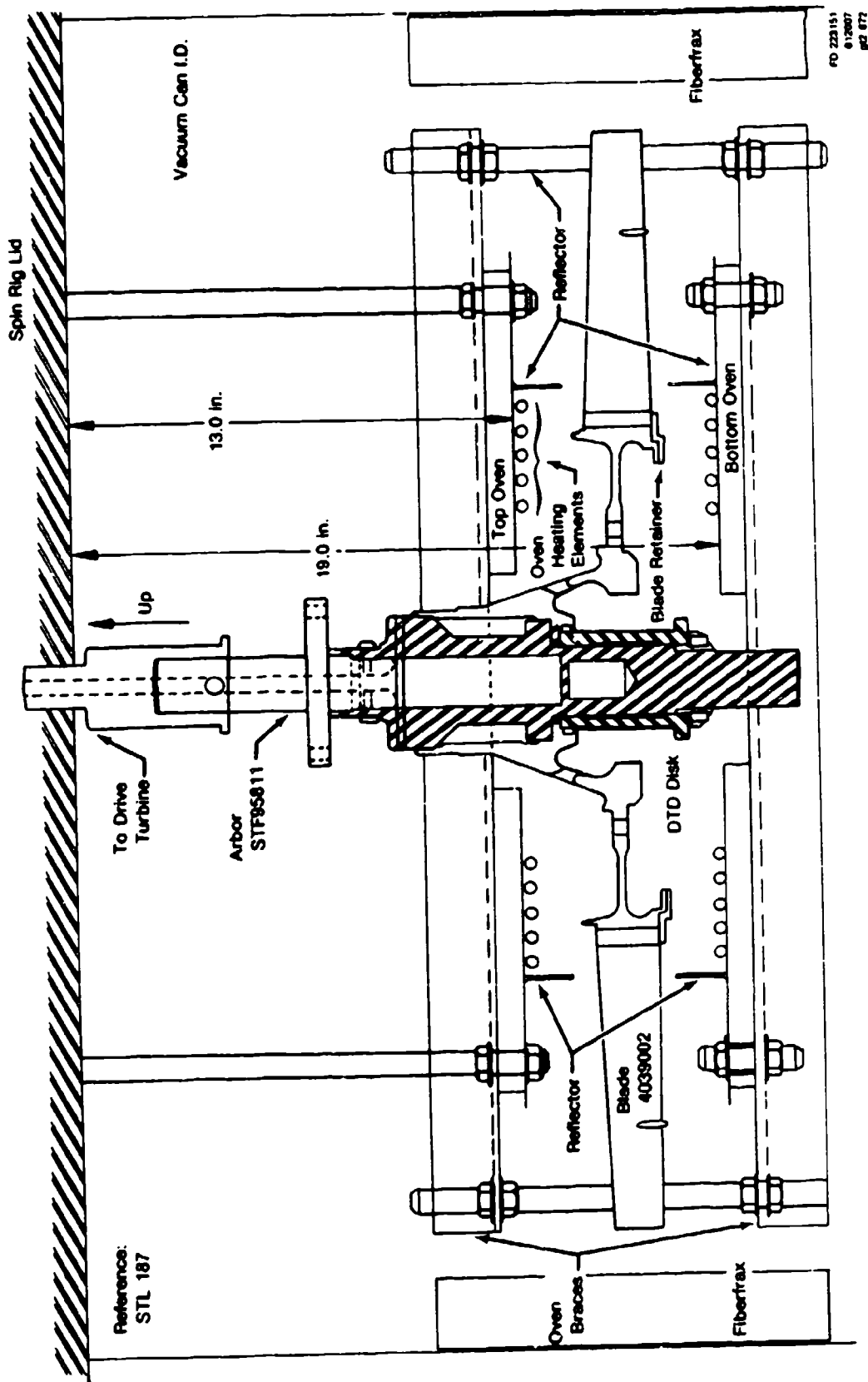
Figure E-1. NE&T Oven Assembly for Hot Spin Test at 500°F. AMS 4928 Titanium Disk Derived from F100 2nd Stage Fan Design. Damage Tolerant Design Disks 1 and 2.
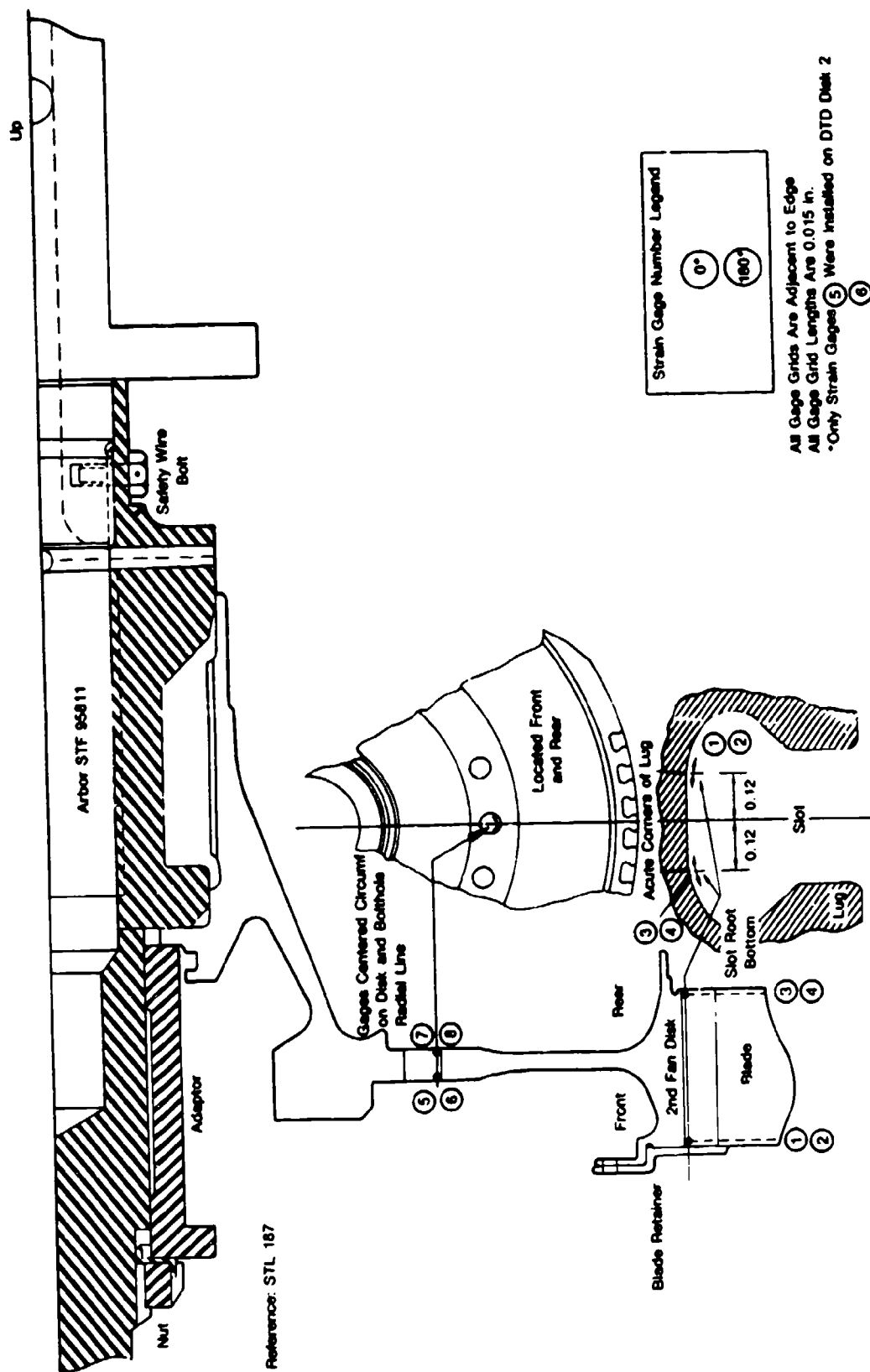
Figure E-2. Strain Gage Locations. AMS 4928 Titanium Disk Derived from F100 2nd Stage Fan Design. Damage Tolerant Design Disks 1 and 2* ME&T Hot Spin in a Partial Vacuum.
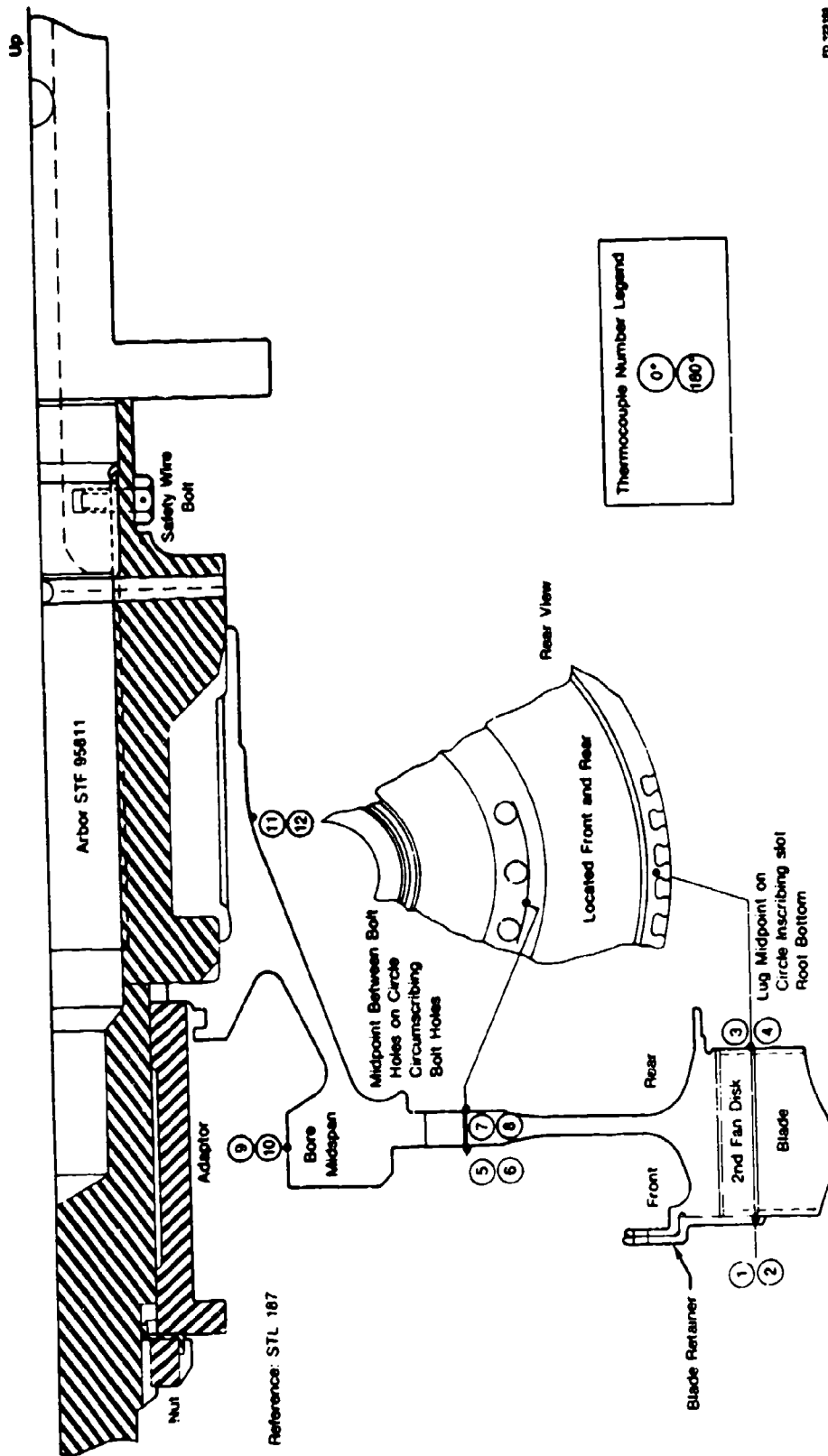
Figure E-3. Thermocouple Locations for Oven Calibration. AMS 4928 Titanium Disk Derived from F100 2nd Stage Fan Design. Damage Tolerant Design Disk 1. ME&T Hot Spin Test in Partial Vacuum.

202

Figure E-4. Strain Gage and Elox Locations. AMS 4928 Titanium Disk Derived from F100 2nd Stage Fan Disk. ME&T Room Temperature Ferris Wheel Test of Damage Tolerant Design Disks 1 and 3. Design.

Figure E-5. Strain Gage and Elox Locations. AMS 4928 Titanium Disk Derived from F100 2nd Stage Fan Design. Damage Tolerant Design. Disks 2 ME&T Room Temperature Ferris Wheel Test.

204
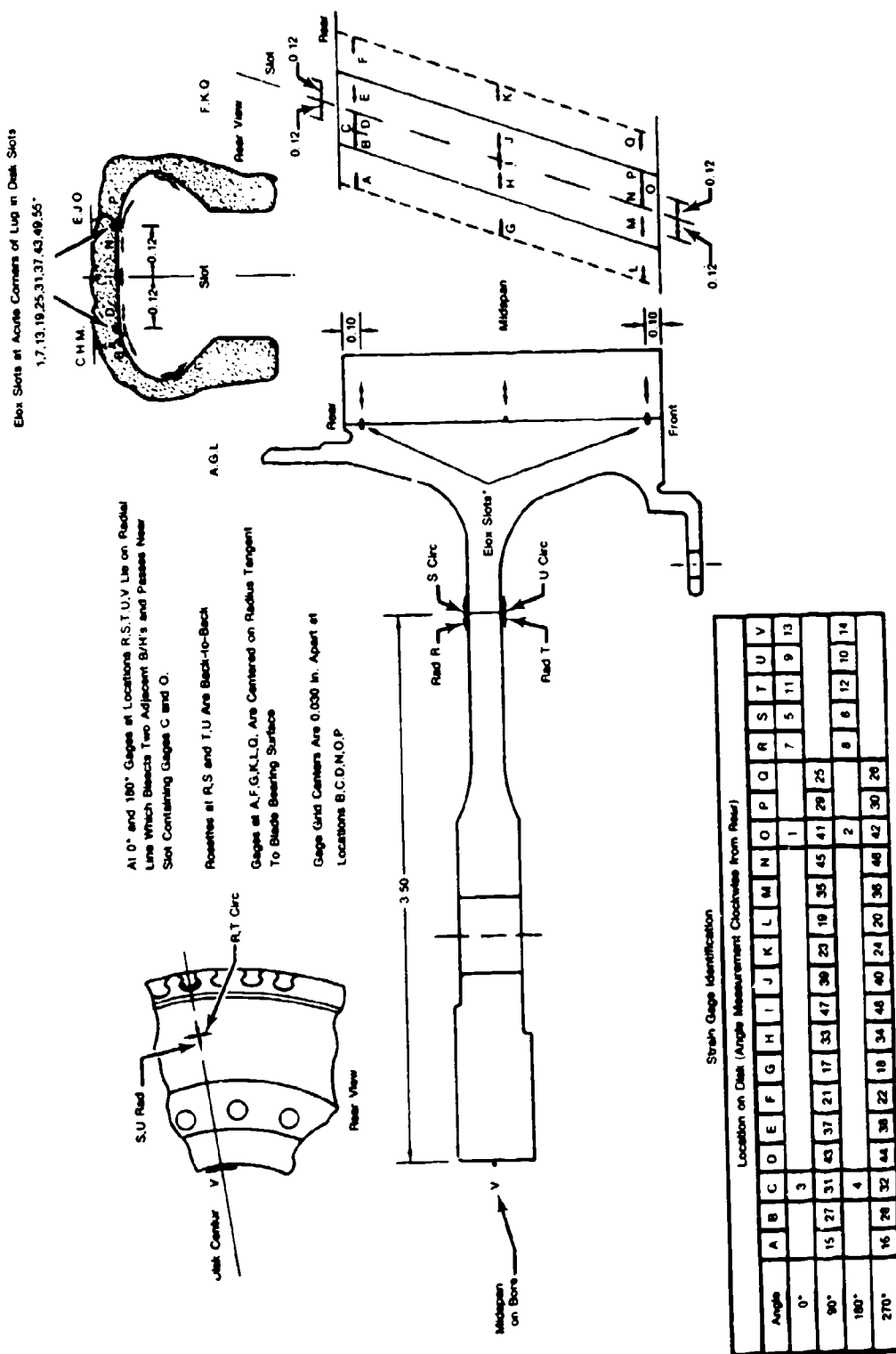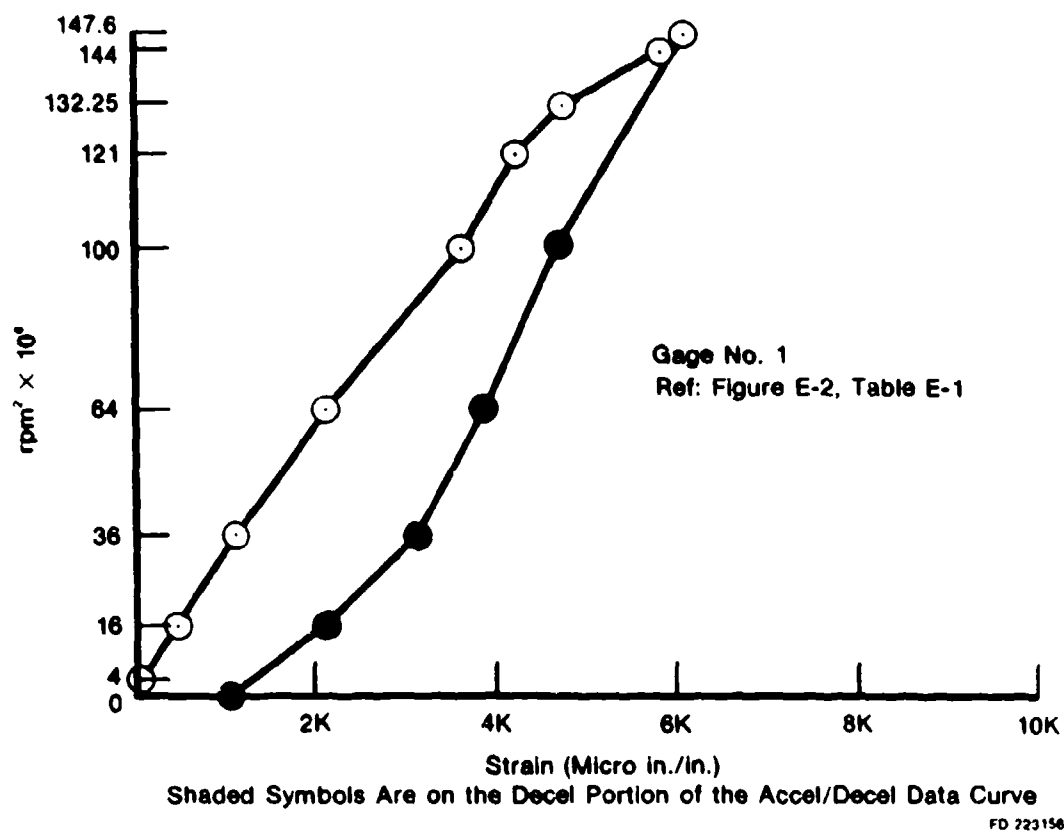
Figure E-6. RPM² vs Spin Strain Accel/Decel Data at 500°F
to 12,150 RPM, Damage Tolerant Design Disk 1.

Gage No. 2
Ref: Figure E-2, Table E-1

Strain (Micro in./in.)

Shaded Symbols Are on the Decel Portion of the Accel/Decel Data Curve

FD 223157
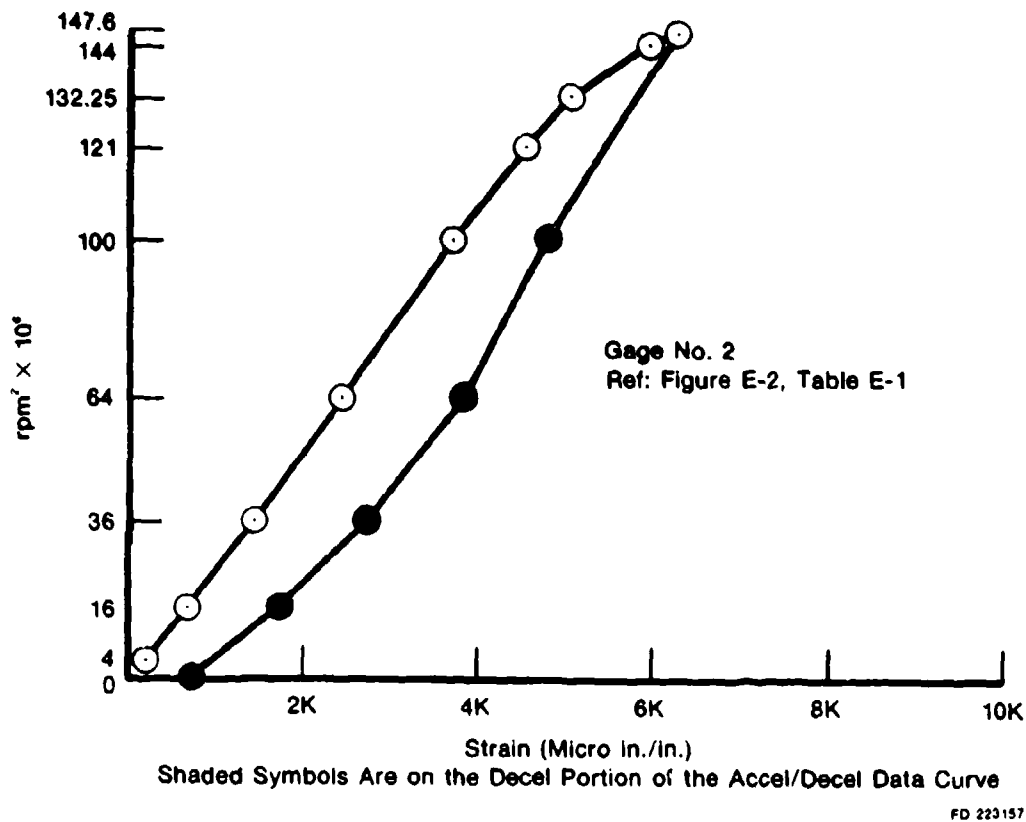
Figure E-7. RPM^2 vs Spin Strain Accel/Decel Data at 500°F to 12,150 RPM Damage Tolerant Design Disk 1.
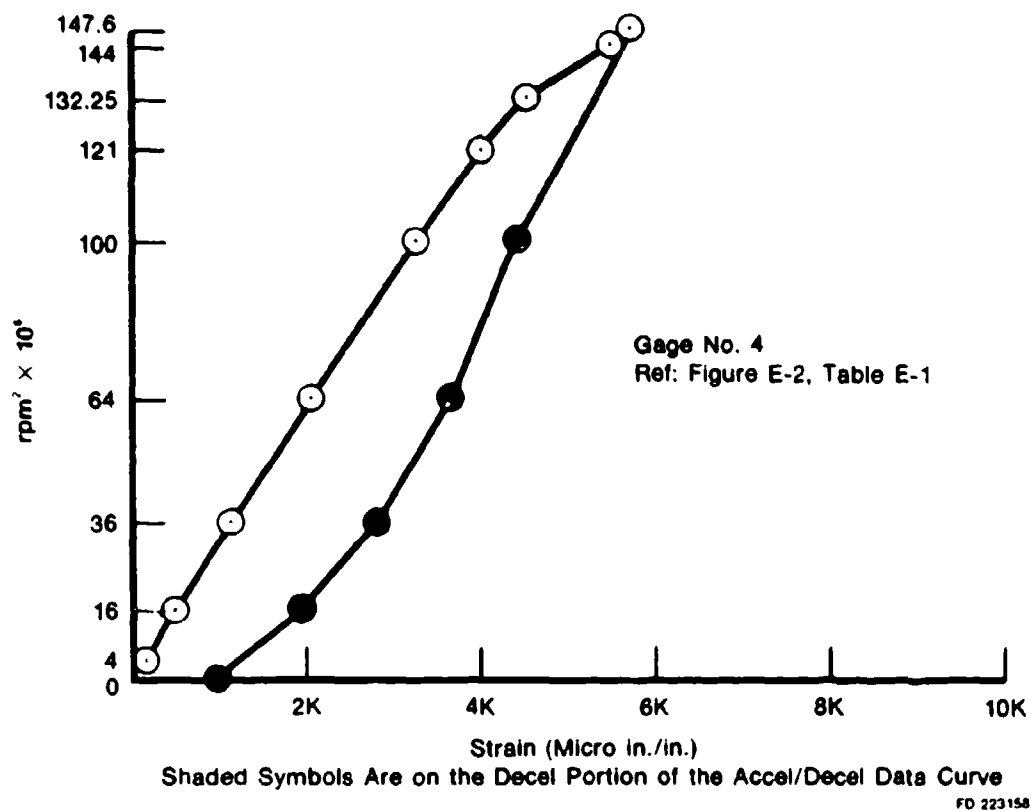
Figure E-8.   RPM^2 vs Spin Strain Accel/Decel Data at 500°F
to 12,150 RPM Damage Tolerant Design Disk 1.
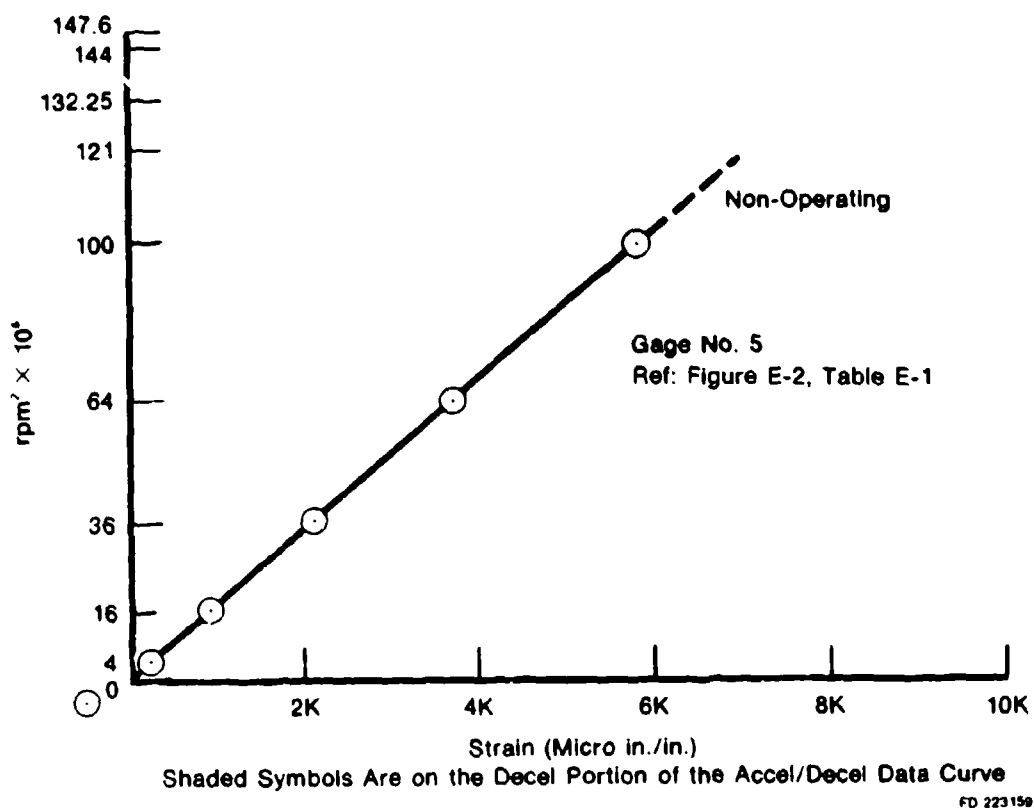
Figure E-9. RPM^2 vs Spin Strain Accel/Decel Data at 500°F
to 12,150 RPM Damage Tolerant Design Disk 1.

FE 186466

Figure E-10. Damage Tolerant Design Disk 1 in ME&T "Ferris Wheel" Test
Facility with Strain Gage and Acoustic Emission Instrumentation.

FE 186467
FD 208994

Figure F-11. Close-Up of Damage Tolerant Design Disk 1 Mounted in ME&T
ferris Wheel" Test Facility. Included in Close-Up is an
Elox Slot (Arrow), Acoustic Emission Detection Probe,
and Strain Gage Instrumentation.

210
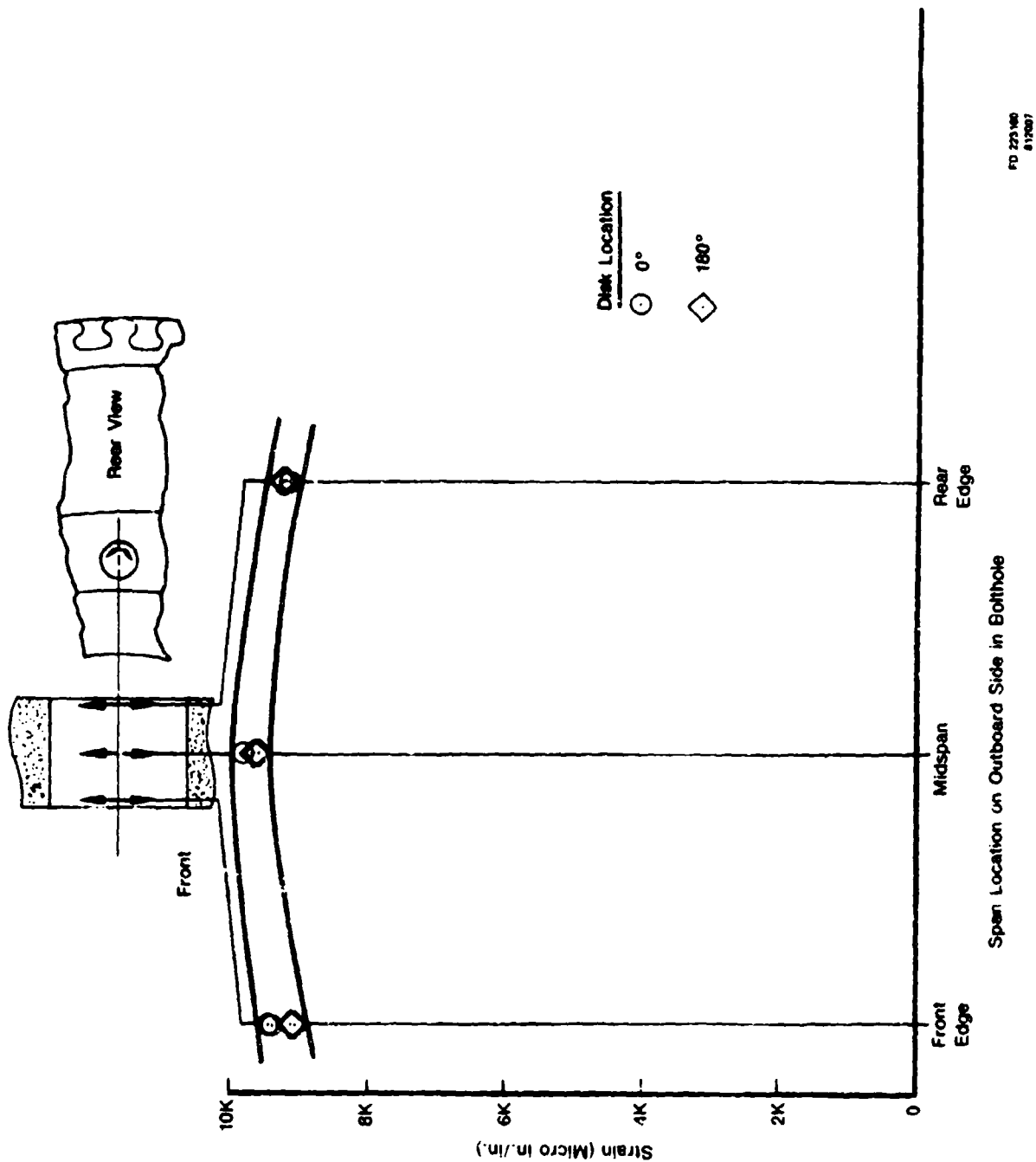
Figure E-12. Static Strain Profile Outside Bolthole Edge. ME&T Room Temperature Ferris Wheel Test at 18,890 lb/Slot. Damage Tolerant Design Disk 1 (Reference Figure E-4 for Strain Gage Locations).
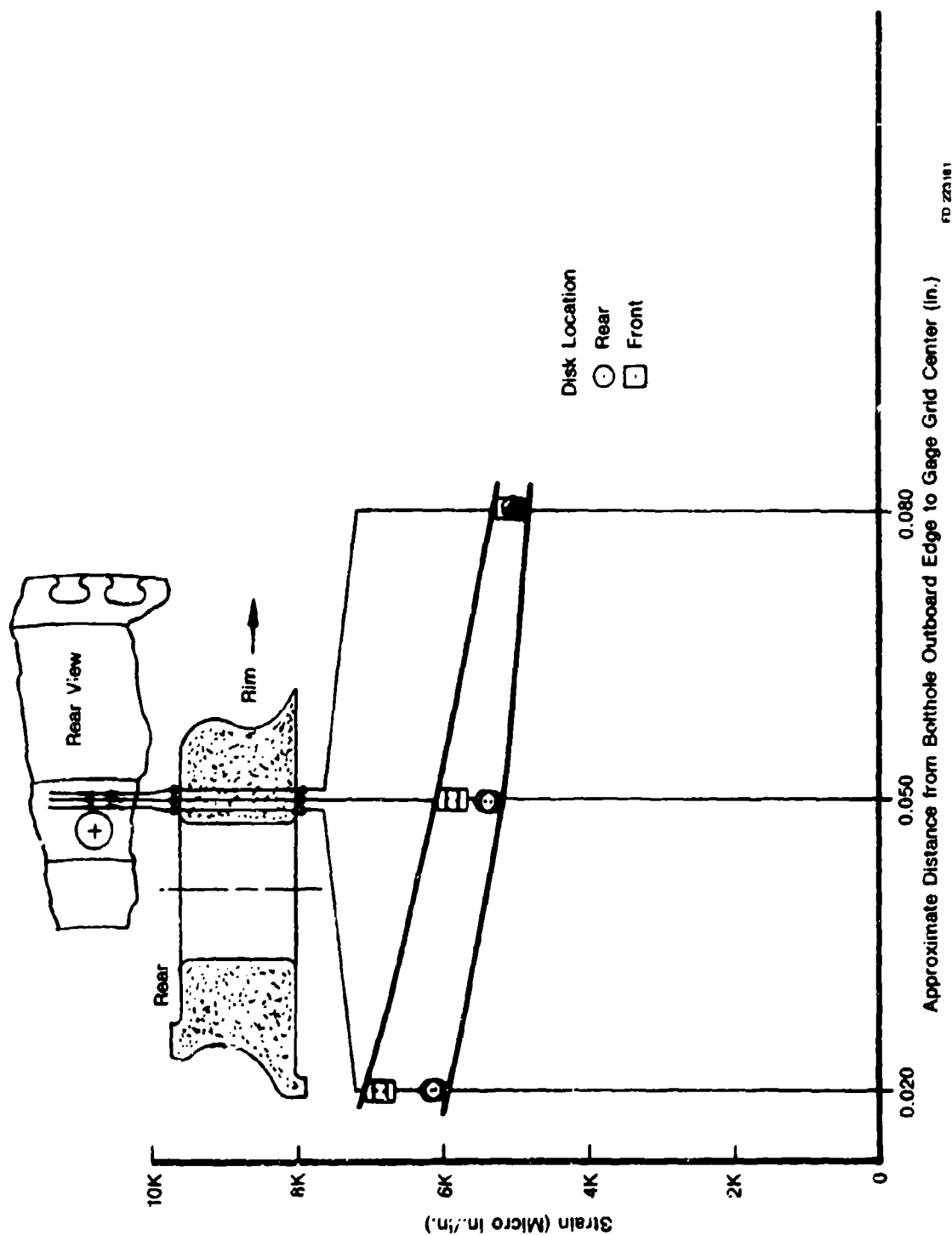
Figure E-13. Static Strain Profile Outside Disk Bolthole Outboard Edge. ME&T Room Temperature Ferris Wheel Test at 18,890 lb/Slot. Damage Tolerant Design Disk 1. (Reference Figure E-4 for Strain Gage Locations).

Figure E-14.   Close-Up of Damage Tolerant Design Disk 2.
Slot Strain Gage Instrumentation Prior to "Ferris Wheel" Testing.

213
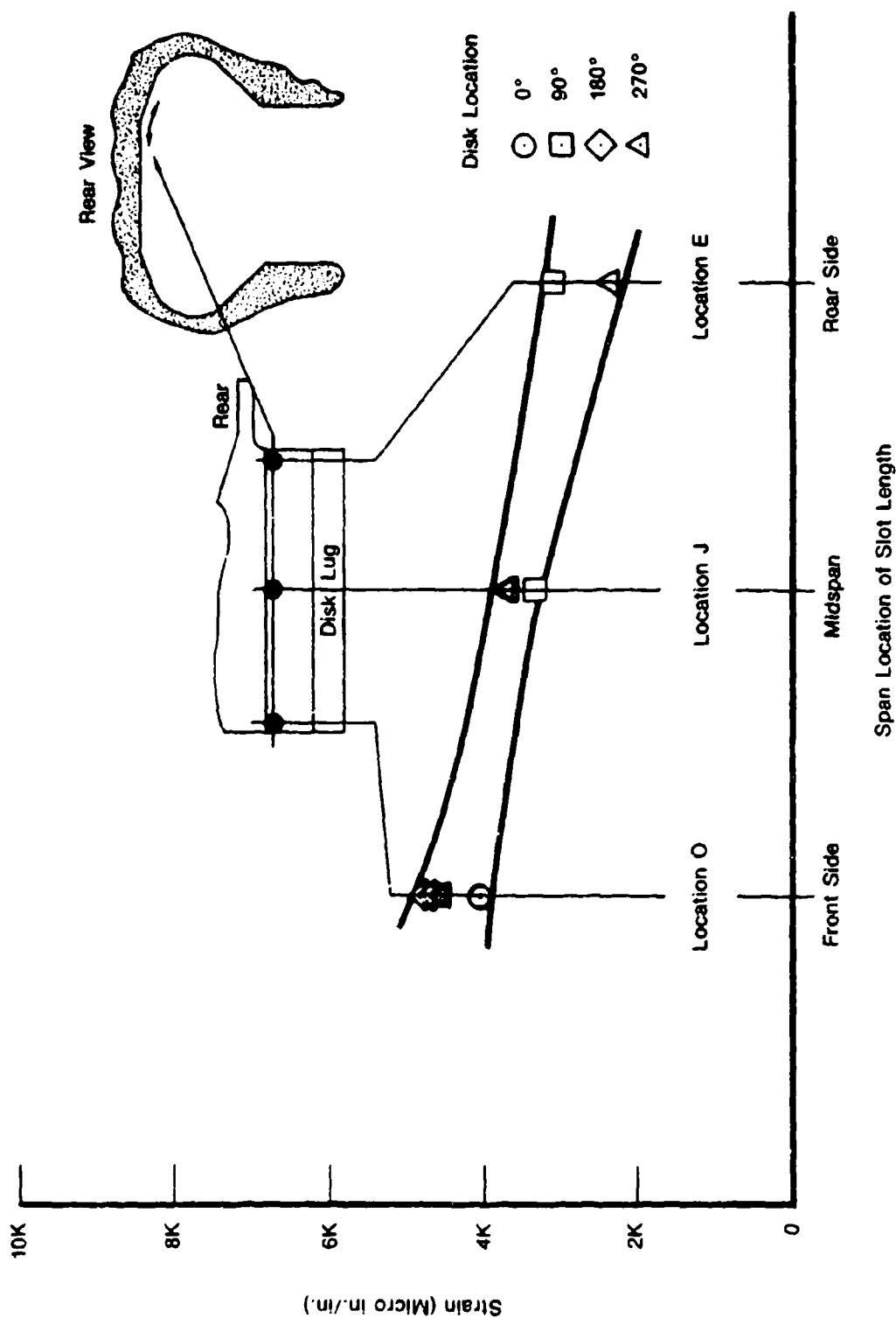
Figure E-15. Static Strain Profile of Disk Slot Live Rim Radius. ME&T Room Temperature
Ferris Wheel Test at 17,700 lb/Slot. Damage Tolerant Design Disk 2.
(Reference Figure E-5 for Strain Gage Locations).

214
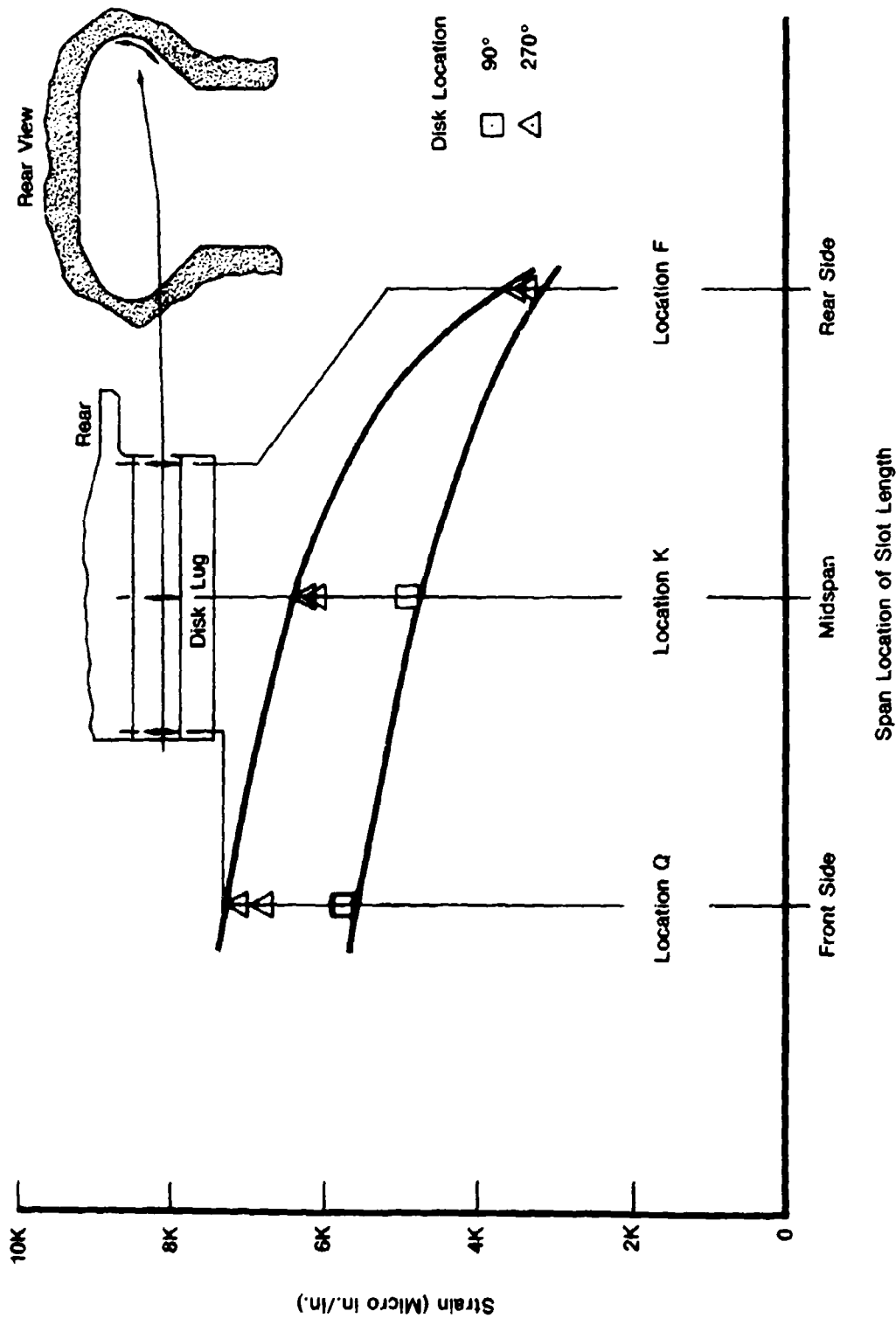
Figure E-16. Static Strain Profile of Disk Lug Bearing Radius. ME&T Room Temperature Ferris Wheel Test at 17,700 lb/Slot. Damage Tolerant Design Disk 2 (Reference Figure E-5 for Strain Gage Locations).
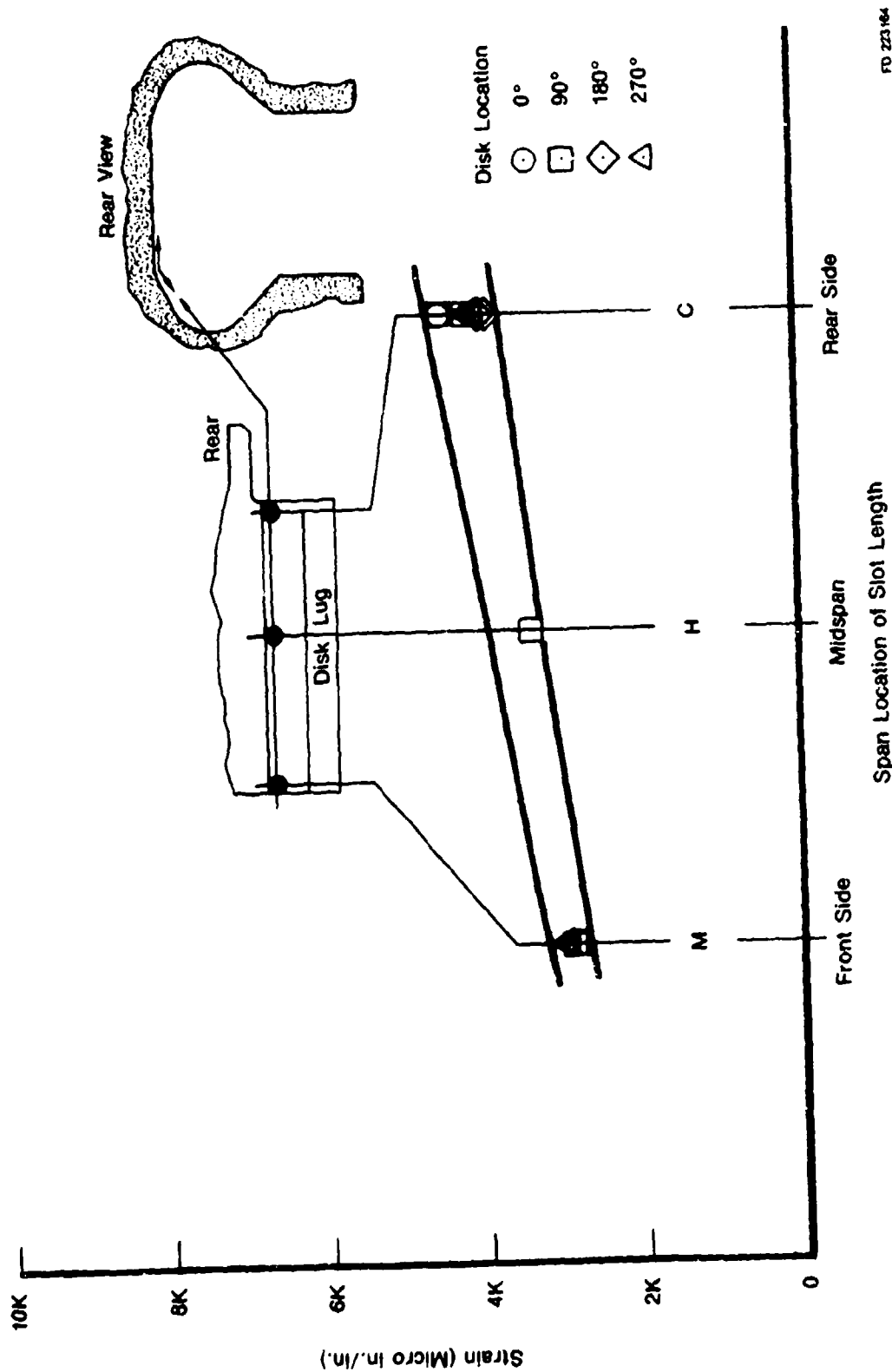
Figure E-17. Static Strain of Disk Slot Live Rim Radius. ME&T Room Temperature
Ferris Wheel Test at 17,700 lb/Slot. Damage Tolerant Design Disk 2
(Reference Figure E-5 for Strain Gage Locations).

216
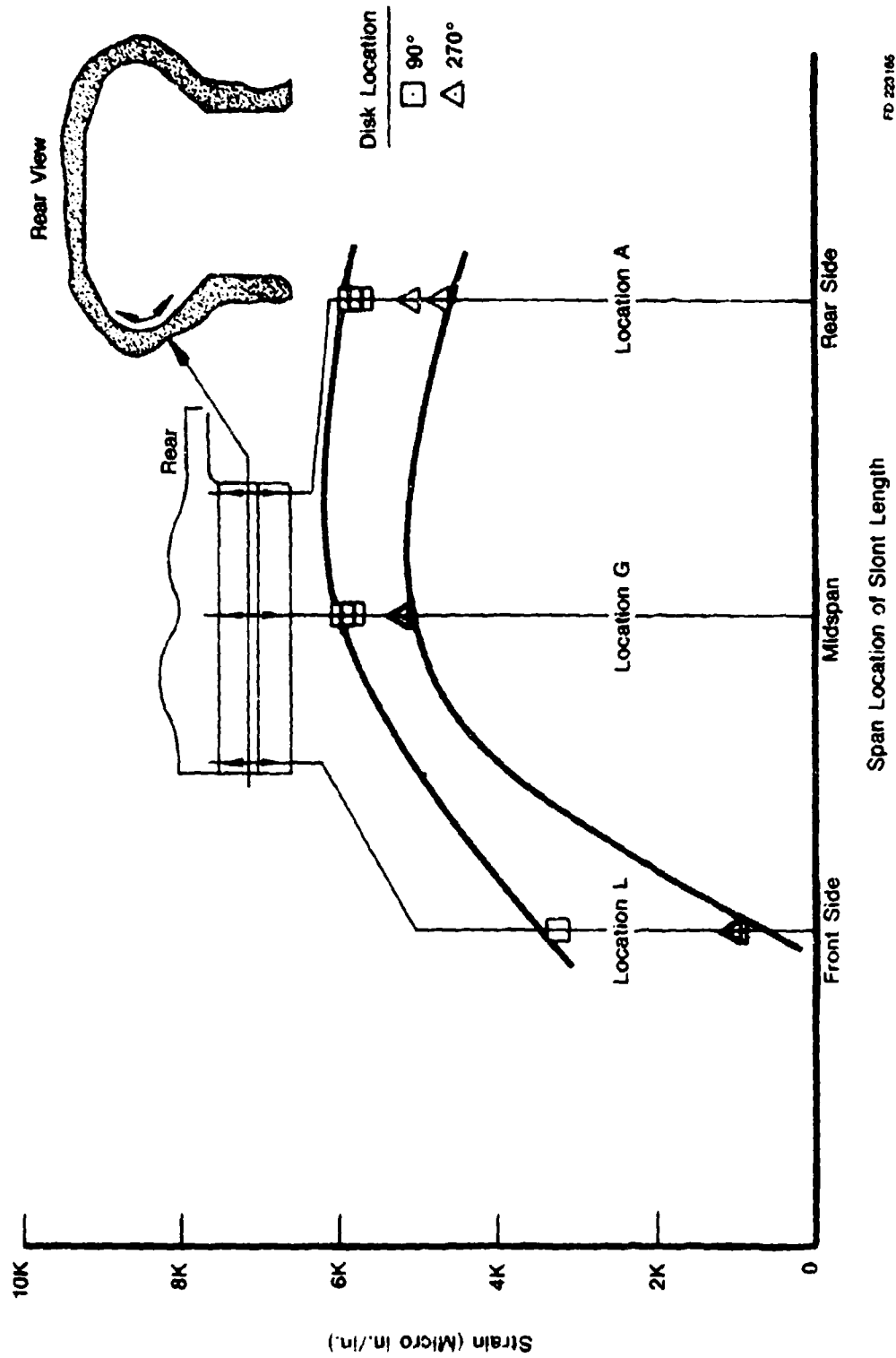
Figure E-18. Static Strain Profile of Disk Lub Bearing Radius. ME&T Room Temperature Ferris Wheel Test at 17,700 lb/Slot. Damage Tolerant Design Disk 2 (Reference Figure E-5 for Strain Gage Locations).
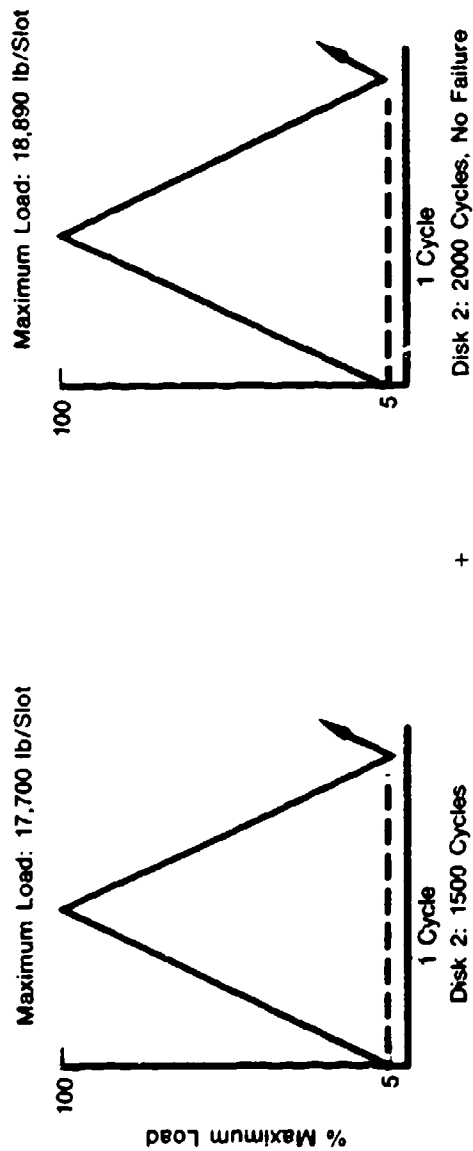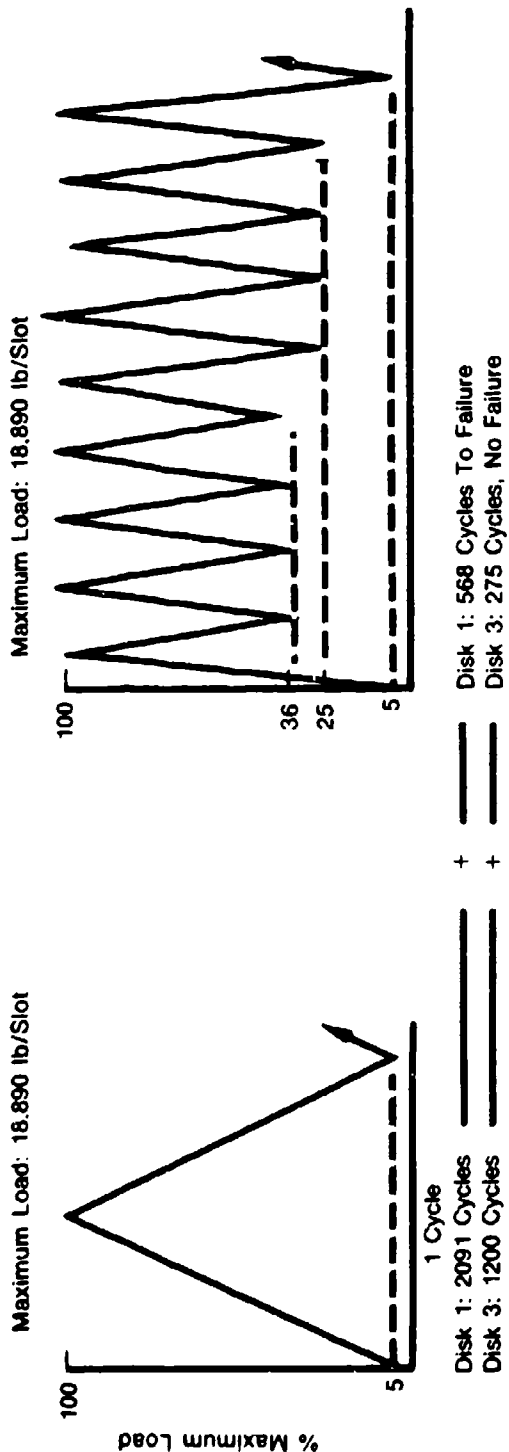
Figure E-19. Load Cycle Definition for Ferris Wheel LCF Test of Damage Tolerant Design Disks 1, 2, and 3.

FD 223168

218

Disk 3

Mag: 100X

Elox Slot in Bolthole 6.
Outboard Side

Disk 2

Mag: 100X

Elox Slot in Slot 19 Live Rim Radius.
Near Front Edge

Disk 1

Mag: 100X

Elox Slot in Bolthole 4.
Outboard Side
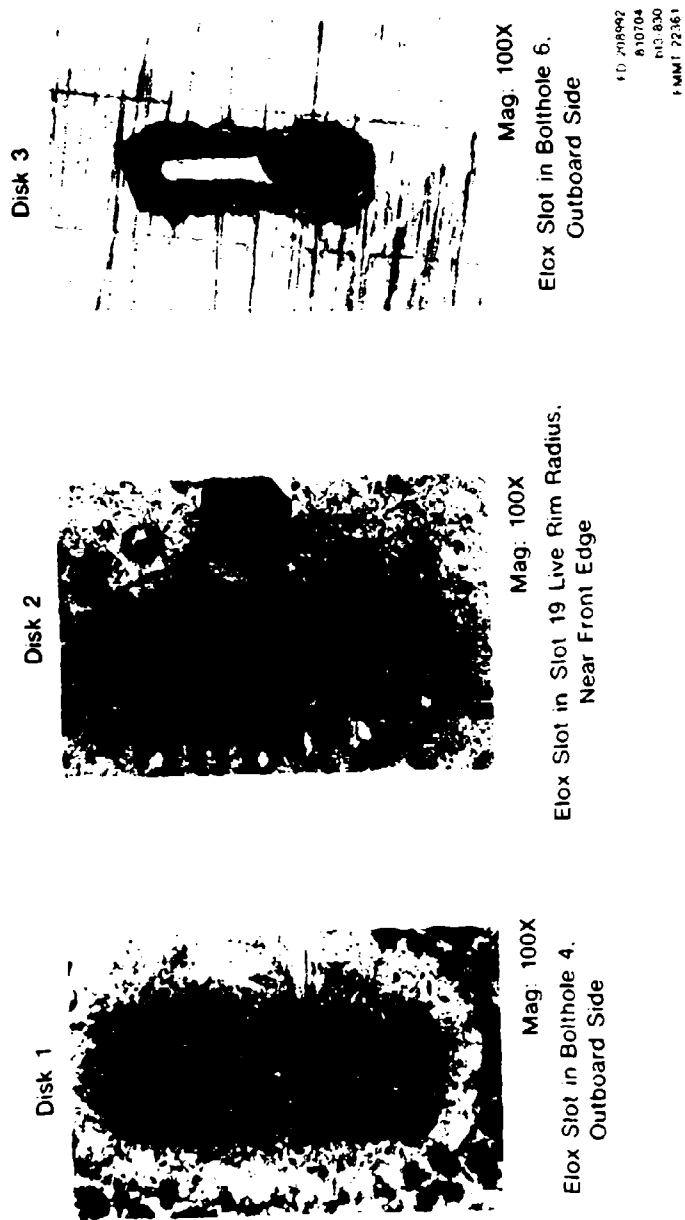
Figure F-20. Typical Baseline Elox Slot Pre-Flaw Indications. ME&T Room Temperature
Ferris Wheel LCF Test. Damage Tolerant Design Disks 1, 2, and 3..

219

Baseline

500 Sawtooth Cycles
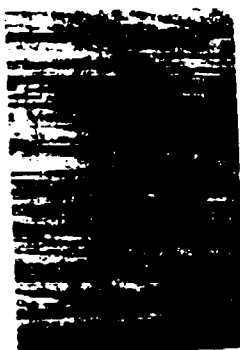
Mag: 50X

1100 Sawtooth Cycles
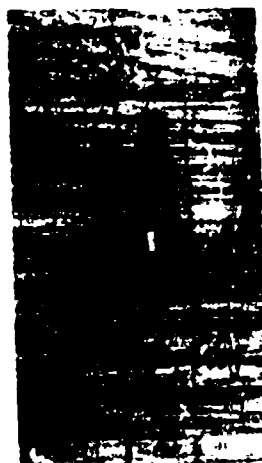
Mag: 50X

1200 Sawtooth + 100 Mission Cycles
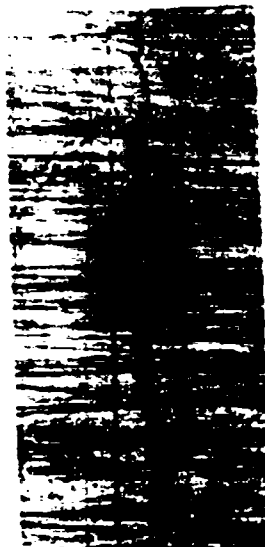
Mag: 50X

1200 Sawtooth + 275 Mission Cycles

Mag: 50X

Mag: 50X

FD 214241

Figure E-21. Replication Crack Growth Progression of Bolt Hole 6 Outboard Side.
ME&T Room Temperature Ferris Wheel LCF Test. Damage Tolerant Design Disk 3
(See Figure E-25 for Fracture Face View of B/H 6).
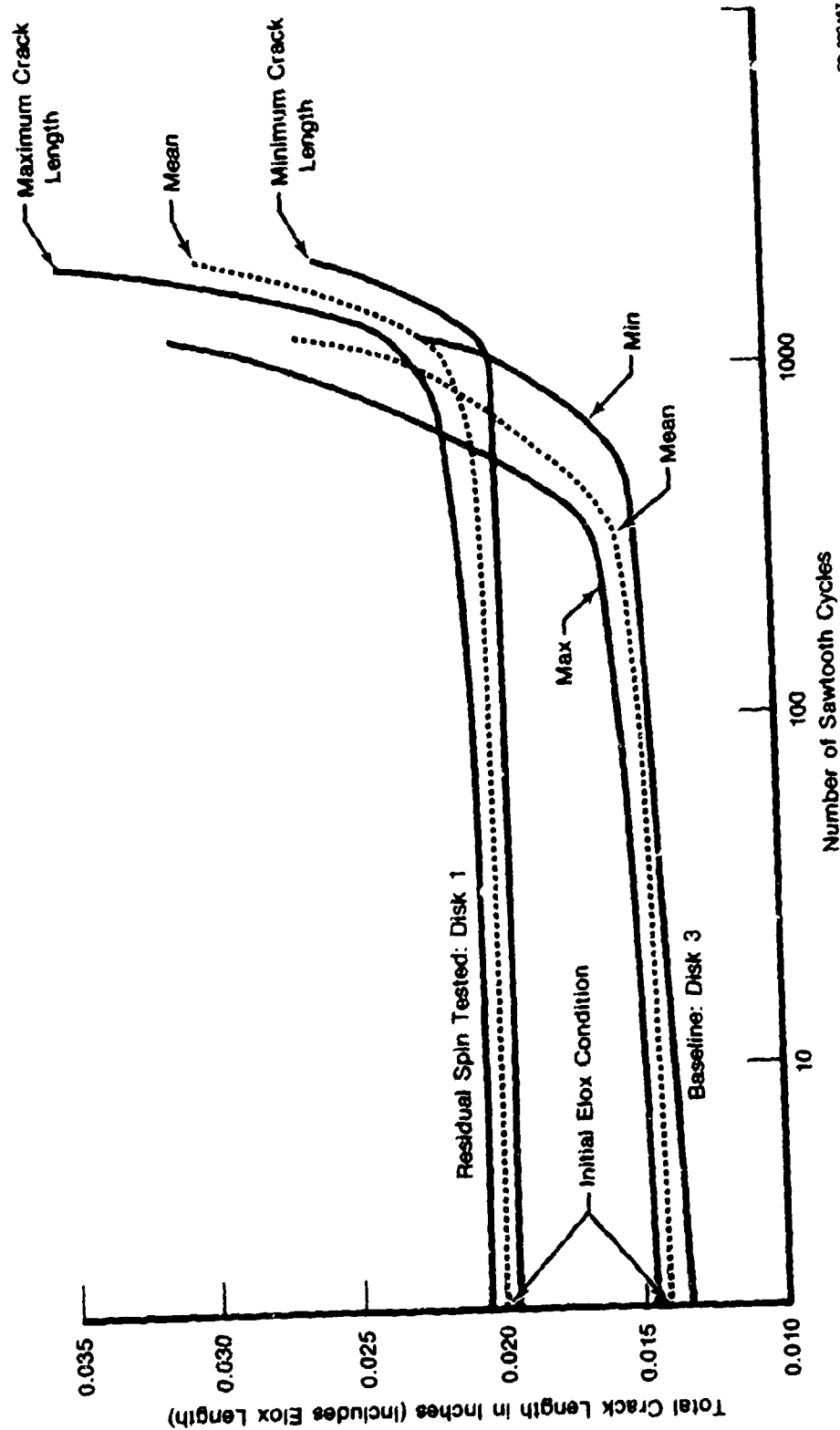
Figure E-22. Bolthole Crack Growth to 1/32 in. Initiation vs Ferris Wheel Sawtooth Cycles. ME&T Room Temperature Ferris Wheel LCF Test (Maximum Load at 18,890 lb/Slot). Damage Tolerant Design Disk 1 and Baseline Disk 3 (Data Taken from Tables V and VI).

221
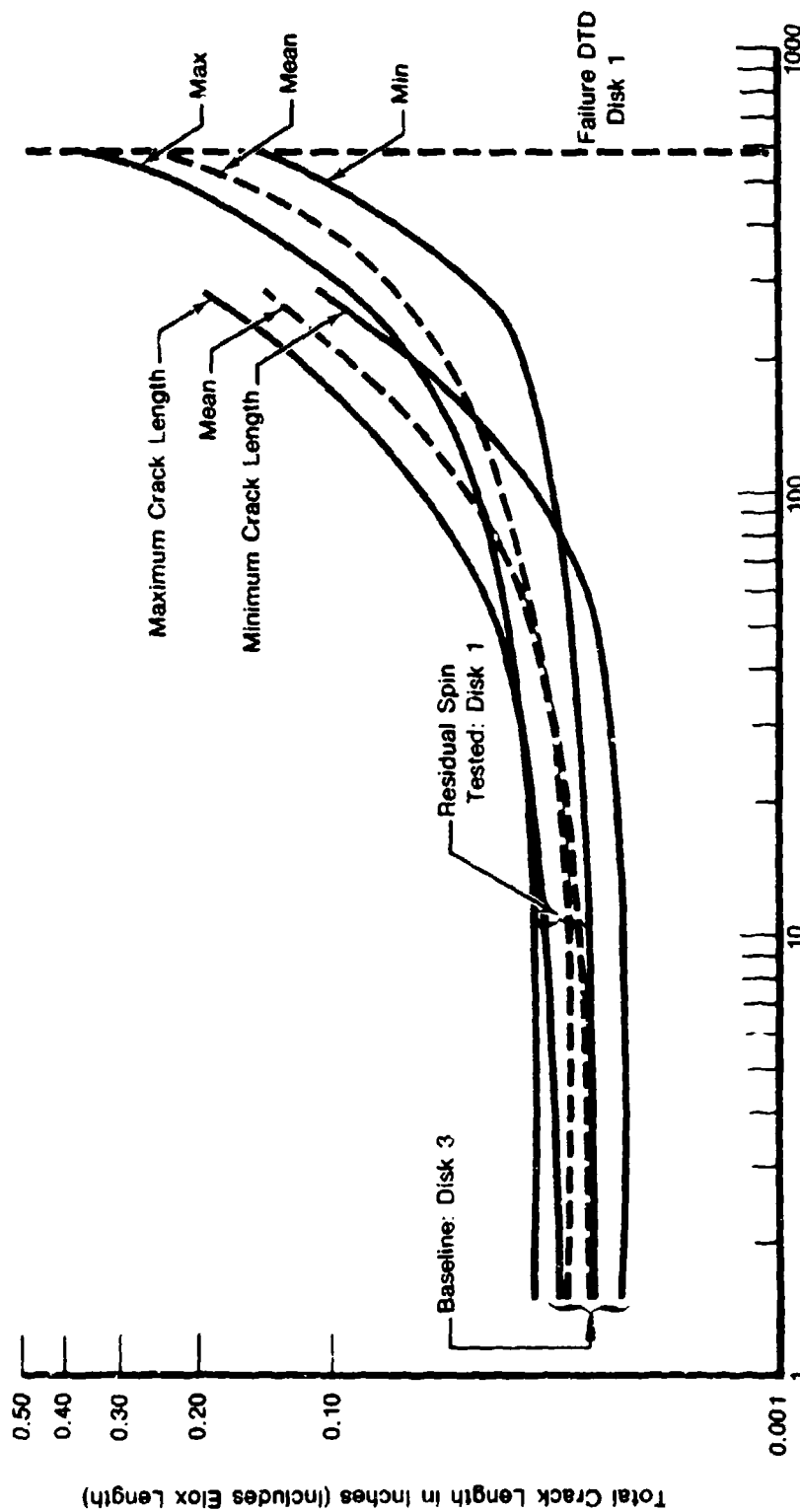
Figure E-23. Bolthole Crack Growth to 1/32 in. Initiation vs Ferris Wheel Mission Cycles. ME&T Room Temperature Ferris Wheel LCF Test (Maximum Load at 18,890 lb/Slot) Damage Tolerant Design Disk 1 and Baseline Disk 3 (Data Taken from Tables V and VI).

222

Elox Slot

Mag: 8.5X
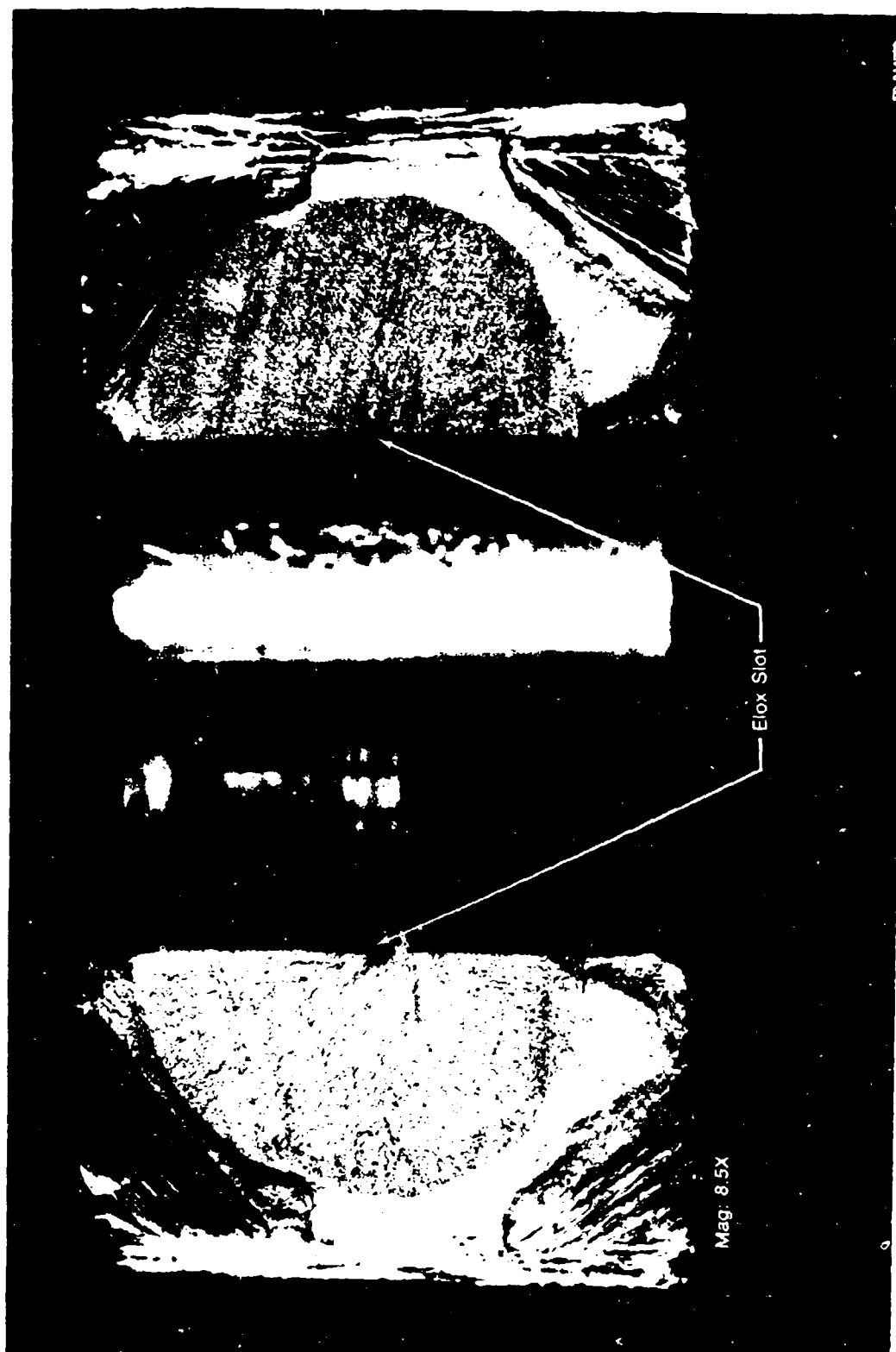
Figure E-24. Close-Up View of Heat Tinted Fracture Face of Elox Initiated Crack in Bolthole 6. MF&T Room Temperature Ferris Wheel LCF Test, Damage Tolerant Design Disk 1.
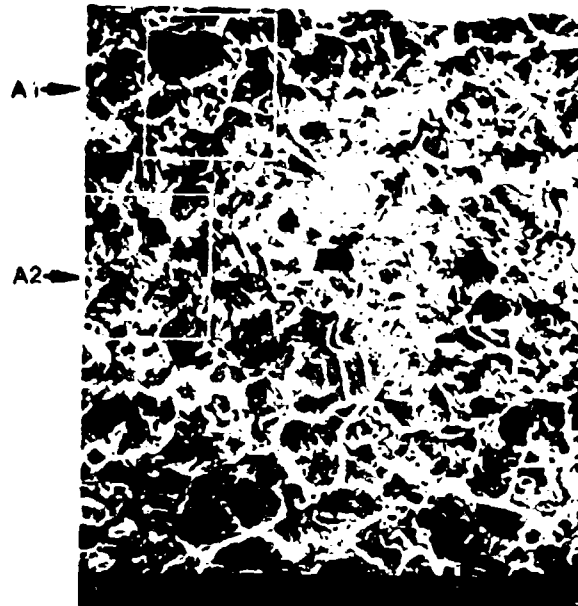
Mag: 8.5X

Figure E-25. Close-Up View of Heat Tinted Fracture Face of Fiox Initiated Crack in Bolthole 6.
ME&T Room Temperature Ferris Wheel LCF Test. Damage Tolerant Design Disk 3.

224

CLEARLY DEFINED THUMBNAIL PATTERN CONTAINING
TRANSGRANULAR FATIGUE WITH WELL DEFINED STRIATIONS

Bolthole 10 With Region A Inset
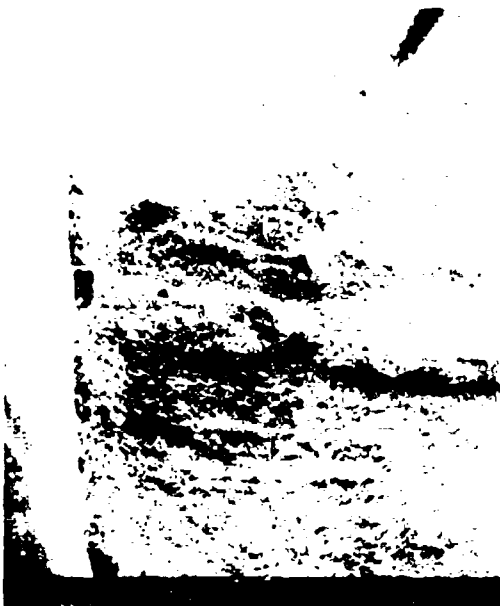
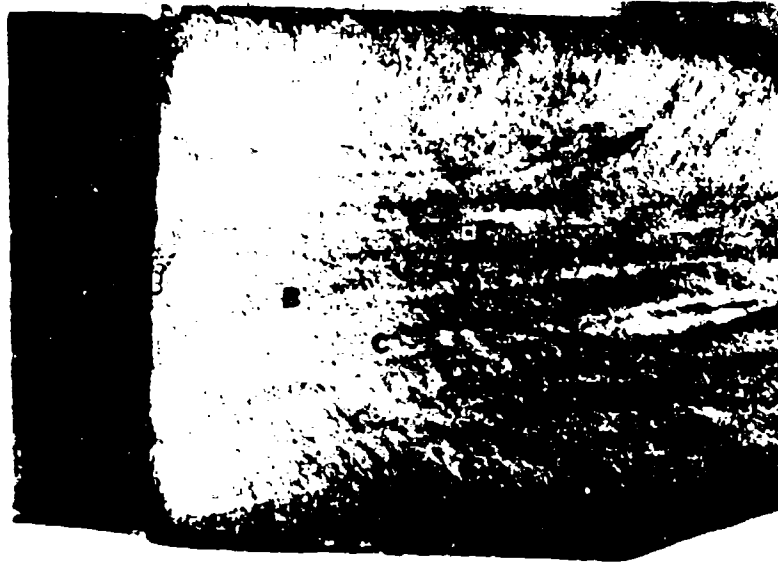Region A With A1, A2 Insets

Mag: 10X

Mag: 500X

A1 Inset

A2 Inset
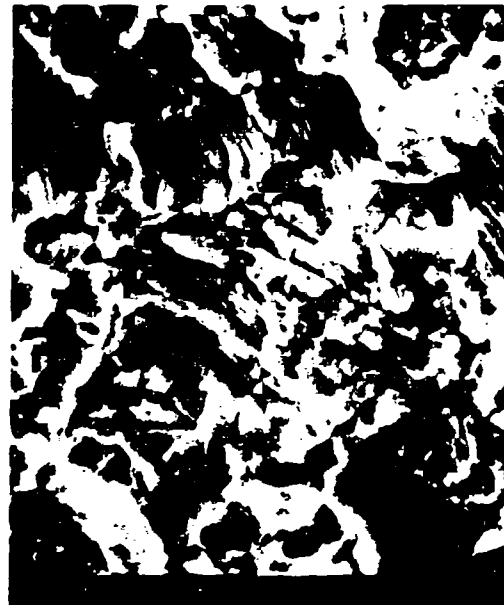
Mag: 2000X

Mag: 2000X

FD 214234

Figure E-26. Scanning Electron Microscope Views of Bolthole 10 Fracture Face.
ME&T Room Temperature Ferris Wheel LCF Test. Damage Tolerant Design Disk 1

Poorly Defined Thumbnail Pattern Containing Mixed Types of Fatigue
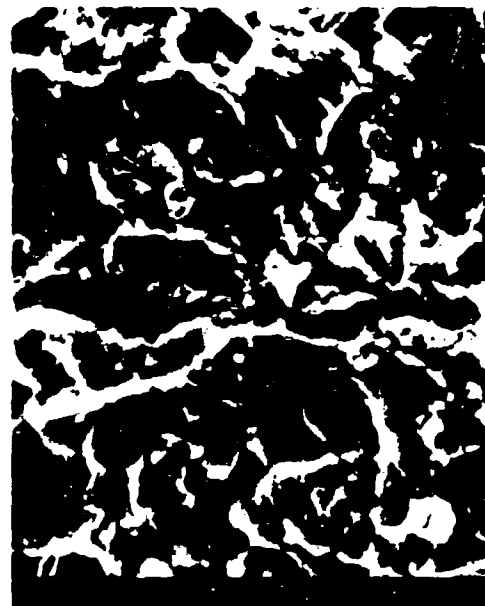Bolthole 20 With Region B, C, D Insets

Region B: Located Same Distance From Elox Slot as Region A.
This Area Shows Transgranular Fatigue With Well Defined Striations

Region B With B1 Inset   B1 Inset

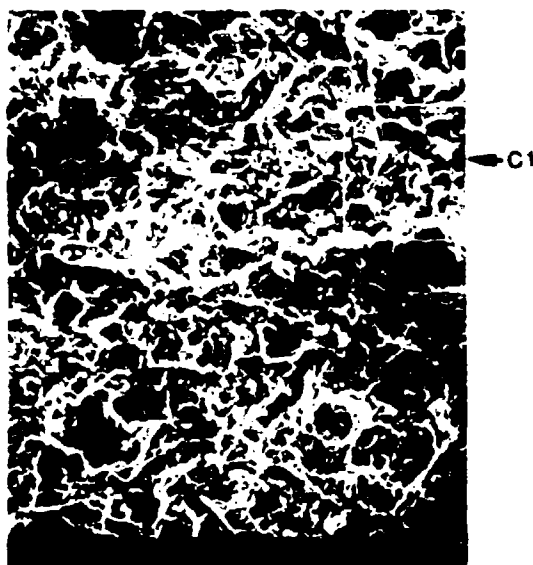Mag: 500X   Mag: 2000X

FD 214235

Figure E-27. Scanning Electron Microscope Views of Bolthole 20 Fracture Face.
ME&T Room Temperature Ferris Wheel LCF Test. Damage Tolerant Design Disk 1.

226

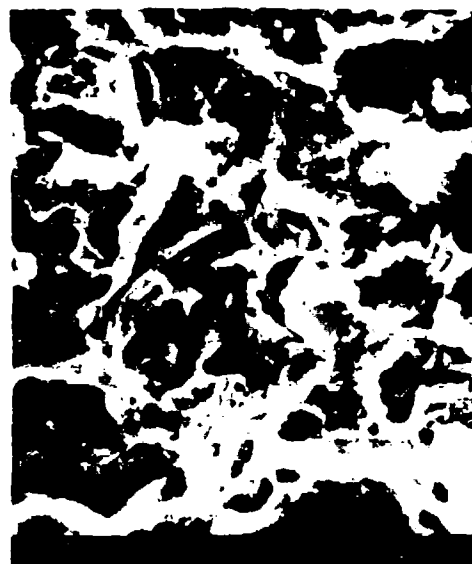Bolthole 20 Views of Regions C and D from Figure 27

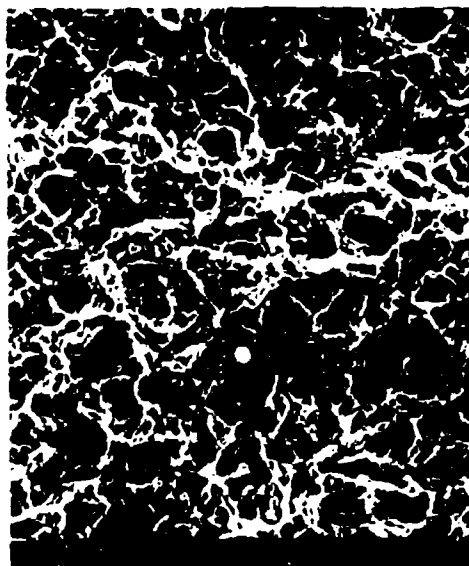Region C: Shows a Transition Area Containing Some Striated Areas

Region C With C1 Inset

C1 Inset

Mag: 500X

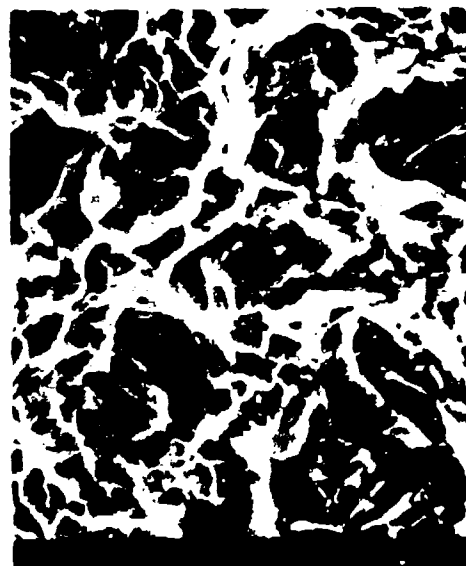Mag: 2000X

Region D: Shows Overstress With Mixed Tensile (Dimpled) and Intergranular

Region D

Enlargement of an Area in Region D

Mag: 500X

Mag: 2000X

FD 214236

Figure E-28. Scanning Electron Microscope Views of Bolthole 20 Fracture Face. ME&T Room Temperature Ferris Wheel LCF Test Damage Tolerant Design Disk 1.

DISTRIBUTION LIST

AFWAL/TST/PO
WPAFB, OH 45433

AFWAL/PS
WPAFB, OH 45433

AFWAL/TST/AA (Library)
WPAFB, OH 45433

Air University Library
Maxwell AFB, AL 36112

DTIA/DDA
Cameron Station
Alexandria, VA 22314
   (2 cys)

AFWAL/POTC
ATTN: W. Troha
WPAFB, OH 45433

AFWAL/POTC
ATTN: J. Holt
WPAFB, OH 45433

AFWAL/POTC
ATTN: J. Petty
WPAFB, OH 45433

AFWAL/POTC
ATTN: D. Finnerty
WPAFB, OH 45433

AFWAL/POTC
ATTN: T. Fecke
WPAFB, OH 45433

AFWAL/POTC
ATTN: R. Hill
WPAFB, OH 45433
   (30 cys)

AFWAL/POTP
ATTN: R. Quigley
WPAFB, OH 45433

AFWAL/POTP
ATTN: R. Panella
WPAFB, OH 45433

AFWAL/POTP
ATTN: R. McNally
WPAFB, OH 45433

AFWAL/MLLN
ATTN: W. Reimann
WPAFB, OH 45433
   (5 cys)

AFWAL/MLLN
ATTN: J. Henderson
WPAFB, OH 45433

AFWAL/MLLN
ATTN: S. Jarvis
WPAFB, OH 45433

Army Applied Tech Lab
ATTN: Library
Fort Eustis, VA 23604

Army Applied Tech Lab
ATTN: J. Lane
Fort Eustis, VA 23604

NASA Lewis Research Center
ATTN: M. Hirschberg
MS-49-1
Cleveland, OH 44135

NASA Lewis Research Center
ATTN: G. Halford
MS-49-1
Cleveland, OH 44135

NASA Lewis Research Center
ATTN: Library
MS-60-3
Cleveland, OH 44135

NAPTC
ATTN: G. Mangano
1440 Parkway Ave.
Trenton, NJ 08628
  (5 cys)

General Electric
AEBG/EMLM
ATTN: L. Beitch
Cincinnati, OH 45215
  (2 cys)

General Electric
AEBG/EMLM
ATTN: A. Coles
Cincinnati, OH 45215
  (5 cys)

General Electric
AEBG/EMLM
ATTN: P. Domas
Cincinnati, OH 45215

Carnegie-Mellon University
ATTN: J. Allison
Dept of M & MS
Pittsburgh, PA 15213

ASD/ENFSF
ATTN: W. Cowie
WPAFB, OH 45433
  (5 cys)

ASD/ENF
ATTN: T. King
WPAFB, OH 45433

ASD/ENFSF
ATTN: J. Ogg
WPAFB, OH 45433
  (3 cys)

ASD/ENFSF
ATTN: L. Smithers
WPAFB, OH 45433

ASD/EN
ATTN: J. Lincoln
WPAFB, OH 45433

ASD/ENFSF
ATTN: W. Taylor
WPAFB, OH 45433

Detroit Diesel Allison
ATTN: N. Provenzano
PO Box 894
Indianapolis, IN 46206
  (5 cys)

Detroit Diesel Allison
ATTN: M. Doner
PO Box 894
Indianapolis, IN 46206
  (3 cys)

Garrett Turbine Engine Co.
ATTN: C. Corrigan
Phoenix, AZ 85010
  (5 cys)

Garrett Turbine Engine Co.
ATTN: L. Matsch
Phoenix, AZ 85010
  (3 cys)

Pratt & Whitney Aircraft
ATTN: D. Hunter
PO Box 2691
West Palm Beach, FL 33402
  (5 cys)

Pratt & Whitney Aircraft
ATTN: D. Hilliard
PO Box 2691
West Palm Beach, FL 33402
  (5 cys)

Pratt & Whitney Aircraft
ATTN: C. Spaeth
PO Box 2691
West Palm Beach, FL 33402
  (3 cys)

Pratt & Whitney Aircraft
ATTN: C. Cook
PO Box 2691
West Palm Beach, FL 33402
  (3 cys)

AFWAL/MLSA
ATTN: G. Petrak
WPAFB, OH 45433

University Of Dayton
Research Institute
ATTN: J. Gallagher
Dayton, OH 45469
  (2 cys)

ASD/YZEA
ATTN: D. Anderson
WPAFB, OH 45433
  (3 cys)

Teledyne CAE
ATTN: B. Lewis
Toledo, OH 45215
  (5 cys)

Systems Research Laboratory
ATTN: H. Bernstein
Dayton, OH 45420

Arnold Engr. Dev. Center
ATTN: T. Cromer/Aero Inc.
Arnold Air Force Station, TN
  (5 cys)